ไลเพสของ *Pseudomonas cepacia* ตรึงรูปบน
เม็ดพอลิสไตรีนที่เคลือบด้วยไคโทซานสำหรับการผลิตไบโอดีเซล

นางสาวภาวิณี ยวงเขียน

วิทยานิพนธ์นี้เป็นส่วนหนึ่งของการศึกษาตามหลักสูตรปริญญาวิทยาศาสตรมหาบัณฑิต
สาขาวิชาปิโตรเคมีและวิทยาศาสตร์พอลิเมอร์
คณะวิทยาศาสตร์ จุฬาลงกรณ์มหาวิทยาลัย
ปีการศึกษา 2558

Pseudomonas cepacia LIPASE IMMOBILIZED ONTO
CHITOSAN-COATED POLYSTYRENE BEADS FOR BIODIESEL PRODUCTION

Miss Pawinee Yuangkian

A Thesis Submitted in Partial Fulfillment of the Requirements
for the Degree of Master of Science Program in Petrochemistry and Polymer Science
Faculty of Science
Chulalongkorn University
Academic Year 2015

Thesis Title	*Pseudomonas cepacia* LIPASE IMMOBILIZED ONTO CHITOSAN-COATED POLYSTYRENE BEADS FOR BIODIESEL PRODUCTION
By	Miss Pawinee Yuangkian
Field of Study	Petrochemistry and Polymer Science
Thesis Advisor	Associate Professor Surachai Pornpakakul, Ph.D.

Accepted by the Faculty of Science, Chulalongkorn University in Partial Fulfillment of the Requirements for the Master's Degree

.....Dean of the Faculty of Science
(Associate Professor Polkit Sangvanich, Ph.D.)

THESIS COMMITTEE

.....Chairman
(Professor Pattarapan Prasassarakich, Ph.D.)

.....Thesis Advisor
(Associate Professor Surachai Pornpakakul, Ph.D.)

.....Examiner
(Associate Professor Voravee Hoven, Ph.D.)

.....External Examiner
(Pravit Singtothong, Ph.D.)

ภาวิณี ยวงเขียน : ไลเพสของ *Pseudomonas cepacia* ตรึงรูปบนเม็ดพอลิสไตรีนที่เคลือบด้วยไคโทซานสำหรับการผลิตไบโอดีเซล (*Pseudomonas cepacia* LIPASE IMMOBILIZED ONTO CHITOSAN-COATED POLYSTYRENE BEADS FOR BIODIESEL PRODUCTION) อ.ที่ปรึกษาวิทยานิพนธ์หลัก: รศ. ดร.สุรชัย พรภคกุล, 173 หน้า.

ในงานวิจัยนี้เม็ดพอลิสไตรีนที่เคลือบด้วยไคโทซาน (CHI-STY/PS beads) ถูกใช้เป็นตัวพยุงชนิดของแข็ง และไลเพสของ *Pseudomonas cepacia* (*P. cepacia*) ถูกตรึงรูปบนเม็ดพอลิสไตรีนที่เคลือบด้วยไคโทซาน โดยใช้กลูตารอลดีไฮด์เป็นสารเชื่อมขวาง (GLU-CHI-STY/PS beads) การตรึงรูปของไลเพสบน GLU-CHI-STY/PS beads ถูกใช้เป็นตัวเร่งปฏิกิริยาสำหรับผลิตไบโอดีเซลผ่านปฏิกิริยาทรานส์เอสเทอร์ริฟิเคชันของน้ำมันถั่วเหลือง สำหรับปฏิกิริยาทรานส์เอสเทอร์ริฟิเคชัน *P. cepacia* (30 มิลลิกรัม) ตรึงรูปบน 15%GLU-2%CHI-15%STY/PS beads (1 กรัม) ที่อุณหภูมิ 30 องศาเซลเซียส เป็นเวลา 72 ชั่วโมง ถูกใช้เป็นตัวเร่งปฏิกิริยาสำหรับผลิตไบโอดีเซล กิจกรรมของเอนไซม์, ปริมาณโปรตีนที่ยึดเกาะ และความจำเพาะของเอนไซม์ของตัวเร่งปฏิกิริยานี้เท่ากับ 54.43 ยูนิตต่อกรัมของตัวพยุง, 72.93% และ 2.49 ยูนิตต่อมิลลิกรัมของโปรตีน ตามลำดับ ศึกษาผลกระทบในปฏิกิริยาการทรานส์เอสเทอร์ริฟิเคชันคือ อัตราส่วนระหว่างน้ำมันต่อแอลกอฮอล์, ปริมาณตัวเร่งปฏิกิริยา, อุณหภูมิที่ใช้ และเวลาในการทำปฏิกิริยา พบว่า สภาวะที่เหมาะสมคือ อัตราส่วน 1:5 ระหว่างน้ำมันต่อเอทานอล (เติมเอทานอลปราศจากน้ำ 3 ครั้ง) ตัวเร่งปฏิกิริยา 0.4294 กรัม ที่อุณหภูมิ 40 องศาเซลเซียส เป็นเวลา 32 ชั่วโมง ได้เปอร์เซ็นต์เอทิลเอสเทอร์สูงสุดคือ 91% หลังจากนำตัวเร่งปฏิกิริยากลับมาใช้ซ้ำ 5 ครั้ง พบว่า เปอร์เซ็นต์เอทิลเอสเทอร์ลดลงเป็น 87%

สาขาวิชา ปิโตรเคมีและวิทยาศาสตร์พอลิเมอร์ ลายมือชื่อนิสิต .....

ปีการศึกษา 2558 ลายมือชื่อ อ.ที่ปรึกษาหลัก .....

5572074123 : MAJOR PETROCHEMISTRY AND POLYMER SCIENCE
KEYWORDS: IMMOBILIZATION OF LIPASE / BIODIESEL PRODUCTION

PAWINEE YUANGKIAN: *Pseudomonas cepacia* LIPASE IMMOBILIZED ONTO CHITOSAN-COATED POLYSTYRENE BEADS FOR BIODIESEL PRODUCTION. ADVISOR: ASSOC. PROF. SURACHAI PORNPAKAKUL, Ph.D., 173 pp.

In this research, chitosan-styrene copolymer coated onto polystyrene beads (CHI-STY/PS beads) was used as the solid support and the lipase of *Pseudomonas cepacia* (*P. cepacia*) was immobilized onto CHI-STY/PS beads by using glutaraldehyde as linker (GLU-CHI-STY/PS beads). Immobilization of lipase onto GLU-CHI-STY/PS beads was used as a catalyst for biodiesel production through transesterification reaction of soybean oil. For transesterification reaction, *P. cepacia* (30 mg) immobilized onto 15%GLU-2%CHI-15%STY/PS beads (1 g) at 30°C for 72 hours was used as a catalyst for biodiesel production. The lipase activity, protein loading yield and specific activity of this catalyst gave the optimal value at 54.43 U/g-support, 72.93% and 2.49 U/mg-protein, respectively. The effects of molar ratio of oil to alcohol, amount of catalyst, temperature and reaction time in the transesterification reaction were investigated. The optimum conditions were 1:5 oil/ethanol molar ratio (three step addition of anhydrous ethanol), 0.4294 g catalyst at 40°C for 32 hours. The highest ethyl esters yield was 91%. The ethyl esters production retained 87% of the original conversion after being reused for 5 batches.

Field of Study: Petrochemistry and Polymer Science Student's Signature .....
Advisor's Signature .....

Academic Year: 2015

ACKNOWLEDGEMENTS

In spite of my efforts in this project, the research could not have been achieved without all guidance and support that I have received from many individuals. I would like to show our sincere gratitude to everyone who dedicated their time to assist, consult and support me throughout the project.

At first, I would like to express my deep and sincere gratitude to my advisor, Associate Professor Dr. Surachai Pornpakakul, for his advises, patience, motivation, and tolerance. The research would not have been possible without the help of his guidance and encouragement all the time throughout this research.

I would also like to extend to Professor Dr. Pattarapan Prasassarakich, Associate Professor Dr. Voravee Hoven and Dr. Pravit Singtothong, attending as the chairman, examiner and external examiner of my thesis committee, respectively, for their kind guidance, helpful discussions and valuable suggestions throughout my study.

I would like to special thanks to all staff at IRPC Co., Ltd. and PTT Global Chemical Public Co., Ltd. for kind suggestion and helpful in providing facilities and materials for my thesis experiment.

In addition, I am grateful to Mr. Suphongphan Srisurichan, Miss Jittranuch Jirapathomkul, Miss Apichaya Thiangtrong and all members on Research Center for Biooraganic Chemistry (RCBC) for their kind gratitude of finding me the information, their friendship, support and helpfulness.

Finally, I would like to express thanks to my family for their care and supports to make my study successful. Thanks are also due to everyone who has contributed suggestions and supports throughout my research.

CONTENTS

Page

Page

Page

Page

Page

Page

LIST OF TABLES

Tables Page

LIST OF FIGURES

LIST OF SCHEMES

LIST OF ABBREVIATIONS

°C	=	Degree of Celsius
mg	=	Milligram
g	=	Gram
g/mol	=	Gram per mole
%w/v	=	Percent weight by volume
min	=	Minute
h	=	Hour
CHI	=	Chitosan
STY	=	Styrene
GLU	=	Glutaraldehyde
PS	=	Polystyrene
ml	=	Milliliter
mM	=	Millimolar
M	=	Molar
mm	=	Millimeter
P. cepacia	=	*Pseudomonas cepacia*
U/g-support	=	Unit per gram of support
ATR-FTIR	=	Fourier transforms infrared spectroscopy in the attenuated total reflectance mode
UV/VIS	=	Ultraviolet-visible
^{1}H-NMR	=	Proton nuclear magnetic resonance
SEM	=	Scanning electron microscopy

SBO	=	Soybean oil
MW	=	Molecular weight
SN	=	Saponification number
TAG	=	Triacylglycerol
FAEE	=	Fatty acid ethyl ester
FAME	=	Fatty acid methyl ester

CHAPTER I
INTRODUCTION

Population growth and economic development have resulted in the increasing energy consumption in the world. Common sources of energy are petroleum, natural gas and coal from fossil fuels. The growth in consumption of energy has caused economic, security, atmospheric pollution and environmental problems. New sources of energy that can be produced from renewable raw materials were needed. Biodiesel is made from renewable biological sources such as vegetable oils and animal fats. The main advantages of biodiesel are biodegradable, nontoxic and low pollutant emissions [1]. There are several methods to make biodiesel production such as direct use of vegetable oils (dilution), thermal cracking (pyrolysis), microemulsion and transesterification. Dilution is not applicable to most of actual diesel fuels because the high viscosity of biodiesel in this method damaged the engine. Other methods of biodiesel production are pyrolysis and microemulsion would lead to incomplete combustion because a low cetane number. The most commonly used method is transesterification of triacylglycerol (TAG) with short chain alcohols [2]. Using alcohol for transesterification is a sequence of three reversible consecutive steps. In the first step, triglycerides are converted to diglycerides. Then, diglycerides are converted to monoglycerides. The last step, monoglycerides are converted to glycerin molecules. It is a reversible reaction and accordingly excess alcohol is used to shift the equilibrium to the product side. The catalyst for the transesterification is classified as chemical or enzymatic catalyst. Chemical catalysts such as acid (H_2SO_4) or base (NaOH and KOH) catalysts are used to produce biodiesel in short time reaction and give high conversion level of biodiesel. On the other hand, major of disadvantage in these catalyst are high-energy requirements, recovery of glycerol is difficult and potential pollution to the environment [3]. Nowadays, enzyme used as catalysts for biodiesel production. The main advantages of enzyme as biocatalyst are mild reaction conditions, easy recovery of glycerol and very high purity product. In addition, free fatty acid content in the oil

can be completely converted to biodiesel and no soap formation. Thus, conversion of the biodiesel has increased.

The enzymatic catalysts are mostly used in term of lipase immobilization for transesterification processes because catalyst can be easy separation from the product and recovery. Besides, lipase immobilization are used in food technology, biotechnology and analytical chemistry [4]. Lipase used in the production of biodiesel as a source of bacteria and fungi such as *Candida antarctica* (Novozym 435), *Candida rugosa* (Lipase AY), *Pseudomonas cepacia* (Lipase PS), *Pseudomonas fluorescens* (lipase AK), *Pseudomonas aeruginosa*, and *Thermomyces lanuginose* (Lipozime TL) [5]. The success of the immobilized lipase is closely related to properties of support and characteristics of the lipase. The interactions between support and lipase are critical for lipase activity [6]. There are several methods for lipase immobilization. Methods for lipase immobilization can be classified as carrier binding and encapsulation. Covalent binding method has been most widely studied. In this way, an enzyme molecule can be immobilized by forming a covalent linkage between the amino acid residue of enzyme and an active group on the support [7, 8].

The properties of immobilized lipase are governed by the properties of both the lipase and the support material. Supports of lipase immobilization can be classified as organic and inorganic support. The organic supports can be divided into natural and synthetic polymers [9]. Organic synthetic supports are widely used as immobilization supports. For example, solid-phase synthesis method has been widely used in the synthesis of peptides, proteins and small organic molecules and combinatorial chemistry. Polystyrene beads are still the most commonly used polymer support for solid-phase synthesis because it has many advantages such as good mechanical, chemical stabilities and the facility of derivations with a wide variety of functional groups for substrate attachment [10].

Chitosan is the principal derivative of chitin. It is obtained by *N*-deacetylation to a varying extent that is characterized by the degree of deacetylation and is consequently a copolymer of *N*-acetyl-d-glucosamine and d-glucosamine. Chitosan can be defined as chitin sufficiently deacetylated to form soluble amine salts, the

degree of deacetylation necessary to obtain a soluble product being 80-85% or higher. Commercially, chitosan are obtained at a relatively low cost from shells of shellfish (mainly crabs, shrimps, lobsters and krills) and wastes of the seafood processing industry. It is insoluble under alkaline and neutral conditions, but it can react with inorganic and organic acids such as hydrochloric acid, lactic acid, acetic acid and glutamic acid under acidic conditions. Chitosan is a polysaccharide easily obtained by alkaline hydrolysis of chitin and has been used in pharmaceutical fields, medicines, drug delivery carriers, wound dressing materials and tissue engineering [11]. It is considered to be a suitable support because it has reactive amino and hydroxyl groups, biocompatible, available in various forms (gel, membrane, fiber, and film), non-toxic and amenable to chemical modifications [12]. Many studies have already shown chitosan to be a good support for lipase immobilization. However, immobilized lipase on chitosan supports usually exhibit lower activity than free lipase. Thus, various kinds of chitosan supports have been developed by modification of the chitosan backbone in order to improve activity of the immobilized lipase. The native amino groups or the active groups resulting from surface modification can be bound to aldehyde groups using glutaraldehyde [13, 14]. Glutaraldehyde activation is shown to be the simple and efficient method to immobilize lipase because it can react with amino groups of support and lipase [15, 16].

Considering the good biological properties of polystyrene beads and chitosan, a combination of these polymers may have beneficial effects on the biological characteristics. In this research, chitosan-styrene copolymer coated onto polystyrene beads (CHI-STY/PS beads) was used as the solid support and the lipase of *Pseudomonas cepacia* was immobilized onto CHI-STY/PS beads by using glutaraldehyde as linker. Lipase activity, protein loading yield and specific activity of the lipase-immobilized catalyst were examined and efficiency of the immobilized catalyst for biodiesel production through transeserification was also evaluated.

1.1 Objectives of the research

- Preparation of *Pseudomonas cepacia* lipase immobilized onto chitosan-styrene copolymer coated onto polystyrene beads activated with glutaraldehyde solution.

- *Pseudomonas cepacia* lipase immobilized onto chitosan-styrene copolymer coated onto polystyrene beads activated with glutaraldehyde solution was used as catalyst for biodiesel production through tranesterification.

CHAPTER II
THEORY AND LITERATURE REVIEWS

2.1 Background

Biodiesel is made from renewable biological sources like vegetable oils and animal fats. It is an alternative diesel fuel because of its environmental benefits such as being biodegradable, nontoxic and low carbon dioxide emission profiles. The cetane number, energy content, viscosity and other physical properties of biodiesel are also similar to those of petroleum diesel. For these reasons, biodiesel is considered an excellent replacement for common petroleum diesel. The most popular method of biodiesel production is the transesterification. In general, there are two methods to produce biodiesel in industrial application: i) chemical-catalyzed method and ii) enzymatic-catalyzed method. Enzymatic transesterification of triglycerides offers an environmentally more attractive option to the conventional process. However, the enzymatic-catalyzed method is not favored in industrial development because the high cost and low stability of lipase limit its potential application. The key step in enzymatic processes lies in successful immobilization of the enzyme, which will allow for its recovery and reuse. Immobilization is the most widely used method for achieving stability in lipases and to make them more attractive for industrial use. Common immobilization techniques include physical adsorption onto a solid support [17], covalent binding to a solid support [18] and entrapment of lipase entails capture of the lipase within a matrix of a polymer [19].

2.2 Production of biodiesel

Biodiesel is environmentally friendly and shows great potential as an alternative liquid fuel and energy product. Globally, there are many efforts to develop and improve vegetable oil properties in order to approximate the properties of diesel fuels. It has been remarked that high viscosity, low volatility and polyunsaturated characters are the mostly associated problems with crude vegetable oils. These problems can be overcome by four methods such as direct use (dilution), thermal

cracking (pyrolysis), microemulsion and transesterification [20]. Dilution of vegetable oil is not applicable to most of actual diesel engines, as the high viscosity would damage the engine. Biodiesel obtained from pyrolysis and microemulsion methods would lead to incomplete combustion due to a low cetane number. Transesterification is the most common method for biodiesel production due to its simplicity and it has been widely studied and industrially used to convert vegetable oil into biodiesel [21].

2.2.1 Direct use (dilution)

The direct usage of vegetable oils as biodiesel is possible by blending it with conventional diesel fuels in a suitable ratio and these ester blends are stable for short term usages. The blending process is simple which involves mixing alone and hence the equipment cost is low. However, direct usage of these triglyceric esters (oils) is unsatisfactory and impractical for long term usages in the available diesel engines due to high viscosity, acid contamination, free fatty acid formation resulting in gum formation by oxidation and polymerization and carbon deposition. Hence vegetables oils are processed so as to acquire properties (viscosity and volatility) similar to that of fossil fuels and the processed fuel can be directly used in the diesel engines available [22].

2.2.2 Thermal cracking (pyrolysis)

Pyrolysis refers to chemical change caused by application of heat to get simpler compounds from a complex compound. The process is also known as cracking. Vegetable oils can be cracked to reduce viscosity and improve cetane number. The products of cracking include alkanes, alkenes and carboxylic acids. Soybean oil, cottonseed oil, rapeseed oil and other oils are successfully cracked with appropriate catalysts to get biodiesel [22]. By using this technique good flow characteristics were achieved due to reduction in viscosity. Disadvantages of this process include high equipment cost and need for separate distillation equipment for separation of various fractions. Also the product obtained was similar to gasoline containing sulfur which makes it less eco-friendly [22]. The mechanisms for the thermal decomposition of a triacylglyceride are given in Scheme 2.1 [23].

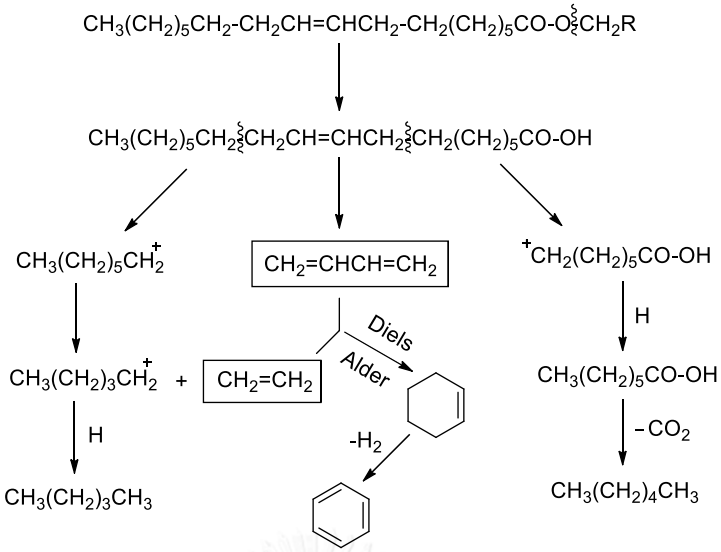

Scheme 2.1 The mechanism of thermal decomposition of triglycerides

2.2.3 Microemulsion

Microemulsion is another technique that has been reported to produce biodiesel and the components of a biodiesel microemulsion include diesel fuel, vegetable oil, alcohol, surfactant and cetane improver in suitable proportions [22]. Alcohols such as methanol, ethanol and propanol are used as viscosity lowering additives, higher alcohols are used as surfactants and alkyl nitrates are used as cetane improvers. Viscosity reduction, increase in cetane number and good spray characters encourage the usage of microemulsion but prolong usage causes problems like injector needle sticking, carbon deposit formation and incomplete combustion [22].

2.2.4 Transesterification (alcoholysis)

The most popular method of biodiesel production is the transesterification (also called alcoholysis). It is the reaction of vegetable oil or animal fat with an alcohol to form esters and glycerol. A catalyst is used to improve the reaction rate and yield. Excess alcohol is used to shift the equilibrium toward the product because of reversible nature of reaction. Transesterification using an alcohol is a sequence of three reversible consecutive steps as shown in Scheme 2.2 [24]. In the first step, triglycerides are converted to diglycerides. Then, diglycerides are converted to monoglycerides and

monoglycerides are converted to glycerin molecules at the last step. Scheme 2.3 shows the overall scheme for the transesterification of triglycerides [22].

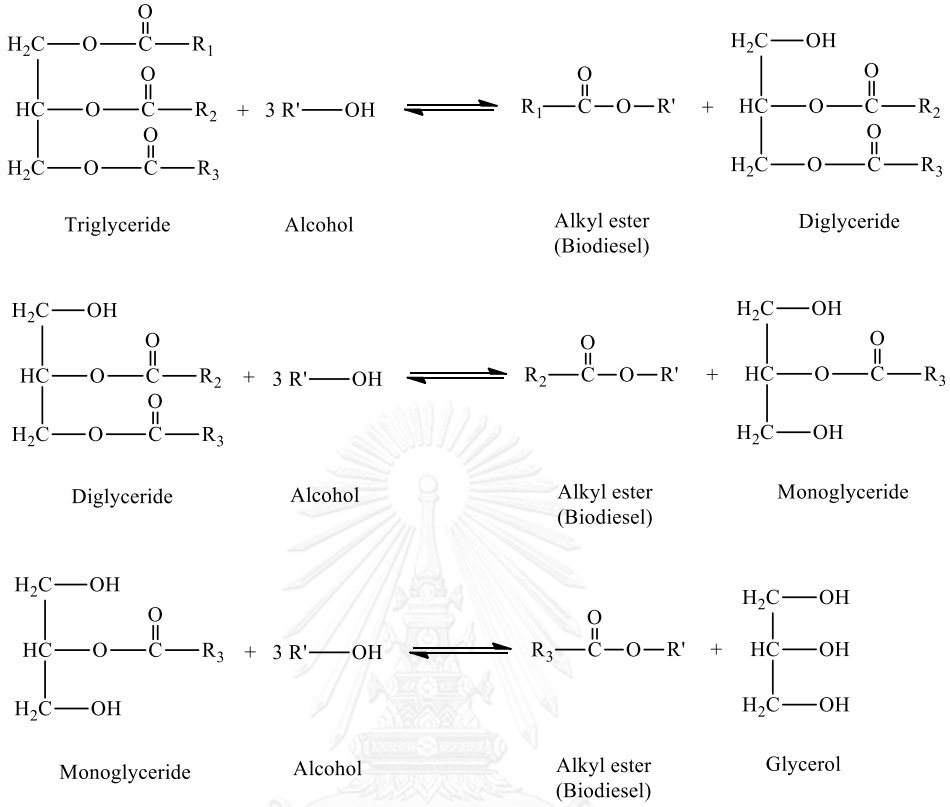

Scheme 2.2 Three reversible consecutive steps of transesterification with alcohol

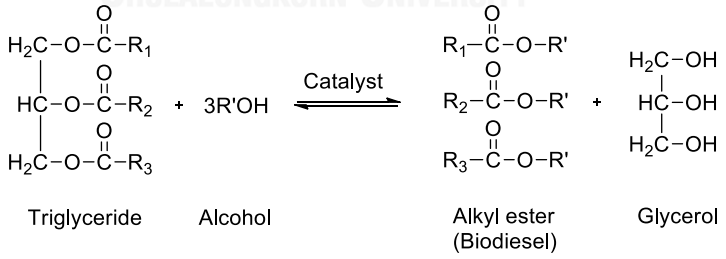

Scheme 2.3 Transesterification of triglycerides with alcohol

2.3 Advantages of biodiesel

There are many advantages of biodiesel including [25]:

• Biodiesel is not harmful to the environment. A car using biodiesel produces lower emissions of contaminants such as carbon monoxide, particulate matter, polycyclic aromatic hydrocarbons and aldehydes. So, the smoke becomes very clean indeed. If a vehicle uses traditional diesel, the vehicle emits black and stinky smoke.

• Biodiesel is lower health risk, due to reduced emissions of carcinogenic substances.

• Biodiesel can make the vehicle perform better. It is noted that biodiesel has a cetane number of over 51. Cetane number is used to measure the quality of the fuels ignition. If your fuel has a high cetane number, you can be sure that what you get is a very easy cold starting coupled with a low idle noise.

• Biodiesel can make your car last longer. Because of the clarity and the purity of biodiesel, you can be sure it will not have too many impurities to harm your car. It is actually more lubrication.

• Biodiesel may not require an engine modification. It is the only alternative fuel that can be used in a conventional diesel engine, without modifications. Some cars can take advantage of biodiesel without the need to undergo engine alterations. Some mix 20% biodiesel with regular diesel. Doing so enables the car to benefit from the good points of biodiesel without the hassle.

• Biodiesel reduces the environmental effect of a waste product because it is made entirely from vegetable sources, so it does not contain any sulfur, aromatic hydrocarbons, metals or crude oil residues.

• Biodiesel is a renewable fuel, obtained from vegetable oils or animal fats. You can even make biodiesel in your backyard. If your engine can work with biodiesel fuel alone, then you really need not go to the gas station to buy fuel. You can just manufacture some for your own personal use.

• Biodiesel is energy efficient. If the production of biodiesel is compared with the production of the regular type, producing the latter consumes more energy. Biodiesel does not need to be drilled, transported, or refined like petroleum diesel. Producing biodiesel is easier and is less time consuming.

2.4 Disadvantages of biodiesel

There are certain disadvantages of using biodiesel as a replacement for diesel fuel that must be taken into consideration [25, 26]:

• Slightly higher fuel consumption due to the lower calorific value of biodiesel.

• Due to the high oxygen content, it produces relatively high NO_x levels during combustion.

• Oxidation stability is lower than that of diesel so that under extended storage conditions it is possible to produce oxidation products that may be harmful to the vehicle components.

• Higher freezing point than diesel fuel. This may be inconvenient in cold climates.

• The kinematic viscosity is higher than diesel fuel. This affects fuel atomization during injection and requires modified fuel injection systems.

• It is less stable than diesel fuel and therefore long-term storage (more than six months) of biodiesel is not recommended.

It must be noted that these disadvantages are significantly reduced when biodiesel is used in blends with diesel fuel.

2.5 Source of Biodiesel

There are many possible raw materials with a potential to obtain biodiesel. Generally, the main feedstock for biodiesel production can be divided in: i) vegetable oils such as sunflower oil, soybean oil, rapeseed oil, jatropha oil, cotton seed oil, palm oil, canola oil and rice bran oil ii) animal fats such as tallow, pork lard, beef tallow, fish oil and chicken fat and iii) waste cooking oils and industrial waste oils. The source of

biodiesel in the form of vegetables oils, animal fats and some other biomass are listed in Table 2.1 [26].

Table 2.1 Source of oil

Vegetable Oils	Animal Fats	Other Sources
Soybeans	Lard	Bacteria
Rapeseed	Tallow	Algae
Canola	Poultry Fat	Fungi
Safflower	Fishoil	Micro algae
Barley		Tarpenes
Coconut		Latexes
Copra		Cooking Oil (Yellow Grease)
Cotton seed		Microalgae (Chlorellavulgaris)
Groundnut		
Oat		
Rice		
Sorghum		
Wheat		
Winter rapeseed oil		

2.6 Chemical composition of biodiesel

It is important to know that the quality and the properties of biodiesel are greatly influenced by the fatty acid composition of fats and oils used for its synthesis. Free fatty acids (FFAs) are the saturated or unsaturated monocarboxylic acids that occur naturally in fats, oils or greases, but FFAs are not attached to glycerol backbones. The different sources of oil have different fatty acid compositions. The fatty acids compositions depend on the number of carbon chain length and in the number of unsaturated bonds (double bonds). One mole of glycerol and three moles of fatty acids are commonly referred to triglycerides as shown in Scheme 2.4.

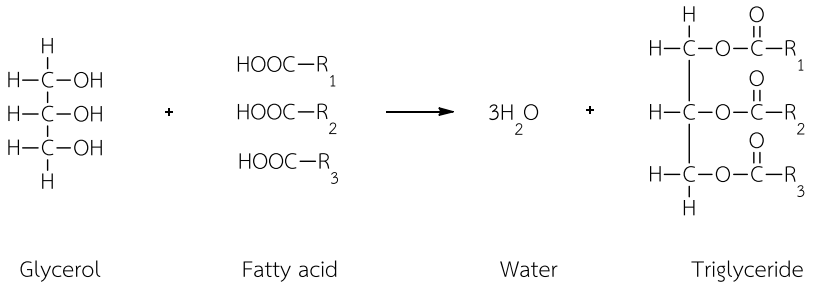

Scheme 2.4 Chemical structure of vegetable oil

The fatty acids are commonly found in vegetable oils such as stearic, palmitic, oleic, linoleic and linolenic. The structures of common fatty acids are given in Table 2.2 [27].

Table 2.2 The chemical structures of common fatty acids

Name of fatty acid	Structure	Chemical name of fatty acids	Formula
Lauric	12:0	Dodecanoic	$C_{12}H_{24}O_2$
Myristic	14:0	Tetradecanoic	$C_{14}H_{28}O_2$
Palmitic	16:0	Hexadecanoic	$C_{16}H_{32}O_2$
Stearic	18:0	Octadecanoic	$C_{18}H_{36}O_2$
Oleic *cis*-9-	18:1	Octadecenoic	$C_{18}H_{34}O_2$
Linoleic *cis*-9, *cis*-12-	18:2	Octadecadienoic	$C_{18}H_{32}O_2$
Linolenic	18:3	*cis*-9, *cis*-12, *cis*-15-Octadecatrienoic	$C_{18}H_{30}O_2$
Arachidic	20:0	Eicosanoic	$C_{20}H_{40}O_2$
Behenic	22:0	Docosanoic	$C_{22}H_{44}O_2$
Erucic	22:1	*cis*-13-Docosenoic	$C_{32}H_{42}O_2$
Lignoceric	24:0	Tetracosanoic	$C_{24}H_{48}O_2$

2.7 Soybean oil

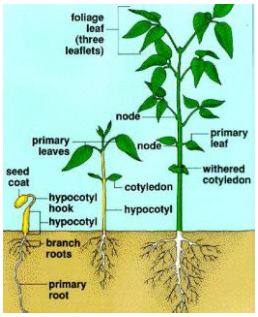

Figure 2.1 Soybean

Soybean is a major source of high quality protein and oil. Soybean seed quality is often determined by seed protein, oil, fatty acid and mineral content. Therefore, improving soybean seed quality is key to improving human and animal nutrition [28]. Soybean oil is a renewable raw material for a wide variety of industrial products, including inks, plasticizers, varnishes, resins, plastics and biodiesel.

There is a need for alternative energy sources to petroleum-based fuels due to the depletion of the world's petroleum reserves, global warming and environmental concerns. Biodiesel is a clean and renewable fuel which is considered to be the best substitution for diesel fuel. Its use reduces particle emissions, non-toxic, renewable and environmentally friendly. Soybean oil is one of the major feedstock for biodiesel production. The oil produced by soybeans is widely used by manufacturers of both food products and industrial manufactured goods. The physical properties of fatty acids vary with their chain length, unsaturation, other substituents and change with temperature. Soybean oil's properties should reflect its constituents, especially, its fatty acid composition and physical properties have frequently been measured for typical soybean oils, but there have been fewer measurements of soybean oils with modified fatty acid compositions [29].

Considerable potential exists for an expanded use of soybean oil as a renewable chemical feedstock. However, the physical and chemical properties of conventional soybean oil limit its use for many industrial applications. Soybean oil is a complex mixture of five fatty acids (palmitic, stearic, oleic, linoleic and linolenic acids)

that have vastly differing melting points, oxidative stabilities and chemical functionalities [30].

2.8 Alcohols used in biodiesel production

Alcohols can be used for biodiesel production such as methanol, ethanol, butanol and amylic alcohol. The most widely used alcohols are methanol (CH_3OH) and ethanol (C_2H_5OH) because of their low cost and properties. Methanol is often preferred to ethanol in spite of its high toxicity because its use in biodiesel production requires simpler technology; excess alcohol may be recovered at a low cost and higher reaction speeds are reached. The comparison between the two alcohols is summarized in Table 2.3 [25].

Table 2.3 Most important alcohols used in biodiesel production

Type of alcohol	Property
Methanol	Most widely used, in spite of its toxicity. It is a substance of petrochemical origin.
Ethanol	Less used, requires more complex production technology and the reaction speeds are lower. It can be produced from biomass.

2.9 Catalyst for biodiesel production

The catalytic for biodiesel production through transesterification is classified as (i) chemical catalyst such as acid (H_2SO_4) or base (NaOH and KOH) catalysts and (ii) enzymatic catalyst as indicated in Figure 2.2.

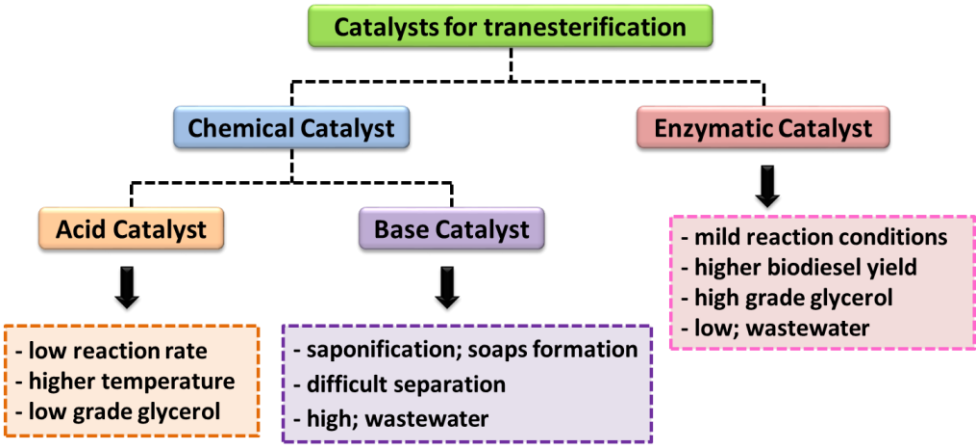

Figure 2.2 Schematic representation of catalytic for transesterification reaction

2.9.1 Acid catalyst

The acid catalysts are widely used such as sulfuric acid, hydrochloric acid and sulfonic acid. These catalysts give very high yields in alkyl esters, but the reactions are slow, temperatures above 100°C and more than 3 hours to reach complete conversion [24]. The mechanism of acid-catalyzed transesterification of vegetable oils as shown in Scheme 2.5 [31]. It can be extended to di- and triglycerides. In the first step, the protonation of the carbonyl group of the ester is change to the carbocation and a nucleophilic attack of the alcohol, which produces the tetrahedral intermediate. This intermediate eliminates glycerol to form the new ester and to regenerate the catalyst H^+ [32]. However, a large excess amount of alcohol makes the recovery of glycerol difficult. Post treatments are required after the completion of transesterification reaction as the end products are a mixture of esters, glycerol, mono and diacylglycerols, pigments, unreacted alcohol, catalyst and tri, di and monoglycerides. These post treatment include a multi-step purification of end products which include: (a) separation of glycerol by gravitational settling or centrifugation, (b) neutralization of the catalyst, (c) deodorization and (d) removal of pigments [33].

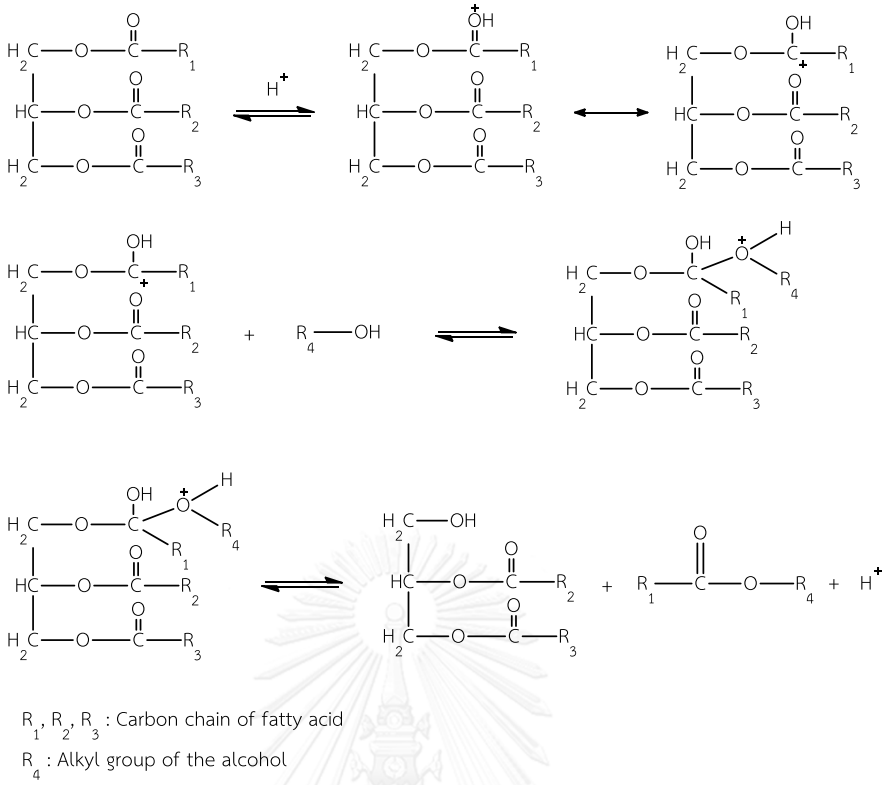

Scheme 2.5 Mechanism of the acid-catalyzed transesterification of vegetable oils

2.9.2 Base catalyst

The mechanism of base-catalyzed transesterification of vegetable oils was produced in three steps as shown in Scheme 2.6 [34]. The first step (Eq. 1) is the reaction of the base with the alcohol, producing an alkoxide and the protonated catalyst. Second step, the nucleophilic attack of the alkoxide at the carbonyl group of the triglyceride generates a tetrahedral intermediate (Eq. 2), from which the alkyl ester and the corresponding anion of the diglyceride are formed (Eq. 3). The latter deprotonates the catalyst, thus regenerating the active species (Eq. 4), which is now able to react with a second molecule of the alcohol, starting another catalytic cycle. Diglycerides and monoglycerides are converted by the same mechanism to a mixture of alkyl esters and glycerol. The most common base catalysts are sodium hydroxide (NaOH) and potassium hydroxide (KOH) [32, 35]. Other base catalysts include carbonates, methoxide, sodium ethoxide, sodium propoxide and sodium butoxide [36]. Advantages of base catalyst including easily react with alcohol to form the alkoxide

group lead to complete the reaction, higher conversion rate of esters under a low temperature, pressure environment and short reaction time for completion of the reaction [37]. However, base catalyzed transesterification needs a high purity feedstock. Triglycerides must contain the lower FFAs (free fatty acids) and alcohol must be anhydrous due to occurrence of water has effect to the reaction, which produces soap through saponification reactions as shown in Scheme 2.7 [38]. The soap formation consumes the catalyst and decreases the ester yields. Moreover, the soap formed during the reaction prevents glycerol separation from biodiesel. Besides, high amounts of water are needed in washing and consequent wastewater treatment of the effluent adds to the overall process cost.

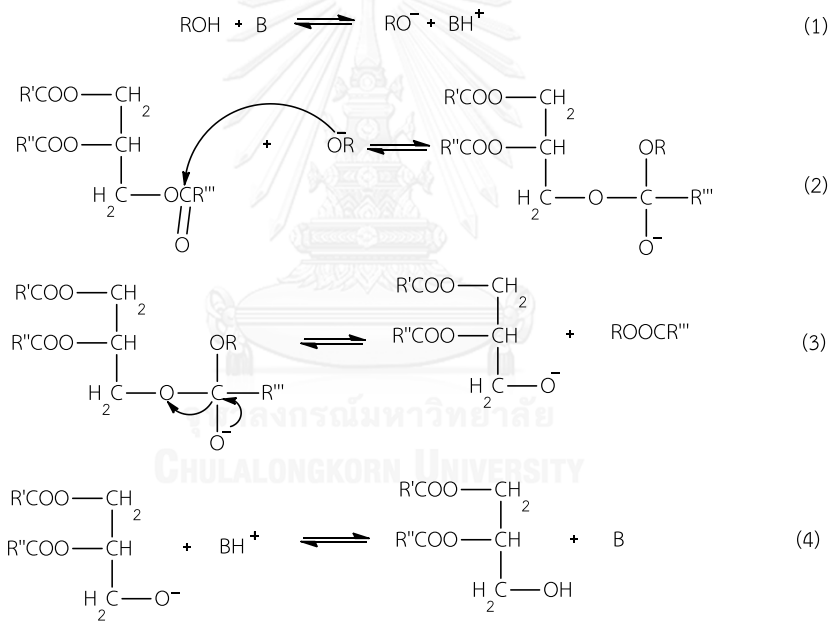

Scheme 2.6 Mechanism of the base-catalyzed transesterification of vegetable oils

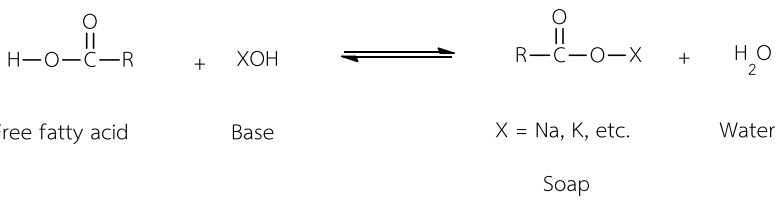

Scheme 2.7 Mechanism of saponification reactions

2.9.3 Enzymatic catalyst

To overcome problem associated with chemical process for biodiesel production, enzymatic process using lipase have been developed. Table 2.4 shows chemical and enzyme methods for biodiesel production [39].

Table 2.4 Comparison of chemical (alkaline and acid) and enzymatic process for biodiesel production

Parameter	Enzymatic process	Chemical process	
		Alkaline process	Acid process
FFA content in the raw material	FFA are converted to biodiesel	Soaps formation	FFA are converted to biodiesel
Water content in the raw material	It is not deleterious for lipase	Soaps formation Oil hydrolysis resulting more soaps	Catalyst deactivation
Biodiesel yield	High, usually around 90%	High, usually >96%	High yields (>90%) only for high alcohol to oil molar ratio, high catalyst concentration and high temperature
Reaction rate	Low	High	Slower than for alkaline process
Glycerol recovery	Easy, high grade glycerol	Complex, low grade glycerol	Complex, low grade glycerol
Catalyst recovery and reuse	Easy Reusability proved but not sufficiently studied.	Difficult; neutralized by an acid Partially lost in post-processing steps	Difficult, the catalyst ends up in the by-products No reusable catalyst
Energy costs	Low, Temperature: 20-50°C	Medium, Temperature: 60-80°C	High, Temperature: >100°C
Catalyst cost	High	Low	Low High cost of equipment due to acid corrosion
Environmental impact	Low; wastewater treatment not needed	High; wastewater treatment needed	High; wastewater treatment needed

Lipases (EC 3.1.1.3 triacylglycerol acylhydrolase) represent a group of water soluble enzymes that originally catalyze the hydrolysis of ester bonds in water insoluble lipid substrates, acting at the interface between the aqueous and the organic phases. Enzymatic action of lipases on the substrate is a result of a nucleophilic attack on the carbonyl carbon atom from ester groups [5]. Lipases are widely used to catalyze hydrolysis, alcoholysis, esterification and transesterification process during biodiesel production. Enzyme catalysts have become more attractive recently since it can avoid soap formation and the purification process is simple to accomplish. However, lipases are less often used commercially because of the longer reaction times and higher cost. To reduce the cost, some researchers developed new biocatalysts. An example is so called whole cell biocatalysts which are immobilized within biomass support particles. The optimal parameters for the use of a specific lipase depend on the origin as well as the formulation of the lipase. The advantages and disadvantages of using enzymes are displayed in Table 2.5.

Table 2.5 The advantages and disadvantages of using enzymes

Advantages	Disadvantages
They are **specific in their action** and are therefore **less likely to produce unwanted by-products**.	They are **highly sensitive to changes in physical and chemical conditions** surrounding them.
They are **biodegradable** and therefore **cause less environmental pollution**.	They are **easily denatured** by even a small increase in temperature and are **highly susceptible to poisons and changes in pH**. Therefore the **conditions in which they work must be tightly controlled**.
They **work in mild conditions**, i.e. low temperatures, neutral pH and normal atmospheric pressure, and therefore **are energy saving**.	The enzyme substrate mixture **must be uncontaminated with other substances** that might affect the reaction.

The classification of lipase on the basis of the sources obtained from microorganism, animal and plant. Lipases can be produced in high yields from microorganisms such as bacteria and fungi. In practice, microbial lipases are commonly used by the industry. The selection of a lipase for lipid modification is based on the

nature of modification sought, for instance, position-specific modification of triacylglycerol, fatty acids specific modification, modification by hydrolysis, and modification by synthesis (direct synthesis and transesterification). The literature survey showed the use of lipases from some of the following sources. Microbial lipases are derived from *Aspergillus niger*, *Bacillus thermoleoVorans*, *Candida cylindracea*, *Candida rugosa*, *Chromobacterium Viscosum*, *Geotrichum candidum*, *Fusarium heterosporum*, *Fusarium oxysporum*, *Humicola lanuginose*, *Mucor miehei*, *Oospora lactis*, *Penicillium cyclopium*, *Penicillium roqueforti*, *Pseudomonas aeruginosa*, *Pseudomonas cepacia*, *Pseudomonas fluorescens*, *Pseudomonas putida*, *Rhizopus arrhizus*, *Rhizopus boreas*, *Rhizopus thermosus*, *Rhizopus usamii*, *Rhizopus stolonifer*, *Rhizopus fusiformis*, *Rhizopus circinans*, *Rhizopus delemar*, *Rhizopus chinensis, Rhizopus japonicus* NR400, *Rhizopus microsporus*, *Rhizomucor miehei*, *Rhizopus nigricans*, *Rhizopus niveus*, *Rhizopus oryzae*, *Rhizopus rhizopodiformis*, *Rhizopus stolonifer* NRRL 1478, *Rhodotorula rubra* and *Staphylococcus hyicus*, to name a few. Animal sources are from pancreatic lipases and plant lipases are from papaya latex, oat seed lipase and castor seed lipase. Several commercial lipases used in free form for biodiesel production are listed in Table 2.6 [40, 41].

Table 2.6 Commercial lipase powders used for biodiesel production

Lipase origin	Substrate (S)	Acyl acceptor (A)	S:A ratios	Temp. (°C)	Time (h)	Yield [%]	Ref.
Pseudomonas cepacia	Jatropha oil	Ethanol	1:4	50	8	98	[17]
Pseudomonas cepacia	Soybean oil	Methanol	1:7.5	35	1	67	[19]
Pseudomonas cepacia	Soybean oil	Methanol	1:3	35	90	80	[42]
Pseudomonas cepacia	Mahua oil	Ethanol	1:4	40	24	80	[43]
Pseudomonas cepacia	Palm kernel oil	Ethanol	1:4	40	8	72	[44]
Candida cylindracea	Palm oil	1-butanol	1:4	37	8	96	[45]
Chromobacterium viscosum	Jatropha oil	Ethanol	1:4	40	8	92	[46]
Mucor miehei	Sunflower oil	Ethanol	1:3	30	5	83	[47]
Rhizopus orzyae	Waste Cooking Oils	Methanol	1:4	40	24	92	[48]
Thermomyces lanuginosus	Soybean oil	Ethanol	1:7.5	31.5	7	96	[49]

2.10 Lipase from *Pseudomonas cepacia*

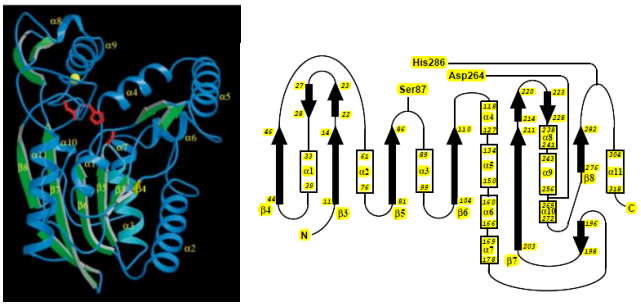

Figure 2.3 A ribbon diagram of *Pseudomonas cepacia* lipase [50]

The structures of lipases from diverse sources are ranging from microbes (including fungi, yeast and bacteria) to enzymes. In the large part all conform to the α/β-hydrolase fold [50]. All of these structures clearly showed these lipases to be serine hydrolases with catalytic triads resembling those of serine proteases. The first three-dimensional structures of lipases was revealed that the active sites were occluded by surface loops and clearly indicated the necessity of a conformational change to expose the catalytic site [51-53].

Figure 2.3 shows a ribbon diagram of *Pseudomonas cepacia* lipase along with a schematic of the topology of the protein [54]. Many of the features of the α/β-hydrolase fold are maintained. The central β sheet in the core of the molecule conforms to strands β_3–β_8 of the α/β-hydrolase fold [55]. Throughout this report the β strands will be numbered to be consistent with the numbering of the consensus α/β-hydrolase fold, so the first strand is named β_3. The active-site Ser87 lies at the C-terminal end of strand β_5 in the strand-turn-helix motif described previously [55, 56]. The main chain takes a sharp turn at Gly110, located at the C-terminal end of strand β_6. Strand β_7 is the longest strand in the β sheet and its N-terminal half forms hydrogen bonds to strand β_6 in a parallel manner. The C-terminal half of strand β_7 hydrogen bonds to both strands β_6 and β_8 in a pattern typical of parallel β strands. This hydrogen-bonding pattern is disrupted by a bulge at Leu278 in strand β_8. The catalytic acid, Asp264, is part of a loop which follows strand β_7 and the triad histidine, His286, is located in a loop following strand β_8. There are 11α helices, of which four pack against the central β sheet. The active site is comprised of Ser87, His286 and Asp264, which form a number of hydrogen bonds.

Pseudomonas cepacia lipase or called *Burkholderia cepacia* lipase has been also known under its commercial trade name as *P. cepacia* lipase. It has been recently proven to be among the most versatile lipases [57]. A recent report has screened lipases form large number of sources and identified *Pseudomonas cepacia* lipase as most promising for transesterification [19, 58]. This lipase was used for immobilized onto various supports with different methods such as the lipase from *Pseudomonas cepacia* was entrapped within a sol-gel polymer matrix, which prepared by

polycondensation of hydrolyzed tetramethylorthosilicate and iso-butyltimethoxysilane [19], adsorption on celite [17] or covalent binding method by crosslinked with polyacrylonitrile (PAN) nanofibrous membrane [18]. However, Lipase PS catalyst can produced high yield of biodiesel through transesterification reaction and was able to use in range of temperature is 30 to 50°C [59].

2.11 Immobilization of enzymes

The term “immobilized enzymes” refers to “enzymes physically confined or localized in a certain defined region of space with retention of their catalytic activities and which can be used repeatedly and continuously” [4]. Immobilization of lipases on solid supports offers several advantages, including simple recovery allowing repeated use of the catalyst, easy separation of enzyme from product, possibility of continuous operation and improvement of enzyme stability. The introduction of immobilized catalysts has greatly improved both the technical performance of the industrial processes and their economy as shown in Table 2.7 [4]. Besides, the immobilization techniques are the basis for making a number of biotechnological products with applications in diagnostics, bio-affinity chromatography and biosensors.

Table 2.7 Technological properties of immobilized enzyme systems

Advantages	Disadvantages
1. Enzyme can be recovered and reused	1. Immobilization may alter shape of enzyme
2. Easier reactor operation	2. Loss or reduction in activity
3. Easier to separate enzyme and products	3. Enzyme may become detached
4. Wider choice of reactor	4. Diffusional limitation
5. Allows catalysis in unfavorable media	5. May alter catalytic ability
6. Increased operational stability of the enzyme and can be manipulated easily	6. Expensive
7. Allows continuous production/enzyme used for longer	
8. Enzyme does not contaminate product/no purification required	

2.11.1 Choice of Supports

In the enzyme immobilization process, the appropriate type of support is the key factor for immobilization. The properties of immobilized enzymes are governed by the properties of both the enzyme and the support material. Supports can be classified as organic and inorganic. The organic supports can be divided into natural and synthetic polymers, according to their chemical composition as shown in Table 2.8 [9].

Table 2.8 Classification of supports

Supports	Advantages	Disadvantages	Samples
Organic			
Organic support from natural sources	Good compatibility with enzymes	Poor binging, weak mechanical stability	• Polysaccharides: cellulose, dextrans, agar, agarose, chitin, alginate • Proteins: collagen, albumin • Carbon
Organic synthetic supports	Custom-made supports	Solid-liquid mass transfer, diffusion limitation	• Polystyrene • Synthetic polymers: polyacrylate, polymethacrylates, polyacrylamide, polyamides, vinyl and allyl polymers
Inorganic			
Natural minerals	Greater stability than organic supports	Abrasion can occur in stirred vessels	• Bentonite, silica and silica derivatives, celite, aluminum based supports
Processed materials			• Glass (non-porous and controlled pore), metals, controlled pore metal oxides

1. Organic support

1.1 Naturally occurring organic support

Natural organic polymers are cheap starting materials for the production of support materials and are available in large quantities such as structural proteins (ceratin, collagen), globular proteins (albumin) or carbohydrates. From this group,

carbohydrates are of special interest because it does not suffer from biological safety aspects like protein matrices isolated from animal sources and because it is highly hydrophilic which provides a desirable microenvironment for many enzymes. Alginate, acidic gelation, carrageenan, chitin or chitosan (prepared from chitin by deacetylation) are particularly useful for encapsulating microorganisms by ionotropic. Enzymes have been linked to carbohydrates simply by adsorption followed by cross-linking [59].

Chitosan is of importance because of its primary amino groups that are susceptible for coupling reactions. Furthermore, porous spherical chitosan particles are commercially available allowing non-covalent or covalent attachment of enzymes. This support matrix can be easily prepared and activation methods have been summarized [60].

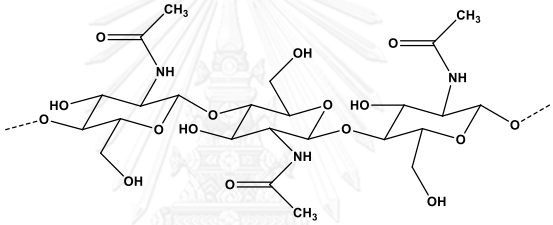

Chitin

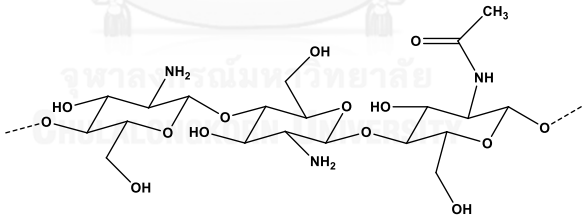

Chitosan

Figure 2.4 Schematic representations of the chemical structures of the chitin and chitosan

1.2 Synthetic organic support

Organic synthetic supports are widely used as immobilization supports. Synthetic organic polymers display the greatest variability with regard to physical and chemical characteristics. The main synthetic polymers are polystyrene, polyacrylate, polyvinyls, polyamide, polypropylene, polyaldehyde and polypeptide structures. The

immobilization in this way is not covalently bound, so the enzyme can be leached from the support in an aqueous medium. It is disadvantage of this immobilization support.

Polystyrene was the first synthetic polymer used for enzyme immobilization. Binding occurred mainly by adsorptive forces. Usually, binding of the enzyme is favored at low salt conditions. However, the hydrophobicity of the matrix often leads to partial enzyme denaturation during the binding process, so it is low activity yields.

2. Inorganic support

Inorganic supports often obtain a greater stability than organic supports, due to the higher inertness to the reaction conditions like high pressure and temperature. Frequently used inorganic supports (glass, silica gel, silica derivatives, celite, bentonite, hydroxyapatite, nickel/nickel oxide, titania, zirconia, aluminum based supports) have been extensively studied and developments have led to the application on both laboratory and industrial scale. It often show good mechanical properties, thermal stability, resistance against microbial attack and organic solvents. On the other hand, non-porous materials like metal and metal oxides only have small binding surfaces. Minerals usually display a broad distribution of pore size.

2.11.2 Methods of immobilization

There are several methods for lipase immobilization. Methods for enzyme immobilization can be classified as carrier binding and encapsulation. Immobilization techniques of lipases used as catalysts in biodiesel production are summarized in Figure 2.5. These immobilization methods have been used to improve lipase stability for biodiesel production and this is discussed in the following sections.

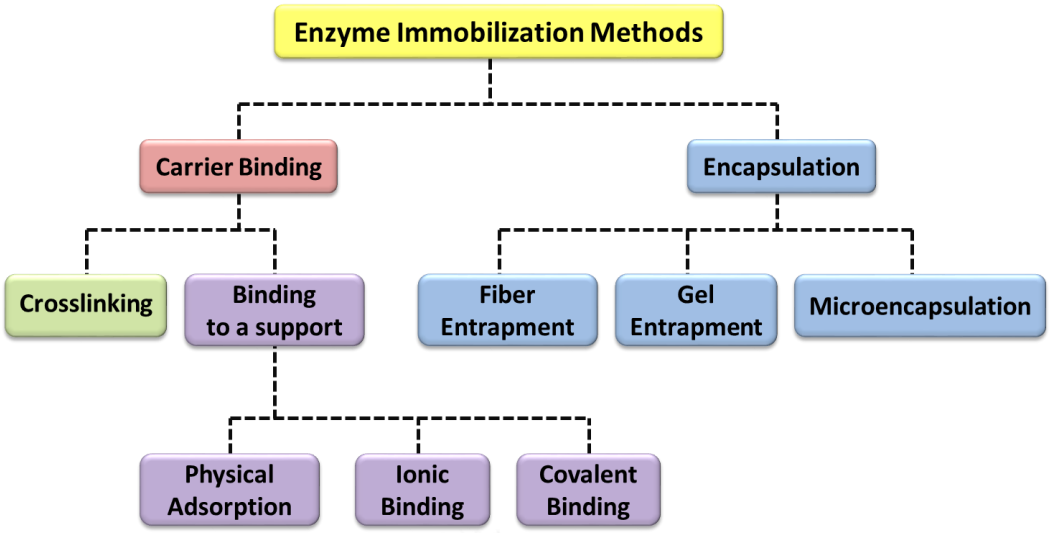

Figure 2.5 Schematic representation of the main different methods of enzyme immobilization

1. Carrier binding

1.1 Crosslinking

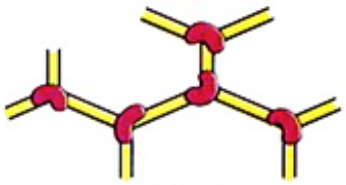

Figure 2.6 Shows pictorial representation of crosslinking between molecules of enzyme

The crosslinking method is based on the formation of covalent bonds between the enzyme and active molecules. In Figure 2.6 shows crosslinking method between molecules of enzyme [61]. The individual biocatalytic units (enzymes, organelles, whole cells) are joined to one another with the help of bi- or multifunctional reagents. The reagents used include glutardialdehyde, glutaraldehyde, glyoxal, diisocyanates, hexamethylene diisocyanate and toluene diisocyanate. The most commonly used being gluteraldehyde. The advantages and disadvantages of a given matrix must be taken into account when considering the appropriate procedure for a given enzyme

immobilization. One advantage is the simplicity of the process. The main disadvantages are the fragility of the particles produced in some cases and diffusion limitations. Since crosslinking and co-crosslinking usually involve covalent bonds, immobilized biocatalysts in this way frequently undergo changes in the conformation with a resultant loss of activity.

1.2 Binding to a support

Physical adsorption is a simple and straightforward route for enzyme immobilization, in which the enzyme is bound to a support by hydrophobic, van der Waals or ionic interactions. It is often used because of the ease and low cost of the procedure. A support is added to an enzyme solution and after a few hours of mixing the enzyme-support complex is ready. Secondly, physical adsorption is reversible that enables the reuse of the support. Denatured enzymes can be removed from the support by changes in pH or ionic strength of the reaction medium and it can be replaced with fresh enzyme. However, hydrophobic and van der Waals bonding is generally too weak to keep the enzyme fixed to the support under industrial conditions of high reactant and product concentrations and high ionic strength. Therefore, the leaking of enzyme upon use can be expected, not all of the enzyme can be reused, and the product might have to be purified. On the other hand, ionic and covalent binding are generally stronger due to the firm bonding between the enzyme and the support, which have the advantages that the biocatalysts do not suffer from desorption or leaching of enzymes during catalytic reactions. Nevertheless, enhancement of the bond strength between the enzyme and the support can cause changes in the enzyme conformation, often into a less favorable one, which can result in deactivation of the enzyme. Moreover, if the enzyme is deactivated (or denatured), both enzyme and the support remained unusable.

1.2.1 Physical adsorption

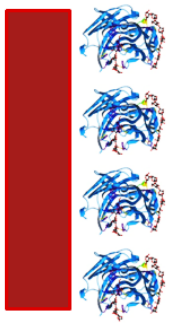

Figure 2.7 Shows pictorial representation of physical adsorption

Immobilization by physical adsorption is a simple method of preparing an immobilized enzymes and the support materials. Physical adsorption between enzymes and supports process is shown in Figure 2.7 [62]. Most of the support materials available have sufficient surface-charge properties suitable for immobilization by adsorption. Several different supports were used for the physical adsorption of lipases such as natural organic carriers (chitosan, dextran, gelatin, cellulose, starch), organic synthetic carriers (nylon, polyethylene, polypropylene, polystyrene) and inorganic carriers (ceramic, alumina, activated carbon, kaolinite, bentonite, porous glass) [63]. This method is cheap, easy for use and least expensive technique to prepare solid-support biocatalysts. The interactions formed between the enzyme and the support material will be dependent on the existing surface chemistry of the support and on the type of amino acids exposed at the surface of the enzyme molecule. The interaction between the enzyme and the surface of the matrix arises from weak forces by van der Walls, hydrophobic interactions, and hydrogen bonds. The method consists of simply mixing an aqueous solution of enzyme with the support material for a period of time, after which the excess enzyme is washed away from the immobilized enzyme on the support. The activity of physically adsorbed enzymes is strongly dependent on the pH of the solution and working temperature. The main advantages of adsorption are the method simplicity, the little effect on the conformation/activity of the biocatalyst and the possibility of regenerating inactive enzyme by addition of fresh enzyme. The main disadvantage is a weak binding force between the carrier and the enzyme, so enzyme can easily be desorbed from the carrier. The enzyme desorption

can easily occur by changes in the environment medium such as pH, temperature, solvent and ionic strength or in the case of extended reactions [64]. This is the main reason why the immobilization of lipases by adsorption is not the best solution for industrial application.

1.2.2. Ionic binding

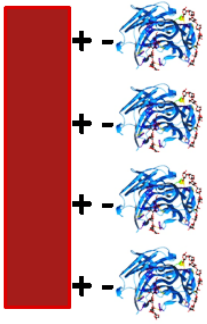

Figure 2.8 Shows pictorial representation of ionic binding

Ionic binding is another simple non-covalent immobilization technique as shown in Figure 2.8 [62]. In this method, the amount of enzyme bound to the carrier and the activity after immobilization depends on the nature of the carrier. The main difference between ionic binding and physical adsorption is the strength of the interaction, which is much stronger for ionic binding, although less strong than covalent binding. The preparation of immobilized enzymes using ionic binding is based on the same procedure as described for physical adsorption [65]. The ionic nature of the binding forces between the enzyme and the support also depends on pH variations, support charge, enzyme concentrations and temperature. The supports used for ionic binding may be based on polysaccharide derivatives (e.g., diethylaminoethylcellulose, dextran, chitosan), synthetic polymers (e.g., polystyrene derivatives, polyethylene vinylalcohol) and inorganic materials (e.g., ambertite, alumina, silicates, bentonite, sepiolite, silica gel) [63]. The immobilization by ionic binding has the advantage that changes in the enzyme conformation only occur in a small extent, resulting in immobilized enzymes with high enzymatic activities. The main disadvantage is the possible interference of other ions, and special attention should be paid in maintaining the correct ionic strength and pH conditions in order to prevent their easy detachment.

1.2.3. Covalent binding

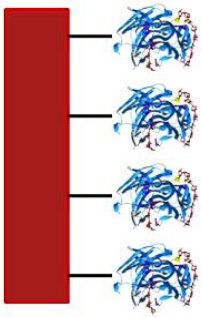

Figure 2.9 Shows pictorial representation of covalent binding

Covalent binding is the most widely used method for enzyme immobilization. It can be achieved by direct attachment with the enzyme and the material through the covalent linkage. The covalent linkage is strong and stable of the bonds formed between enzyme and matrix as shown in Figure 2.9 [63]. The enzyme is not released into the solution upon use. In addition, covalent immobilization offers the greatest advantages by increasing the stability of the enzyme and preventing it from leaking into solution. The bond is normally formed between a functional group present on the support surface and amino acid residues on the surface of the enzyme. There are numerous inorganic and organic supports available for lipase immobilization, including porous alumina, metallic oxides, stainless steel, and controlled pore glass (CPG), cellulose, starch, chitin and synthetic polymers. This covalent binding of the enzyme with the support material involves two main steps: (i) the activation of the support material by the addition of the reactive compound and (ii) the second one is the modification of the polymer backbone to activate the matrix**.** The activation step produces the electrophilic group on the support material, so that the support material couples/reacts with the strong nucleophiles on the proteins. The covalent bond is usually formed by using active bridge molecules such as CNBr, and bi- or multifunctional reagents. For example glutaraldehyde in this reaction the amine group reacts with the activated matrix to give imine.

2. Encapsulation

(a) (b) (c)

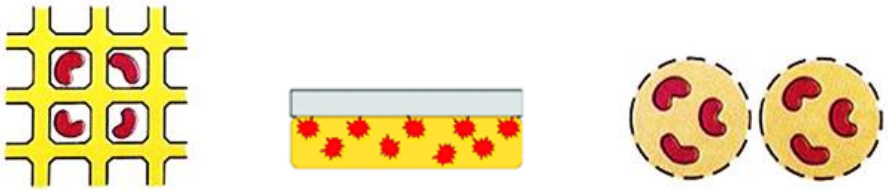

Figure 2.10 Shows pictorial representation of encapsulation in a fiber entrapment (a), gel entrapment (b) and microencapsulation (c) ionic binding

The encapsulation method can be achieved by film, gel, fiber entrapping and microencapsulation as shown in Figure 2.10 [61]. This method can be achieved by mixing an enzyme or active molecule with a polymer and then crosslinking the polymer to form a lattice structure that traps the enzyme [66]. This method can be carried out by using natural polymers (alginate and carrageenan), synthetic polymers (photo-cross linkable resins and polyurethane polymers), acrylic polymers, hydrogels, microemulsion based gels and those obtained by sol-gel methods. Lipases immobilized by entrapment are more stable than physically adsorbed lipase. Entrapment of lipase includes capture of the lipase within a matrix of a polymer. Microencapsulation method is that the enzyme molecules are capsulated within spherical semipermeable membranes with a selective controlled permeability. Microencapsulated enzymes are formed by enclosing enzymes solution within spherical semipermeable polymer membranes with controlled porosity. This method provides the large surface area between polymeric material and the enzyme. The drawback of this method is inactivation of enzyme during encapsulation [66]. The advantages of this immobilization method are the extremely large surface area between the substrate and the enzyme, fast, cheap, mild conditions required for reaction process, within a relatively small volume and the real possibility of simultaneous immobilization. However, with the increase of the substrate concentration limitation by diffusion occurs. The solution is to produce an

encapsulated enzyme with smaller size to overcome the mass transfer problems and to use the enzymes of highest purity.

The choice of the most appropriate technique also depends on the nature of the enzyme (biochemical and kinetics properties) and the carrier (chemical characteristics, mechanical properties). Therefore, the interaction between the enzyme and support provides an immobilized enzyme with particular biochemical and physicochemical properties that determine their applicability to specific processes. A comparison of these different immobilized methods is summarized in Table 2.9.

Table 2.9 Comparison of different enzyme immobilization methods

Methods and binding nature	Advantages	Disadvantages
Crosslinking		
Enzymes molecules are cross-linked by a functional reactant. E.g. cellulose or glyceraldehyde	- Biocatalyst stabilization - The interaction between the lipase and the carrier is strong and the immobilized lipase is stable.	- Cross-linked biocatalysts are less useful for packed beds. - Mass transfer limitations - Loss of activity - The cross-linking conditions are intense and the mechanical strength of the immobilized lipase is low.
Physical adsorption		
Enzyme is attached to the outside of an inert material. Weak bonds: hydrophobic, Van der Waals or ionic interactions	- Simple and cheap - Little conformational change of the enzyme - Preparing conditions are mild and easy with low cost. The carrier can be regenerated for repeated use.	- Desorption - Nonspecific adsorption - The interaction between the lipase and the carrier is weak, so the immobilized lipase was sensitive to pH, ionic strength and temperature etc. The adsorption capacity is small and the protein might be stripped off from the carrier.
Covalent binding		
Chemical binding between functional groups of the enzyme and support	- No enzyme leakage - Potential for enzyme stabilization - The immobilized lipase is rather stable because of the strong forces between the protein and the carrier.	- Matrix and enzyme are not regenerable - Major loss of activity - The preparation conditions are rigorous, so the lipase might lose its activity during the immobilized process. Some coupling reagents are toxic.
Encapsulation		
Enzyme is held in a mesh or capsule of an inert material. Occlusion of an enzyme within a polymeric network	- Wide applicability - The entrapment conditions are moderate and the immobilized method is applicable to a wide range of carrier and lipases.	- Mass transfer limitations - Enzyme leakage - This immobilized lipase always has the mass transfer restriction during the catalytic process, so the lipase is only effective for low molecular weight substrates.

2.12 Literature review

In 2002, Kose and coworkers [67] studied transesterification of cotton seed oil with primary and secondary alcohols. The immobilization of lipase from *Candida antarctica* (Novozym 435) in solvent-free medium was used as a catalyst. The optimum conditions of the methanolysis were as follows 30% enzyme based on oil weight, 1:4 oil/alcohol molar ratio and 7 hours reaction time at 50°C. Maximum methyl esters yield was 91.5%. At the same conditions cotton seed oil was converted with short-chain primary and secondary alcohols to its corresponding esters with conversions between 72% and 94%, respectively. The results indicated that alcoholysis products of cotton seed oil could be used as valuable intermediates for the oleochemical industry.

In 2003, Hung and coworkers [68] studied immobilization of *Candida rugosa* lipase on chitosan beads. Lipase was immobilized to chitosan beads by a binary method in which lipase was first immobilized to the hydroxyl groups of chitosan activated with carbodiimide (EDC) followed by cross-linking more lipase to the amino groups of chitosan using glutaraldehyde. Binary immobilization method yielded the highest protein loading and activity of 287.2 μg/g-chitosan and 13.8 U/g-chitosan, respectively. The activity is highest in comparison with the immobilized lipase prepared by activation with EDC (4.3 U/g-chitosan) and by cross-linking with glutaraldehyde (6.98 U/g-chitosan). The protein coupling and activity yields were 25.2 and 91.5%, respectively. Immobilized lipase retained 74% residual activity after ten hydrolysis cycles and 67% after 7 days of storage.

In 2005, Noureddini and coworkers [19] studied enzymatic transesterification of soybean oil with methanol and ethanol using immobilized lipase from *Pseudomonas cepacia* as catalyst. Lipase from *Pseudomonas cepacia* was immobilized by entrapment within a sol-gel structure which was prepared by polycondensation of hydrolyzed tetramethoxysilane (TMOS) and iso-butyltrirnethoxysilene (iso-BTMS). The effects of enzyme loading, water concentration, alcohol concentration and temperature in the transesterification reaction were investigated. The optimal conditions for processing 10 g of soybean oil were 475 mg lipase for the reactions with

methanol, 0.5 g water and 1:7.5 oil/methanol molar ratio at 35°C and 475 mg lipase for the reactions with ethanol, 0.3 g water and 1:15.2 oil/ethanol molar ratio at 35°C. This reaction can be produce methyl and ethyl esters formation of 67 and 65 mol% in 1 hour of reaction. The triglycerides reached negligible levels after the first 30 min of the reaction and the immobilized lipase was consistently more active than the free enzyme toward the transesterification of soybean oil. The immobilized lipase also proved to be stable and lost little activity when was subjected to repeated uses.

In 2007, Royon and coworkers [69] studied enzymatic production of biodiesel from cotton seed oil with *t*-butanol as a solvent using immobilized lipase from *Candida antarctica* (Novozyme 435) as catalyst. It was found that enzyme inhibition, caused by undissolved methanol, was eliminated by adding *t*-butanol to the reaction medium, which also gave a noticeable increasing of reaction rate and ester yield. The effect of *t*-butanol and methanol concentrations and temperature on this system was determined. A 97% yield of methanolysis was observed from a reaction mixture containing 32.5% *t*-butanol and 13.5% methanol, 54% oil and 0.017 g enzyme after 24 hours at 50°C.

In 2008, Halim and Kamaruddin [70] studied transesterification to produce fatty acid methyl ester (FAME) from waste cooking palm oil (WCPO) in a *tert*-butanol system. *Candida antarctica* lipase B immobilized on acrylic resin (Novozyme 435) was used as biocatalyst. Biodiesel production of WCPO with methanol was successfully carried out in *tert*-butanol as the reaction medium, which eliminated both negative effect caused by excessive methanol and glycerol as the byproduct. The optimum conditions for this reaction were 1:4 oil/methanol molar ratio, 4% Novozyme 435 based on oil weight, 200 rpm and 12 hours reaction time at 40°C. Transesterification of WCPO can reach up to 88% FAME yield under optimum condition.

In 2008, Dizge and Keskinler [71] studied enzymatic production of biodiesel from canola oil using immobilized lipase. In the present work, lipase from *Thermomyces lanuginosus* was immobilized in polyurethane foams by using polyglutaraldehyde as a cross-linking agent. The immobilized lipase was used as catalyst for biodiesel production through transesterification reaction of canola oil with

methanol. The optimum pH for free and immobilized enzyme were 6, resulting in 80% immobilization yield. The effects of enzyme loading, oil/alcohol molar ratio, water concentration and temperature in the transesterification reaction were investigated. The optimal conditions were 20 g canola oil, 430 μg immobilized lipase, 1:6 oil/methanol molar ratio (three-step addition), 0.1 g water at 40°C for 24 hours. The highest methyl esters yield was 90% of which enzymatic activity remained after 10 batches, when *tert*-butanol was adopted to remove by product glycerol during repeated use of the lipase. The immobilized lipase proved to be stable and lost little activity when was subjected to repeated uses.

In 2009, Dizge and coworkers [72] studied methanolysis of canola oil with methanol and using immobilization of lipase from *Thermomyces lanuginosus* as catalyst. This lipase was immobilized onto styrene-divinylbenzene (STY-DVB) copolymer and STY-DVB copolymer containing polyglutaraldehyde (STY-DVB-PGA). Lipase from *T. lanuginosus* was immobilized with 60% and 85% yield on the hydrophobic microporous STY-DVB and STY-DVB-PGA copolymer, respectively. Therefore, Lipase from *T. lanuginosus* was immobilized onto STY-DVB-PGA copolymer as catalyst for transesterification. Biodiesel production using the latter lipase preparation was realized by a three-step addition of methanol to avoid strong substrate inhibition. Under the optimized conditions were 92 g canola oil, 1 g immobilized lipase onto STY-DVB-PGA copolymer, 1:6 oil/methanol molar ratio at 50°C for 24 hours. The highest methyl esters yield was 97%. Lipase immobilized onto STY-DVB-PGA copolymer retained its activity during 10 batch reactions.

In 2009, Nasratun and coworkers [73] studied immobilization of lipase from *Candida rugosa* on chitosan beads for transesterification reaction of cooking oil. The porous bead of chitosan was used for immobilization of lipase from *Candida rugosa* by physical adsorption. The effect of reaction time and oil to methanol molar ratios were studied to compare the transesterification performance between free lipase and immobilized lipase. The experiment results show that the maximum conversion of ester using immobilized lipase and free lipase were 71.25 and 76.5%, respectively which was obtained at conditions of 1:4 oil/methanol molar ratio at 40°C for 48 hours.

However, the conversion of ester for free lipase was higher than ester conversion of immobilized lipase on transesterification reaction. On the other hand, immobilized lipase was provided an important advantage such as easy separation from the product and has a high potential to reuse.

In 2012, Egwim and coworkers [74] studied optimization of lipase immobilized on chitosan beads for biodiesel production. The optimum lipase loading, immobilization time and concentration of immobilized enzyme were determined. The effect of pH, reaction temperature, reaction time, operational and storage stabilities were studied. The optimal immobilization conditions were enzyme loading 0.2 g/g chitosan, temperature of 40ºC, pH of 7.0, oil/methanol molar ratio of 1:4, amount of beads of 2 g and immobilization time of 3 hours. Thermal, operational and storage stabilities of the enzyme were found to improve after immobilization. In conclusion, optimization of immobilization conditions was found to offer additional advantage on enzyme activity.

In 2012, Xie and Wang [75] studied immobilized lipase from *Candida rugosa* on magnetic chitosan microspheres for transesterification of soybean oil with methanol. The magnetic chitosan microspheres were prepared by the chemical co-precipitation approach using glutaraldehyde as cross-linking reagent for lipase immobilization. The immobilization of lipase onto the magnetic particles was confirmed by magnetic measurements, transmission electron microscopy (TEM) and Fourier transform infrared (FT-IR) spectra. The optimal conditions were 1:4 oil/methanol molar ratio (three step addition) at 35°C for 30 hours. The highest methyl esters yield was 87%. The obtained results showed that the conversion to methyl esters was decreased to 85%, 83%, 78% and 72% after 1, 2, 3 and 4 cycles, respectively. Thus, the immobilized lipase could be used for four times without significant decrease of the activity.

In 2012, Kuo and coworkers [76] studied lipase immobilization on chitosan-coated Fe_3O_4 nanoparticles. Magnetic Fe_3O_4-chitosan nanoparticles are prepared by the coagulation of an aqueous solution of chitosan with Fe_3O_4 nanoparticles. The Fe_3O_4-chitosan nanoparticles are used for the covalent immobilization of lipase from *Candida rugosa* using N-(3-dimethylaminopropyl)-N-ethylcarbodiimide (EDC) and

Nhydroxysuccinimide (NHS) as coupling agents. The optimum conditions were immobilization time 2.14 hours, pH 6.37 and enzyme/support ratio 0.73 (w/w). The highest activity obtained was 20 U/g Fe_3O_4-chitosan. After twenty repeated uses, the immobilized lipase retains over 83% of its original activity.

CHAPTER III

EXPERIMANTAL

3.1 Materials and equipments

3.1.1 Chemicals

1. Styrene monomer; PTT Global Chemical Public Co., Ltd.

2. Sodium hydroxide; Merck

3. Sodium sulfate anhydrous; Merck

4. Sorbitan monooleate (Tween 80); Ajax Finechem Pty., Ltd.

5. Chitosan powder (MW 500,000 g/mol with ~85% degree of deacetylation); Seafresh Industry Public Co., Ltd.

6. Potassium persulphate; Carlo Erba

7. Polystyrene beads (PS beads); IRPC Co., Ltd.

8. Glutaraldehyde solution (25% solution in water); Merck

9. Lipase from *Pseudomonas cepacia* (*P. cepacia*), activity = 35 U/mg; Sigma

10. Disodium hydrogen phosphate; Merck

11. Potassium dihydrogen phosphate; Merck

12. Sodium chloride; Ajax Finechem Pty., Ltd.

13. Potassium chloride; Carlo Erba

14. Sodium carbonate anhydrous; Carlo Erba

15. *p*-nitrophenyl palmitate; Sigma

16. *p*-nitrophenol; Hopkin and Williams Ltd.

17. Coomassie Brilliant Blue G-250; Sigma

18. ortho-Phosphoric acid 85%; RCI Labscan Limited

19. Methanol; analytical grade; Merck

20. Ethanol; analytical grade; Merck

21. Ethanol; absolute for analysis grade; Merck

22. Dry ethanol: Dry ethanol was prepared by placing 5 g of clean dry magnesium turnings and 0.5 g of iodine (or a few drops of CCl_4), to activate the Mg, in a 2 l flask, followed by 50-75 ml of absolute ethanol, and warming the mixture until a vigorous reaction occurs. When this subsides, heating is continued until all the magnesium is converted to magnesium ethoxide. Up to 1 l of ethanol is added and, after an hour's reflux, the dry ethanol is distilled off.

23. Chloroform-d ($CDCl_3$); NMR spectroscopy grade; Merck KGaA Darmstadt, Germany

3.1.2 Equipments

1. Hotplate stirrer with magnetic bar

2. Thermometer

3. Vessel vial, round bottom flask, volumetric flask and Erlenmeyer flask

4. Beaker

5. Whatman no.1 filter paper

6. Centrifuge

7. Rotary evaporator

8. Buchner funnel

9. UV/VIS spectrophotometer (HP 8453)

10. The versatile digital microscope (Dino-Lite & Dino-Eye) Dino Capture 2.0 Version 1.5.11.A

11. Fourier transforms infrared spectroscopy in the attenuated total reflectance mode (ATR-FTIR; Nicolet 6700). Attenuated Total Reflection (ATR) formally

examined solid samples. In ATR, a highly refracting prism (diamond probe) is used to contact to the sample.

12. Scanning electron microscopy (SEM; JSM-5800 LV) analysis

13. NMR spectrometer; ^{1}NMR was recorded on Varian Model Mercury +400 nuclear magnetic resonance spectrometer operating at 400 MHz for ^{1}H. Chemical shifts are reported in part per million (ppm) relative to tetramethylsilane (TMS) or using the residual protonated solvent signal as a reference (for ^{1}H-NMR; $CDCl_3$ 7.26 ppm, Methanol-d_4 3.31 ppm, DMSO-d_6 2.50 ppm and D_2O 4.79 ppm).

3.2 Preparation and modification of solid supports for enzyme immobilization

3.2.1 Preparation of chitosan-styrene copolymer coated onto polystyrene beads (CHI-STY/PS beads)

Chitosan solution (2% w/v) was prepared by dissolving 2.00 g of chitosan powder in 100 ml of aqueous acetic acid solution (0.1% v/v). To 15 ml of the chitosan solution (2% w/v) in 50 ml round bottom flask, 2.25 g of styrene monomer solution (15% w/v) and tween 80 (1.32 g) were added. After stirring at room temperature for 15 min, 0.35 g of potassium persulphate ($K_2S_2O_8$) as initiator for polymerization and 4.55 g of polystyrene beads were added into the mixture and continuously stirred at 60°C for 24 hours. The resulting beads were filtered by suction and washed with distilled water until the pH was 7.0. Then, CHI-STY/PS beads were dried over silica gel in desiccator for 24 hours. The average diameter of CHI-STY/PS beads was obtained by the versatile digital microscope. The coated beads were characterized by ATR-FTIR spectroscopy and percentage in coating was calculated according to the following equation (1):

$$\text{Coating yield (\%)} = \frac{\text{(weight of the coated beads - weight of PS beads introduced)}}{\text{weight of PS beads introduced}} \times 100 \quad (1)$$

To optimize conditions for the preparation of CHI-STY/PS beads various concentration of chitosan solution (15 ml, 1-3% w/v), concentration of styrene

monomer (5-20% w/v), polymerization temperature (50-80°C) and polymerization time (6-36 h) were studied.

3.2.2 Activation of CHI-STY/PS beads with glutaraldehyde solution (GLU-CHI-STY/PS beads)

The process of chitosan-styrene copolymer coated onto polystyrene beads support (CHI-STY/PS beads) were activated with glutaraldehyde solution as a linker. This support was prepared by covalent binding method. The concentration of glutaraldehyde solution (GLU; 25% w/v solution in water) was diluted by distill water to concentration at 5, 10, 15 and 20% w/v.

To 15 ml of each concentration of glutaraldehyde solution in 50 ml round bottom flask and 4.55 g of CHI-STY/PS beads were added. The mixture was stirred at 80°C for 24 hours and the activated beads (GLU-CHI-STY/PS beads) were filtered off and washed with distilled water until the pH was 7.0. Then, the GLU-CHI-STY/PS beads were dried over silica gel in desiccator for 24 hours. The average diameter of CHI-STY/PS beads was obtained by the versatile digital microscope. The resulting beads (GLU-CHI-STY/PS beads) were characterized by ATR-FTIR spectroscopy and percentage in coating was calculated according to the following equation (2):

$$\text{Increased weight (\%)} = \frac{\text{(weight of GLU-CHI-STY/PS beads - weight of CHI-STY/PS beads introduced)}}{\text{weight of CHI-STY/PS beads introduced}} \times 100 \quad (2)$$

To optimize conditions for the preparation of GLU-CHI-STY/PS beads various concentration of glutaraldehyde solution (15 ml, 5-25% w/v), temperature (40-80°C) and time (4-32 h) were studied.

3.3 Immobilization of lipase

3.3.1 Preparation of phosphate buffer solution (PBS buffer) 25 mM, pH 7.0

Phosphate buffer solution (0.1 M, pH 7.0) as stock solution was prepared by dissolving disodium hydrogen phosphate (Na_2HPO_4) 1.4196 g, potassium dihydrogen phosphate (KH_2PO_4) 1.3609 g, sodium chloride (NaCl) 0.8006 g and potassium chloride (KCl) 0.0201 g in 100 ml of distilled water. Then, phosphate buffer solution (25 mM,

pH 7.0) was prepared by dissolving 62.50 ml of phosphate buffer solution (0.1 M, pH 7.0) in 250 ml of distilled water.

3.3.2 Immobilization of lipase from *Pseudomonas cepacia* (*P. cepacia*)

The lipase from *Pseudomonas cepacia* was immobilized onto GLU-CHI-STY/PS beads. To a solution of 18.0 mg of *P. cepacia* lipase and 5 ml of PBS buffer (25 mM, pH 7.0) in 25 ml round bottom flask, 1.0 g of GLU-CHI-STY/PS beads were added and stirred at 30°C for 72 hours. The suspension was filtered through a filter paper Whatman no.1 to obtain immobilized beads and unbound lipase. The immobilized beads were dried over silica gel in desiccator for 8 hours and stored in a refrigerator (-20°C) until use. Lipase activity, protein loading yield and specific activity were analyzed. Lipase activity assay was performed by a colorimetric method by using *p*-nitophenol (*p*-NP) as the standard [68]. The amount of protein was determined by the Bradford method by using *P. cepacia* as the standard [77].

To optimize the conditions for lipase immobilization onto GLU-CHI-STY/PS beads various concentration of glutaraldehyde solution (5-25% w/v), amounts of lipase (6.0-48.0 mg) in phosphate buffer solution (25 mM, pH 7.0) at 30°C and immobilization time (48-96 h) were studied.

3.3.3 Determination of lipase activity

Lipase activity was measured using 0.01 g of *p*-NPP dissolved in 2 ml of ethanol as substrate (*p*-NPP; 0.5% w/v, 13.25 μmol/ml). The increase in absorbance at 410 nm caused by the release of *p*-nitrophenol (*p*-NP) in the hydrolysis of *p*-nitrophenyl palmitate (*p*-NPP) was measured spectrophometrically [68, 78]. To a mixture of 1.1 ml of PBS buffer (25 mM, pH 7.0) and 1 ml of *p*-NPP solution (0.5% w/v), 50 mg of immobilized lipase was added. The reaction mixture was incubated under continuous stirring (1,400 rpm) in a water bath at 40°C for 5 min and then terminated by adding 2 ml of 0.5 N Na_2CO_3 followed by centrifuging for 10 min (5,000 rpm). The supernatant of 0.10 ml was diluted with 10 ml of PBS:EtOH:Na_2CO_3 (1.1:1:2) and absorbance of the solution was measured at 410 nm using a UV/VIS spectrophotometer (HP 8453). The activity for immobilized lipase was calculated using a standard calibration curve of *p*-

NP. One unit (U) of lipase activity was defined as the amount of enzyme necessary to produce 1 μmol of *p*-nitrophenol (*p*-NP) per min from *p*-nitrophenyl palmitate (*p*-NPP) under the standard conditions. Specific activity was defined as the number of enzyme unit per mg of protein.

3.3.4 Protein assay

The amount of protein was determined by the Bradford method by using *P. cepacia* as the standard. The amount of bound protein was determined indirectly from the difference between the amount of protein introduced and the amount of protein remained in the solution [77].

3.3.4.1 Preparation of protein reagent

10.0 mg of Coomassie Brilliant Blue G-250 was dissolved in 5 ml of 95% ethanol. The mixture was continuously stirred at room temperature for 20 min. To this solution 10 ml of 85% (w/v) phosphoric acid was added and stirred at room temperature for 5 min. The resulting solution was diluted to a final volume of 100 ml by distilled water. The mixture was continuously stirred at room temperature for 5 min. Then, protein reagent was filtered through Whatman no.1 paper and stored at room temperature in brown glass bottle until use. Final concentrations in the reagent were 0.01% (w/v) Coomassie Brilliant Blue G-250, 4.7% (w/v) ethanol and 8.5% (w/v) phosphoric acid [77].

3.3.4.2 Protein determination

Lipase solution (sample solution) (1.0 ml) was pipetted into the test tubes. Then, 5 ml of protein reagent was added and mixed by vortexing. The absorbance at 595 nm was measured after 2 min in 3 ml cuvettes against a reagent blank prepared from 1.0 ml of the appropriate PBS buffer (25 mM, pH 7.0) and 5 ml of protein reagent. The protein loading was calculated using a standard calibration curve of protein concentration.

3.3.5 Immobilization efficiency

The efficiency of immobilization was evaluated in terms of lipase activity, protein loading yield and specific activity as follows [72]:

$$\text{Lipase activity (U/g-support)} = \frac{\text{activity of immobilized lipase}}{\text{amount of support used}} \quad (1)$$

$$\text{Protein loading (\%)} = \frac{\text{amount of protein loaded}}{\text{amount of protein introduced}} \times 100\% \quad (2)$$

$$\text{Specific activity (U/mg protein)} = \frac{\text{activity of immobilized lipase}}{\text{amount of protein loaded}} \quad (3)$$

3.4 Enzymatic transesterification for biodiesel production

The lipase-immobilized GLU-CHI-STY/PS beads were used as catalyst for biodiesel production through transesterification reaction of soybean oil with anhydrous methanol and anhydrous ethanol. The reaction parameters were investigated in term of the optimal amount of catalyst, temperature, molar ratio of oil to alcohol and reaction time.

3.4.1 Determination of molecular weight of soybean oil

Molecular weight of soybean oil was estimated by using saponification value. Saponification value (AOAC 920.160) is the weight of KOH in milligram (mg) needed to saponify 1 g of fat and oil. It is also the average triacylglycerol molecule weight index in fat and oil sample. The reason for the determination is to describe molecular weight and the length of fatty acid chains in fat and oil. The saponification value is inversely proportional with the molecular weight and the chain's length. In determining saponification value, about 1 ± 0.005 g of soybean oil was weighed in a 50 ml round bottom flask and 25 ml of 0.5 N KOH solution was added. Next, boiling chip was added and connected to the reflux condenser. The solution was heated for 1 hour and left to cool before it was added with 1 ml phenolphthalein and titrated with 0.5 N HCl until the pink color disappeared. The same process was conducted to determine blank

(without oil). The molecular weight of soybean oil was calculated from saponification value [79] (see detail in Appendix B).

3.4.2 Enzymatic production of biodiesel

Experiments were performed to optimize the amount of ester product by varying the anhydrous ethanol concentration. In this study, transesterification reaction was investigated the role of substrate molar ratio in transesterification of soybean oil, conducting the reactions at 1:1, 1:2, 1:3, 1:4, 1:5 and 1:6 oil/ethanol molar ratios. The reaction using immobilized lipase (0.4294 g) as catalyst was carried out by reacting soybean oil (10 g) with one-step addition of anhydrous ethanol on basis of molar ratios as shown in Table 3.1. The transesterification was carried out in a 50 ml round bottom flask and heated at 40°C with stirring (700 rpm) for 192 hours in the oil bath as shown in Figure 3.1. At the end of the reaction, a sample was taken from the reaction mixture. The mixtures were filtered to separate the catalyst and the product. After centrifuge of the product, fatty acid ethyl esters (FAEEs) in upper layer were analyzed by NMR spectroscopy.

Table 3.1 Amount of ethanol was added in one step for biodiesel production

Type of Alcohol	Oil/ethanol molar ratio	Amount of anhydrous ethanol (g)
Anhydrous ethanol	1:1	0.53
	1:2	1.05
	1:3	1.58
	1:4	2.11
	1:5	2.63
	1:6	3.16

Figure 3.1 Transesterification reaction

In addition, the reaction was also conducted by adding alcohol stepwise. The effect of molar ratio of oil to alcohol was investigated in the range of 1:4 to 1:6 molar ratios. The transesterification of soybean oil with anhydrous ethanol and anhydrous methanol were investigated. The reaction using immobilized lipase (0.4294 g) as catalyst was carried out by reacting soybean oil (10 g) with three-step addition of alcohol on basis of molar ratios at 40°C for 32 hours. Amount of alcohol was added at the beginning of the reaction, 8 and 16 hours, respectively as shown in Table 3.2. At the end of the reaction, a sample was taken from the reaction mixture. The mixtures were filtered to separate the catalyst and the product. After centrifuge of the product, biodiesel in upper layer were analyzed by NMR spectroscopy.

Table 3.2 Amount of alcohol was added in three steps for biodiesel production

Type of Alcohol	Oil/alcohol molar ratio	Amount of alcohol (g)		
		0 h	8 h	16 h
Anhydrous ethanol	1:4	1.58 (3.0 eq.)	0.26 (0.5 eq.)	0.26 (0.5 eq.)
	1:5	1.58 (3.0 eq.)	0.53 (1.0 eq.)	0.53 (1.0 eq.)
	1:6	1.58 (3.0 eq.)	0.79 (1.5 eq.)	0.79 (1.5 eq.)
Anhydrous methanol	1:4	1.10 (3.0 eq.)	0.18 (0.5 eq.)	0.18 (0.5 eq.)
	1:5	1.10 (3.0 eq.)	0.37 (1.0 eq.)	0.37 (1.0 eq.)
	1:6	1.10 (3.0 eq.)	0.55 (1.5 eq.)	0.55 (1.5 eq.)

*eq. = equivalent

3.4.2.1 Optimization of the transesterification reaction

Since the transesterification reaction is reversible, an increase in the amount of one of the reactants will cause in higher ester yield and at least 3 molar equivalents of alcohol are required for the complete conversion alkyl ester. Experiments were performed by varying reaction parameters such as amount of catalyst, temperature, molar ratio of oil to alcohol and reaction time. In this study, amount of catalyst was measured based on oil mass with the variability from 0.2147, 0.3221 and 0.4294 g. In order to investigate the effect of temperature on enzymatic transesterification for biodiesel production, the reaction conditions were conducted at 30, 40 and 50°C. The

transesterification reaction was investigated the role of substrate molar ratio in transesterification of soybean oil, conducting the reactions at 1:1, 1:2, 1:3, 1:4, 1:5 and 1:6 oil/ethanol molar ratios. The reaction time was ranged from 8 to 64 hours.

3.5 Stability and reusability of immobilized lipase

The operational stability or reusability of immobilized lipase was conducted by carrying out transesterification reaction. The reaction using immobilized lipase (0.4294 g) as catalyst was carried out by reacting soybean oil (10 g) with 1:5 molar ratio of oil to ethanol (three-step addition of anhydrous ethanol) at 40°C for 32 hours. At the end of the reaction, a sample was taken from the reaction mixture. The mixtures were filtered to separate the catalyst and the product. After centrifuge of the product, fatty acid ethyl esters (FAEEs) in upper layer were analyzed by NMR spectroscopy. The recovered immobilized lipase was used in the next batch transesterification with new substrates. The reusability was determined by estimating the product as in the original cycle.

CHAPTER IV
RESULTS AND DISCUSSION

Since *Pseudomonas cepacia* lipase, recently proven to be the most versatile lipases [57], has identified as most promising for transesterification, this work studied process for immobilization of *Pseudomonas cepacia* lipase onto modified support and evaluated efficiency of the catalyst for the biodiesel production through transesterification. The experiments were divided into four steps: preparation of supporting material (chitosan-styrene copolymer coated onto polystyrene beads), activation of the support using glutaraldehyde, lipase immobilization and biodiesel production. For preparation of chitosan-styrene copolymer coated onto polystyrene beads (CHI-STY/PS beads), effect of the concentration of chitosan solution, the concentration of styrene monomer solution, temperature and time in the reaction on coating of chitosan onto polystyrene beads were studied. In the second step, CHI-STY/PS beads was activated with glutaraldehyde solution (GLU-CHI-STY/PS beads) as linker and effect of the concentration of glutaraldehyde solution, temperature and time reaction on attachment of glutaraldehyde onto CHI-STY/PS beads were investigated. In immobilization step, the lipase from *Pseudomonas cepacia* was used and effect of the concentration of glutaraldehyde solution, amount of lipase and time for immobilization onto modified support (GLU-CHI-STY/PS beads) were studied by evaluating the lipase activity, amount of lipase in the form of protein loading yield and specific activity. In the final step, the lipase immobilized onto GLU-CHI-STY/PS beads were used as catalyst for biodiesel production through transesterification. The variables that influence the production of biodiesel such as amount of the catalyst, temperature, molar ratio of oil to alcohol and time were studied.

4.1 Coating chitosan-styrene copolymer onto polystyrene beads (CHI-STY/PS beads)

Chitosan-styrene copolymer was coated onto polystyrene beads (CHI-STY/PS beads) by emulsion polymerization technique. The CHI-STY/PS beads were prepared

by emulsion polymerization between chitosan solution copolymer with styrene monomer solution by using potassium persulphate as an initiator.

4.1.1 Effect of concentrations of chitosan and styrene monomer solution

The effect of various concentrations of chitosan solution (the range from 1 to 3% w/v) copolymer with styrene monomer solution (the range from 5 to 20% w/v) on coating chitosan-styrene copolymer onto polystyrene beads was studied. Appearance of those beads was shown in Figure 4.2 to 4.4. Average diameter and percentage in coating of the CHI-STY/PS beads, prepared by emulsion polymerization at 60°C for 24 hours, were examined and results were summarized in Table 4.1. Concentration of chitosan and styrene monomer solution for the polymerization was significantly affected on appearance and average diameter and percentage in coating of CHI-STY/PS beads. In Figure 4.2 to 4.4, the success of coating easily indicated by consideration beads surface and a lump of beads. The good preparation was CHI-STY/PS beads with smooth surface or without crack or hold together or no lump of beads. Chitosan-styrene copolymer were successfully coated onto polystyrene beads when 1%CHI-15%STY, 2%CHI-15%STY and 3%CHI-15%STY were used.

Figure 4.1 showed percentage in coating chitosan-styrene copolymer onto polystyrene beads using various concentrations of chitosan and styrene monomer solution at 60°C for 24 hours. The percentage in coating from the batches using 1, 2 and 3% (w/v) chitosan solution was gradually increased when higher concentrations of styrene monomer solution was used in in range of 5 to 15% (w/v). Using 20% styrene monomer solution, the percentage in coating was suddenly decreased. This may be caused by too high concentration of styrene monomer solution. At high concentration of styrene monomer solution, styrene could be polymerized itself or copolymerized with chitosan and then resulted in self-forming polymer particles and attaching the coated beads to form lumps of the beads. Thus, coating chitosan-styrene copolymer onto polystyrene beads was less and percentage in coating was decreased. In case low concentration, when used 5% (w/v) of styrene monomer solution in each batch, coating chitosan-styrene copolymer onto polystyrene beads was also incomplete.

Using 15% (w/v) styrene monomer solution gave the highest percentage in coating in each batch using 1, 2 and 3% (w/v) chitosan solution. The percentage in coating of 1%CHI-15%STY/PS beads, 2%CHI-15%STY/PS beads and 3%CHI-15%STY/PS beads were 31.19%, 54.18% and 30.47%, respectively while the average diameter of 1%CHI-15%STY/PS beads, 2%CHI-15%STY/PS beads and 3%CHI-15%STY/PS beads were 1.560, 1.577 and 1.552 mm, respectively as shown in Table 4.1. The size of these supports was bigger than PS beads (1.288 mm).

Among of those coated beads, chitosan-styrene copolymer coated polystyrene beads (CHI-STY/PS beads) were well formed in the batches using 1% chitosan solution-15% styrene solution, 2% chitosan solution-15% styrene solution and 3% chitosan solution-15% styrene solution. Thus, 1%CHI-15%STY/PS beads, 2%CHI-15%STY/PS beads and 3%CHI-15%STY/PS beads were activated with various concentrations of glutaraldehyde solution for before lipase immobilization.

Table 4.1 Average diameter and percentage in coating of the CHI-STY/PS beads prepared by using 1, 2 and 3% (w/v) chitosan solution copolymerizing with various concentrations of styrene monomer solution at 60°C for 24 hours

Concentration of styrene monomer solution (%w/v)	1% (w/v) chitosan solution		2% (w/v) chitosan solution		3% (w/v) chitosan solution	
	Average diameter (mm)	Coating yield (%)	Average diameter (mm)	Coating yield (%)	Average diameter (mm)	Coating yield (%)
5	1.405	2.38	1.392	1.61	1.384	1.03
10	1.521	15.12	1.547	15.42	1.530	12.92
15	1.560	31.19	1.577	54.18	1.552	30.47
20	1.510	10.69	1.571	49.54	1.547	23.02

*average diameter of PS beads = 1.288 mm

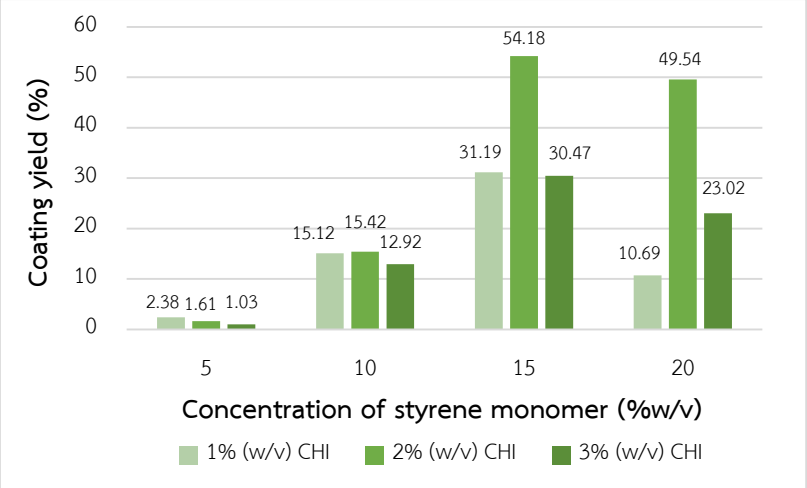

Figure 4.1 Percentage in coating chitosan-styrene copolymer onto polystyrene beads using styrene monomer solution in the range of 5 to 20% (w/v) in each batch of 1, 2 and 3% (w/v) chitosan solution at 60°C for 24 hours

(a) 5% (w/v) styrene monomer solution (b) 10% (w/v) styrene monomer solution

(c) 15% (w/v) styrene monomer solution (d) 20% (w/v) styrene monomer solution

Figure 4.2 Variation concentration of styrene monomer solution copolymer with 1% (w/v) chitosan solution coated onto polystyrene beads at 60°C for 24 hours (a) 5% (w/v) styrene monomer solution (b) 10% (w/v) styrene monomer solution (c) 15% (w/v) styrene monomer solution and (d) 20% (w/v) styrene monomer solution

(a) 5% (w/v) styrene monomer solution

(b) 10% (w/v) styrene monomer solution

(c) 15% (w/v) styrene monomer solution

(d) 20% (w/v) styrene monomer solution

Figure 4.3 Variation concentration of styrene monomer solution copolymer with 2% (w/v) chitosan solution coated onto polystyrene beads at 60°C for 24 hours (a) 5% (w/v) styrene monomer solution (b) 10% (w/v) styrene monomer solution (c) 15% (w/v) styrene monomer solution and (d) 20% (w/v) styrene monomer solution

(a) 5% (w/v) styrene monomer solution (b) 10% (w/v) styrene monomer solution

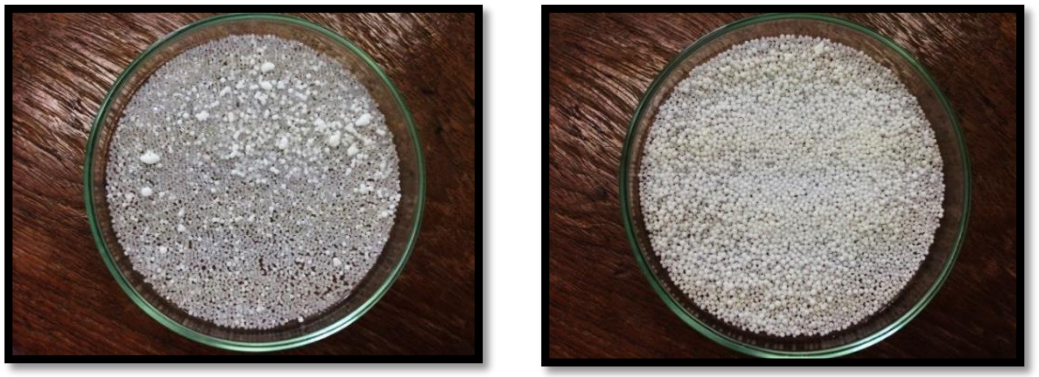

(c) 15% (w/v) styrene monomer solution (d) 20% (w/v) styrene monomer solution

Figure 4.4 Variation concentration of styrene monomer solution copolymer with 3% (w/v) chitosan solution coated onto polystyrene beads at 60°C for 24 hours (a) 5% (w/v) styrene monomer solution (b) 10% (w/v) styrene monomer solution (c) 15% (w/v) styrene monomer solution and (d) 20% (w/v) styrene monomer solution

In Figure 4.5-4.7, ATR-FTIR spectra displayed the characteristic chemical structures of the CHI-STY/PS beads obtained from polymerization using various concentrations of chitosan and styrene monomer solution at 60°C for 24 hours. The ATR-FTIR spectra of PS beads are shown in Figure 4.5 (a), 4.6 (a) and 4.7 (a). The absorption bands at 3025, 2921 and 2850 cm^{-1} were absorption of =C-H stretching vibration (aromatic), -C-H stretching vibration (aromatic) and -C-H stretching vibration (alkane), respectively. The absorption band at 1601 cm^{-1} was attributed to C=C stretching vibration (aromatic). The absorption band at 1492, 1452 and 754 cm^{-1} were ascribed to CH_2 bending vibration, $-CH_3$ bending vibration and C-H bending vibration (aromatic), respectively [80]. After coating with chitosan-styrene copolymer, the spectra indicated the absorption bands of -OH and -NH stretching vibrations at around 3358 cm^{-1}. The new absorption band at 1635 cm^{-1} was ascribed to -NH bending vibration in $-NH_2$. Besides, the absorption band at 1070 cm^{-1} was attributed to -CO stretching vibration in -CH-O-CH [81]. Therefore, it can be confirmed that chitosan-styrene copolymer were successfully coated onto polystyrene beads. In the study, the FTIR spectra of the CHI-STY/PS beads obtained from using 1, 2 and 3% (w/v) chitosan solution copolymer with 5 to 10% (w/v) styrene monomer solution showed that intensity of -NH bending vibration in $-NH_2$ position at 1635 cm^{-1} were decreased. When using 1, 2 and 3% (w/v) chitosan solution copolymer with 15% (w/v) styrene monomer solution, the FTIR spectra of the CHI-STY/PS beads showed that intensity of -NH bending vibration in $-NH_2$ position at 1635 cm^{-1} were increased. This indicated that the CHI-STY/PS beads contained more chitosan-styrene copolymer on the beads than other beads. Since intensity of -NH bending vibration at 1635 cm^{-1} of the beads obtanined from using 1, 2 and 3% (w/v) chitosan solution copolymer with 20% (w/v) styrene monomer solution was less than the beads coated with copolymer using 15% (w/v) styrene monomer solution, these indicated that less amount of copolymer were coated onto the PS beads and also were consistent with the percentage in coating as shown in Figure 4.1.

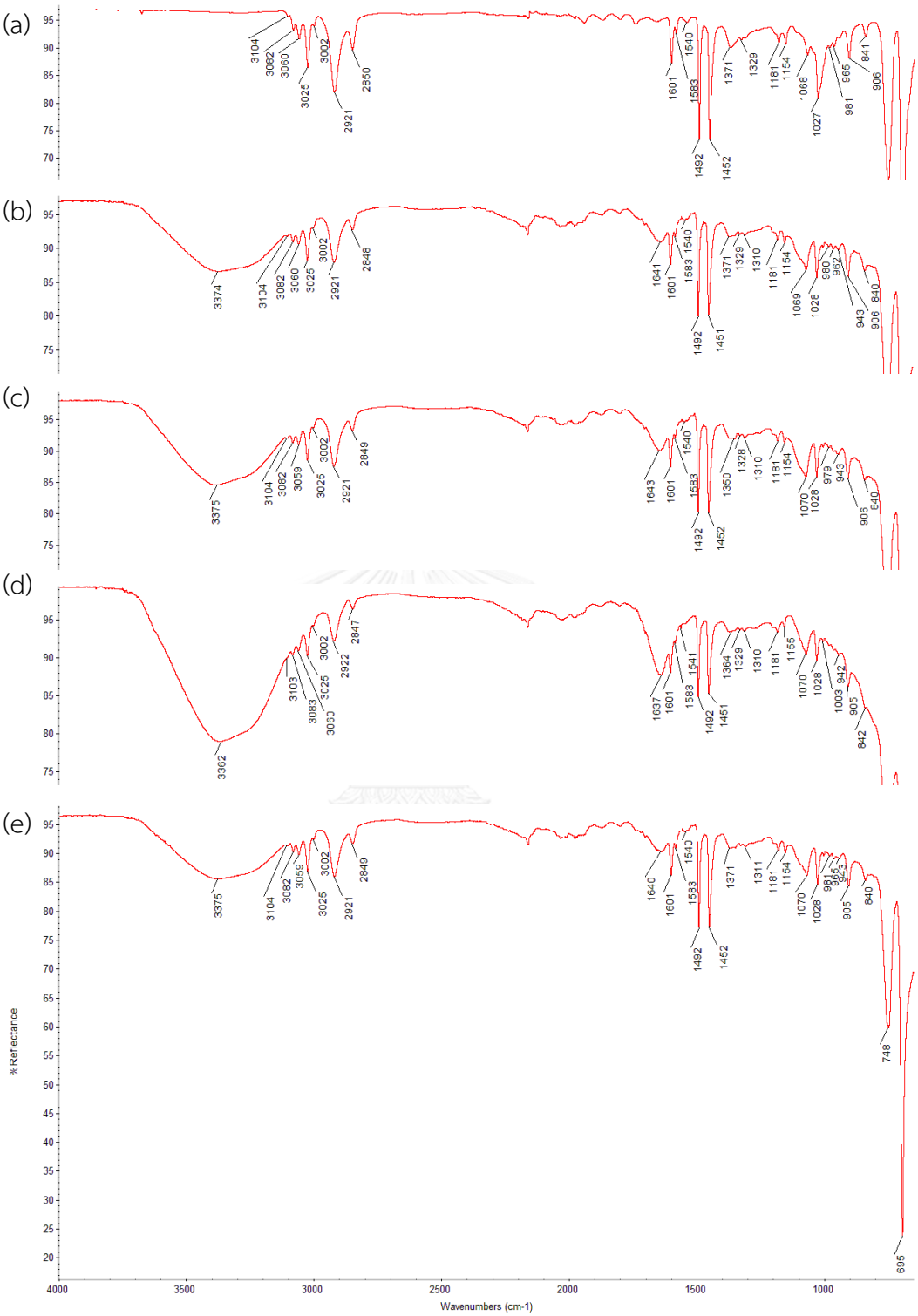

Figure 4.5 ATR-FTIR spectra of (a) polystyrene beads (PS beads) and of the CHI-STY/PS beads prepared at 60°C for 24 hours using 1% (w/v) chitosan solution copolymerized with (b) 5% (w/v) styrene monomer solution (c) 10% (w/v) styrene monomer solution (d) 15% (w/v) styrene monomer solution and (e) 20% (w/v) styrene monomer solution

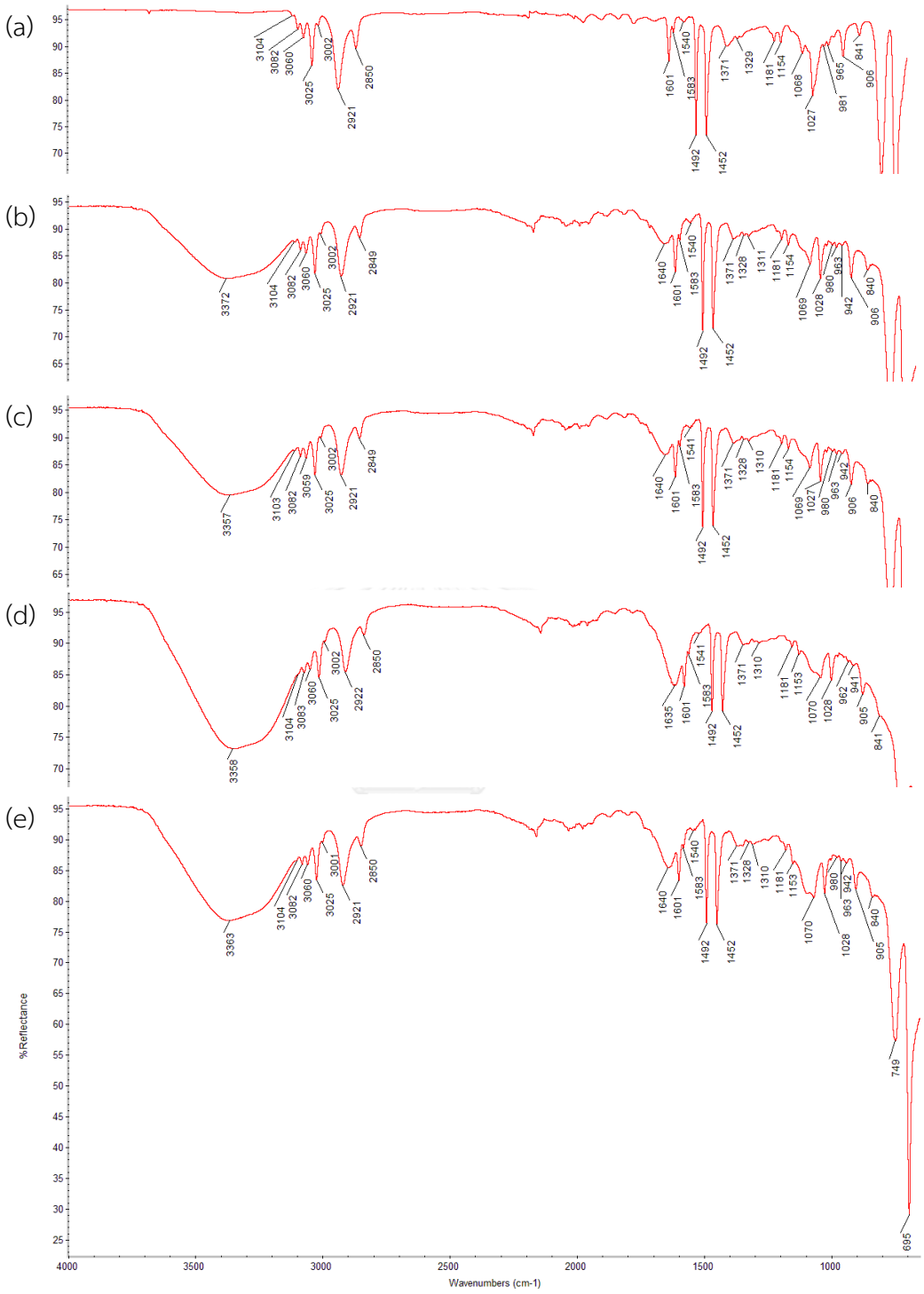

Figure 4.6 ATR-FTIR spectra of (a) polystyrene beads (PS beads) and of the CHI-STY/PS beads prepared at 60°C for 24 hours using 2% (w/v) chitosan solution copolymerized with (b) 5% (w/v) styrene monomer solution (c) 10% (w/v) styrene monomer solution (d) 15% (w/v) styrene monomer solution and (e) 20% (w/v) styrene monomer solution

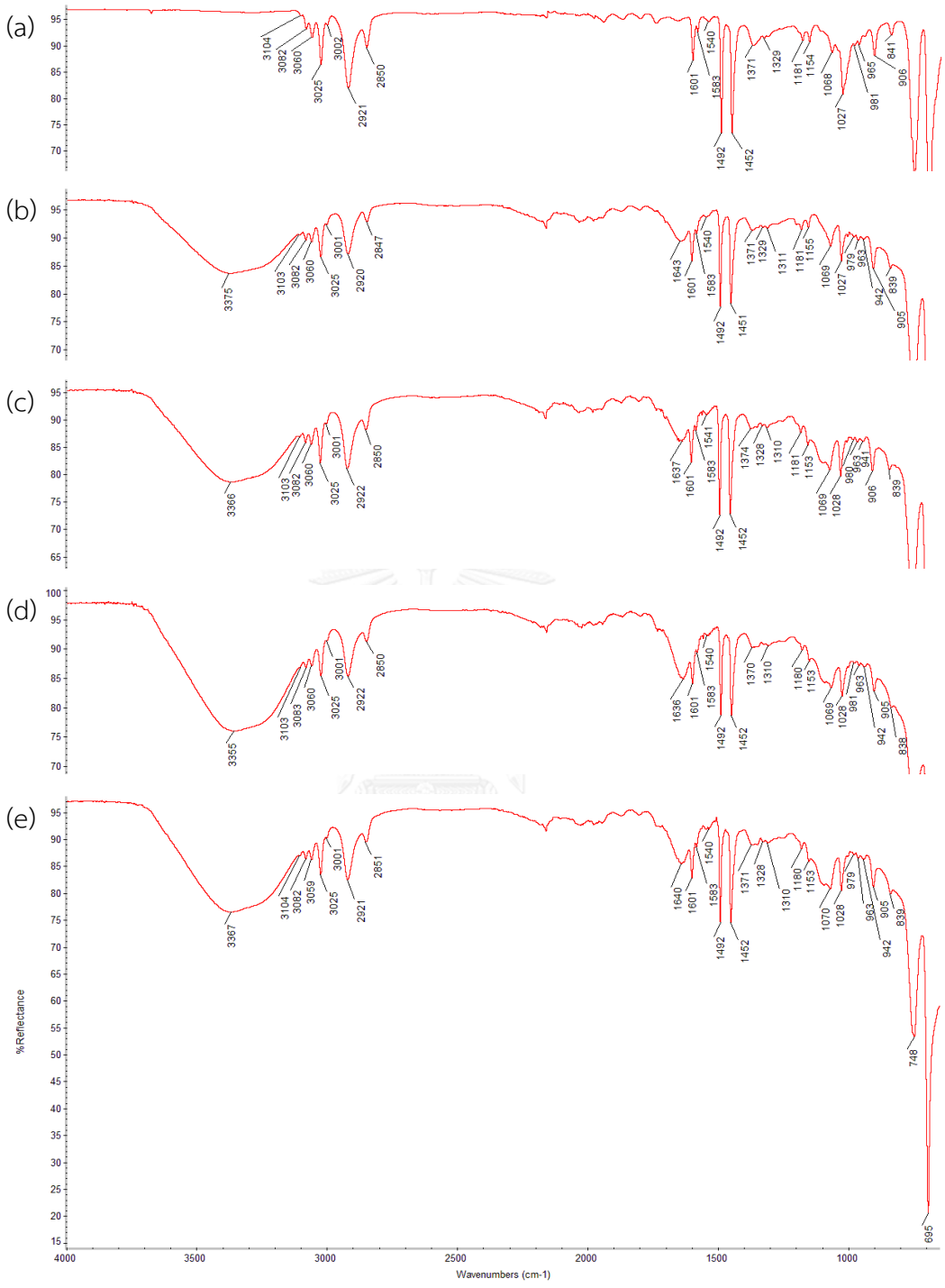

Figure 4.7 ATR-FTIR spectra of (a) polystyrene beads (PS beads) and of the CHI-STY/PS beads prepared at 60°C for 24 hours using 3% (w/v) chitosan solution copolymerized with (b) 5% (w/v) styrene monomer solution (c) 10% (w/v) styrene monomer solution (d) 15% (w/v) styrene monomer solution and (e) 20% (w/v) styrene monomer solution

In Figure 4.8, SEM micrographs showed that the CHI-STY/PS beads were different from the original PS beads. The original PS beads was a spherical smooth surface beads as shown in Figure 4.8 (a) and magnification (500X) of the PS beads (Figure 4.8 b) showed good structural integrity without any pores or cracks. After coating copolymer from using 1, 2, and 3% (w/v) chitosan solution copolymer with 15% (w/v) styrene monomer solution at 60°C for 24 hours SEM images (Figure 4.8 c-h) showed spherical beads with holes and some holes seemed to be filled with copolymer. At higher amount of chitosan solution used, SEM image (Figure 4.8 e) showed that most of the holes were filled up copolymer. Since a number of holes is descending sort: 2% (w/v) chitosan solution > 1% (w/v) chitosan solution > 3% (w/v) chitosan solution was similar to descending order of the percentage of coating, 2% (w/v) chitosan solution (54.18%) > 1% (w/v) chitosan solution (31.19%) > 3% (w/v) chitosan solution (30.47%), and consistent with the ATR-FTIR spectra as well as shown in Figure 4.5-4.7, these indicated that the holes were responsible for the storage of chitosan. In Figure 4.8 (d, f, h) SEM images with magnification of 500X showed the surface roughness of the CHI-STY/PS beads obtained from 1, 2, and 3% (w/v) chitosan solution copolymerized with 15% (w/v) styrene monomer solution and also displayed good phase compatibility between the chitosan-styrene copolymer and PS beads.

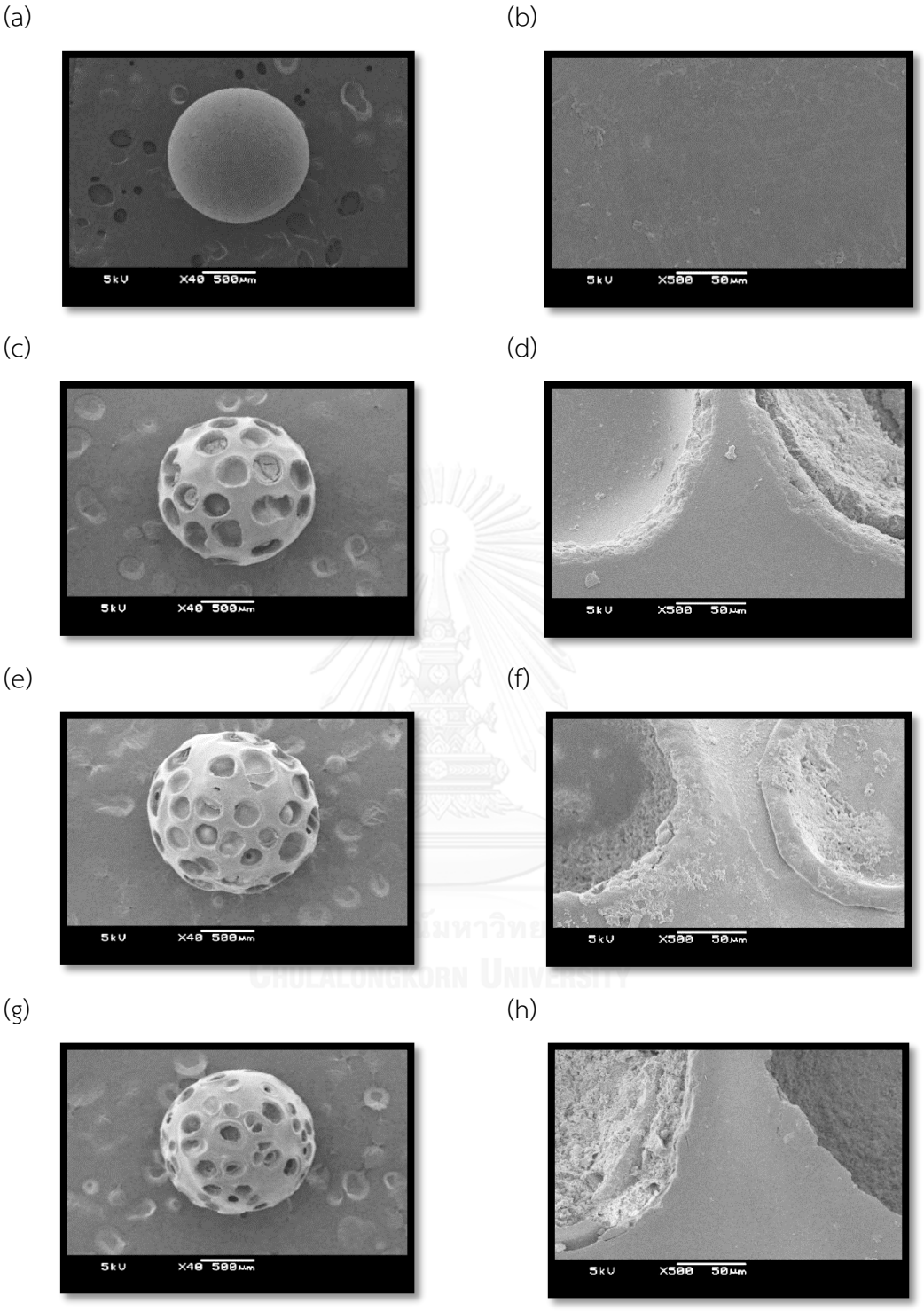

Figure 4.8 SEM micrographs of (a) PS beads X40 (b) PS beads X500 (c) 1%CHI-15%STY/PS beads X40 (d) 1%CHI-15%STY/PS beads X500 (e) 2%CHI-15%STY/PS beads X40 (f) 2%CHI-15%STY/PS beads X500 (g) 3%CHI-15%STY/PS beads X40 and (h) 3%CHI-15%STY/PS beads X500

4.1.2 Effect of temperature on coating chitosan-styrene copolymer onto polystyrene beads

The effect of temperature on coating 2%chitosan-15%styrene copolymer onto polystyrene beads was investigated at 50, 60, 70 and 80°C. Results (Table 4.2 and Figure 4.9) obviously showed that temperature affected coating of chitosan-styrene copolymer onto polystyrene beads.

Table 4.2 Average diameter and percentage in coating of 2%CHI-15%STY/PS beads at various temperatures for 24 hours

Temperature (°C)	Average diameter of 2%CHI-15%STY/PS beads (mm)	Coating yield (%)
50	1.366	6.64
60	1.577	54.18
70	1.598	43.42
80	1.612	33.37

*average diameter of PS beads = 1.288 mm

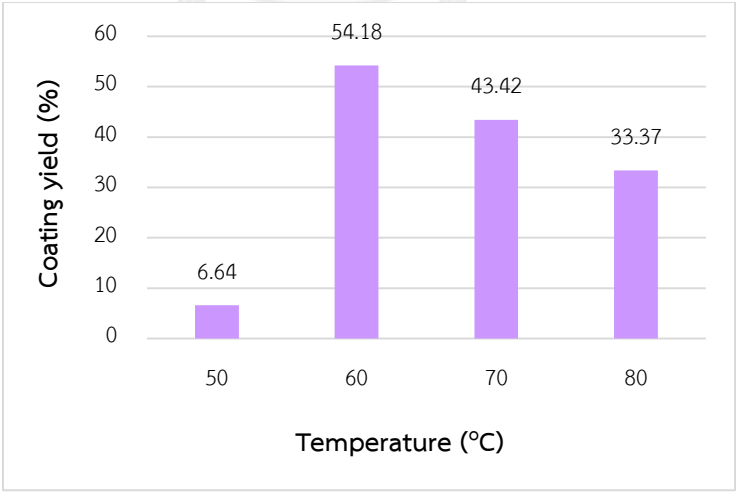

Figure 4.9 Percentage of coating of 2%CHI-15%STY/PS beads at various temperatures for 24 hours

Table 4.2, it was found that average diameter of 2%CHI-15%STY/PS beads was in the range of 1.366-1.612 mm while the PS beads was 1.288 mm and the higher temperature the larger average diameter. The highest percentage of coating with 54.18% was obtained from 60°C of copolymerizing temperature while small amount of copolymer was coated onto the beads at 50°C of copolymerizing temperature. The results revealed that polymerization of styrene and copolymer coating were slow at 50°C of temperature and coating was well performed at 60°C or above. However, the percentage of coating decreased when the temperature was higher than 60°C. These may be caused by coating chitosan-styrene copolymer onto the polystyrene beads competing with expansion of the PS beads and self-forming of copolymer. In Figure 4.10, polystyrene beads were expanded at high temperature upper 60°C. Therefore, chitosan-styrene copolymer coated onto the polystyrene beads will happen less. It can be summarized that the suitable temperature of CHI-STY/PS beads were achieved at 60°C because it gave the highest percentage in coating.

(a) 50°C (b) 60°C

(c) 70°C (d) 80°C

Figure 4.10 Pictures of 2%CHI-15%STY/PS beads prepared at (a) 50°C (b) 60°C (c) 70°C and (d) 80°C for 24 hours

In Figure 4.11, the ATR-FTIR spectra of the 2%CHI-15%STY/PS beads obtained from various temperatures for 24 hours displayed that chitosan-styrene copolymer were successfully coated onto polystyrene beads as confirmed by absorption bands of chitosan, around 3358, 1635 and 1070 cm^{-1} for absorption of -OH and -NH stretching vibrations, -NH bending vibration in -NH_2 and -CO stretching vibration in -CH-O-CH, respectively [81]. In the study, intensity of -NH bending vibration of -NH_2 group at 1635 cm^{-1} was low when took more temperature in the coating upper 60°C. This is consistent with the percentage in coating as shown in Figure 4.9 and highest coating of chitosan-styrene copolymer onto polystyrene beads at 60°C for 24 hours.

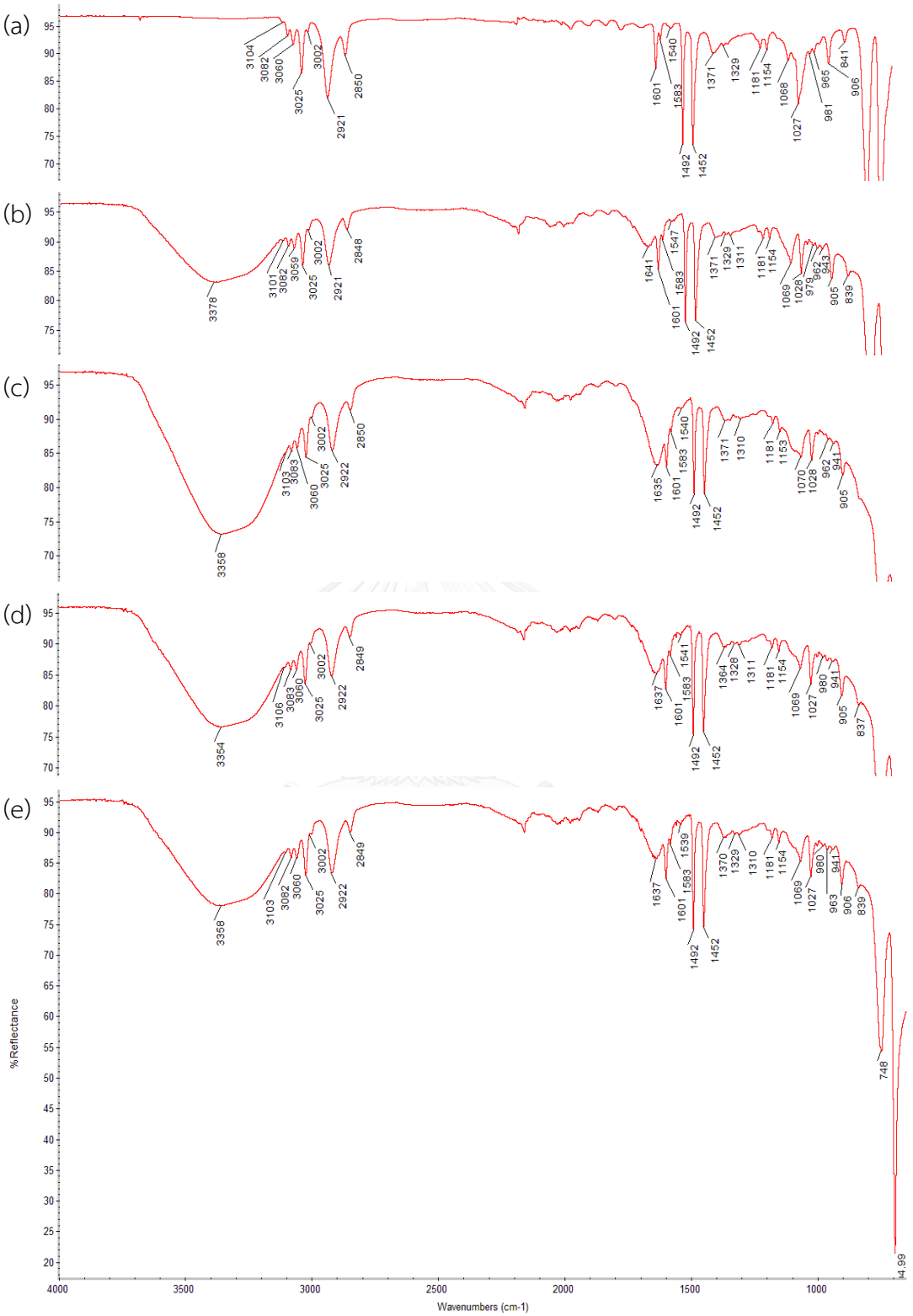

Figure 4.11 ATR-FTIR spectra of (a) polystyrene beads (PS beads) and 2%CHI-15%STY/PS beads obtained at temperatures, (b) 50°C (c) 60°C (d) 70°C and (e) 80°C, for 24 hours

4.1.3 Effect of coating time on coating chitosan-styrene copolymer onto polystyrene beads

The effect of coating time on 2%CHI-15%STY/PS beads was investigated at 6, 12, 18, 24, 30 and 36 hours. As the results, the various coating time have effect to coating of chitosan onto polystyrene beads. Results (Table 4.3 and Figure 4.12) showed that the average diameter of 2%CHI-15%STY/PS beads was in range 1.474-1.630 mm and was increased by coating time increased while copolymer was fully coated onto the beads within 24 hours to reach maximal coating with about 50%. Accordingly, the suitable time to perform the coating was around 24 hours. Figure 4.13 showed that surfaces of the 2%CHI-15%STY/PS beads obtained from each time for coating were smooth without crack or hold together as a pack. Thus, the CHI-STY/PS beads obtained at 60°C for 24 hours were used for immobilization step.

Table 4.3 Average diameter and percentage in coating of 2%CHI-15%STY/PS beads at 60°C for various coating times

Coating time (h)	Average diameter of 2%CHI-15%STY/PS beads (mm)	Coating yield (%)
6	1.474	7.59
12	1.548	13.54
18	1.563	32.42
24	1.577	54.18
30	1.609	50.27
36	1.630	46.58

*average diameter of PS beads = 1.288 mm

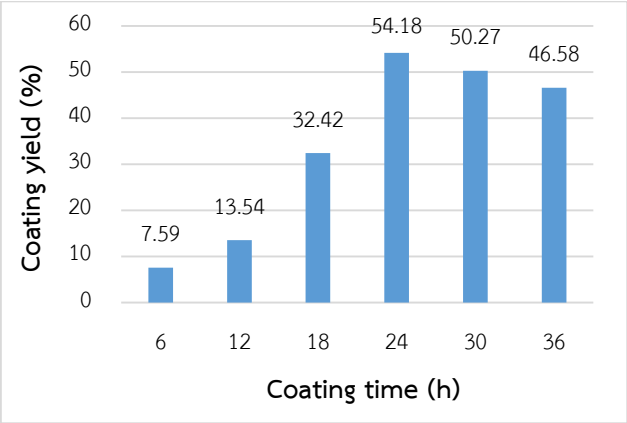

Figure 4.12 Percentage of coating of 2%CHI-15%STY/PS beads at 60°C for various coating times

(a) 6 hours

(b) 12 hours

(c) 18 hours

(d) 24 hours

(e) 30 hours

(f) 36 hours

Figure 4.13 Coating time of 2%CHI-15%STY/PS beads at 60°C (a) 6 hours (b) 12 hours (c) 18 hours (d) 24 hours (e) 30 hours and (f) 36 hours

In Figure 4.14, the ATR-FTIR spectra of the 2%CHI-15%STY/PS beads at 60°C for various coating times. It was found that chitosan-styrene copolymer were successfully coated onto polystyrene beads as confirmed from absorption bands of chitosan. As the results, the ATR-FTIR spectra showed the absorption bands around 3358 cm^{-1} was indexed to -OH and -NH stretching vibrations. The new absorption band at 1635 cm^{-1} was ascribed to -NH bending vibration in $-NH_2$. Besides, the absorption band at 1070 cm^{-1} was attributed to -CO stretching vibration in -CH-O-CH [81]. Therefore, it can be confirmed that chitosan can be coated onto polystyrene beads. In the study, -NH bending vibration in $-NH_2$ position at 1635 cm^{-1} to the decreased intensity when increasing coating time upper 24 hours. This is consistent with the percentage in coating as shown in Figure 4.12. In the results, it was found that chitosan-styrene copolymer were successfully coated onto polystyrene beads at 60°C for 24 hours.

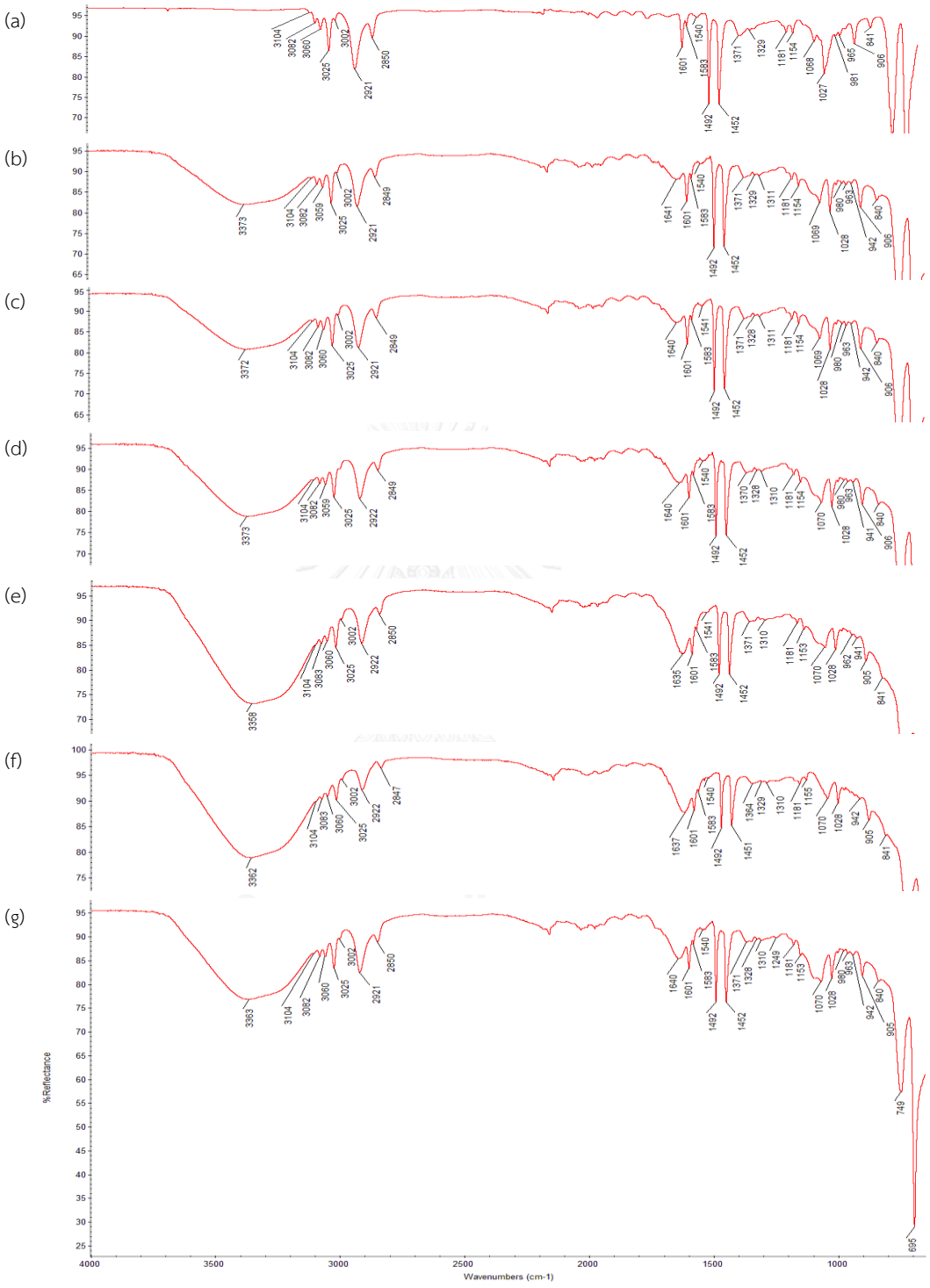

Figure 4.14 ATR-FTIR spectra of (a) polystyrene beads (PS beads) and 2%CHI-15%STY/PS beads at 60°C for coating times, (b) 6 hours (c) 12 hours (d) 18 hours (e) 24 hours (f) 30 hours and (g) 36 hours

4.2 Activation of CHI-STY/PS beads with glutaraldehyde solution (GLU-CHI-STY/PS beads)

The CHI-STY/PS beads were activated with glutaraldehyde solution as a linker to give the support (GLU-CHI-STY/PS beads) ready for immobilization via covalent binding. In immobilization process amino groups of the support reacted with glutaraldehyde solution as shown in Scheme 4.1.

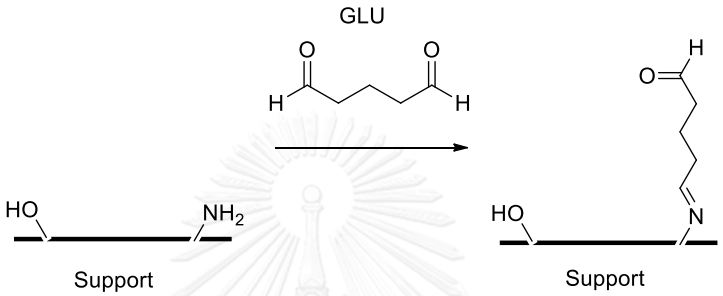

Scheme 4.1 Scheme of activation and lipase immobilization using glutaraldehyde as linker

4.2.1 Effect of concentration of glutaraldehyde solution and temperature

1%CHI-15%STY/PS beads, 2%CHI-15%STY/PS beads and 3%CHI-15%STY/PS beads were activated with various concentrations of glutaraldehyde solution. The concentration of glutaraldehyde solution (GLU; 25% w/v solution in water) was diluted by distill water to concentration at 5, 10, 15 and 20% (w/v). The effect of temperature was also investigated at 40, 60 and 80°C.

Table 4.4 Average diameter and percentage of increased weight of 1%CHI-15%STY/PS beads, 2%CHI-15%STY/PS beads and 3%CHI-15%STY/PS beads activated with various concentrations of glutaraldehyde solution at 40, 60 and 80°C for 24 hours

concentration of chitosan solution (%w/v)	concentration of glutaraldehyde solution (%w/v)	temperature (40°C)		temperature (60°C)		temperature (80°C)	
		average diameter (mm)	increased weight (%)	average diameter (mm)	increased weight (%)	average diameter (mm)	increased weight (%)
1	5	1.578	7.03	1.589	10.07	1.591	12.34
	10	1.611	19.15	1.644	23.07	1.665	27.69
	15	1.622	22.86	1.652	26.77	1.719	33.67
	20	1.683	29.28	1.720	33.64	1.767	37.13
	25	1.708	32.09	1.783	41.11	1.799	44.28
2	5	1.581	8.04	1.594	12.19	1.598	14.19
	10	1.642	21.05	1.662	27.02	1.673	31.07
	15	1.657	25.65	1.683	31.35	1.742	36.03
	20	1.722	33.88	1.787	38.08	1.798	41.49
	25	1.778	37.52	1.827	44.67	1.848	46.38
3	5	1.563	5.20	1.582	9.96	1.591	12.14
	10	1.609	18.67	1.647	21.70	1.658	25.73
	15	1.640	21.15	1.651	23.78	1.677	30.09
	20	1.658	26.99	1.682	31.84	1.733	34.21
	25	1.685	31.86	1.784	38.85	1.802	42.97

*average diameter of original 1%CHI-15%STY/PS beads = 1.560 mm

*average diameter of original 2%CHI-15%STY/PS beads = 1.577 mm

*average diameter of original 3%CHI-15%STY/PS beads = 1.552 mm

4.2.1.1 1%CHI-15%STY/PS beads activated with various concentrations of glutaraldehyde solution at 40, 60 and 80°C for 24 hours

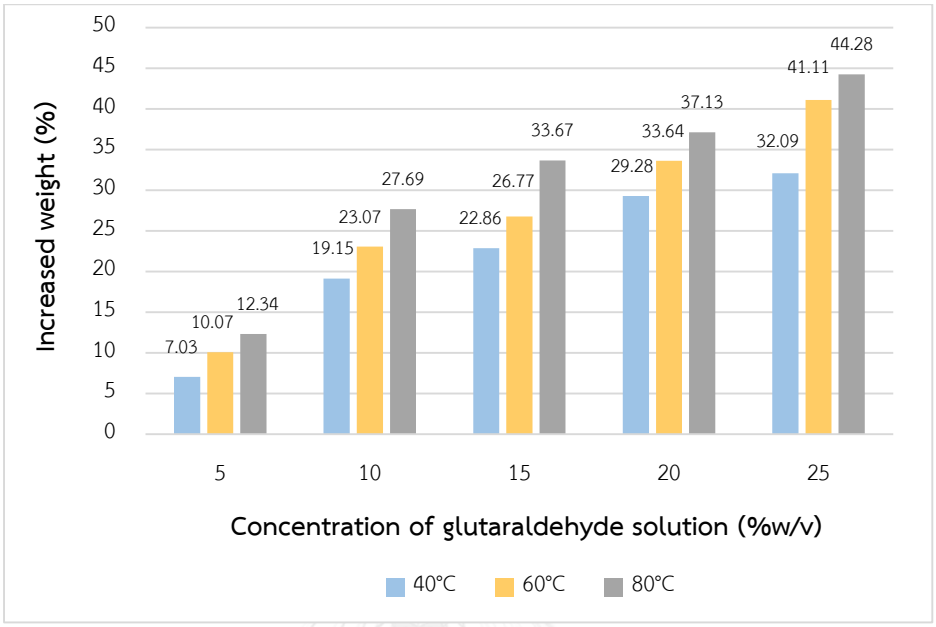

Figure 4.15 Percentage of increased weight of 1%CHI-15%STY/PS beads activated with various concentrations of glutaraldehyde solution at 40, 60 and 80°C for 24 hours

Table 4.4 presented the average diameter and percentage of increased weight of 1%CHI-15%STY/PS beads activated with various concentrations of glutaraldehyde solution at 40, 60 and 80°C for 24 hours. The effect of concentration of glutaraldehyde solution (the range from 5 to 25% w/v) activated with 1%CHI-15%STY/PS beads at various temperature (the range from 40 to 80°C) for 24 hours were studied. The results showed that increasing concentration of glutaraldehyde solution resulted in increase of weight of the beads at each temperature as presented in Figure 4.15. Because of increase of the average diameter when used glutaraldehyde solution (5 to 25% w/v) at 40 to 60°C, it indicated that the amino group not only reacted with glutaraldehyde but also with polyglutaraldehyde. In Figure 4.16-4.17, color of the 1%CHI-15%STY/PS beads activated with higher concentration of glutaraldehyde or higher temperature was more yellow than of the lower ones. At 80°C color of the 1%CHI-15%STY/PS beads obtained from each concentration of glutaraldehyde solution used became brown

color beads as shown in Figure 4.18. Changing in color due to concentration and temperature also supported that polyglutaraldehyde present in the glutaraldehyde solution could react with amino group and was presented on the beads. Thus, the highest percentage of increased weight was obtained from 80°C when compared at other temperatures.

(a) 5% (w/v) GLU

(b) 10% (w/v) GLU

(c) 15% (w/v) GLU

(d) 20% (w/v) GLU

(e) 25% (w/v) GLU

Figure 4.16 Comparison of 1%CHI-15%STY/PS beads activated with various concentrations of glutaraldehyde solution at 40°C for 24 hours (a) 5% (w/v) GLU (b) 10% (w/v) GLU (c) 15% (w/v) GLU (d) 20% (w/v) GLU and (e) 25% (w/v) GLU

(a) 5% (w/v) GLU

(b) 10% (w/v) GLU

(c) 15% (w/v) GLU

(d) 20% (w/v) GLU

(e) 25% (w/v) GLU

Figure 4.17 Comparison of 1%CHI-15%STY/PS beads activated with various concentrations of glutaraldehyde solution at 60°C for 24 hours (a) 5% (w/v) GLU (b) 10% (w/v) GLU (c) 15% (w/v) GLU (d) 20% (w/v) GLU and (e) 25% (w/v) GLU

(a) 5% (w/v) GLU

(b) 10% (w/v) GLU

(c) 15% (w/v) GLU

(d) 20% (w/v) GLU

(e) 25% (w/v) GLU

Figure 4.18 Comparison of 1%CHI-15%STY/PS beads activated with various concentrations of glutaraldehyde solution at 80°C for 24 hours (a) 5% (w/v) GLU (b) 10% (w/v) GLU (c) 15% (w/v) GLU (d) 20% (w/v) GLU and (e) 25% (w/v) GLU

In comparison of ATR-FTIR spectra (Figure 4.19 to 4.22) of 1%CHI-15%STY/PS beads and activated 1%CHI-15%STY/PS beads, low intensity of the absorption of -OH and -NH stretching vibrations (around 3362 cm^{-1}) and of -NH bending vibration in $-NH_2$ (1637 cm^{-1}) and appearance of absorption at about 1723 and 2723 cm^{-1} (for -CO

stretching vibration and C-H stretching vibration of aldehyde, respectively) indicated that most of amino group was reacted with the aldehydes. Because of stronger intensity of the absorption at about 1723 cm^{-1} obtained from the higher temperature, it indicated that higher temperature provided the beads with more aldehyde functional group and this was also an important evidence that polyglutaraldehyde was on the activated beads.

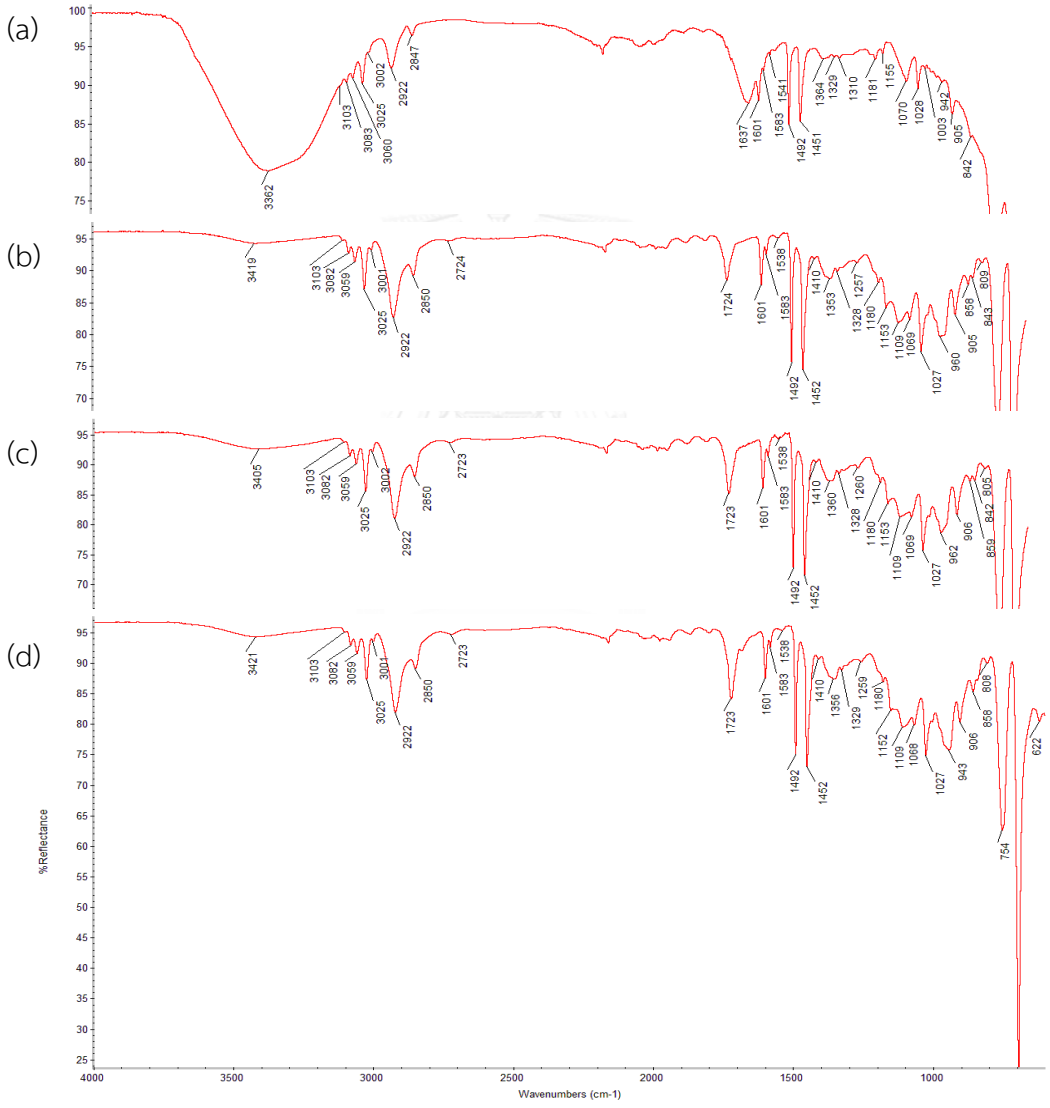

Figure 4.19 ATR-FTIR spectra of (a) 1%CHI-15%STY/PS beads and 1%CHI-15%STY/PS beads activated with 25% (w/v) glutaraldehyde solution at temperatures, (b) 40°C, (c) 60°C and (d) 80°C, for 24 hours

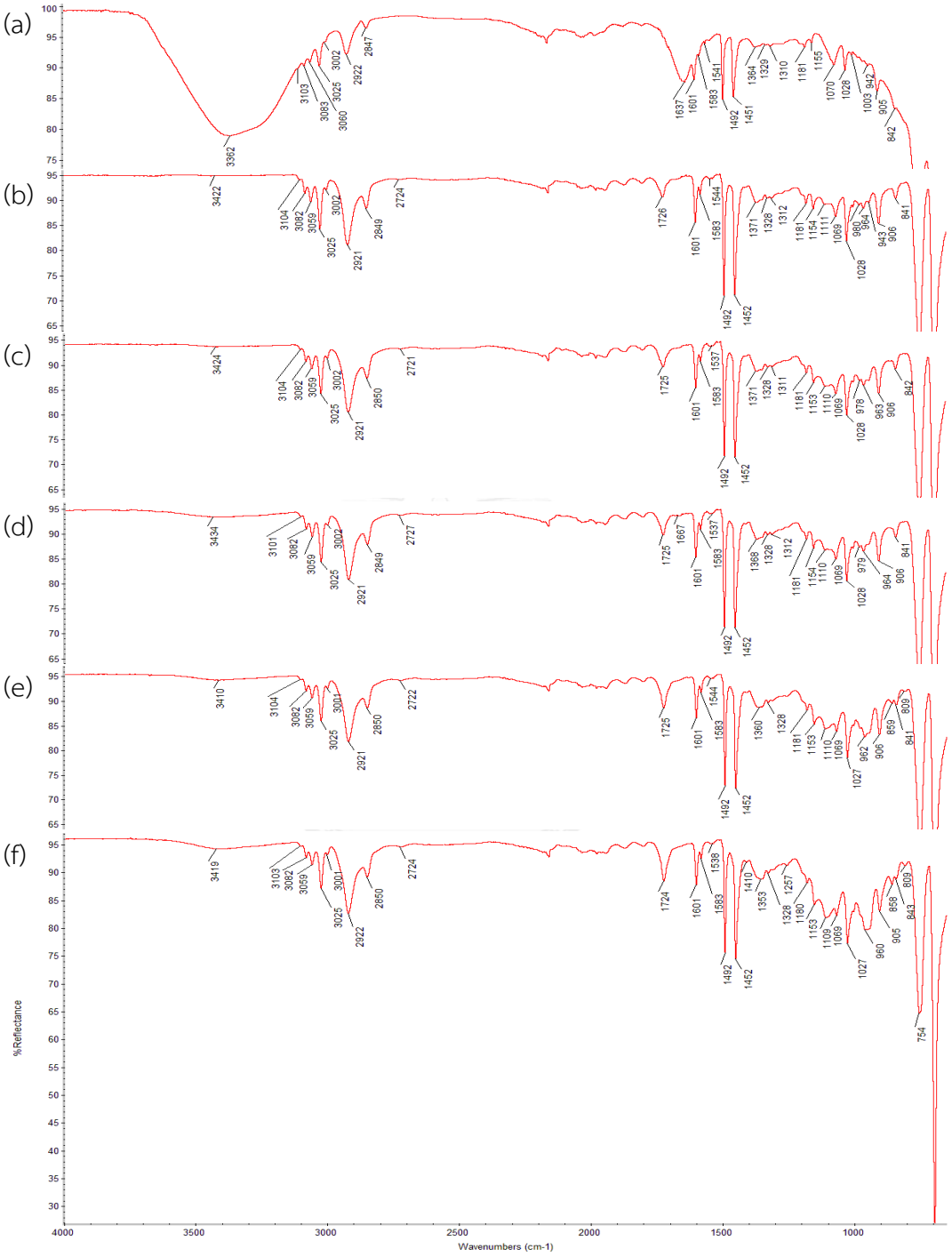

Figure 4.20 ATR-FTIR spectra of 1%CHI-15%STY/PS beads activated with various concentrations of glutaraldehyde solution at 40°C for 24 hours (a) 1%CHI-15%STY/PS beads (b) 5% (w/v) GLU (c) 10% (w/v) GLU (d) 15% (w/v) GLU (e) 20% (w/v) GLU and (f) 25% (w/v) GLU

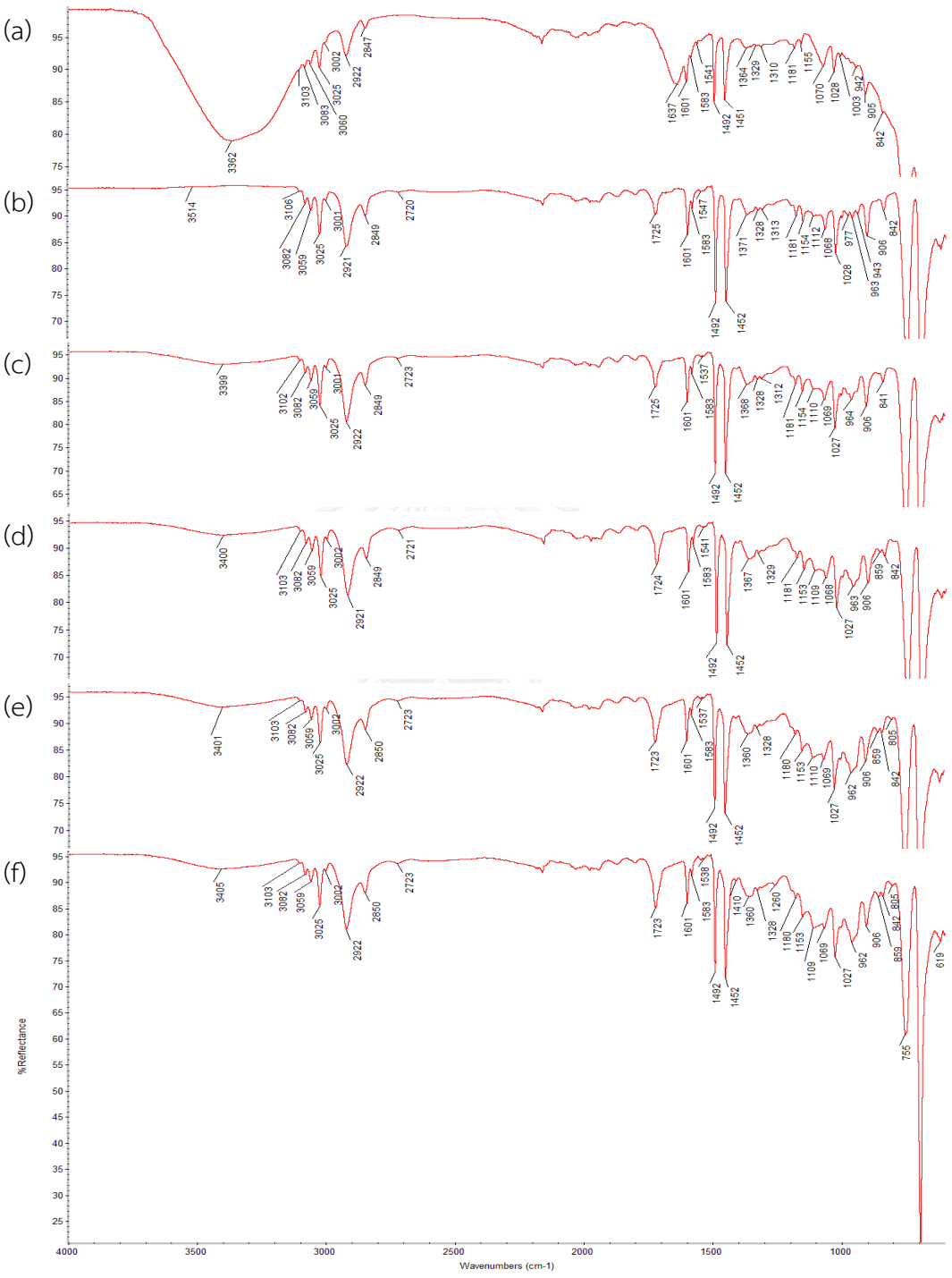

Figure 4.21 ATR-FTIR spectra of 1%CHI-15%STY/PS beads activated with various concentrations of glutaraldehyde solution at 60°C for 24 hours (a) 1%CHI-15%STY/PS beads (b) 5% (w/v) GLU (c) 10% (w/v) GLU (d) 15% (w/v) GLU (e) 20% (w/v) GLU and (f) 25% (w/v) GLU

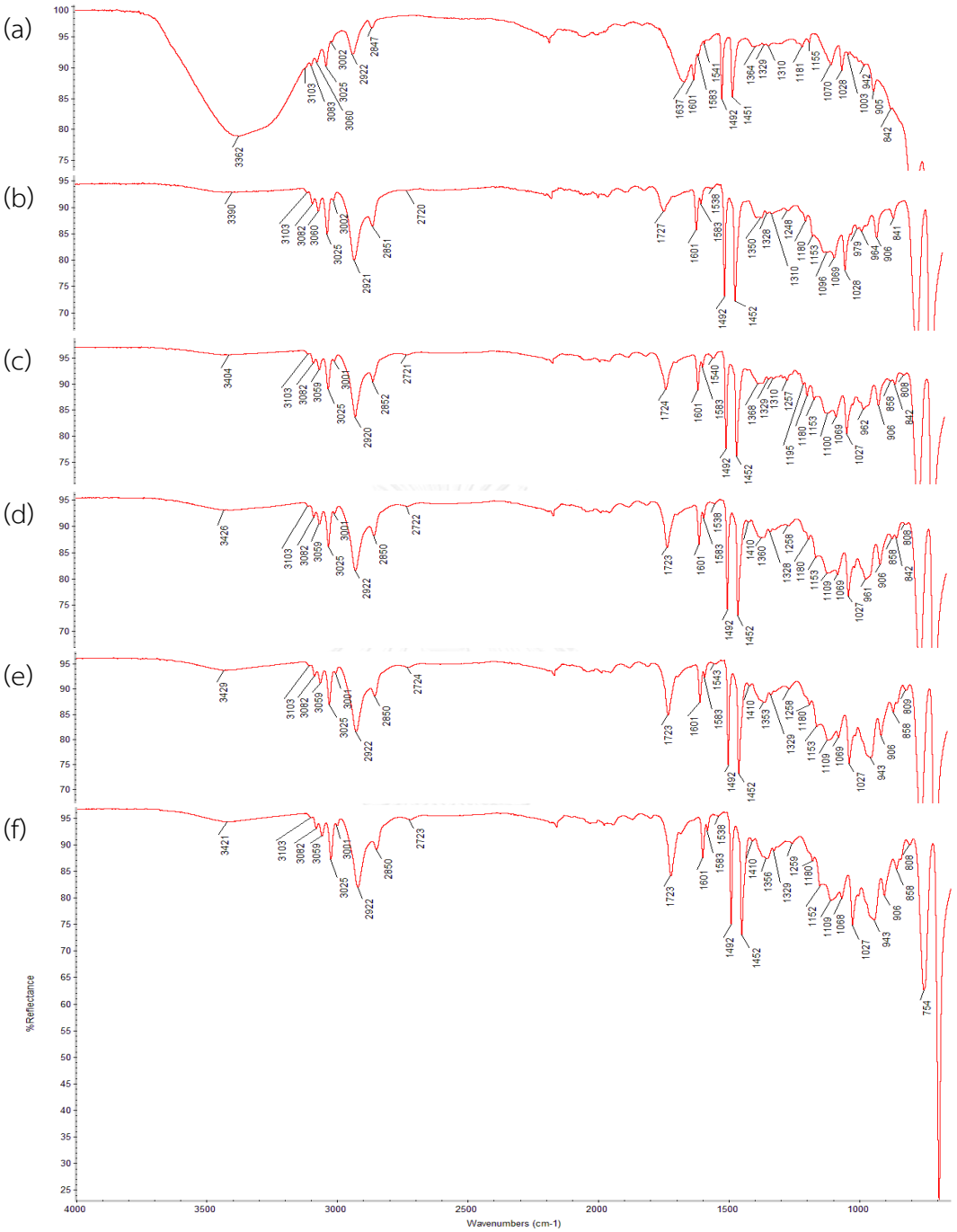

Figure 4.22 ATR-FTIR spectra of 1%CHI-15%STY/PS beads activated with various concentrations of glutaraldehyde solution at 80°C for 24 hours (a) 1%CHI-15%STY/PS beads (b) 5% (w/v) GLU (c) 10% (w/v) GLU (d) 15% (w/v) GLU (e) 20% (w/v) GLU and (f) 25% (w/v) GLU

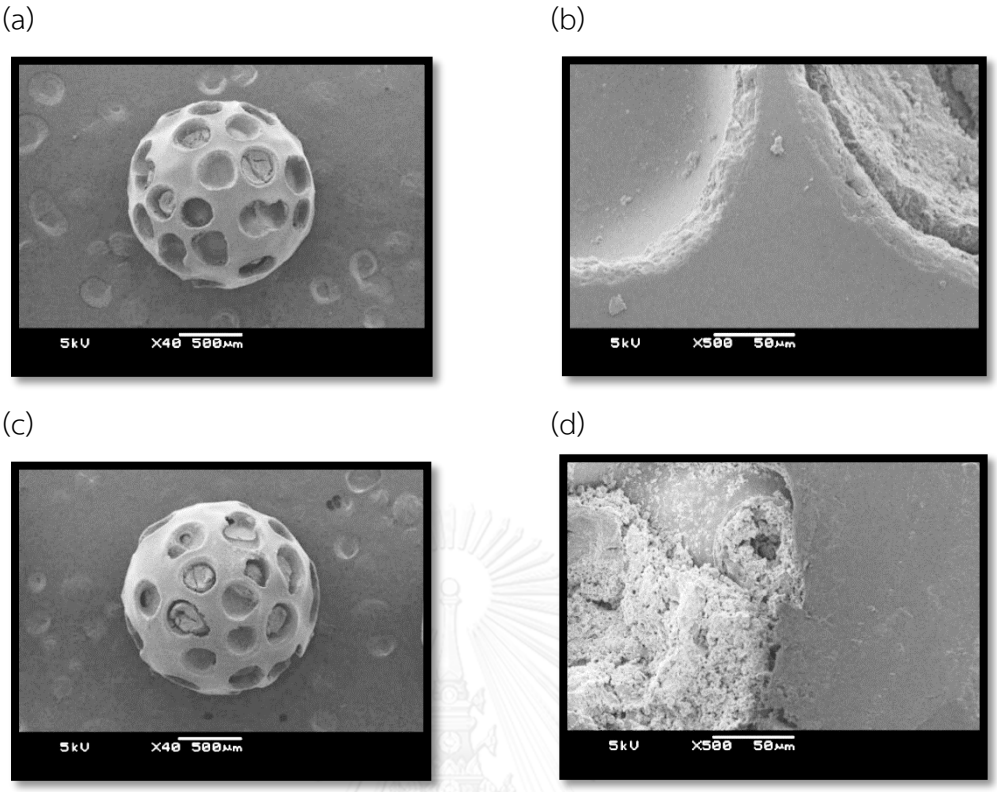

Figure 4.23 SEM micrographs of 1%CHI-15%STY/PS beads, (a) (X40) and (b) (X500) and 20%GLU-1%CHI-15%STY/PS beads obtained at 80°C for 24 hours, (c) (X40) and (d) (X500)

In Figure 4.23, SEM micrographs of 20%GLU-1%CHI-15%STY/PS beads are almost the same as 1%CHI-15%STY/PS beads except 20%GLU-1%CHI-15%STY/PS beads at magnification of 500X in Figure 4.23 (b) showed rough surface roughness in the hole. This indicated that chitosan-styrene copolymer might only be retained in the holes of the beads and styrene monomer might serve to help coating or holding the chitosan onto polystyrene beads through copolymerization. In addition, SEM micrographs of the 20%GLU-1%CHI-15%STY/PS beads also showed good phase compatibility between the chitosan-styrene copolymer and glutaraldehyde.

4.2.1.2 2%CHI-15%STY/PS beads activated with various concentrations of glutaraldehyde solution at 40, 60 and 80°C for 24 hours

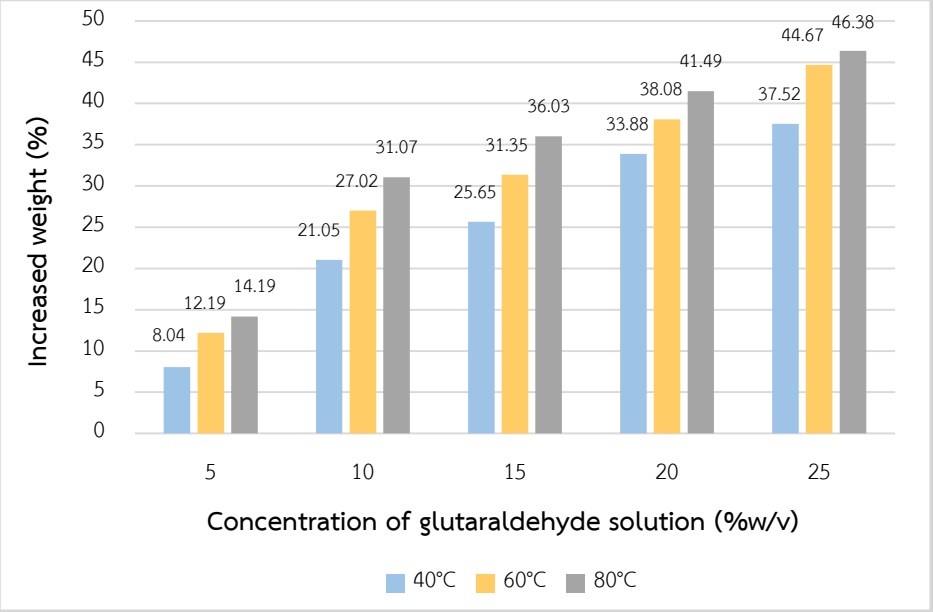

Figure 4.24 Percentage of increased weight of 2%CHI-15%STY/PS beads activated with various concentrations of glutaraldehyde solution at 40, 60 and 80°C for 24 hours

Table 4.4 presented the average diameter and percentage of increased weight of 2%CHI-15%STY/PS beads activated with various concentrations of glutaraldehyde solution at 40, 60 and 80°C for 24 hours. The effect of concentration of glutaraldehyde solution (the range from 5 to 25% w/v) activated with 2%CHI-15%STY/PS beads at various temperature (the range from 40 to 80°C) for 24 hours were studied. The results showed that increasing concentration of glutaraldehyde solution resulted in increase of weight of the beads at each temperature as presented in Figure 4.24. Because of increase of the average diameter when used glutaraldehyde solution (5 to 25% w/v) at 40 to 60°C, it indicated that the amino group not only reacted with glutaraldehyde but also with polyglutaraldehyde. In Figure 4.25-4.26, color of the 2%CHI-15%STY/PS beads activated with higher concentration of glutaraldehyde or higher temperature was more yellow than of the lower ones. At 80°C color of the 2%CHI-15%STY/PS beads obtained from each concentration of glutaraldehyde solution used became brown color beads as shown in Figure 4.27. Changing in color due to concentration and

temperature also supported that polyglutaraldehyde present in the glutaraldehyde solution could react with amino group and was presented on the beads. Thus, the highest percentage of increased weight was obtained from 80°C when compared at other temperatures.

(a) 5% (w/v) GLU

(b) 10% (w/v) GLU

(c) 15% (w/v) GLU

(d) 20% (w/v) GLU

(e) 25% (w/v) GLU

Figure 4.25 Comparison of 2%CHI-15%STY/PS beads activated with various concentrations of glutaraldehyde solution at 40°C for 24 hours (a) 5% (w/v) GLU (b) 10% (w/v) GLU (c) 15% (w/v) GLU (d) 20% (w/v) GLU and (e) 25% (w/v) GLU

(a) 5% (w/v) GLU

(b) 10% (w/v) GLU

(c) 15% (w/v) GLU

(d) 20% (w/v) GLU

(e) 25% (w/v) GLU

Figure 4.26 Comparison of 2%CHI-15%STY/PS beads activated with various concentrations of glutaraldehyde solution at 60°C for 24 hours (a) 5% (w/v) GLU (b) 10% (w/v) GLU (c) 15% (w/v) GLU (d) 20% (w/v) GLU and (e) 25% (w/v) GLU

(a) 5% (w/v) GLU

(b) 10% (w/v) GLU

(c) 15% (w/v) GLU

(d) 20% (w/v) GLU

(e) 25% (w/v) GLU

Figure 4.27 Comparison of 2%CHI-15%STY/PS beads activated with various concentrations of glutaraldehyde solution at 80°C for 24 hours (a) 5% (w/v) GLU (b) 10% (w/v) GLU (c) 15% (w/v) GLU (d) 20% (w/v) GLU and (e) 25% (w/v) GLU

In comparison of ATR-FTIR spectra (Figure 4.28 to 4.31) of 2%CHI-15%STY/PS beads and activated 2%CHI-15%STY/PS beads, low intensity of the absorption of -OH and -NH stretching vibrations (around 3358 cm^{-1}) and of -NH bending vibration in $-NH_2$

(1635 cm^{-1}) and appearance of absorption at about 1723 and 2723 cm^{-1} (for -CO stretching vibration and C-H stretching vibration of aldehyde, respectively) indicated that most of amino group was reacted with the aldehydes. Because of stronger intensity of the absorption at about 1723 cm^{-1} obtained from the higher temperature, it indicated that higher temperature provided the beads with more aldehyde functional group and this was also an important evidence that polyglutaraldehyde was on the activated beads.

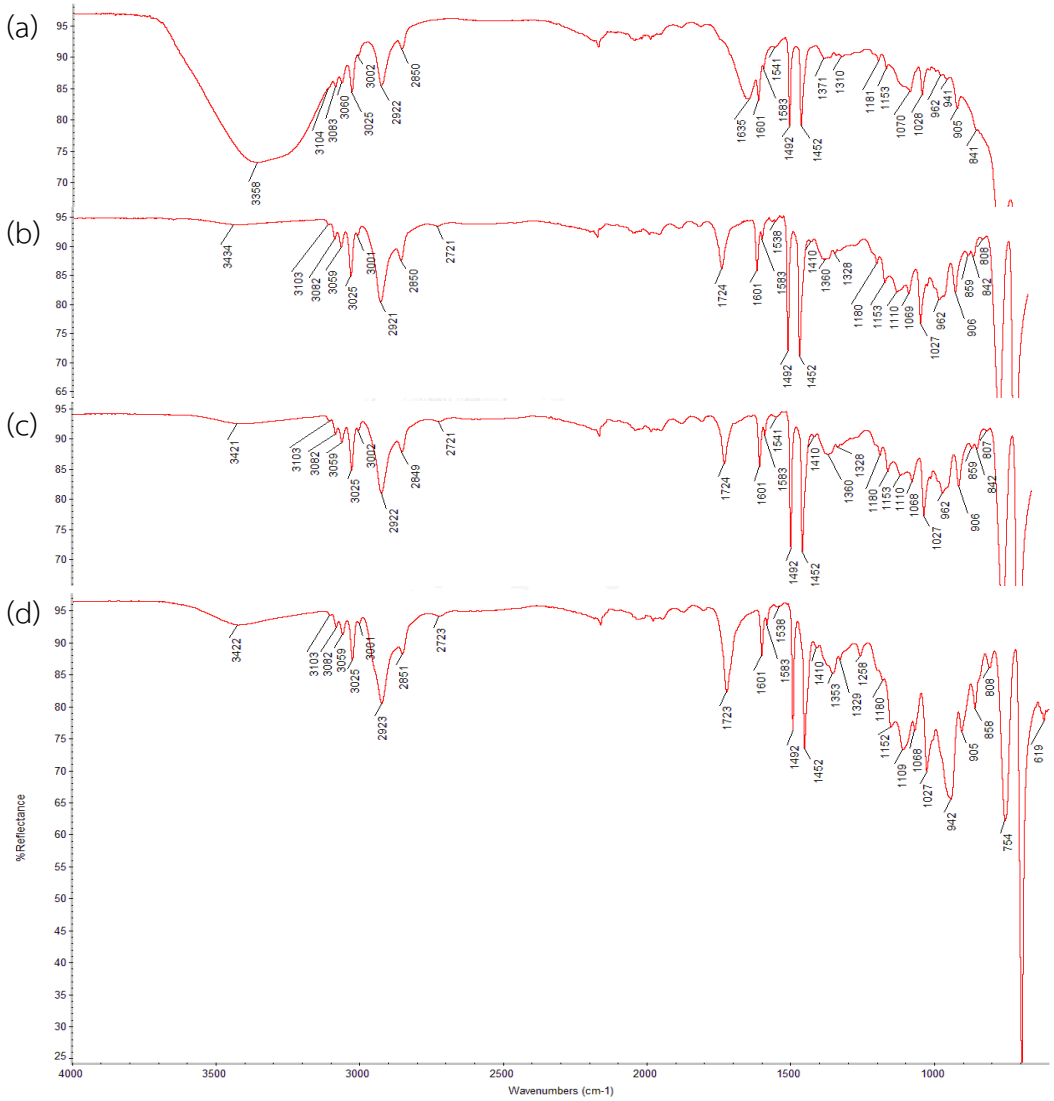

Figure 4.28 ATR-FTIR spectra of (a) 2%CHI-15%STY/PS beads and 2%CHI-15%STY/PS beads activated with 25% (w/v) glutaraldehyde solution at temperatures, (b) 40°C, (c) 60°C and (d) 80°C, for 24 hours

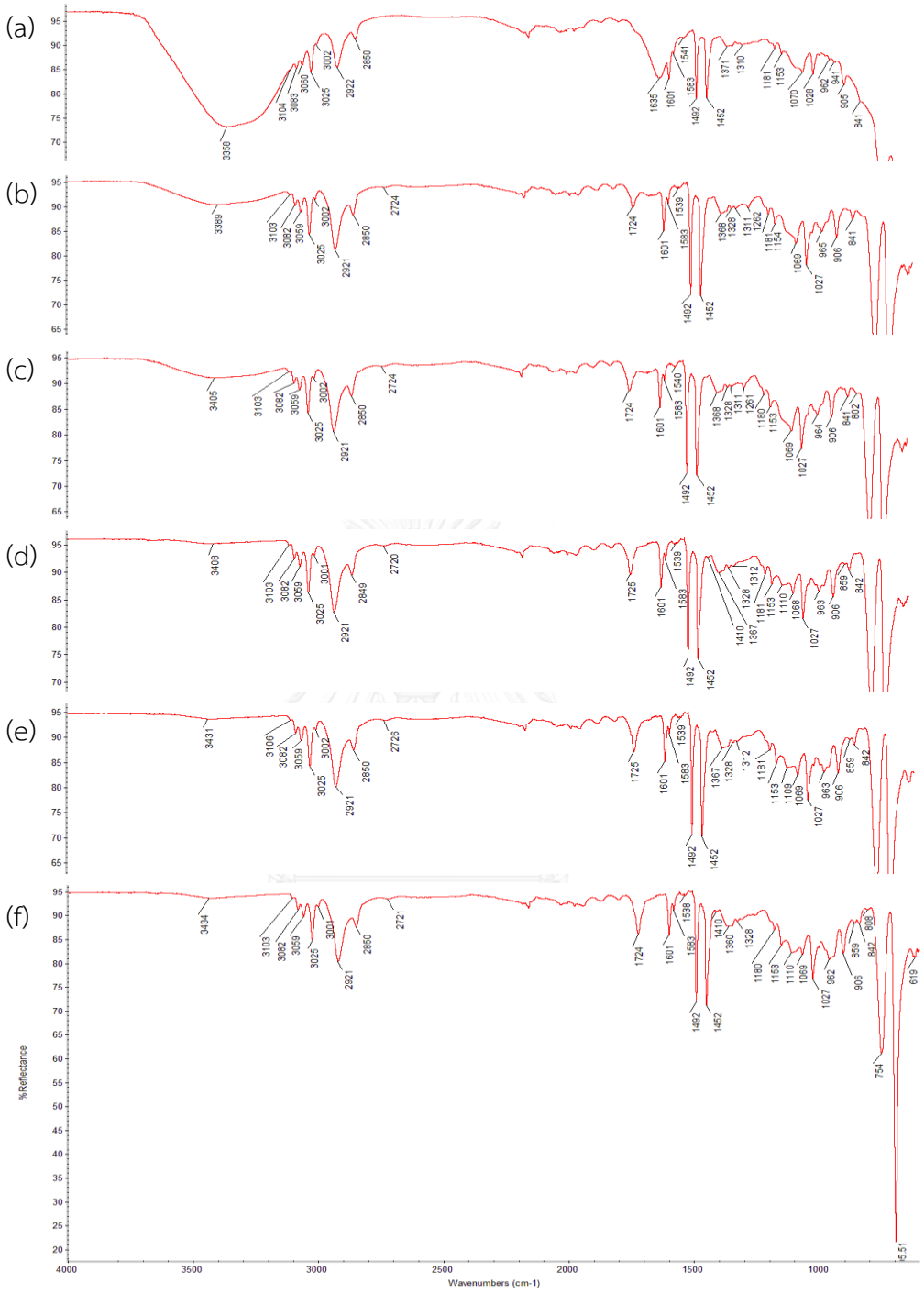

Figure 4.29 ATR-FTIR spectra of 2%CHI-15%STY/PS beads activated with various concentrations of glutaraldehyde solution at 40°C for 24 hours (a) 2%CHI-15%STY/PS beads (b) 5% (w/v) GLU (c) 10% (w/v) GLU (d) 15% (w/v) GLU (e) 20% (w/v) GLU and (f) 25% (w/v) GLU

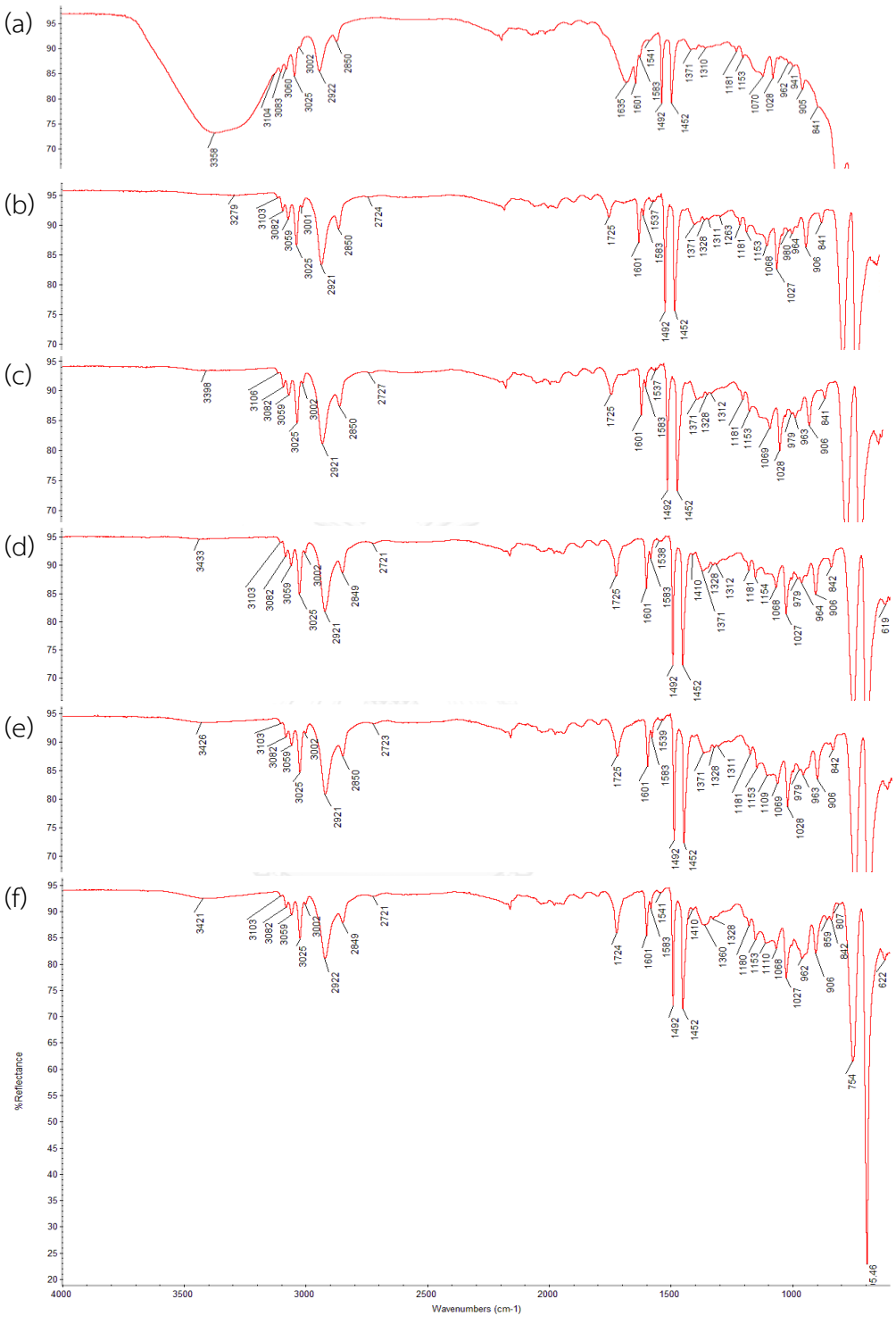

Figure 4.30 ATR-FTIR spectra of 2%CHI-15%STY/PS beads activated with various concentrations of glutaraldehyde solution at 60°C for 24 hours (a) 2%CHI-15%STY/PS beads (b) 5% (w/v) GLU (c) 10% (w/v) GLU (d) 15% (w/v) GLU (e) 20% (w/v) GLU and (f) 25% (w/v) GLU

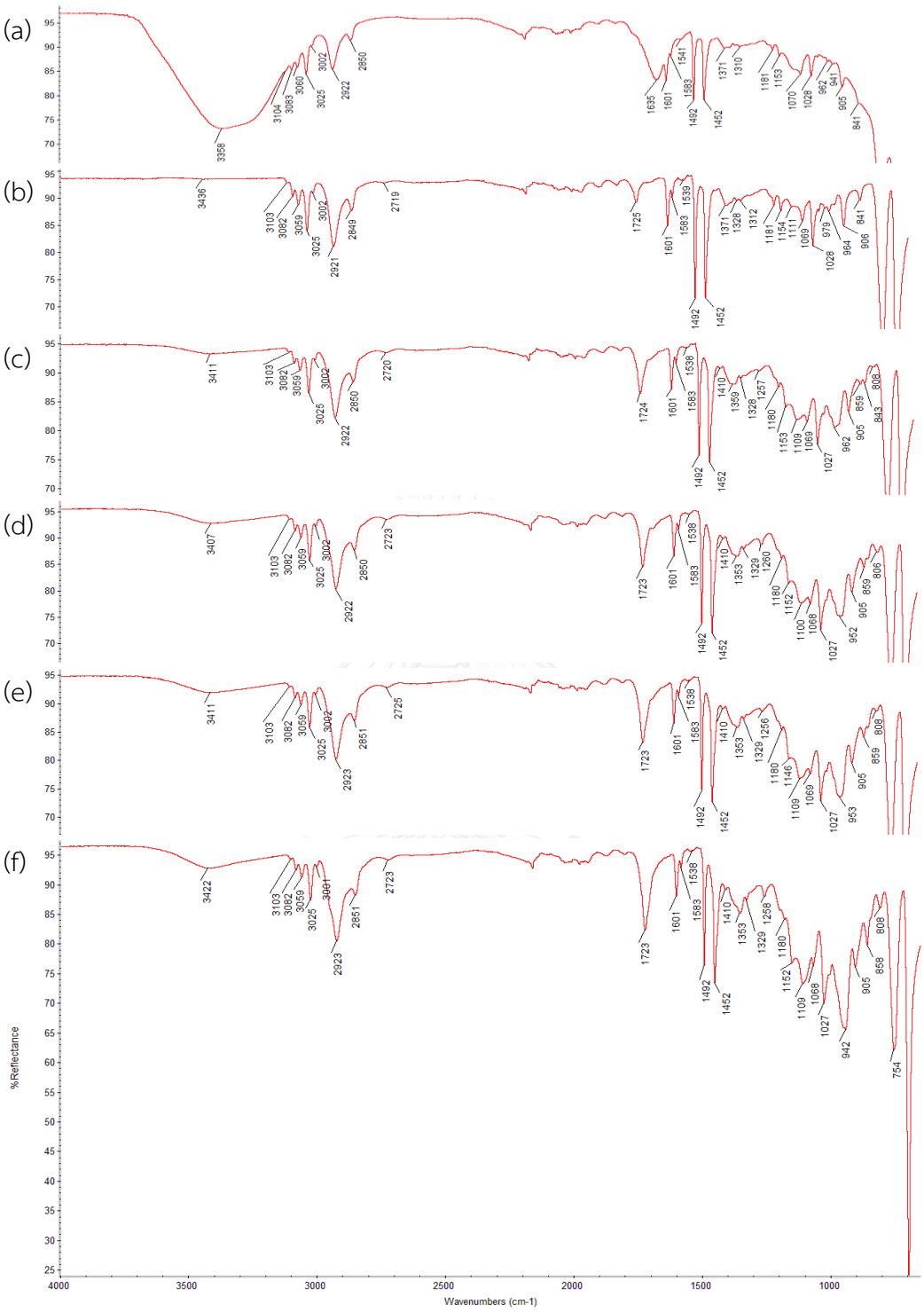

Figure 4.31 ATR-FTIR spectra of 2%CHI-15%STY/PS beads activated with various concentrations of glutaraldehyde solution at 80°C for 24 hours (a) 2%CHI-15%STY/PS beads (b) 5% (w/v) GLU (c) 10% (w/v) GLU (d) 15% (w/v) GLU (e) 20% (w/v) GLU and (f) 25% (w/v) GLU

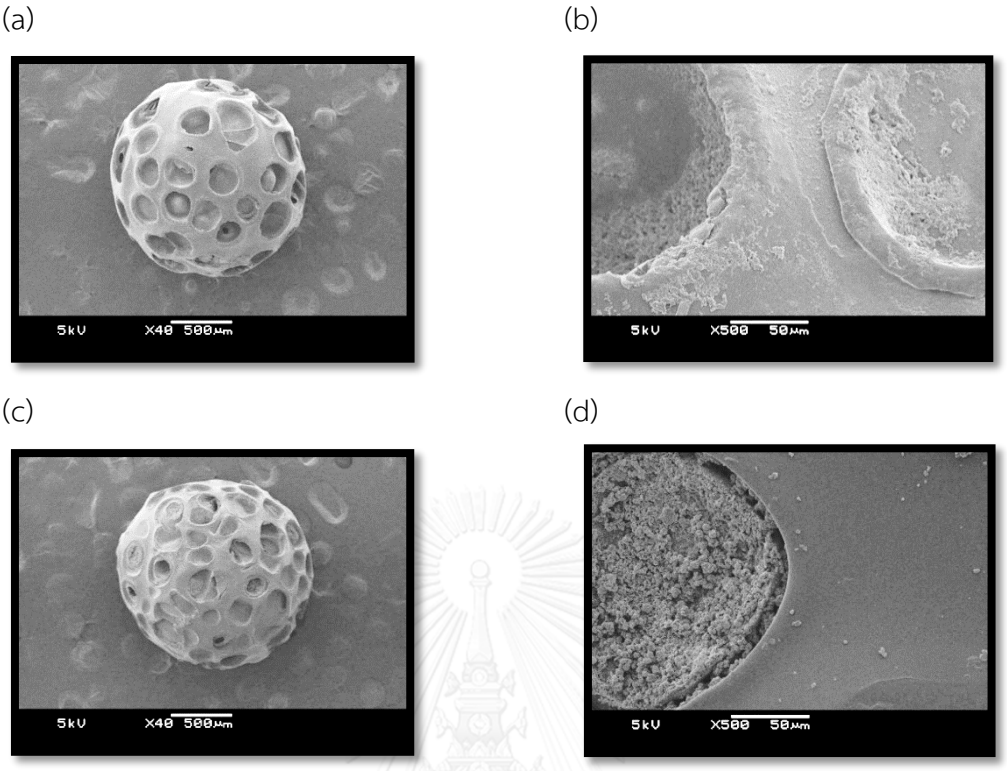

Figure 4.32 SEM micrographs of 2%CHI-15%STY/PS beads, (a) (X40) and (b) (X500) and 15%GLU-2%CHI-15%STY/PS beads obtained at 80°C for 24 hours, (c) (X40) and (d) (X500)

In Figure 4.32, SEM micrographs of 15%GLU-2%CHI-15%STY/PS beads are almost the same as 2%CHI-15%STY/PS beads except 15%GLU-2%CHI-15%STY/PS beads at magnification of 500X in Figure 4.32 (b) showed rough surface roughness in the hole. This indicated that chitosan-styrene copolymer might only be retained in the holes of the beads and styrene monomer might serve to help coating or holding the chitosan onto polystyrene beads through copolymerization. In addition, SEM micrographs of the 15%GLU-2%CHI-15%STY/PS beads also showed good phase compatibility between the chitosan-styrene copolymer and glutaraldehyde.

4.2.1.3 3%CHI-15%STY/PS beads activated with various concentrations of glutaraldehyde solution at 40, 60 and 80°C for 24 hours

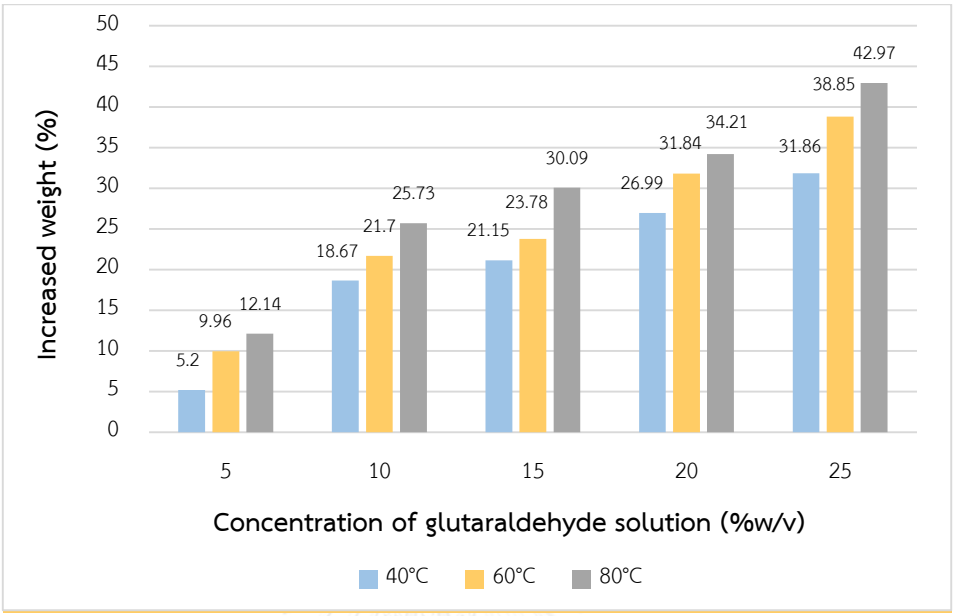

Figure 4.33 Percentage of increased weight of 3%CHI-15%STY/PS beads activated with various concentrations of glutaraldehyde solution at 40, 60 and 80°C for 24 hours

Table 4.4 presented the average diameter and percentage of increased weight of 3%CHI-15%STY/PS beads activated with various concentrations of glutaraldehyde solution at 40, 60 and 80°C for 24 hours. The effect of concentration of glutaraldehyde solution (the range from 5 to 25% w/v) activated with 3%CHI-15%STY/PS beads at various temperature (the range from 40 to 80°C) for 24 hours were studied. The results showed that increasing concentration of glutaraldehyde solution resulted in increase of weight of the beads at each temperature as presented in Figure 4.33. Because of increase of the average diameter when used glutaraldehyde solution (5 to 25% w/v) at 40 to 60°C, it indicated that the amino group not only reacted with glutaraldehyde but also with polyglutaraldehyde. In Figure 4.34-4.35, color of the 3%CHI-15%STY/PS beads activated with higher concentration of glutaraldehyde or higher temperature was more yellow than of the lower ones. At 80°C color of the 3%CHI-15%STY/PS beads obtained from each concentration of glutaraldehyde solution used became brown color beads as shown in Figure 4.36. Changing in color due to concentration and

temperature also supported that polyglutaraldehyde present in the glutaraldehyde solution could react with amino group and was presented on the beads. Thus, the highest percentage of increased weight was obtained from 80°C when compared at other temperatures.

(a) 5% (w/v) GLU

(b) 10% (w/v) GLU

(c) 15% (w/v) GLU

(d) 20% (w/v) GLU

(e) 25% (w/v) GLU

Figure 4.34 Comparison of 3%CHI-15%STY/PS beads activated with various concentrations of glutaraldehyde solution at 40°C for 24 hours (a) 5% (w/v) GLU (b) 10% (w/v) GLU (c) 15% (w/v) GLU (d) 20% (w/v) GLU and (e) 25% (w/v) GLU

(a) 5% (w/v) GLU

(b) 10% (w/v) GLU

(c) 15% (w/v) GLU

(d) 20% (w/v) GLU

(e) 25% (w/v) GLU

Figure 4.35 Comparison of 3%CHI-15%STY/PS beads activated with various concentrations of glutaraldehyde solution at 60°C for 24 hours (a) 5% (w/v) GLU (b) 10% (w/v) GLU (c) 15% (w/v) GLU (d) 20% (w/v) GLU and (e) 25% (w/v) GLU

(a) 5% (w/v) GLU

(b) 10% (w/v) GLU

(c) 15% (w/v) GLU

(d) 20% (w/v) GLU

(e) 25% (w/v) GLU

Figure 4.36 Comparison of 3%CHI-15%STY/PS beads activated with various concentrations of glutaraldehyde solution at 80°C for 24 hours (a) 5% (w/v) GLU (b) 10% (w/v) GLU (c) 15% (w/v) GLU (d) 20% (w/v) GLU and (e) 25% (w/v) GLU

In comparison of ATR-FTIR spectra (Figure 4.37 to 4.40) of 3%CHI-15%STY/PS beads and activated 3%CHI-15%STY/PS beads, low intensity of the absorption of -OH

and -NH stretching vibrations (around 3355 cm^{-1}) and of -NH bending vibration in $-NH_2$ (1636 cm^{-1}) and appearance of absorption at about 1722 and 2720 cm^{-1} (for -CO stretching vibration and C-H stretching vibration of aldehyde, respectively) indicated that most of amino group was reacted with the aldehydes. Because of stronger intensity of the absorption at about 1722 cm^{-1} obtained from the higher temperature, it indicated that higher temperature provided the beads with more aldehyde functional group and this was also an important evidence that polyglutaraldehyde was on the activated beads.

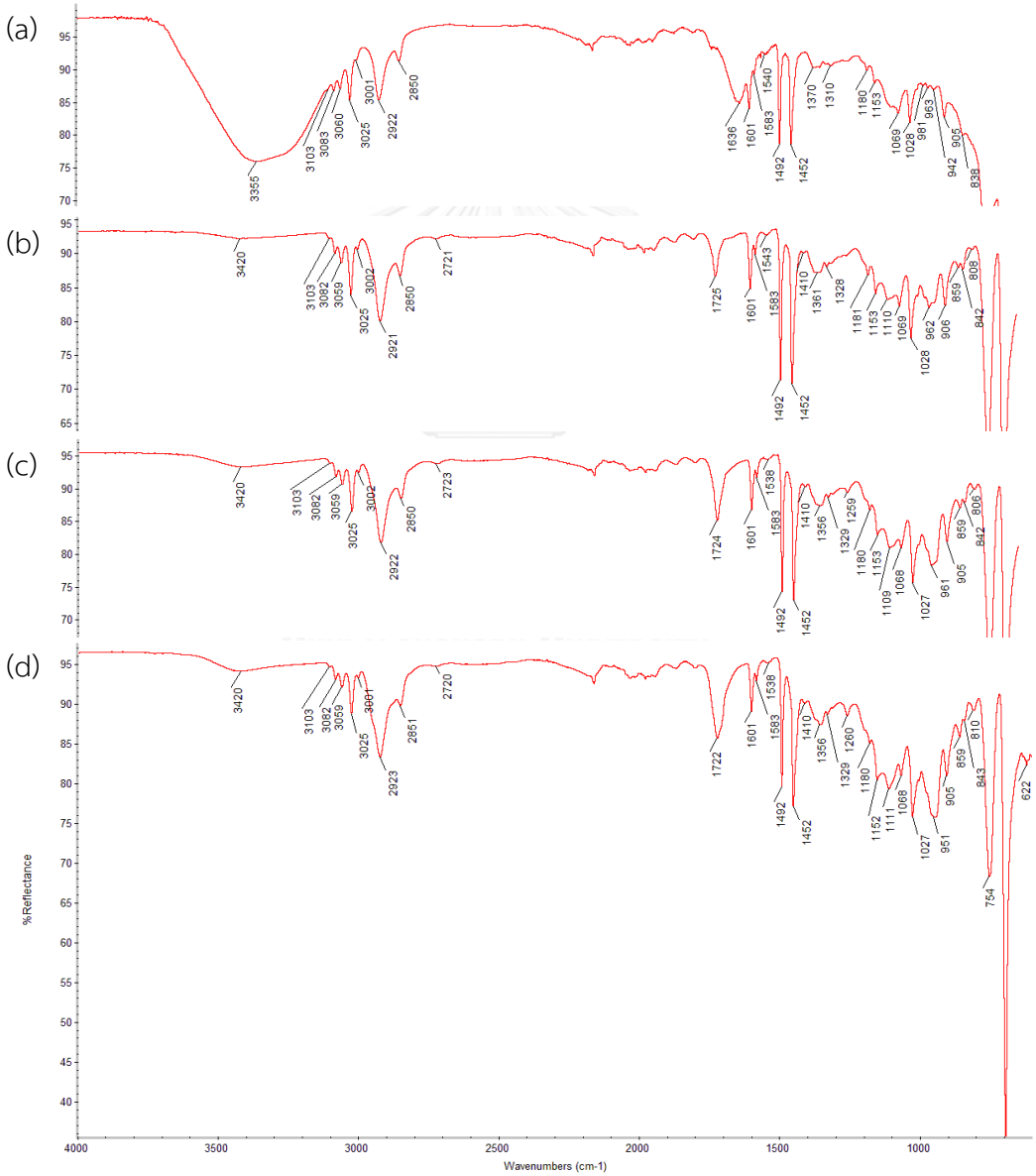

Figure 4.37 ATR-FTIR spectra of (a) 3%CHI-15%STY/PS beads and 3%CHI-15%STY/PS beads activated with 25% (w/v) glutaraldehyde solution at temperatures, (b) 40°C, (c) 60°C and (d) 80°C, for 24 hours

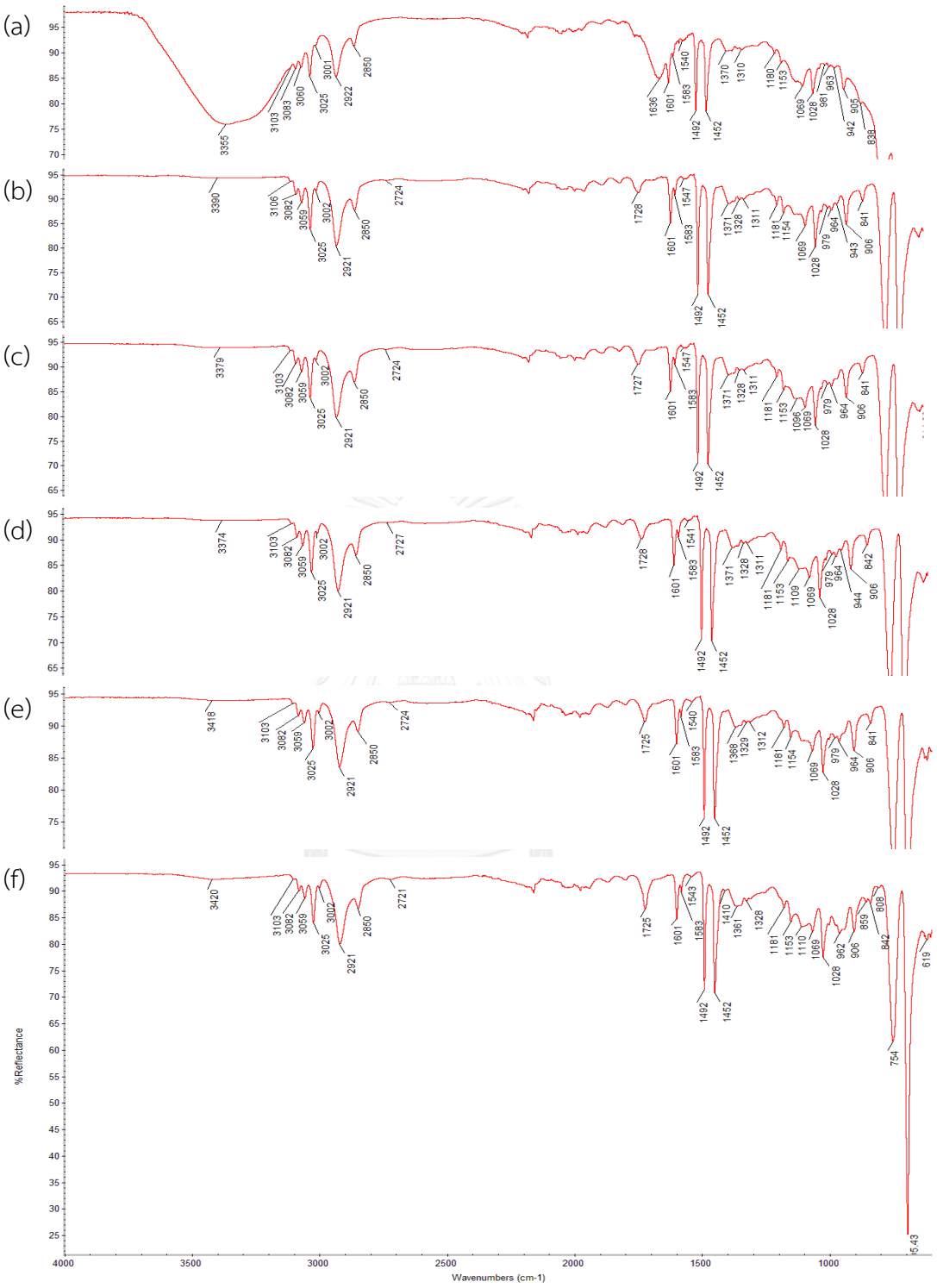

Figure 4.38 ATR-FTIR spectra of 3%CHI-15%STY/PS beads activated with various concentrations of glutaraldehyde solution at 40°C for 24 hours (a) 3%CHI-15%STY/PS beads (b) 5% (w/v) GLU (c) 10% (w/v) GLU (d) 15% (w/v) GLU (e) 20% (w/v) GLU and (f) 25% (w/v) GLU

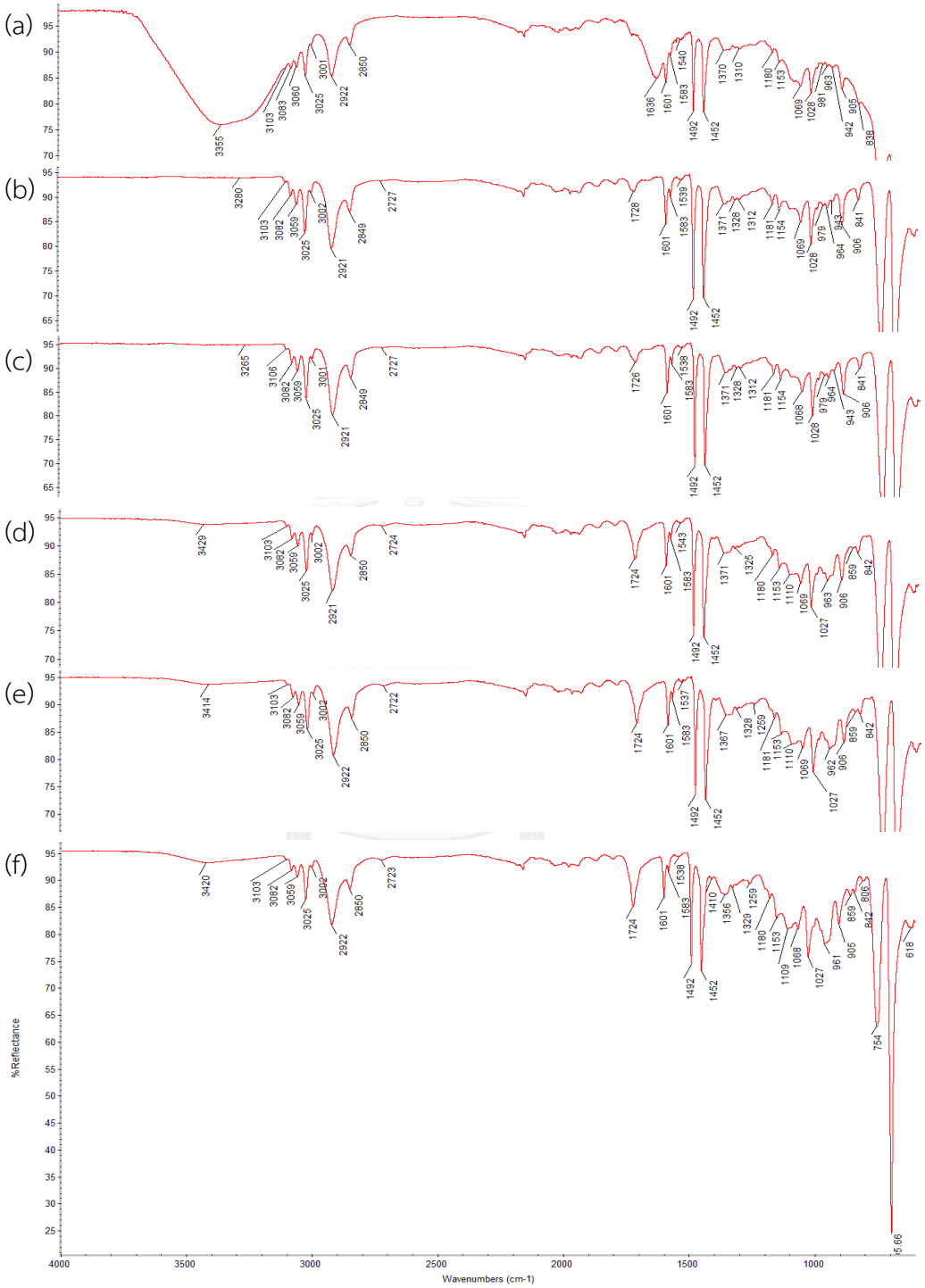

Figure 4.39 ATR-FTIR spectra of 3%CHI-15%STY/PS beads activated with various concentrations of glutaraldehyde solution at 60°C for 24 hours (a) 3%CHI-15%STY/PS beads (b) 5% (w/v) GLU (c) 10% (w/v) GLU (d) 15% (w/v) GLU (e) 20% (w/v) GLU and (f) 25% (w/v) GLU

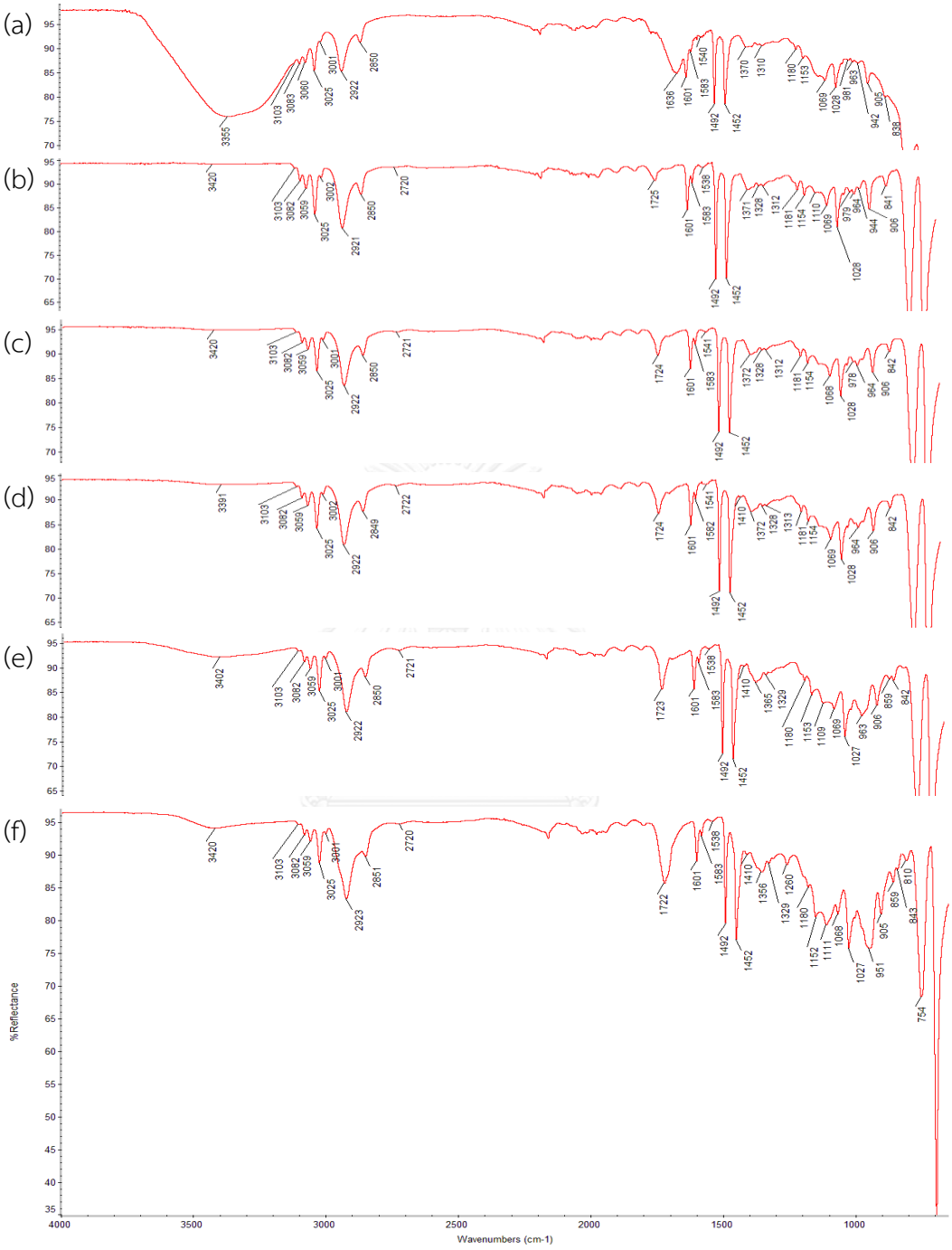

Figure 4.40 ATR-FTIR spectra of 3%CHI-15%STY/PS beads activated with various concentrations of glutaraldehyde solution at 80°C for 24 hours (a) 3%CHI-15%STY/PS beads (b) 5% (w/v) GLU (c) 10% (w/v) GLU (d) 15% (w/v) GLU (e) 20% (w/v) GLU and (f) 25% (w/v) GLU

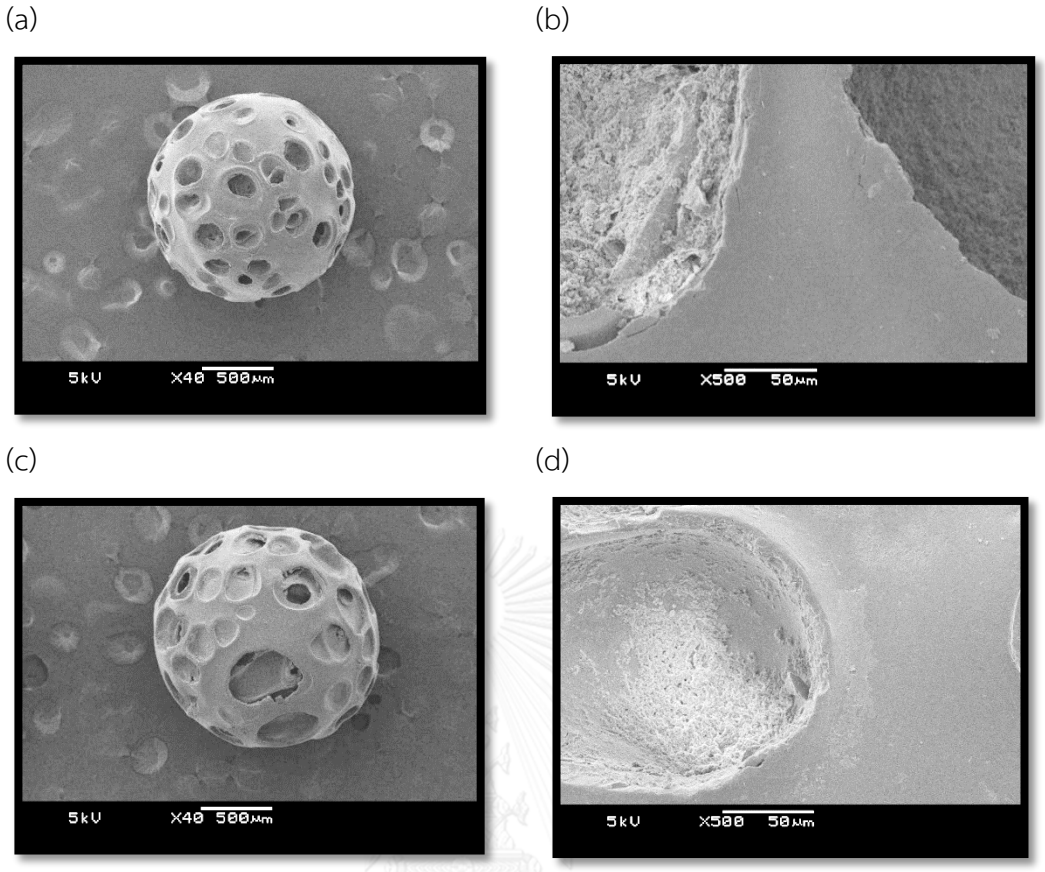

Figure 4.41 SEM micrographs of 3%CHI-15%STY/PS beads, (a) (X40) and (b) (X500) and 20%GLU-3%CHI-15%STY/PS beads obtained at 80°C for 24 hours, (c) (X40) and (d) (X500)

In Figure 4.41, SEM micrographs of 20%GLU-3%CHI-15%STY/PS beads are almost the same as 3%CHI-15%STY/PS beads except 20%GLU-3%CHI-15%STY/PS beads at magnification of 500X in Figure 4.41 (b) showed rough surface roughness in the hole. This indicated that chitosan-styrene copolymer might only be retained in the holes of the beads and styrene monomer might serve to help coating or holding the chitosan onto polystyrene beads through copolymerization. In addition, SEM micrographs of the 20%GLU-3%CHI-15%STY/PS beads also showed good phase compatibility between the chitosan-styrene copolymer and glutaraldehyde.

4.2.2 Effect of time

The effect of glutaraldehyde-treated time on 2%CHI-15%STY/PS beads was investigated at 4, 8, 12, 24, 28 and 32 hours and glutaraldehyde solution (25% w/v). As the results, the various time have effect to activate with glutaraldehyde.

Table 4.5 Average diameter and percentage of increased weight of 25%GLU-2%CHI-15%STY/PS beads at 80°C for various times

concentration of chitosan solution (%w/v)	concentration of glutaraldehyde solution (%w/v)	time (h)	temperature (80°C)	
			average diameter (mm)	increased weight (%)
2	25	4	1.599	16.52
		8	1.670	28.43
		12	1.769	37.97
		24	1.848	46.38
		28	1.851	46.80
		32	1.864	47.51

*average diameter of original 2%CHI-15%STY/PS beads = 1.577 mm

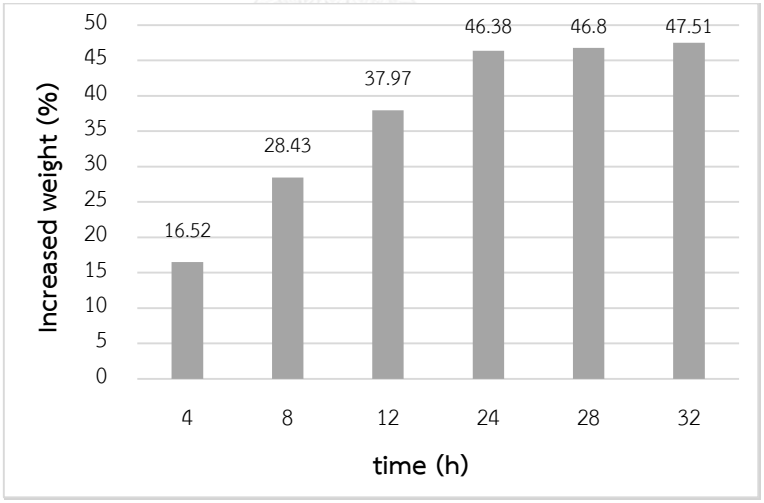

Figure 4.42 Percentage of increased weight of 25%GLU-2%CHI-15%STY/PS beads at 80°C for 4, 8, 12, 24, 28 and 32 hours of reaction time

Table 4.5 presented the average diameter and percentage of increased weight of 25%GLU-2%CHI-15%STY/PS beads at 80°C for various times. The results showed that increasing time resulted in increase of weight of the beads at each time as

presented in Figure 4.42. The color of the 25%GLU-2%CHI-15%STY/PS beads obtained from each time used became brown color beads as shown in Figure 4.43. Changing in color due to time also supported that polyglutaraldehyde present in the glutaraldehyde solution could react with amino group and was presented on the beads. Thus, the highest percentage of increased weight was obtained for 24 hours when compared at other time.

(a) 4 hours

(b) 8 hours

(c) 12 hours

(d) 24 hours

(e) 28 hours

(f) 32 hours

Figure 4.43 25%GLU-2%CHI-15%STY/PS beads obtained at 80°C for (a) 4 hours (b) 8 hours (c) 12 hours (d) 24 hours (e) 28 hours and (f) 32 hours of glutaraldehyde-treated time

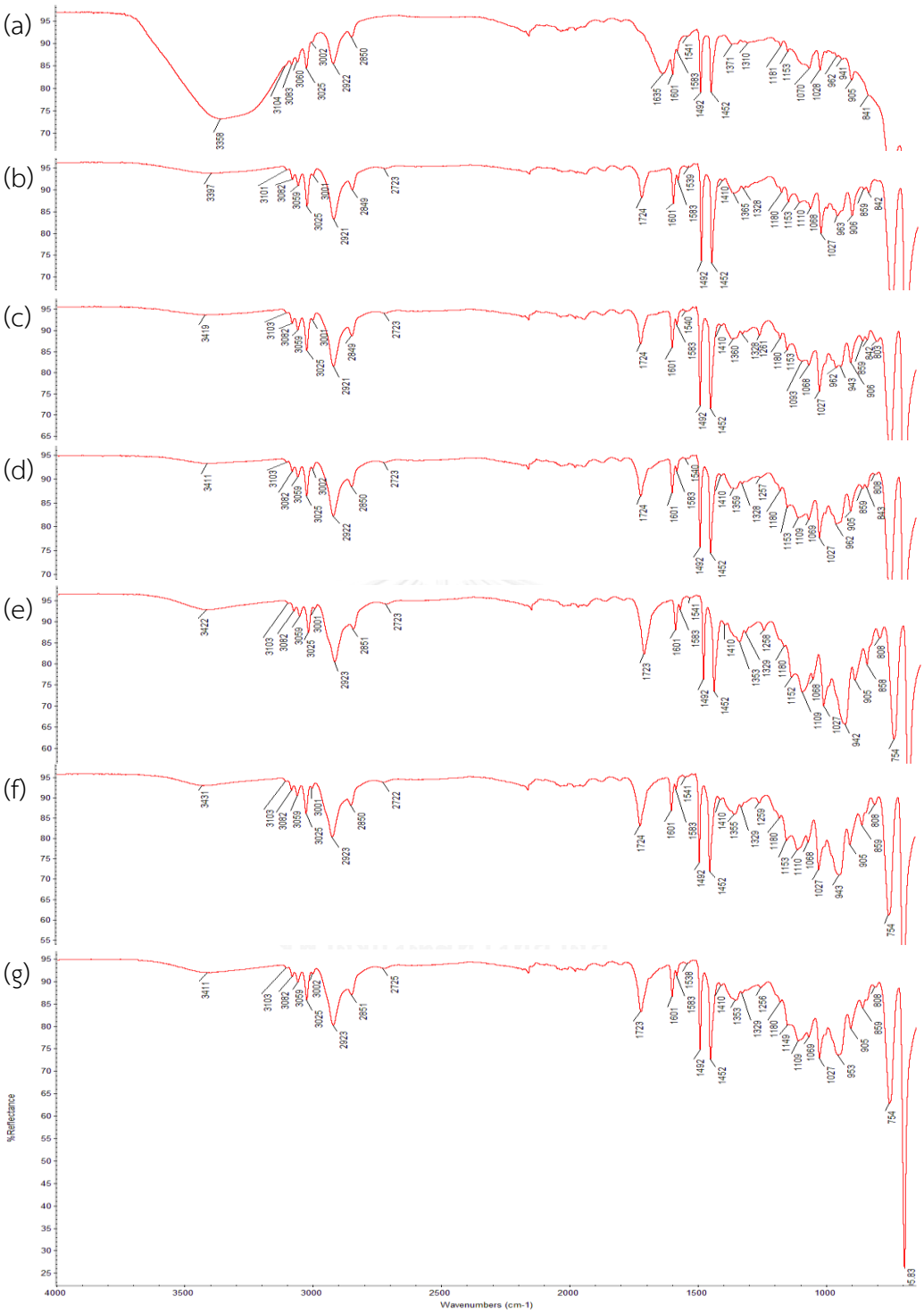

Figure 4.44 ATR-FTIR spectra of (a) 2%CHI-15%STY/PS beads and 2%CHI-15%STY/PS beads activated with 25% (w/v) glutaraldehyde solution at time, (b) 4 hours (c) 8 hours (d) 12 hours (e) 24 hours (f) 28 hours and (g) 32 hours for (a) 4 hours (b) 8 hours (c) 12 hours (d) 24 hours (e) 28 hours and (f) 32 hours, at 80°C

In comparison of ATR-FTIR spectra (Figure 4.44) of 2%CHI-15%STY/PS beads and activated 2%CHI-15%STY/PS beads, low intensity of the absorption of -OH and -NH stretching vibrations (around 3358 cm^{-1}) and of -NH bending vibration in $-NH_2$ (1635 cm^{-1}) and appearance of absorption at about 1723 and 2723 cm^{-1} (for -CO stretching vibration and C-H stretching vibration of aldehyde, respectively) indicated that most of amino group was reacted with the aldehydes. Because of stronger intensity of the absorption at about 1723 cm^{-1} obtained from the higher time, it indicated that higher time provided the beads with more aldehyde functional group and this was also an important evidence that polyglutaraldehyde was on the activated beads. In the results, it was found that chitosan-styrene copolymer were successfully activated with glutaraldehyde at 80°C for 24 hours because intensity of signal was relatively constant after 24 hours. This is consistent with the percentage in coating as shown in Figure 4.42.

4.3 Immobilization of lipase onto GLU-CHI-STY/PS beads

To optimize the conditions for lipase immobilization onto GLU-CHI-STY/PS beads various concentration of glutaraldehyde solution (5-25% w/v), amounts of lipase (6.0-48.0 mg) and immobilization time (48-96 h) were studied and efficiency of *P. cepacia* lipase immobilized onto GLU-CHI-STY/PS beads was evaluated in term of lipase activity, protein loading yield and specific activity. Immobilization of lipase onto GLU-CHI-STY/PS beads were presented in Scheme 4.2.

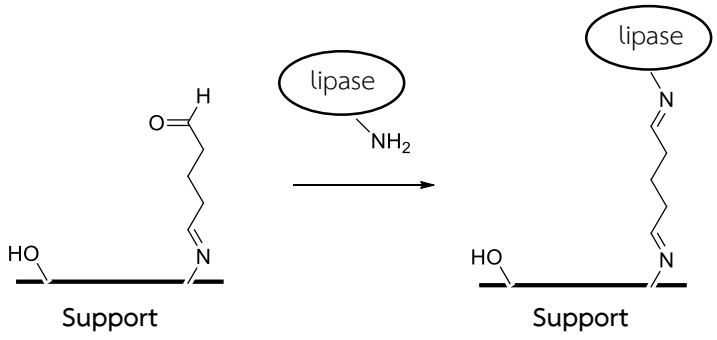

Scheme 4.2 Schematic representative for lipase immobilized of onto GLU-CHI-STY/PS beads

4.3.1 Effect of concentration of glutaraldehyde solution

4.3.1.1 Immobilization on lipase activity

The immobilization of *P. cepacia* lipase on GLU-CHI-STY/PS beads was performed via covalent binding method. For immobilization step, 18 mg of *P. cepacia* lipase were immobilized onto fifteen modified supports at 30°C of immobilization temperature for 72 hours in order to find out how much aldehyde functional group was suitable for immobilization of the lipase. The fifteen supports consisted the beads obtained from the 1%CHI-15%STY/PS beads, 2%CHI-15%STY/PS beads and 3%CHI-15%STY/PS beads activated with glutaraldehyde solution in the range from 5 to 25% (w/v) at 80°C for 24 hours.

The results (Figure 4.45) showed that increasing the concentration of glutaraldehyde solution resulted in increase of the lipase activity of the immobilized *P. cepacia* lipase except the beads activated by high glutaraldehyde concentration, > 20% glutaraldehyde for 1%CHI-15%STY/PS beads and 3%CHI-15%STY/PS beads and >15% glutaraldehyde for 2%CHI-15%STY/PS beads, resulted in decrease of lipase activity. Since chitosan is a product from deacetylation of chitin and it contains many free amino groups, using lower concentration of glutaraldehyde will provide low aldehyde groups for immobilization that gave low amount of the immobilized lipase and also low lipase activity. When the concentration of glutaraldehyde solution was increased and the more amino groups of chitosan were activated and resulted in increase of the immobilized lipase and of lipase activity. However, when too much concentration of glutaraldehyde solution was used, the lipase activity was decreased because the increasing amount of the lipase bound to the active aldehyde may change the spatial structure of the active center of the enzyme as described by Chen and coworker [82]. The maximal value of lipase activity onto 20%GLU-1%CHI-15%STY/PS beads, 15%GLU-2%CHI-15%STY/PS beads and 20%GLU-3%CHI-15%STY/PS beads obtained from immobilization at 30°C for 72 hours were 34.39, 36.12 and 31.38 U/g-support, respectively.

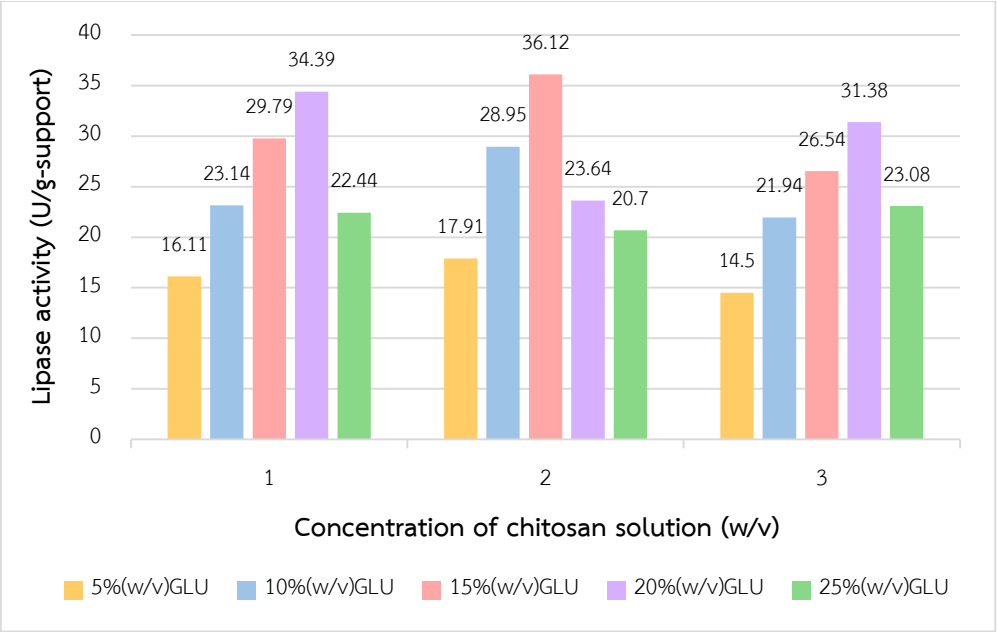

Figure 4.45 Effect of glutaraldehyde concentration on activity of *P. cepacia* lipase (18 mg) immobilized onto 1 g of GLU-CHI-STY/PS beads at 30°C for 72 hours

4.3.1.2 Immobilization on protein loading yield

18 mg of *P. cepacia* lipase was immobilized onto 1 g of GLU-CHI-STY/PS beads in phosphate buffer (25 mM, pH 7.0) at 30°C for 72 hours. Then, protein loading yield was analyzed. The amount of protein was determined by the Bradford method by using *P. cepacia* as the standard. The amount of bound protein was determined indirectly from the difference between the amount of protein introduced and the amount of protein remain in the solution [77]. The effect of glutaraldehyde on protein loading yield was showed in Figure 4.46. In the study, the percentage of protein loading yield gave at high value when increasing concentration of glutaraldehyde solution. This is not consistent with the lipase activity because the lipase activity was decreased when increasing concentration of glutaraldehyde solution as shown in Figure 4.47. Because of, the extensive interaction of individual lipase with aldehyde groups on the surface of the microspheres possibly changes the lipase conformation. So, the lipase activity was decreased [82]. In the result, 18 mg of *P. cepacia* lipase were successfully immobilized onto 1 g of 20%GLU-1%CHI-15%STY/PS beads, 15%GLU-2%CHI-15%STY/PS beads and 20%GLU-3%CHI-15%STY/PS beads at 30°C for 72 hours because

it gave high value of lipase activity and protein loading yield. The protein loading yield onto 20%GLU-1%CHI-15%STY/PS beads, 15%GLU-2%CHI-15%STY/PS beads and 20%GLU-3%CHI-15%STY/PS beads at 30°C for 72 hours were 67.00, 67.11 and 65.72%, respectively.

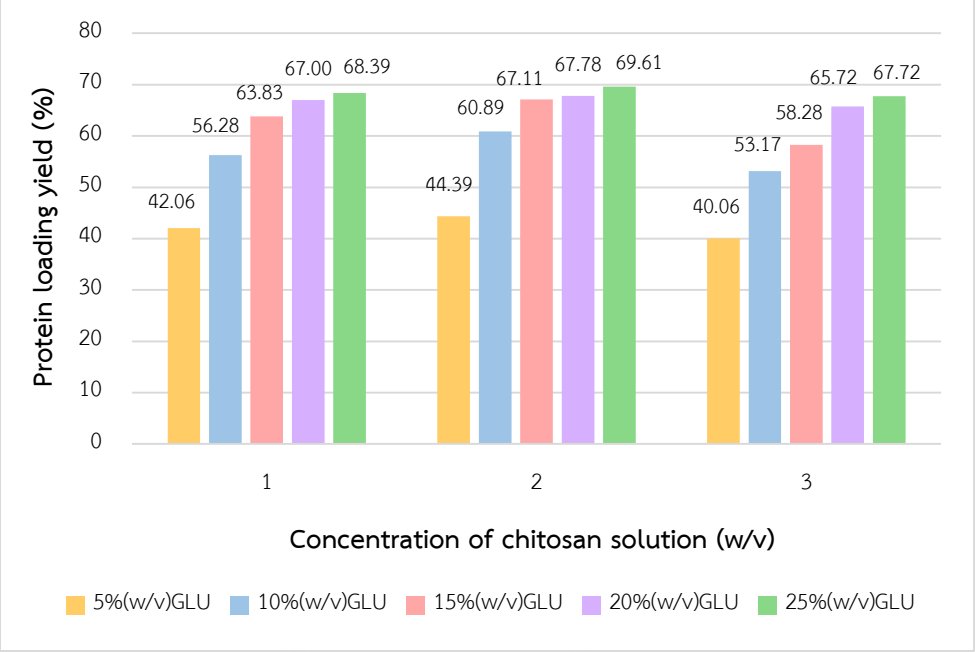

Figure 4.46 Effect of glutaraldehyde concentration on protein loading yield of *P. cepacia* lipase (18 mg) immobilized onto GLU-CHI-STY/PS beads (1 g. of support) at 30°C for 72 hours

(a)

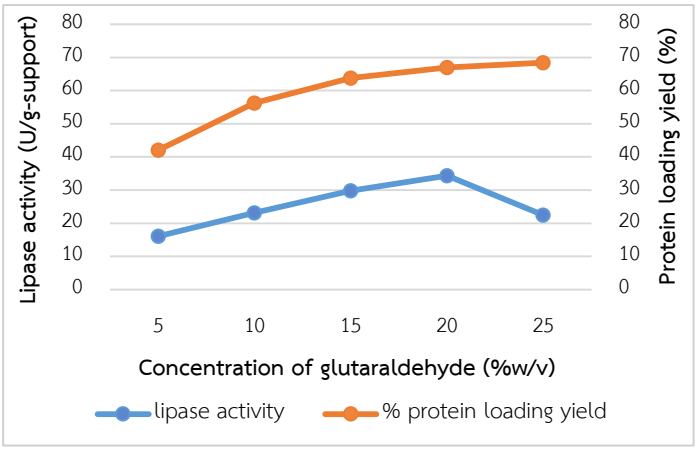

(b)

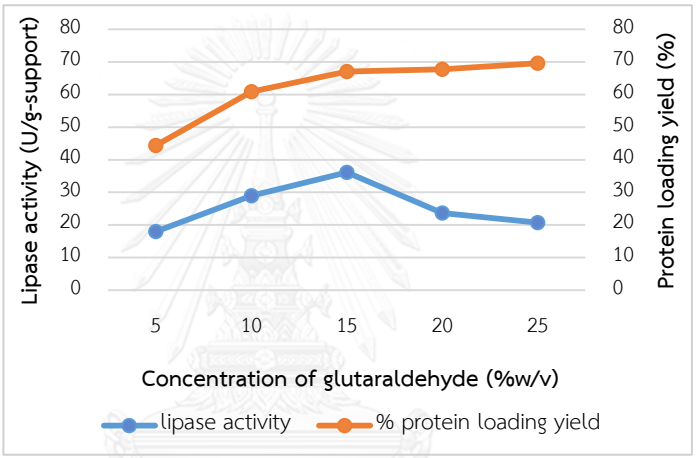

(c)

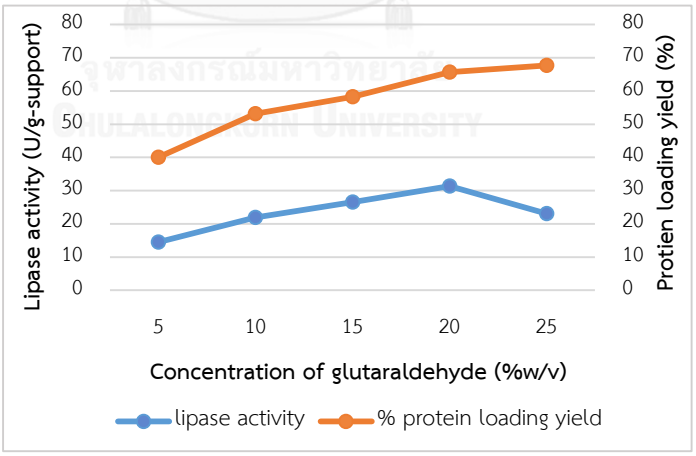

Figure 4.47 Effect of glutaraldehyde concentration of *P. cepacia* lipase (18 mg) immobilized onto GLU-CHI-STY/PS beads in phosphate buffer (25 mM, pH 7.0) at 30°C for 72 hours on lipase activity and protein loading yield; (a) GLU-1%CHI-15%STY/PS beads, (b) GLU-2%CHI-15%STY/PS beads and (c) GLU-3%CHI-15%STY/PS beads

4.3.1.3 Immobilization on specific activity

Since glutaraldehyde not only acts as the cross-linker but also denature lipase, glutaraldehyde at high concentration can directly affect lipase activity and specific activity of the lipase as seen in Table 4.6.

Table 4.6 Lipase activity, protein loading yield and specific activity of *P. cepacia* lipase (18 mg) immobilized onto 1 g of GLU-CHI-STY/PS beads in phosphate buffer (25 mM, pH 7.0) at 30°C for 72 hours

Concentration of chitosan solution (%w/v)	Concentration of glutaraldehyde solution (%w/v)	Immobilization time (h)	Amount of protein introduced (mg/g-support)	Amount of protein loaded (mg/g-support)	Lipase activity (U/g-support)	Protein loading yield (%)	Specific activity (U/mg-protein)
1	5	72	18	7.57	16.11	42.06	2.13
	10	72	18	10.13	23.14	56.28	2.28
	15	72	18	11.49	29.78	63.83	2.59
	20	72	18	12.06	34.39	67.00	2.85
	25	72	18	12.31	22.44	68.39	1.82
2	5	72	18	7.99	17.91	44.39	2.24
	10	72	18	10.96	28.95	60.89	2.64
	15	72	18	12.08	36.12	67.11	2.99
	20	72	18	12.20	23.64	67.78	1.94
	25	72	18	12.53	20.70	69.61	1.65
3	5	72	18	7.21	14.50	40.06	2.01
	10	72	18	9.57	21.94	53.17	2.29
	15	72	18	10.49	26.54	58.28	2.53
	20	72	18	11.83	31.38	65.72	2.65
	25	72	18	12.19	23.08	67.72	1.89

The ATR-FTIR spectra (Fig 4.48-4.50) of immobilization lipase (18 mg of *P. cepacia*) onto GLU-CHI-STY/PS beads (1 g of support) showed absorption of C=N bond at 1558 cm^{-1} and less intensity of absorption of C=O stretching of aliphatic aldehyde at 1726 cm^{-1}. Results from FTIR spectra revealed that the lipase was immobilized onto the beads via reaction between the amine group of lipase and carbonyl group of aldehyde.

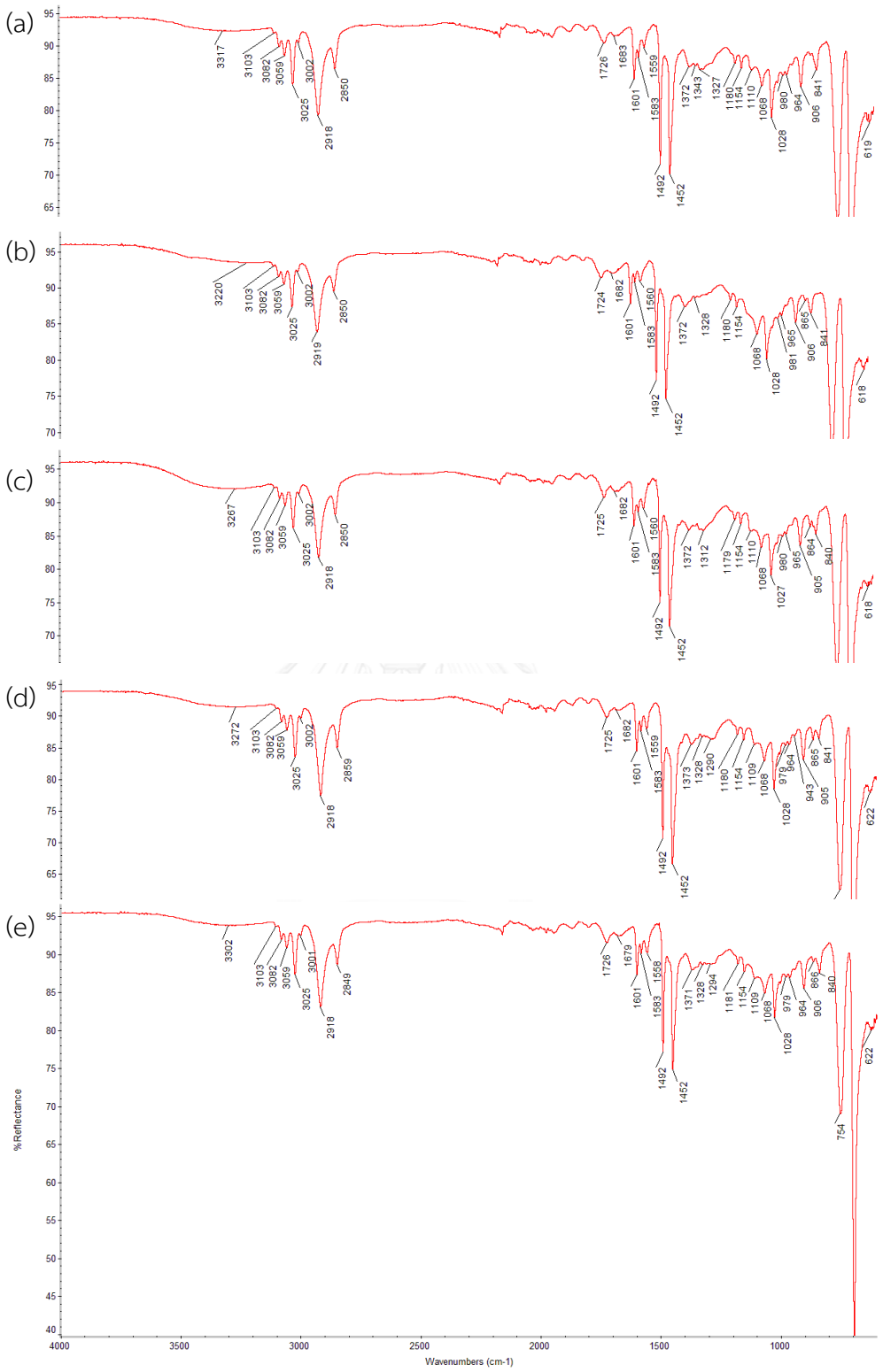

Figure 4.48 ATR-FTIR spectra of lipase (18 mg of *P. cepacia*) immobilized onto GLU-1%CHI-15%STY/PS beads at 30°C for 72 hours (a) 5% (w/v) GLU (b) 10% (w/v) GLU, (c) 15% (w/v) GLU (d) 20% (w/v) GLU and (e) 25% (w/v) GLU

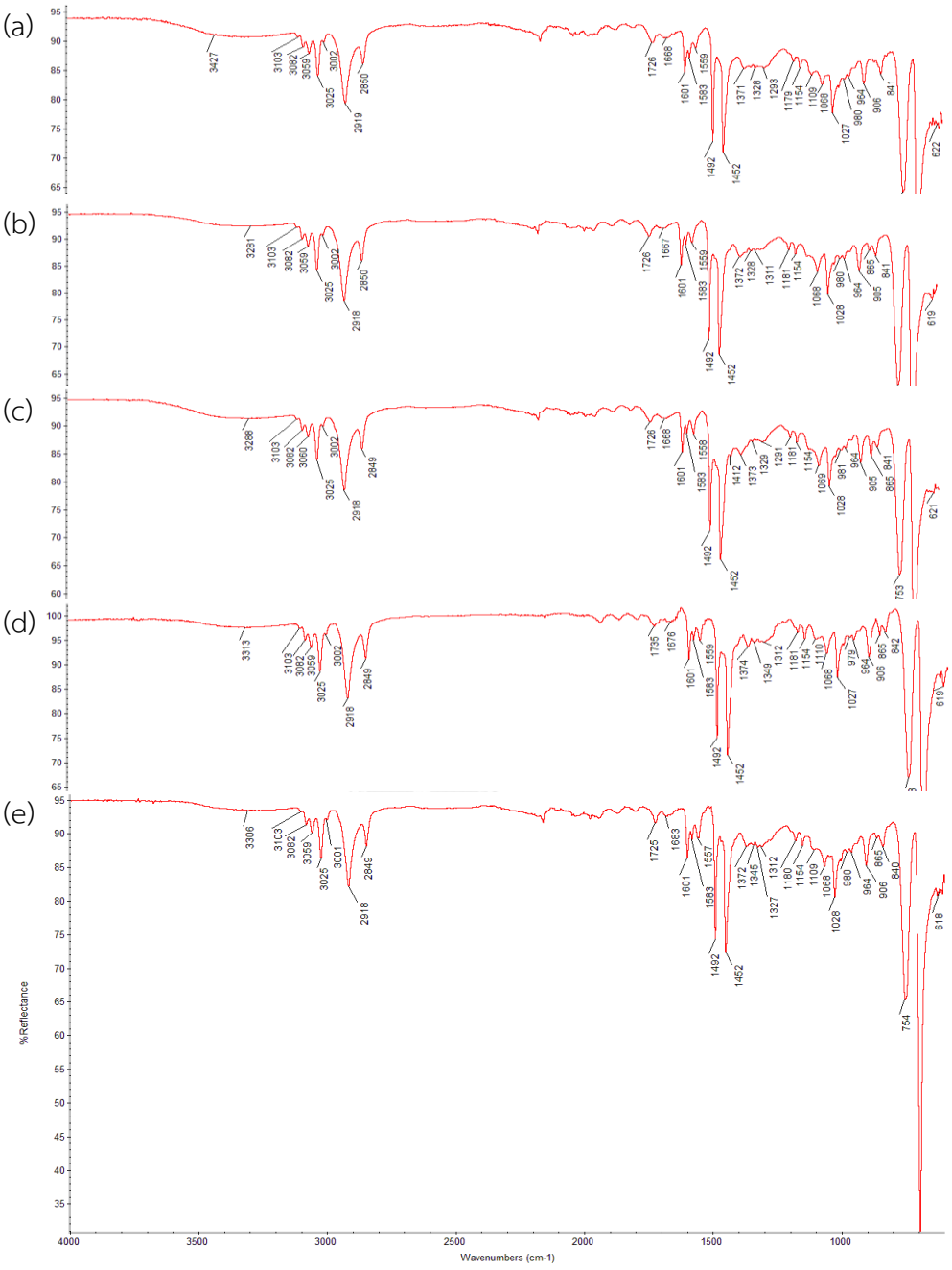

Figure 4.49 ATR-FTIR spectra of lipase (18 mg of *P. cepacia*) immobilized onto GLU-2%CHI-15%STY/PS beads at 30°C for 72 hours (a) 5% (w/v) GLU (b) 10% (w/v) GLU, (c) 15% (w/v) GLU (d) 20% (w/v) GLU and (e) 25% (w/v) GLU

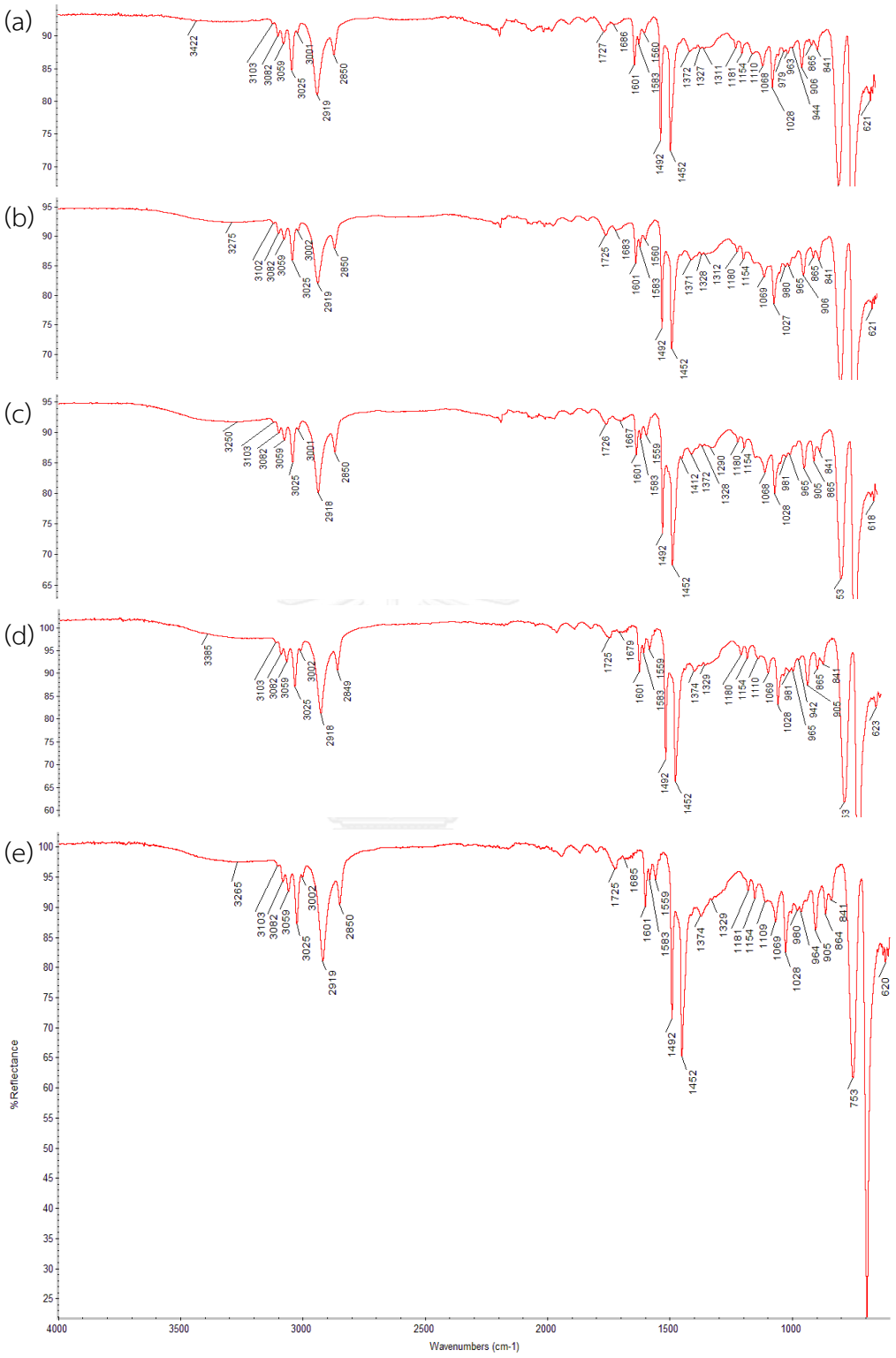

Figure 4.50 ATR-FTIR spectra of lipase (18 mg of *P. cepacia*) immobilized onto GLU-3%CHI-15%STY/PS beads at 30°C for 72 hours (a) 5% (w/v) GLU (b) 10% (w/v) GLU, (c) 15% (w/v) GLU (d) 20% (w/v) GLU and (e) 25% (w/v) GLU

Figure 4.51-4.53 showed SEM micrographs of immobilized lipase onto 20%GLU-1%CHI-15%STY/PS beads, 15%GLU-2%CHI-15%STY/PS beads and 20%GLU-3%CHI-15%STY/PS beads, respectively at 30°C for 72 hours. It was found that SEM micrographs of every immobilized lipase on beads are almost the same as activated glutaraldehyde on beads except every immobilized lipase on beads at magnification of 500X in Figure 4.51, 4.52, 4.53 (d) showed rough surface roughness on the surface. This indicated that *P. cepacia* lipase might only be retained on the surface of the beads.

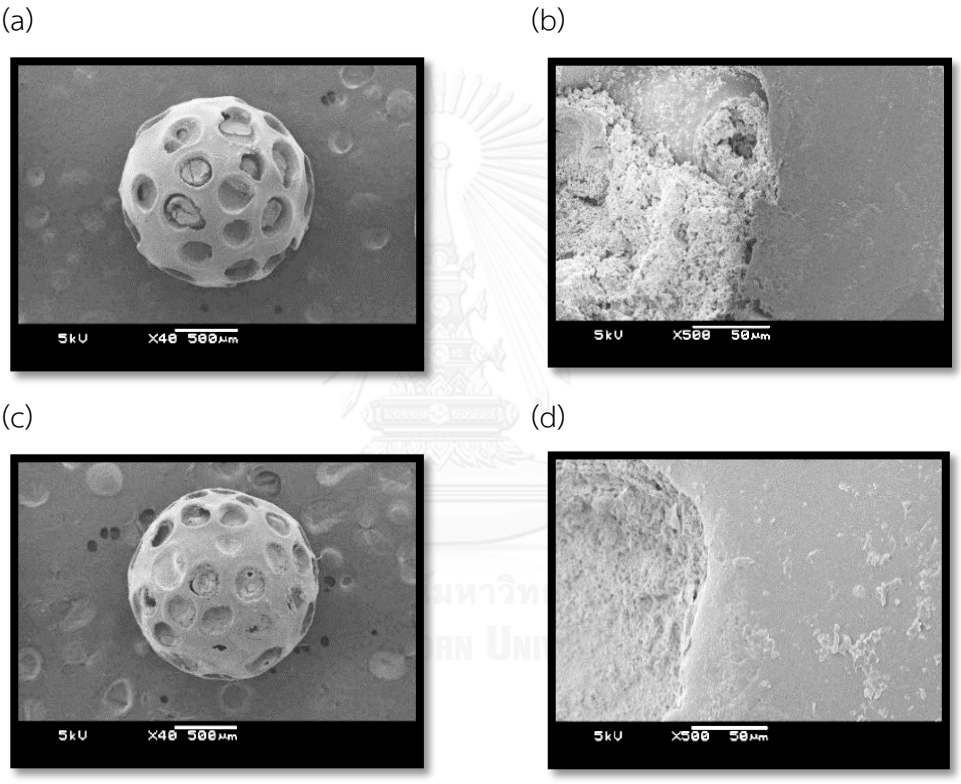

Figure 4.51 SEM micrographs of (a) 20%GLU-1%CHI-15%STY/PS beads at 80°C for 24 hours [X40] (b) 20%GLU-1%CHI-15%STY/PS beads at 80°C for 24 hours [X500] (c) immobilized lipase on 20%GLU-1%CHI-15%STY/PS beads at 30°C for 72 hours [X40] and (d) immobilized lipase on 20%GLU-1%CHI-15%STY/PS beads at 30°C for 72 hours [X500]

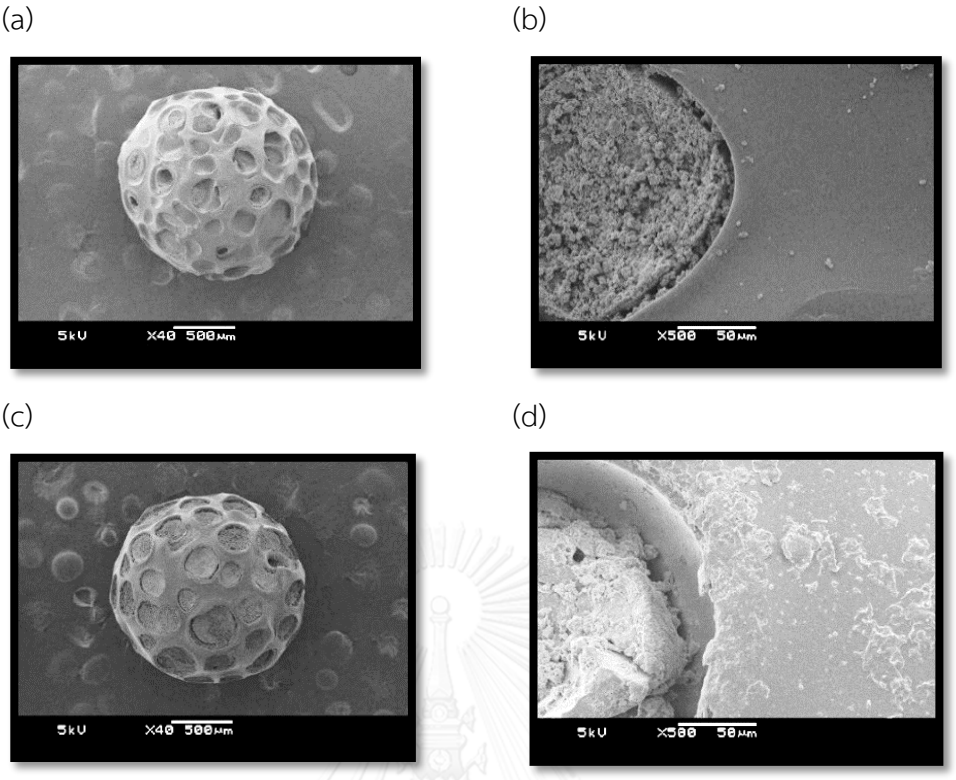

Figure 4.52 SEM micrographs of (a) 15%GLU-2%CHI-15%STY/PS beads at 80°C for 24 hours [X40] (b) 15%GLU-2%CHI-15%STY/PS beads at 80°C for 24 hours [X500] (c) immobilized lipase on 15%GLU-2%CHI-15%STY/PS beads at 30°C for 72 hours [X40] and (d) immobilized lipase on 15%GLU-2%CHI-15%STY/PS beads at 30°C for 72 hours [X500]

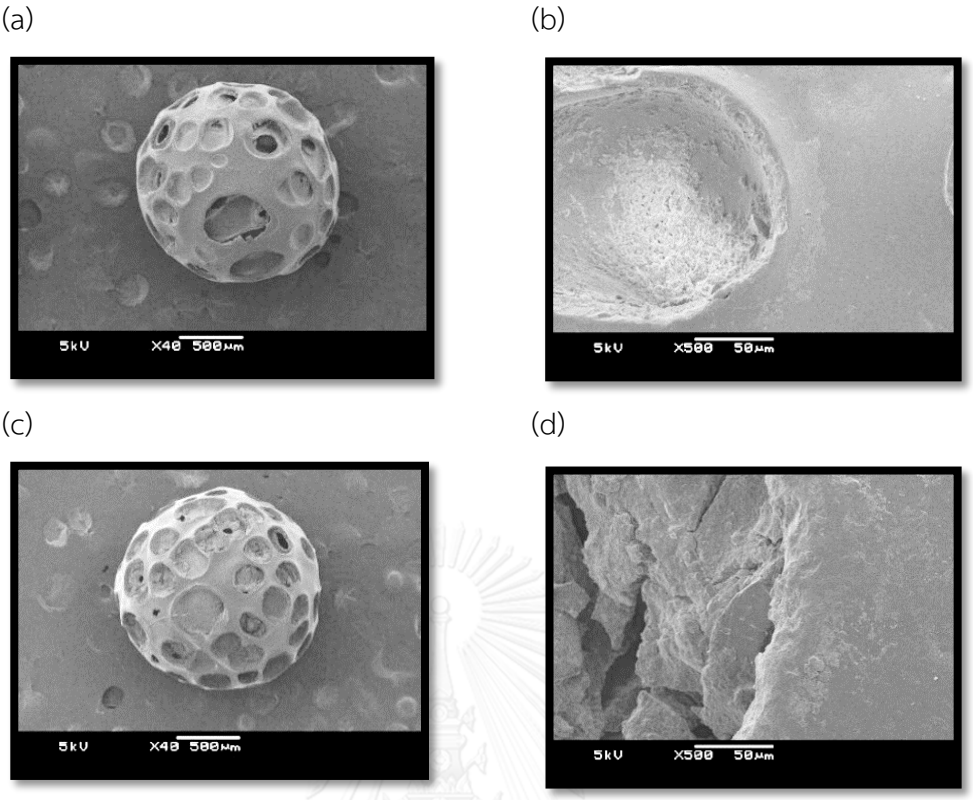

Figure 4.53 SEM micrographs of (a) 20%GLU-3%CHI-15%STY/PS beads at 80°C for 24 hours [X40] (b) 20%GLU-3%CHI-15%STY/PS beads at 80°C for 24 hours [X500] (c) immobilized lipase on 20%GLU-3%CHI-15%STY/PS beads at 30°C for 72 hours [X40] and (d) immobilized lipase on 20%GLU-3%CHI-15%STY/PS beads at 30°C for 72 hours [X500]

4.3.2 Effect of amount of lipase

4.3.2.1 Immobilization on lipase activity

Variation of amount of *P. cepacia* lipase (6 to 48 mg) in phosphate buffer (25 mM, pH 7.0) was immobilized onto 1 g of 15%GLU-2%CHI-15%STY/PS beads at 30°C for 72 hours and lipase activity, protein loading and specific lipase activity of the immobilized beads were then examined. In Figure 4.54, high lipase activity was obtained when amount of *P. cepacia* lipase was increased. Using 6 and 12 mg of *P. cepacia* lipase gave also lower activity, which there were 4.10 and 15.76 U/g-support, respectively. After using 12 mg, it was a sudden surge on lipase activity. In the study, using 18 mg gave high value at 36.12 U/g-support. After using 18 mg, lipase activity was

continually increased until more than 30 mg found that lipase activity was rarely increased. The results, 30 mg was sufficiently immobilized onto 1 g of the 15%GLU-2%CHI-15%STY/PS beads and it arrived at high value at 54.43 U/g-support. These lipase activity was performed to determine the optimal amount of lipase.

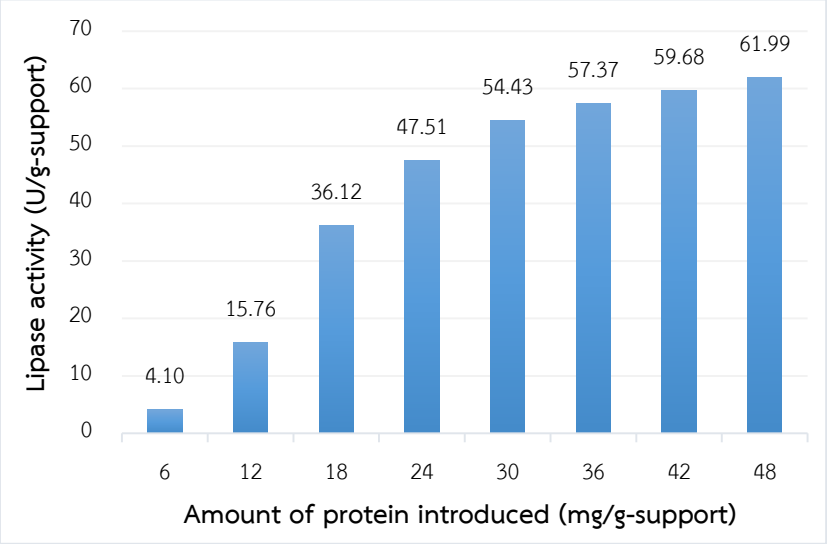

Figure 4.54 Effect of amount of lipase immobilized onto 15%GLU-2%CHI-15%STY/PS beads in phosphate buffer (25 mM, pH 7.0) at 30°C for 72 hours on lipase activity

4.3.2.2 Immobilization on protein loading yield

Variation of amount of *P. cepacia* lipase (6 to 48 mg) were immobilized onto 1 g of 15%GLU-2%CHI-15%STY/PS beads in phosphate buffer (25 mM, pH 7.0) at 30°C for 72 hours. Then, the immobilized lipase onto 15%GLU-2%CHI-15%STY/PS beads were analyzed by the percentage of protein loading yield. The results, the percentage of protein loading yield were present in Figure 4.55. In the study, the percentage of protein loading yield gave at high value when increasing amount of *P. cepacia* lipase. This is consistent with the lipase activity as shown in Figure 4.56. After using 30 mg of *P. cepacia* lipase found that the percentage of protein loading yield was relatively constant. Therefore, 30 mg was sufficiently immobilized onto 1 g of the 15%GLU-2%CHI-15%STY/PS beads and it gave protein loading yield at 72.93%. These the

percentage of protein loading yield was performed to determine the optimal amount of lipase.

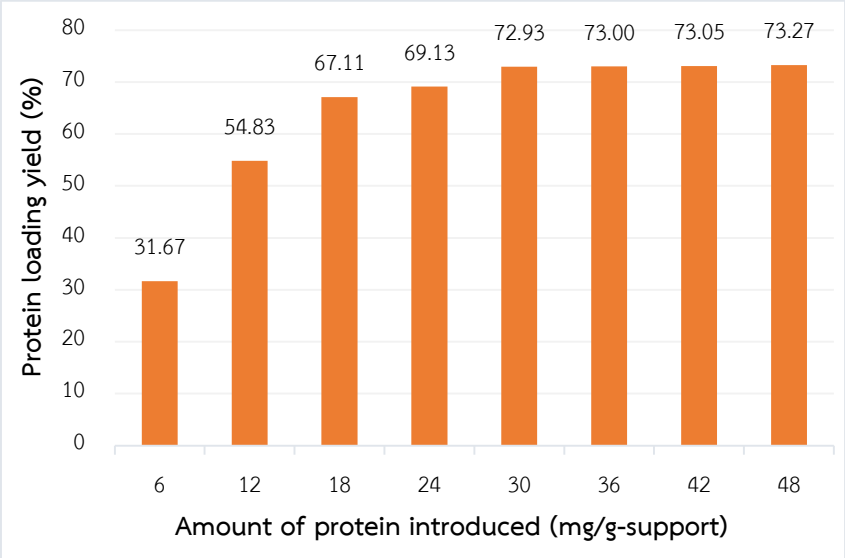

Figure 4.55 Variation of *P. cepacia* lipase were immobilized onto 1 g of 15%GLU-2%CHI-15%STY/PS beads in phosphate buffer (25 mM, pH 7.0) at 30°C for 72 hours on protein loading yield

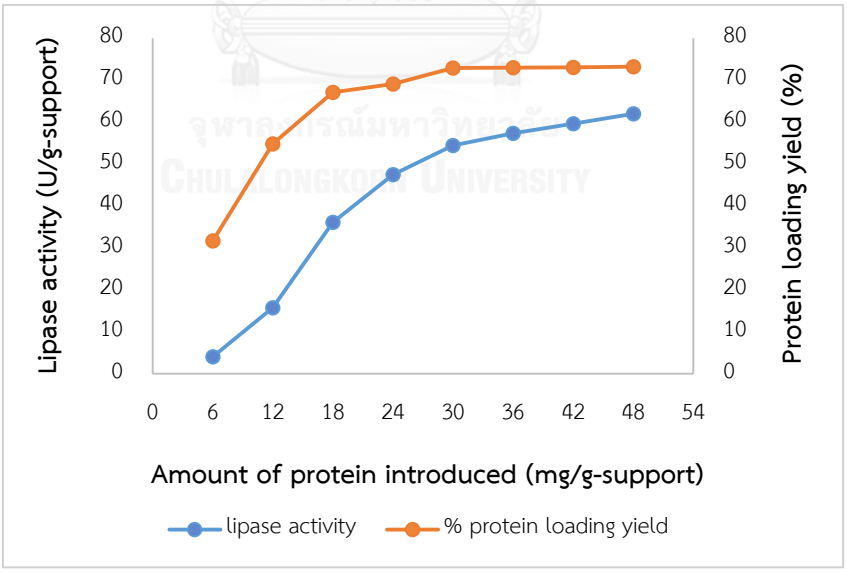

Figure 4.56 Variation of *P. cepacia* lipase were immobilized onto 1 g of 15%GLU-2%CHI-15%STY/PS beads in phosphate buffer (25 mM, pH 7.0) at 30°C for 72 hours on lipase activity and protein loading yield

4.3.2.3 Immobilization on specific activity

The results for specific activity were present in Table 4.7.

Table 4.7 Lipase activity, protein loading yield and specific activity of *P. cepacia* lipase (6 to 48 mg) immobilized onto 1 g of GLU-CHI-STY/PS beads in phosphate buffer (25 mM, pH 7.0) at 30°C for 72 hours

Concentration of chitosan solution (%w/v)	Concentration of glutaraldehyde solution (%w/v)	Immobilization time (h)	Amount of protein introduced (mg/g-support)	Amount of protein loaded (mg/g-support)	Lipase activity (U/g-support)	Protein loading yield (%)	Specific activity (U/mg-protein)
2	15	72	6	1.90	4.10	31.67	2.16
2	15	72	12	6.58	15.76	54.83	2.40
2	15	72	18	12.08	36.12	67.11	2.99
2	15	72	24	16.59	47.51	69.13	2.86
2	15	72	30	21.88	54.43	72.93	2.49
2	15	72	36	26.28	57.37	73.00	2.18
2	15	72	42	30.68	59.68	73.05	1.95
2	15	72	48	35.17	61.99	73.27	1.76

The ATR-FTIR spectra of various amount of *P. cepacia* lipase (6 to 48 mg) immobilized onto 1 g of 15%GLU-2%CHI-15%STY/PS beads at 30°C for 72 hours were analyzed to confirm optimal amount of lipase that was appropriate reacted with active group of surface of the support as shown in Figure 4.57. The absorption of C=N bond at 1558 cm^{-1} and less intensity of absorption of C=O stretching of aliphatic aldehyde at 1726 cm^{-1}. Results from FTIR spectra revealed that the lipase was immobilized onto the beads via reaction between the amine group of lipase and carbonyl group of aldehyde.

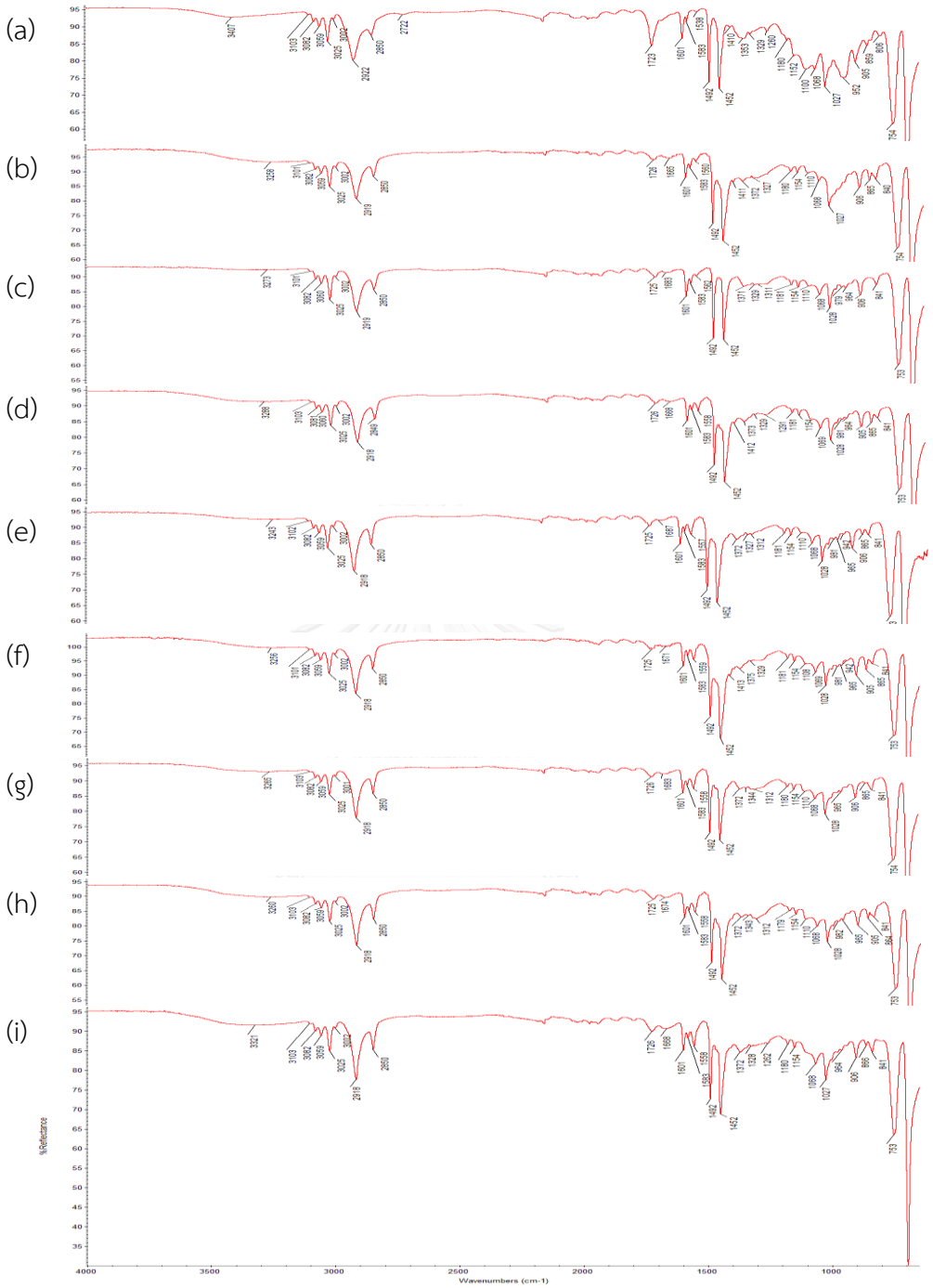

Figure 4.57 ATR-FTIR spectra of lipase immobilized onto 15%GLU-2%CHI-15%STY/PS beads at 30°C for 72 hours (a) 15%GLU-2%CHI-15%STY/PS beads at 80°C for 24 hours (b) 6 mg of *P. cepacia* (c) 12 mg of *P. cepacia* (d) 18 mg of *P. cepacia* (e) 24 mg of *P. cepacia* (f) 30 mg of *P. cepacia* (g) 36 mg of *P. cepacia* (h) 42 mg of *P. cepacia* and (i) 48 mg of *P. cepacia*

4.3.3 Effect of immobilization time

4.3.3.1 Immobilization on lipase activity

18 mg of *P. cepacia* lipase was immobilized onto 1 g of 15%GLU-2%CHI-15%STY/PS beads in phosphate buffer (25 mM, pH 7.0) at 30°C with variation of immobilization time at 48, 60, 72, 84 and 96 hours. After that, the immobilized lipase onto 15%GLU-2%CHI-15%STY/PS beads were tested by lipase activity. In the study, lipase activity at various times were 21.91, 27.67, 36.12, 37.48 and 39.76 U/g-support, respectively as shown in Figure 4.58. The results, lipase activity gave at high value when increasing immobilization time. It was found that 18 mg of *P. cepacia* lipase was completely immobilized onto 15%GLU-2%CHI-15%STY/PS beads at 30°C for 72 hours because increasing immobilization time (beyond 72 hours) for this reaction was relatively constant the lipase activity. Therefore, the optimum reaction time for immobilization lipase was 72 hours.

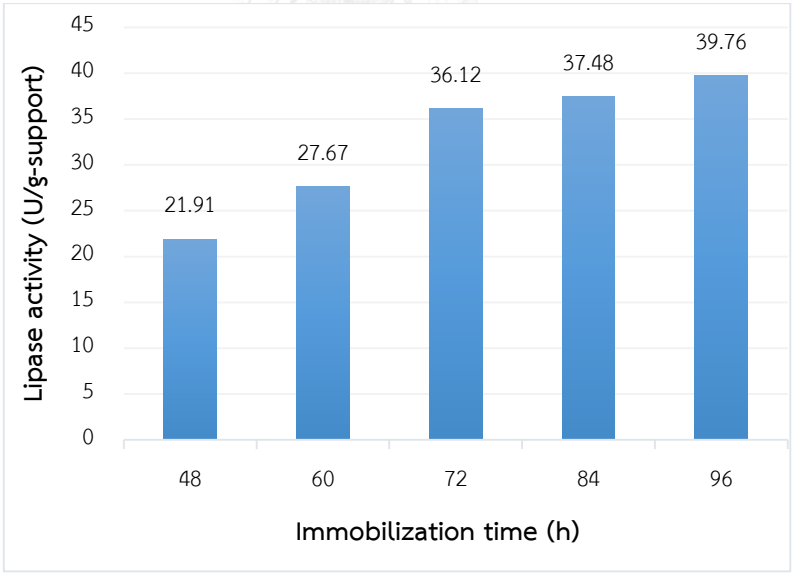

Figure 4.58 Effect of immobilization time on lipase activity of *P. cepacia* lipase (18 mg) immobilized onto 1 g of 15%GLU-2%CHI-15%STY/PS beads in phosphate buffer (25 mM, pH 7.0) at 30°C

4.3.3.2 Immobilization on protein loading yield

18 mg of *P. cepacia* lipase was immobilized onto 1 g of 15%GLU-2%CHI-15%STY/PS beads in phosphate buffer (25 mM, pH 7.0) at 30°C with variation of immobilization time at 48, 60, 72, 84 and 96 hours. Then, the immobilized lipase onto 15%GLU-2%CHI-15%STY/PS beads were tested by protein loading yield. The results that protein loading yield at various times were 52.78%, 60.39%, 67.11%, 67.61 and 67.72%, respectively as shown in Figure 4.59. In the study, the percentage of protein loading yield gave at high value when increasing immobilization time. This is consistent with the lipase activity as shown in Figure 4.60. Therefore, 18 mg of *P. cepacia* lipase was completely immobilized onto 15%GLU-2%CHI-15%STY/PS beads at 30°C for 72 hours because protein loading yield was relatively constant. These protein loading yield was performed to determine the optimal immobilization time.

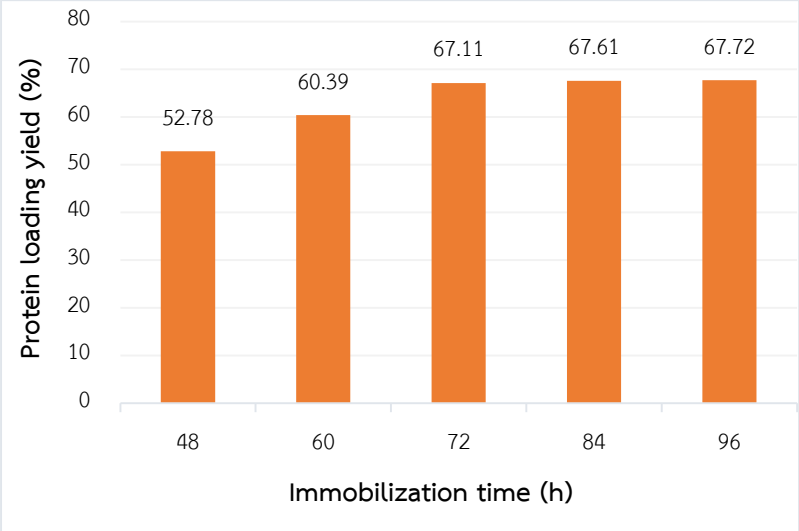

Figure 4.59 The variation of immobilization time of *P. cepacia* lipase (18 mg) were immobilized onto 1 g of 15%GLU-2%CHI-15%STY/PS beads in phosphate buffer (25 mM, pH 7.0) at 30°C on protein loading yield

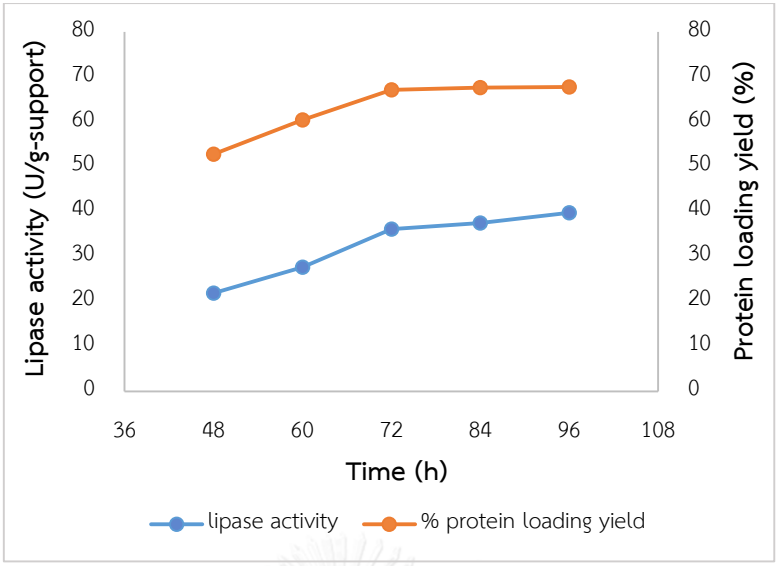

Figure 4.60 The variation of immobilization time of *P. cepacia* lipase (18 mg) were immobilized onto 1 g of 15%GLU-2%CHI-15%STY/PS beads in phosphate buffer (25 mM, pH 7.0) at 30°C on lipase activity and protein loading yield

4.3.3.3 Immobilization on specific activity

The results for specific activity were present in Table 4.8.

Table 4.8 Lipase activity, protein loading yield and specific activity of *P. cepacia* lipase (18 mg) immobilized onto 1 g of GLU-CHI-STY/PS beads in phosphate buffer (25 mM, pH 7.0) at 30°C for 48 to 96 hours

Concentration of chitosan solution (%w/v)	Concentration of glutaraldehyde solution (%w/v)	Immobilization time (h)	Amount of protein introduced (mg/g-support)	Amount of protein loaded (mg/g-support)	Lipase activity (U/g-support)	Protein loading yield (%)	Specific activity (U/mg-protein)
2	15	48	18	9.50	21.91	52.78	2.31
2	15	60	18	10.87	27.67	60.39	2.55
2	15	72	18	12.08	36.12	67.11	2.99
2	15	84	18	12.17	37.48	67.61	3.08
2	15	96	18	12.19	39.76	67.72	3.26

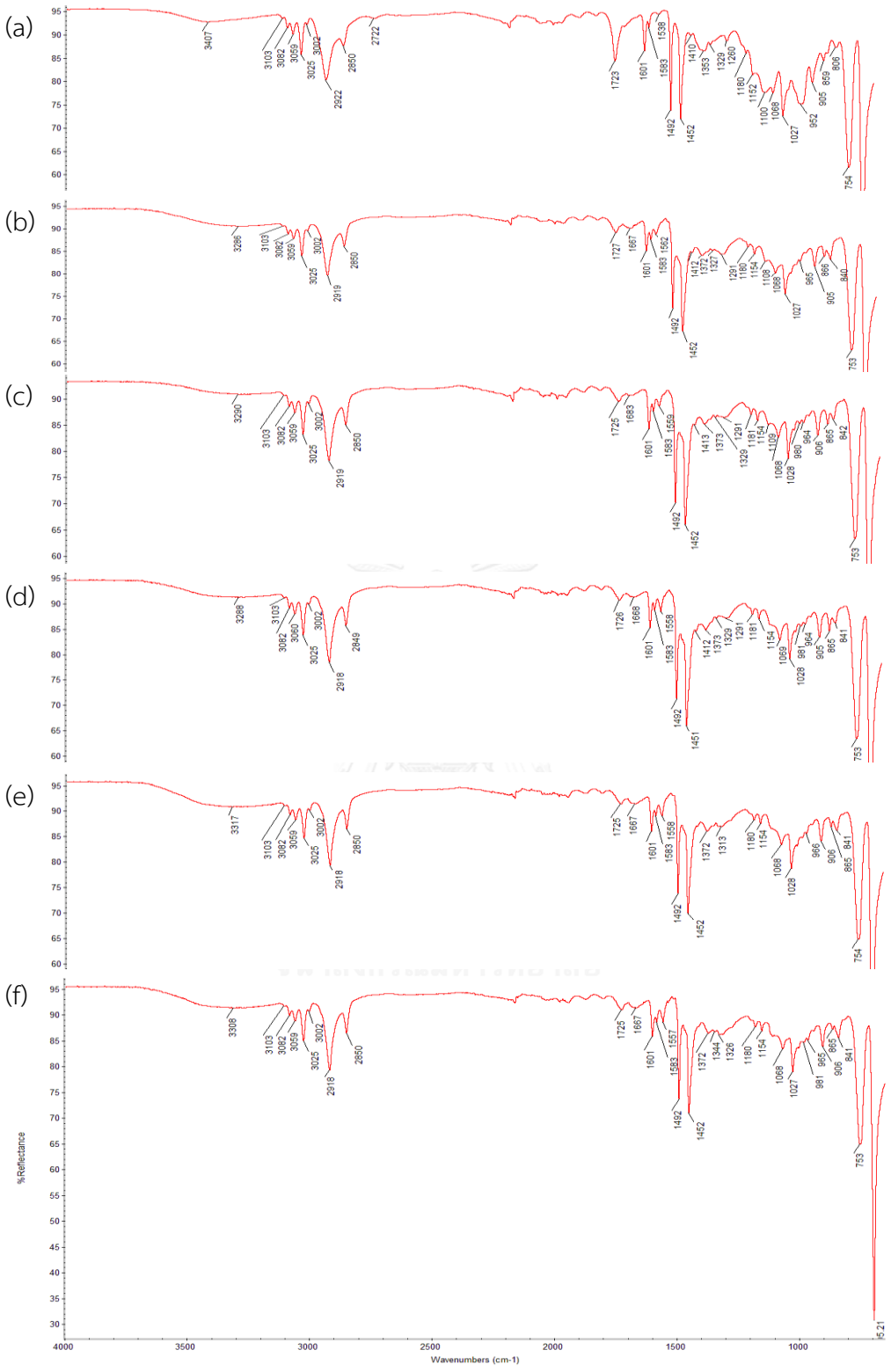

Figure 4.61 ATR-FTIR spectra of *P. cepacia* lipase (18 mg) immobilized onto 1 g of 15%GLU-2%CHI-15%STY/PS beads at 30°C for variation of immobilization times (a) 15%GLU-2%CHI-15%STY/PS beads at 80°C for 24 hours (b) 48 hours (c) 60 hours (d) 72 hours (e) 84 hours and (f) 96 hours

The ATR-FTIR spectra of immobilization lipase (18 mg) onto 15%GLU-2%CHI-15%STY/PS beads at 30°C were analyzed to confirm optimal immobilization time that was appropriate reacted with active group of surface of the support as shown in Figure 4.61. The absorption of C=N bond at 1557 cm^{-1} and less intensity of absorption of C=O stretching of aliphatic aldehyde at 1725 cm^{-1}. Results from FTIR spectra revealed that the lipase was immobilized onto the beads via reaction between the amine group of lipase and carbonyl group of aldehyde.

4.3.4 The optimization of immobilization

The efficiency of *P. cepacia* lipase immobilized onto GLU-CHI-STY/PS beads were investigated in term of lipase activity, protein loading yield and specific activity. The lipase activity, protein loading yield and specific activity of *P. cepacia* lipase (30 mg) immobilized onto 1 g of 15%GLU-2%CHI-15%STY/PS beads at 30°C for 72 hours gave the optimal value at 54.43 U/g-support, 72.93% and 2.49 U/mg-protein, respectively.

4.4 Enzymatic transesterification for biodiesel production

Transesterification reaction of soybean oil using lipase from *P. cepacia* (30 mg) immobilized onto 15%GLU-2%CHI-15%STY/PS beads (1 g) at 30°C for 72 hours were used as a catalyst for biodiesel production. For biodiesel production, the effects of amount of catalyst, temperature, molar ratio of oil to alcohol and time in the transesterification reaction were investigated.

4.4.1 Lipase-immobilized 15%GLU-2%CHI-15%STY/PS beads for transesterification reaction of soybean oil

4.4.1.1 Effect of amount of catalyst on transesterification

To determine the effect of amount of lipase-immobilized 15%GLU-2%CHI-15%STY/PS beads on transesterification reaction, experiments were performed using the catalyst with unit/g of enzyme activity in the range of 0.2147-0.4294 g. The transesterification was carried out by using 10 g of soybean oil reacted with anhydrous ethanol (one-step addition) using 1:3 molar ratio of oil at 40°C for 192 hours. Results, presented in Table 4.9 and Figure 4.62, showed that increasing amount of catalysts

increased rate of reaction and fatty acid ethyl esters (FAEEs) production. In this work, it was found that the highest ethyl esters formation (84%) was obtained by using 0.4294 g of catalyst within 192 hours.

Table 4.9 Effect of amount of catalyst on transesterification of soybean oil (10 g) with anhydrous ethanol, using 1:3 molar ratio oil to anhydrous ethanol (one-step addition), at 40°C for 192 hours

Amount of catalyst (g)	Ethyl esters production (%)																	
	Time (h)																	
	2	4	6	8	24	28	32	48	52	56	72	76	80	96	120	144	168	192
0.2147	3	3	4	4	7	7	9	13	15	15	29	29	30	36	55	64	64	64
0.3221	4	4	5	8	10	11	15	27	28	29	39	45	49	62	78	80	80	80
0.4294	15	19	23	33	51	54	56	59	62	65	72	76	78	79	81	83	84	84

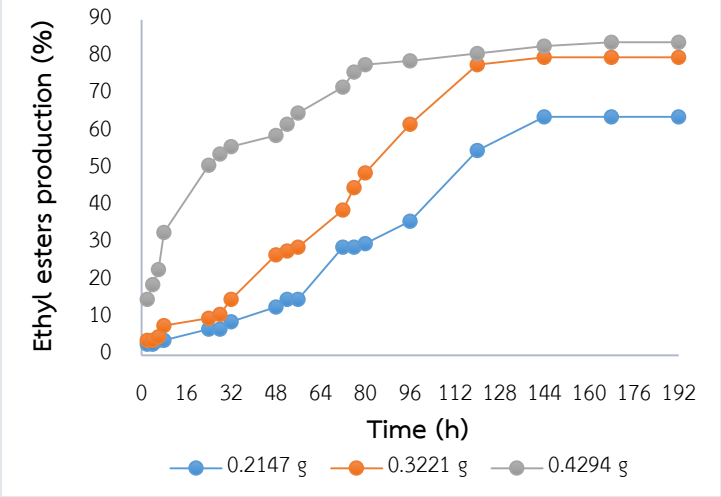

Figure 4.62 FAEEs obtained by transesterification of soybean oil (10 g) with anhydrous ethanol, using 1:3 molar ratio oil to anhydrous ethanol (one-step addition), at 40°C for 192 hours

4.4.1.2 Effect of temperature on transesterification

Since enzyme activity and enzymatic transesterification depend on temperature [62], the transesterification of soybean oil with anhydrous ethanol was carried out at 30, 40 and 50°C using 1:3 molar ratio oil to anhydrous ethanol (one-step addition), 10 g of soybean oil and 0.4294 g of catalyst for 192 hours. Results (Table

4.10 and Figure 4.63) showed that rate of reaction carried out at 40°C was higher than at 30°C and the reaction at 30 and 40°C reached the maximal ethyl esters production within 80 hours. The highest ethyl esters production (84%) were obtained at 40°C. When the reaction temperature was carried out at 50°C, rate of reaction into ethyl esters was suddenly reduced and the highest FAEEs was 60% within 192 hours. The results indicated that the immobilized lipase might be slightly inactivated at 50°C and the reaction thus resulted in low reaction rate and yield. Therefore, the ethyl esters production was rarely decreased due to higher temperatures could reduce the lipase activity. Experiments were also performed to examine thermal stability of the immobilized *P. cepacia* lipase in the transesterification of soybean oil with anhydrous ethanol at 40°C.

Table 4.10 Effect of temperature on transesterification of soybean oil (10 g) with anhydrous ethanol, using 1:3 molar ratio oil to anhydrous ethanol (one-step addition), 0.4294 g of catalyst at 30, 40 and 50°C for 192 hours

Temp (°C)	Ethyl esters production (%)																	
	Time (h)																	
	2	4	6	8	24	28	32	48	52	56	72	76	80	96	120	144	168	192
30	3	3	4	4	11	12	16	47	49	54	71	72	72	79	80	80	82	82
40	15	19	23	33	51	54	56	59	62	65	72	76	78	79	81	83	84	84
50	3	3	4	4	9	9	11	17	20	21	24	34	34	37	47	51	57	60

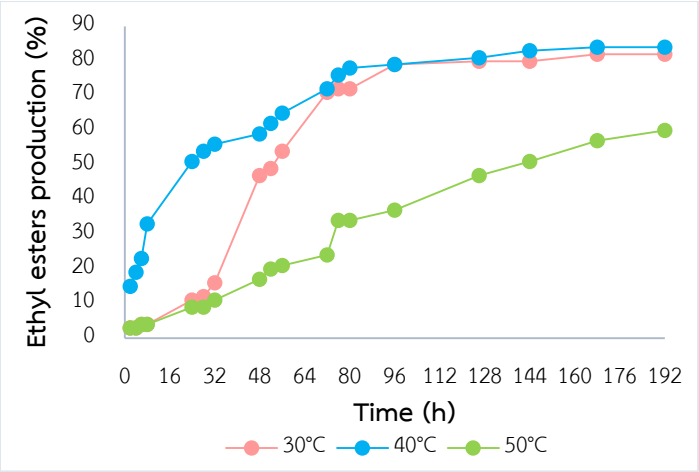

Figure 4.63 FAEEs obtained by transesterification of soybean oil (10 g) with anhydrous ethanol, using 1:3 molar ratio oil to anhydrous ethanol (one-step addition), 0.4294 g of catalyst at 30, 40 and 50°C for 192 hours

4.4.1.3 Effect of molar ratio of oil to alcohol on transesterification

The enzymatic transesterification is well known that excessive short-chain alcohols such as methanol or ethanol might inactivate lipase seriously [19]. Theoretically, at least three molar equivalents of alcohol are required for the complete conversion of the oil to its corresponding alkyl ester. Generally, the greater the molar ratio of oil to alcohol the faster the reaction rate. In this work, experiments were performed to optimize the amount of ester production by various concentrations of anhydrous ethanol. The amount of anhydrous ethanol added was varied from 1 to 6 molar equivalents for anhydrous ethanol, based on the moles of triglycerides (amount of anhydrous ethanol as showed Table 3.1). The effect of oil to anhydrous ethanol molar ratio was presented in Table 4.11. It was found that an increase in the number of moles of alcohol with respect to the triglycerides resulted in an increase in the production of esters. In the study, increasing the molar equivalents of anhydrous ethanol up to three initially in the soybean oil increased the transesterification as shown in Figure 4.64. The highest ethyl esters production (84%) could be obtained by using 1:3 oil/ethanol molar ratio. However, the ethyl esters production was decreased as oil to higher ethanol molar ratio (more than 3 molar equivalent of anhydrous

ethanol) because the excess alcohol levels may inhibit the enzyme activity and thereby decrease its catalytic activity toward the transesterification reaction [19].

Table 4.11 Effect of oil/ethanol molar ratio on transesterification of soybean oil (10 g) with anhydrous ethanol (one-step addition), using 0.4294 g of catalyst at 40°C for 192 hours

Oil:dry ethanol	Ethyl esters production (%)																	
	Time (h)																	
	2	4	6	8	24	28	32	48	52	56	72	76	80	96	120	144	168	192
1:1	4	5	6	6	7	8	11	12	17	22	25	29	32	39	51	54	54	56
1:2	6	7	8	8	19	23	27	46	47	50	52	54	56	56	58	61	64	64
1:3	15	19	23	33	51	54	56	59	62	65	72	76	78	79	81	83	84	84
1:4	4	5	6	6	9	9	10	11	13	13	16	17	19	23	31	37	45	53
1:5	6	6	6	7	8	8	9	9	10	11	12	13	13	19	25	33	39	45
1:6	4	6	6	7	7	7	7	8	9	11	12	12	13	15	20	24	27	34

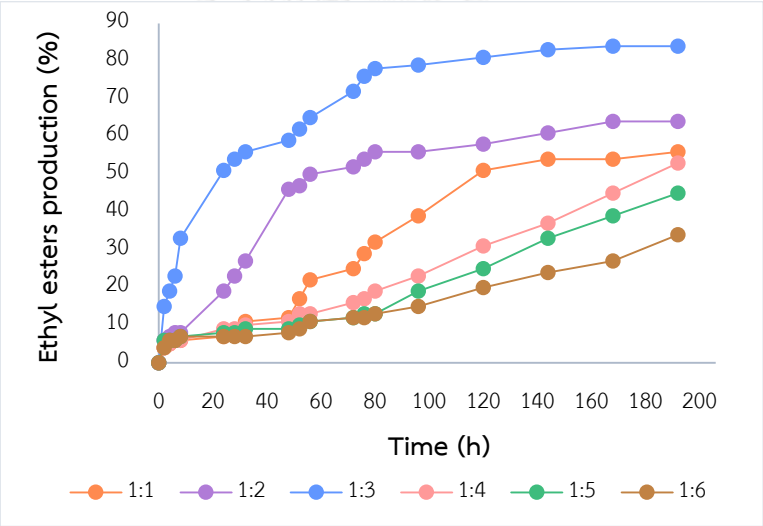

Figure 4.64 Effect of oil/ethanol molar ratio on transesterification of soybean oil with anhydrous ethanol (one-step addition). The reactions were performed with 10 g of soybean oil and 0.4294 g of catalyst at 40°C for 192 hours

The results indicated that an increase in the number of moles of ethanol resulted in an increase in the ester production until the formation of esters reached a maximum level. However, further increases in the ethanol concentrations resulted in a decrease in the formation of esters due to excess alcohol levels may inhibit the enzyme activity and thereby decrease its catalytic activity toward the

transesterification reaction [19]. Thus, the reaction was conducted by adding ethanol stepwise to avoid enzyme inactivation. In the study, effect of adding anhydrous ethanol in the range of 1:4 to 1:6 molar ratios in three steps on biodiesel production was investigated and results were presented in Figure 4.65. The first addition (1:3 oil/ethanol molar ratio) was done at the beginning of the reaction and the other portions of anhydrous ethanol were adding at 8 and 16 hours for three-step addition. The reaction was carried out at 40°C for 32 hours of the total accumulated reaction time (amount of anhydrous ethanol as showed Table 3.2). The reactions were performed with anhydrous ethanol (three-step addition), 10 g of soybean oil and 0.4294 g of catalyst at 40°C for 32 hours. In comparison of FAEEs production from one-step addition and three-step addition, it was found that three-step addition of ethanol could improve FAEEs production with a shorter time and 91% FAEEs production was obtained by three-step addition of 1:5 oil/ethanol molar ratio.

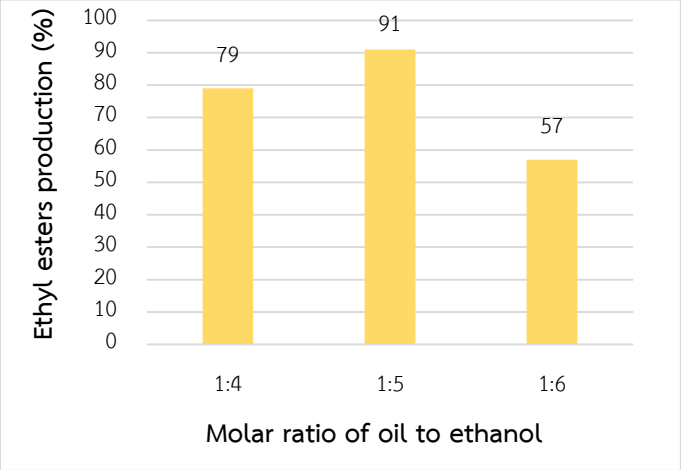

Figure 4.65 Effect of oil/ethanol molar ratio on transesterification of soybean oil. The reactions were performed with anhydrous ethanol (three-step addition), 10 g of soybean oil and 0.4294 g of catalyst at 40°C for 32 hours

In three-step addition of 1:6 oil/ethanol molar ratio, the FAEEs production was higher than that using one-step addition. This indicated that the last two portions of three-step addition still inactivated the enzyme. Thus, adding anhydrous ethanol in four steps was performed for further investigation. The reactions were performed with

1:6 molar ratio oil to anhydrous ethanol (four-step addition), 10 g of soybean oil and 0.4294 g of catalyst at 40°C for 64 hours. The first addition (1:3 oil/ethanol molar ratio) was done at the beginning of the reaction and another three addition of one equivalent anhydrous ethanol was continued at 8, 16 and 32 hours.

Results as shown in Figure 4.66 showed that FAEEs production was increased when adding anhydrous ethanol in four steps. It gave the highest ethyl esters production (92%) at 40°C within 48 hours. However, 1:6 molar ratio oil to anhydrous ethanol (four-step addition) did not have much effect on ethyl esters production when compared to 1:5 molar ratio oil to anhydrous ethanol (three-step addition) and reaction time is longer. Thus, the optimal of molar ratio of oil to ethanol on ethyl esters production was 1:5 molar ratio (three-step addition). It gave the highest ethyl esters production (91%) at 40°C for 32 hours.

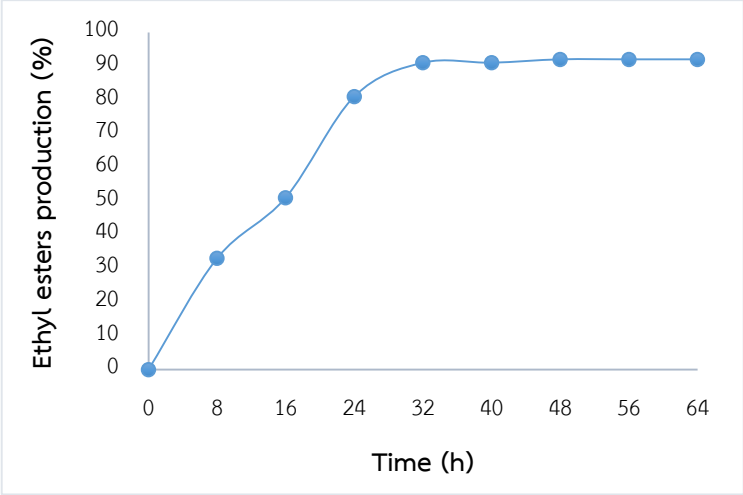

Figure 4.66 Effect of oil/ethanol molar ratio on transesterification of soybean oil. The reactions were performed with 1:6 molar ratio oil to anhydrous ethanol (four-step addition), 10 g of soybean oil and 0.4294 g of catalyst at 40°C for 64 hours

Also, the reaction was conducted by adding methanol stepwise to avoid enzyme inactivation. The effect of molar ratio of oil to methanol was investigated in the range of 1:4 to 1:6 molar ratio. In the study, anhydrous methanol was added in three steps for biodiesel production. The first addition was done at the beginning of

the reaction and the other additions were carried out in 8 and 16 hours for three-step addition during the reaction which took 32 hours at 40°C (amount of anhydrous methanol as showed Table 3.2). The reactions were performed with anhydrous methanol (three-step addition), 10 g of soybean oil and 0.4294 g of catalyst at 40°C for 32 hours. In the result, the optimal of molar ratio of oil to methanol on methyl esters production was 1:4 molar ratio. It gave the highest ethyl esters production (87%) as shown in Figure 4.67.

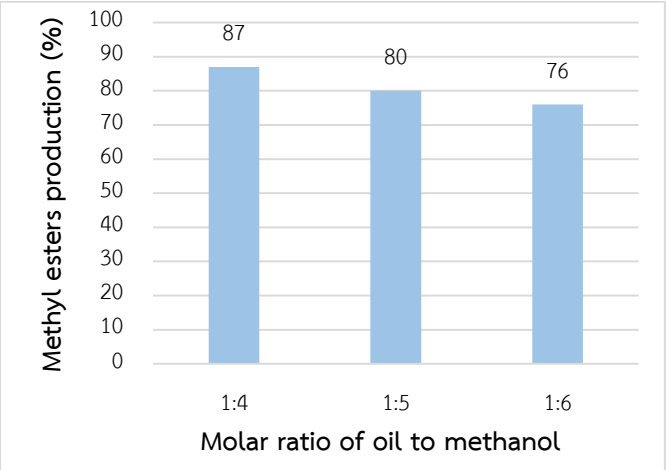

Figure 4.67 Effect of oil/methanol molar ratio on transesterification of soybean oil. The reactions were performed with anhydrous methanol (three-step addition), 10 g of soybean oil and 0.4294 g of catalyst at 40°C for 32 hours

The reactions were performed to examine the effect of molar ratio of oil to alcohol on transesterification. It was investigated by the comparison between anhydrous ethanol and anhydrous methanol. Results, only anhydrous ethanol gave the highest biodiesel conversion at 91%. The reactions were performed with 1:5 molar ratio oil to anhydrous ethanol (three-step addition), 10 g of soybean oil and 0.4294 g of catalyst at 40°C for 32 hours as presented in Figure 4.68.

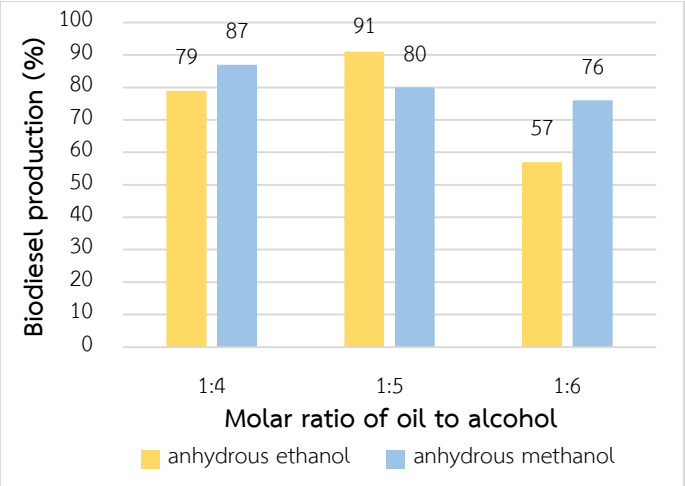

Figure 4.68 Effect of type of alcohol on transesterification of soybean oil with anhydrous ethanol and anhydrous methanol (three-step addition). The reactions were performed with 10 g of soybean oil and 0.4294 g of catalyst at 40°C for 32 hours

In addition, the water content in the reaction mixture is important to transesterification reaction. The effect of water on the reaction was investigated by using ethanol (AR, 95%) and anhydrous ethanol for transesterificaion of the soybean oil. The reactions were performed with 1:5 molar ratio oil to alcohol (three-step addition), 10 g of soybean oil and 0.4294 g of catalyst at 40°C for 64 hours. Results presented in Figure 4.69 showed that anhydrous ethanol used gave higher FAEEs production rate than ethanol and transesterification with ethanol (AR, 95%) possibly reached the maximal value almost the same as using anhydrous ethanol. This indicated that transesterification, hydrolysis and esterification possibly occurred during the reaction process. In a presence of water, partial soybean oil might be hydrolyzed and fatty acids, generated by the hydrolysis, were further reacted with alcohol to give FAEEs. Because of competition between those reactions, it needed time for transesterification of soybean oil until amount of glycerol was enough to dissolve most water presented in the reaction and then the conversion into FAEEs was finally equilibrated.

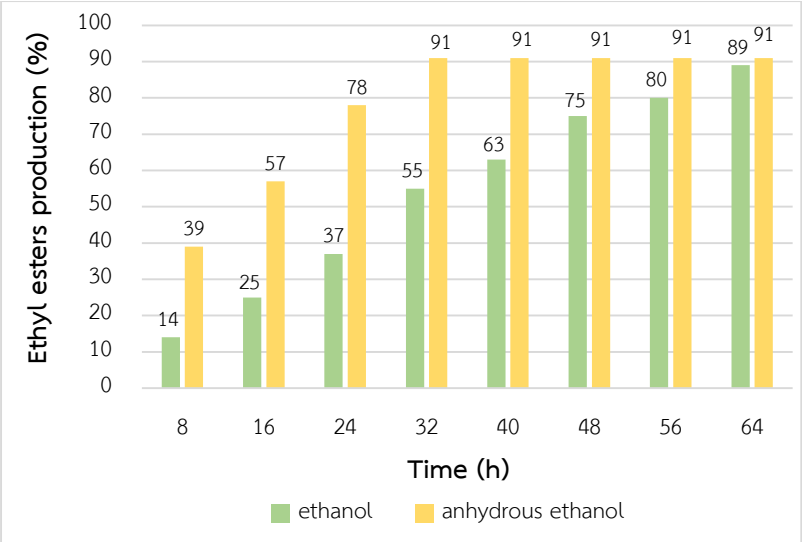

Figure 4.69 Effect of type of alcohol on transesterification of soybean oil with ethanol and anhydrous ethanol. The reactions were performed with 1:5 molar ratio oil to anhydrous ethanol (three-step addition), 10 g of soybean oil and 0.4294 g of catalyst at 40°C for 64 hours

4.4.1.4 Effect of reaction time on transesterification

The reaction time on transesterification reaction of soybean oil with anhydrous ethanol using immobilized lipase is an important parameter. As shown in Figure 4.70, transesterification reaction at 1:5 oil/ethanol molar ratio was not inhibited lipase activity because anhydrous ethanol (2.64 g) was added in three steps for biodiesel production. The first addition was realized at the beginning of the reaction and the other additions were carried out in 8 and 16 hours for three-step addition during the reaction which took 64 hours at 40°C. The first addition of anhydrous ethanol (1.58 g) was slowly increased ethyl esters production (39%) at the beginning of the reaction. Then, the other additions of anhydrous ethanol (0.53 g in each step) were noticeably increased ethyl esters production after added anhydrous ethanol at 8 and 16 hours. The ethyl esters production gave the higher conversion at 57% and 78%, respectively. The ethyl esters productions were practically constant (91%) over reaction time ranges between 32 and 64 hours, indicating the optimum reaction time could be 32 hours. The maximal value at 32 hours gave ethyl esters production at 91%.

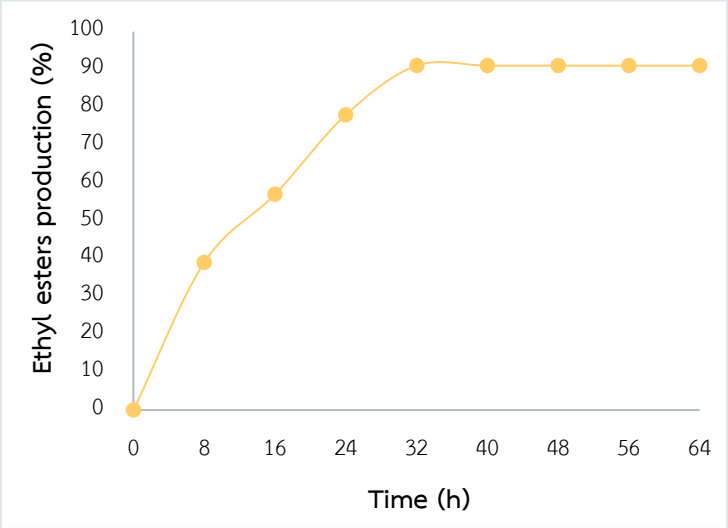

Figure 4.70 Effect of reaction time on transesterification of soybean oil with anhydrous ethanol. The reactions were performed with 1:5 molar ratio oil to anhydrous ethanol (three-step addition), 10 g of soybean oil and 0.4294 g of catalyst at 40°C for 64 hours

4.4.2 Operational stability and reusability of immobilized lipase

In general, the stability and reusability are the major advantage of immobilized lipase and cost of production process can be reduced by enhancing the reusability of immobilized lipase. Thus, the lipase-immobilized 15%GLU-2%CHI-15%STY/PS beads were reused in order to examine their stability and the recyclability. In this study, catalyst of immobilized lipase from *P. cepacia* onto GLU-CHI-STY/PS beads through transesterification of soybean oil with anhydrous ethanol was investigated. The effect of recycle usage on the biodiesel conversion of soybean oil by using the immobilized *P. cepacia* lipase (30 mg) immobilized onto 15%GLU-2%CHI-15%STY/PS beads (1 g) at 30°C for 72 hours. The three-step anhydrous ethanol was repeated every 32 hours. After completion of the reaction in 32 hours of each cycle, the lipase was transferred into the same system for a new cycle. The result was shown in in Figure 4.71. The original biodiesel conversion of soybean oil using the immobilized *P. cepacia* lipase was 91%. The obtained results showed that the conversion to ethyl esters production was decreased to 90%, 90%, 89%, 89% and 87% after 1, 2, 3, 4 and 5 cycles, respectively. However, the conversion was significantly decreased to 70% if it was

reused ten cycles. It was indicated that the lipase bound on GLU-CHI-STY/PS beads performed a good reusability, which was desirable for applications in biotechnology. In the reusability studies, the loss of activity may be ascribed to conformational changes of enzyme or to anhydrous ethanol deactivation of lipase during the reaction procedures. This result suggests that the immobilized *P. cepacia* lipase onto GLU-CHI-STY/PS beads enhances the stability of enzyme. The improved reusability of immobilized enzyme would make its application more economical. This immobilized system is applicable not only to the batch reaction but also to the continuous reaction and different reactor configurations.

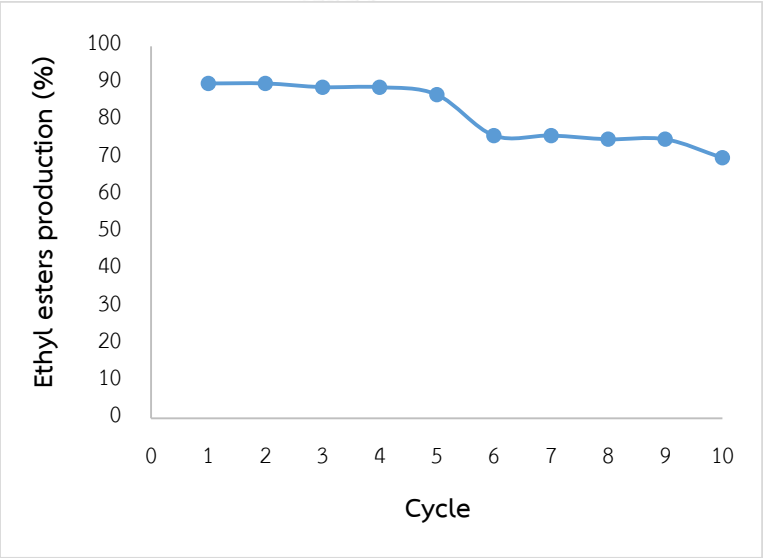

Figure 4.71 Operational stability and reusability of biodiesel from soybean oil with anhydrous ethanol. The reactions were performed with 1:5 molar ratio oil to anhydrous ethanol (three-step addition), 10 g of soybean oil and 0.4294 g of catalyst at 40°C for 32 hours.

CHAPTER V
CONCLUSION

This research studied biodiesel production through transesterification reaction of soybean oil with anhydrous ethanol and anhydrous methanol using lipase immobilized GLU-CHI-STY/PS beads. Lipase from *Pseudormonas cepacia* (*P. cepacia*) was immobilized onto the support, chitosan-styrene copolymer coated onto polystyrene beads activated with glutaraldehyde solution (GLU-CHI-STY/PS beads). The GLU-CHI-STY/PS beads were an excellent support for lipase immobilization because glutaraldehyde had been used as a cross-linking agent between free amine groups and increased the enzyme stability. For immobilization, the lipase activity, protein loading yield and specific activity of *P. cepacia* (30 mg) immobilized onto 15%GLU-2%CHI-15%STY/PS beads (1 g) gave the optimal value at 54.43 U/g-support, 72.93% and 2.49 U/mg-protein, respectively. The optimum conditions were 1:5 oil/ethanol molar ratio (three step addition of anhydrous ethanol), 0.4294 g catalyst at 40°C for 32 hours. It gave the highest ethyl esters production at 91%. Under optimal reaction conditions, the catalyst could be reused for 5 batches with 91% biodiesel and this catalysts after more than 5 batches of the reuse could produce only 87% of FAEEs. Since the immobilization method is very simple, the method could also be used for the immobilization of other enzymes.

REFERENCES

[1] Lu, J., Nie, K., Xie, F., Wang, F. and Tan, T. Enzymatic synthesis of fatty acid methyl esters from lard with immobilized *Candida sp.* 99-125. Process Biochemistry 42(9) (2007): 1367-1370.

[2] Srivastava, A. and Prasad, A. Triglycerides-based diesel fuels. Renewable and Sustainable Energy Reviews 4 (2000): 111-133.

[3] Rashid, U., Anwar, F., Moser, B.R. and Ashraf, S. Production of sunflower oil methyl esters by optimized alkali-catalyzed methanolysis. Biomass and Bioenergy 32(12) (2008): 1202-1205.

[4] Katchalski, K.E. Immobilized enzymes-learning from past successes and failures. Trends Biotechnol 11 (1993): 471-478.

[5] Stoytcheva, M., Montero, G., Toscano, L., Gochev, V. and Valdez, B. The Immobilized Lipases in Biodiesel Production. Biodiesel-Feedstocks and Processing Technologies (2011): 397-411.

[6] Miletić, N., Rohandi, R., Vuković, Z., Nastasović, A. and Loos, K. Surface modification of macroporous poly(glycidyl methacrylate-co-ethylene glycol dimethacrylate) resins for improved *Candida antarctica* lipase B immobilization. Reactive and Functional Polymers 69(1) (2009): 68-75.

[7] Shaw, S.Y., Chen, Y., Qu, J. and Ho, L. Preparation and characterization of *Pseudomonas putida esterase* immobilized on magnetic nanoparticles. Enzyme and Microbial Technology 39(5) (2006): 1089-1095.

[8] Xie, W. and Ma, N. Enzymatic transesterification of soybean oil by using immobilized lipase on magnetic nano-particles. Biomass and Bioenergy 34(6) (2010): 890-896.

[9] Tischer, W. and Wedekind, F. Immobilized Enzymes: Methods and Applications. Topics in Current Chemistry 200 (1999): 95-126.

[10] Wang, Y., Zhang, G., Yan, H., Fan, Y., Shi, Z., Lu, Y., Sun, Q., Jiang, W., Zheng, Y.,

Lib, S. and Liu, Z. Polystyrene resins cross-linked with di- or tri(ethylene glycol) dimethacrylates as supports for solid-phase peptide synthesis. Tetrahedron 62(20) (2006): 4948-4953.

[11] Kumar, M.N.V., Muzzarelli, R.A.A., Muzzarelli, C., Sashiwa, H. and Domb, A.J. Chitosan Chemistry and Pharmaceutical Perspectives. Chemical Reviews 104(12) (2004): 6017-6084.

[12] Krajewska, B. Application of chitin- and chitosan-based materials for enzyme immobilizations: a review. Enzyme and Microbial Technology 35(2-3) (2004): 126-139.

[13] Anita, A., Sastry, C.A. and Hashim, M.A. Immobilization of urease on vermiculite. Bioprocess Engineering 16 (1997): 375-380.

[14] Anita, A., Sastry, C.A. and Hashim, M.A. Immobilization of urease using Amberlite MB-1. Bioprocess Engineering 17 (1997): 355-359.

[15] Migneault, I., Dartiguenave, C., Bertrand, M.J. and Waldron, K.C. Glutaraldehyde: behavior in aqueous solution, reaction with proteins, and application to enzyme crosslinking. Biotechnology Techniques 37 (2004): 790-802.

[16] Lopez-Gallego, F., Betancor, L., Hidalgo, A., Dellamora-Ortiz, G., Mateo, C., Fernandez-Lafuente, R. and Guisan, J.M. Stabilization of different alcohol oxidases via immobilization and post immobilization techniques. Enzyme and Microbial Technology 40(2) (2007): 278-284.

[17] Shah, S. and Gupta, M.N. Lipase catalyzed preparation of biodiesel from *Jatropha* oil in a solvent free system. Process Biochemistry 42(3) (2007): 409-414.

[18] Li, S.F., Fan, Y.H., Hu, R.F. and Wu, W.T. *Pseudomonas cepacia* lipase immobilized onto the electrospun PAN nanofibrous membranes for biodiesel production from soybean oil. Journal of Molecular Catalysis B: Enzymatic 72(1-2) (2011): 40-45.

[19] Noureddini, H., Gao, X. and Philkana, R.S. Immobilized *Pseudornonas cepacia* lipase for biodiesel fuel production from soybean oil. Bioresource Technology 96 (2005): 769-777.

[20] Helwani, Z., Othman, M.R., Aziz, N., Fernando, W.J.N., and Kim, J. Technologies for production of biodiesel focusing on green catalytic techniques: A review. Fuel Processing Technology 90(12) (2009): 1502-1514.

[21] Juan, J.C., Kartika, D.A., Wu, T.Y., and Hin, T.Y. Biodiesel production from Jatropha oil by catalytic and non-catalytic approaches: an overview. Bioresource Technology 102(2) (2011): 452-460.

[22] Ma, F. and Hanna, M.A. Biodiesel production: a review. Bioresource Technology 70 (1999): 1-15.

[23] Schwab, A.W., Dykstra, G.J., Selke, E., Sorenson, S.C. and Pryde, E.H. Diesel Fuel from Thermal Decomposition of Soybean Oil. Journal of the American Oil Chemists Society 65(11) (1988): 1781-1786.

[24] Freedman, B., Butterfield, R.O. and Pryde, E.H. Transesterification Kinetics of Soybean Oil. Journal of the American Oil Chemists Society 63(10) (1986): 1375-1380.

[25] Romano, S.D. and Sorichetti, P.A. Introduction to Biodiesel Production. Green Energy and Technology (2010): 7-27.

[26] Singh, S.P. and Singh, D. Biodiesel production through the use of different sources and characterization of oils and their esters as the substitute of diesel: A review. Renewable and Sustainable Energy Reviews 14(1) (2010): 200-216.

[27] Atabani, A.E., Silitonga, A.S., Badruddin, I.A., Mahlia, T.M.I., Masjuki, H.H., and Mekhilef, S. A comprehensive review on biodiesel as an alternative energy resource and its characteristics. Renewable and Sustainable Energy Reviews 16(4) (2012): 2070-2093.

[28] Bellaloui, N., Bruns, H.A., Gillen, A.M., Abbas, H.K., Zablotowicz, R.M., Mengistu, A. and Paris, R.L. Soybean seed protein, oil, fatty acids, and mineral composition as influenced by soybean-corn rotation. Agricultural Sciences 01(03) (2010): 102-109.

[29] Kummerow, F.A. The Effects of Hydrogenation on Soybean Oil. InTech (2013): 353-373.

[30] Cahoon, E.B. Genetic Enhancement of Soybean Oil for Industrial Uses: Prospects and Challenges. AgBioForum 6(1&2) (2003): 11-13.

[31] Lotero, E., Liu, Y., Lopez, D.E., Suwannakam, K., Bruce, D.A. and Goodwin, J.R. J.G. Synthesis of Biodiesel via Acid Catalysis. Industrial and Engineering Chemistry Research 44 (2005): 5353-5363.

[32] Schuchardt, U., Sercheli, R. and Vargas, R.M. Transesterification of Vegetable Oils: a Review. J. Braz. Chem. Soc. 9(1) (1998): 199-210.

[33] Banerjee, A. and Chakraborty, R. Parametric sensitivity in transesterification of waste cooking oil for biodiesel production-A review. Resources, Conservation and Recycling 53(9) (2009): 490-497.

[34] Lee, D.W., Park, Y.M. and Lee, K.Y. Heterogeneous Base Catalysts for Transesterification in Biodiesel Synthesis. Catalysis Surveys from Asia 13(2) (2009): 63-77.

[35] Marchetti, J.M., Miguel, V.U. and Errazu, A.F. Techno-economic study of different alternatives for biodiesel production. Fuel Processing Technology 89(8) (2008): 740-748.

[36] Fukuda, H., Kondo A. and Noda H. Biodiesel Fuel Production by Transesterification of Oils. Journal of Bioscience and Bioengineering 92(5) (2001): 405-416.

[37] Leung, D.Y.C., Wu, X. and Leung, M.K.H. A review on biodiesel production using catalyzed transesterification. Applied Energy 87(4) (2010): 1083-1095.

[38] Akoh, C.C., Chang, S., Lee, G. and Shaw, J. Enzymatic Approach to Biodiesel Production. Journal of Agricultural and Food Chemistry 55 (2007): 8995–9005.

[39] Robles-Medina, A., Gonzalez-Moreno, P.A., Esteban-Cerdan, L. and Molina-Grima, E. Biocatalysis: towards ever greener biodiesel production. Biotechnol Adv 27(4) (2009): 398-408.

[40] Fjerbaek, L., Christensen, K.V. and Norddahl, B. A review of the current state of biodiesel production using enzymatic transesterification. Biotechnol Bioeng 102(5) (2009): 1298-315.

[41] Kaieda, M., Samukawa, T., Matsumoto, T., Ban, K., Kondo, A. and Shimada, Y. Biodiesel Fuel Production from Plant Oil Catalyzed by *Rhizopus oryzae* Lipase in a Water-Containing System without an Organic Solvent. Journal of bioscience and bioengineerwg 88(6) (1999): 627-631.

[42] Kaieda, M., Samukawa, T., Kondo, A. and Fukuda, H. Effect of Methanol and water contents on production of biodiesel fuel from plant oil catalyzed by various lipases in a solvent-free system. Journal of Bioscience and Bioengineering 91(1) (2001): 12-15.

[43] Kumari, V., Shah, S. and Gupta, M.N. Preparation of biodiesel by lipase-catalyzed transesterification of high free fatty acid containing oil from *Madhuca indica.* Energy and Fuels 21 (2007): 368-372.

[44] Abigor, R.D., Uadia, P.O., Foglia, T.A., Haas, M.J., Jones, K.C. and Okpefa, E. Lipase catalysed production of biodiesel fuel from some Nigerian lauric oils. Biochemical Society Transactions 28 (2000): 979-981.

[45] Lara, P.V. and Park, E.Y. Potential application of waste activated bleaching earth on the production of fatty acid alkyl esters using *Candida cylindracea* lipase in organic solvent system. Enzyme and Microbial Technology 34(3-4) (2004): 270-277.

[46] Shah, S., Sharma, S. and Gupta, M.N. Biodiesel preparation by lipase-catalyzed transesterification of *Jatropha* oil. Energy Fuels 18 (2004): 154-159.

[47] Selmi, B. and Thomas, D. Immobilized lipase-catalyzed ethanolysis of sunflower oil in a solvent-free medium. Journal of the American Oil Chemists' Society 75(6) (1998): 691-695.

[48] Chen, G., Ying, M. and Li, W. . Enzymatic conversion of waste-cooking oils into alternative fuel biodiesel. Applied Biochemistry and Biotechnology 132 (2006): 911-921.

[49] Rodrigues, R.C., Volpato, G., Ayub, M.A.Z. and Wada, K. Lipase-catalyzed ethanolysis of soybean oil in a solvent-free system using central composite design and response surface methodology. Journal of Chemical Technology & Biotechnology 83(6) (2008): 849-854.

[50] Brady, L. and Menge, U. A serine protease triad forms the catalytic centre of a triacylglycerol lipase. Letters Nature 343 (1990): 767-770.

[51] Winkler, F.K., D'Arcy, A. and Hunziker, W. Structure of human pancreatic lipase. Letters Nature 343 (1990): 771-774.

[52] Schrag, J.D., Li, Y., Wu, S. and Cygler, M. . Ser-His-Glu triad forms the catalytic site of the lipase from *Geotrichum candidum*. Letters Nature 351 (1991): 761-764.

[53] Schrag, J.D., Li, Y., Cygler, M., Lang, D., Burgdorf, T., Hecht, H. J., Schmid, R., Schomburg, D., Rydel, T. J., Oliver, J. D., Strickland, L. C., Dunaway, C. M., Larson, S. B., Day, J. and Pherson, A. M. The open conformation of a *Pseudomonas* lipase. Biotechnol. Researc. Instit. 5 (1997): 187-202.

[54] Ollis, D.L., Cheah, E., Cyglerl, M., Dijkstra, B., Frolow, F., Franken, S.M., Harel, M., Remington, S.J., Silman, I., Schragl, J., Sussman, J.L., Verschueren, K.H.G. and Goldmans, A. The α/β hydrolase fold. Protein Engineering 5 (1992): 197-211.

[55] Cygler, M., Schrag, J.D., Sussman, J.L., Harel, M., Silman, I., Gentry, M.K. and Doctor, B.P. Relationship between sequence conservation and three-dimensional structure in a large family of esterases, lipases, and related proteins. Protein Science 2 (1993): 366-382.

[56] Liu, Y., Zhang, X., Tan, H., Yan, Y. and Hameed, B.H. Effect of pretreatment by different organic solvents on esterification activity and conformation of immobilized *Pseudomonas cepacia* lipase. Process Biochemistry 45(7) (2010): 1176-1180.

[57] Otero, C., Berrendero, M.A., Cardenas, F., Alvarez, E. and Elson, S.W. General characterization of non-commercial microbial lipases in hydrolytic and synthetic reactions. Applied Biochemistry and Biotechnology 120 (2005): 209-223.

[58] Ranganathan, S.V., Narasimhan, S.L. and Muthukumar, K. An overview of enzymatic production of biodiesel. Bioresource Technology 99(10) (2008): 3975-3981.

[59] Tosa, T., Sato, T., Mori, T., Yamamoto, K., Takata, I., Nishida, Y. and Chibata, I. Immobilization of enzymes and microbial cells using carrageenan as matrix Biotechnology and Bioengineering 21 (1979): 1697-1709.

[60] Tan, T., Lu, J., Nie, K., Deng, L. and Wang, F. Biodiesel production with immobilized lipase: A review. Biotechnology Advances 28(5) (2010): 628-634.

[61] Nisha, S., Arun, K.S. and Gobi, N. A Review on Methods, Application and Properties of Immobilized Enzyme. Chemical Science Review and Letters 1 (2012): 148-155.

[62] Cetinus, S.A. and Oztop, H.N. Immobilization of catalase into chemically crosslinked chitosan beads. Enzyme and Microbial Technology 32 (2003): 889.

[63] Brady, D. and Jordaan, J. Advances in enzyme immobilisation. Biotechnol Lett 31(11) (2009): 1639-50.

[64] Solas, M.T. et al. Ionic adsorption of catalase on bioskin-kinetic and ultrastructural studies. Journal of Biotechnology 33 (1994): 63.

[65] Torres, R. et al. Reversible immobilization of invertase on Sepabeads coated with polyethyleneimine: Optimization of the biocatalyst's stability. . Biotechnology Progress 18 (2002): 1221.

[66] Yadav, G.D. and Jadhav, S.R. Synthesis of reusable lipases by immobilization on hexagonal mesoporous silica and encapsulation in calcium alginate: Transesterification in non-aqueous medium. Microporous and Mesoporous Materials 86(1-3) (2005): 215-222.

[67] Köse, Ö., Tüter, M. and Aksoy, H.A. Immobilized *Candida antarctica* lipase-catalyzed alcoholysis of cotton seed oil in a solvent-free medium. Bioresource Technology 83(2) (2002): 125-129.

[68] Hung, T.C., Giridhar, R., Chiou, S.H. and Wu, W.T. Binary immobilization of *Candida rugosa* lipase on chitosan. Journal of Molecular Catalysis B: Enzymatic 26(1-2) (2003): 69-78.

[69] Royon, D., Daz, M., Ellenrieder, G. and Locatelli, S. Enzymatic production of biodiesel from cotton seed oil using t-butanol as a solvent. Bioresour Technol 98(3) (2007): 648-653.

[70] Halim, S.F.A. and Harun Kamaruddin, A. Catalytic studies of lipase on FAME production from waste cooking palm oil in a tert-butanol system. Process Biochemistry 43(12) (2008): 1436-1439.

[71] Dizge, N. and Keskinler, B. Enzymatic production of biodiesel from canola oil using immobilized lipase. Biomass and Bioenergy 32(12) (2008): 1274-1278.

[72] Dizge, N., Keskinler, B. and Tanriseven, A. Biodiesel production from canola oil by using lipase immobilized onto hydrophobic microporous styrene-divinylbenzene copolymer. Biochemical Engineering Journal 44(2-3) (2009): 220-225.

[73] Nasratun, M., Said, H.A., Noraziah, A. and Abd Alla, A.N. Immobilization of Lipase from *Candida rugosa* on Chitosan Beads for Transesterification Reaction American Journal of Applied Sciences 6(9) (2009): 1653-1657.

[74] Egwim, E.C., Adesina, A.A., Oyewole, O.A. and Okoliegbe, I.N. Optimization of Lipase Immobilized on Chitosan Beads for Biodiesel Production. Global Research Journal of Microbiology 2(2) (2012): 103-112.

[75] Xie, W. and Wang, J. Immobilized lipase on magnetic chitosan microspheres for transesterification of soybean oil. Biomass and Bioenergy 36 (2012): 373-380.

[76] Kuo, C.H., Liu, Y.C., Chang, C.M.J., Chen, J.H., Chang, C., and Shieh, C.J. Optimum conditions for lipase immobilization on chitosan-coated Fe3O4 nanoparticles. Carbohydrate Polymers 87(4) (2012): 2538-2545.

[77] Bradford, M.M. A rapid and sensitive method for quantitation of microgram quantities of protein utilizing the principle of protein-dye binding. Analytical Biochemistry 72 (1976): 248-254.

[78] Winkler, U.K. and Stuckmann, M. Glycogen, hyaluronate and some other polysaccharides greatly enhance the formation of exolipase by *Serratia marcescens*. Journal of Bacteriology 138 (1979): 663-670.

[79] Khalid, K., Musa, M., Jusoff, K., Abdullah, R., Zaini, Z.M.M. and Samsudin, A. Lowering of palm oil cloud point by enzymatic acidolysis. World Applied Sciences 12 (2011): 28-31.

[80] Naim, A.A., Umar, A., Sanagi, M.M. and Basaruddin, N. Chemical modification of chitin by grafting with polystyrene using ammonium persulfate initiator. Carbohydrate Polymers 98(2) (2013): 1618-1623.

[81] Silva, J.A., Macedo, G.P., Rodrigues, D.S., Giordano, R.L.C. and Gonçalves, L.R.B. Immobilization of *Candida antarctica* lipase B by covalent attachment on chitosan-based hydrogels using different support activation strategies. Biochemical Engineering Journal 60 (2012): 16-24.

[82] Chen, H., Zhang, Q., Dang, Y. and Shu, G. The effect of glutaraldehyde cross-linking on the enzyme activity of immobilized β-Galactosidase on chitosan bead. Advance Journal of Food Science and Technology 5(7) (2013): 932-935.

APPENDIX

APPENDIX A

ENZYMATIC ASSAY

1. Analysis of lipase activity

1.1 Preparation of *p*-nitrophenol (*p*-NP) standard curve

The concentration of *p*-NP (10 μmol/ml) was prepared by dissolving 34.8 mg of *p*-NP in 25 ml of PBS:EtOH:Na_2CO_3 (1.1:1:2). *p*-NP (0.25 μmol/ml) as stock solution was prepared by dissolving 2.50 ml of *p*-NP solution (10 μmol/ml) in 100 ml of PBS:EtOH:Na_2CO_3 (1.1:1:2). The standard curve was performed by diluted of *p*-NP solution (0.25 μmol/ml) in the range of 0.006 - 0.042 μmol/ml was investigated.

Table A-1 Variation of concentration of p-nitrophenol solution

Sample number	Required *p*-NP concentration (μmol/ml)	Volume of *p*-NP (0.25 μmol/ml) (ml)	Volume of solution used to dilute (PBS:EtOH:Na_2CO_3 = 1.1:1:2) (ml)
Blank	0.000	0.00	10.00
1	0.006	0.24	9.76
2	0.012	0.48	9.52
3	0.018	0.72	9.28
4	0.024	0.96	9.04
5	0.030	1.20	8.80
6	0.036	1.44	8.56
7	0.042	1.68	8.32

1.2 The *p*-NP solution was measured by colorimetric method at 410 nm. Results were presented on Figure A-1.

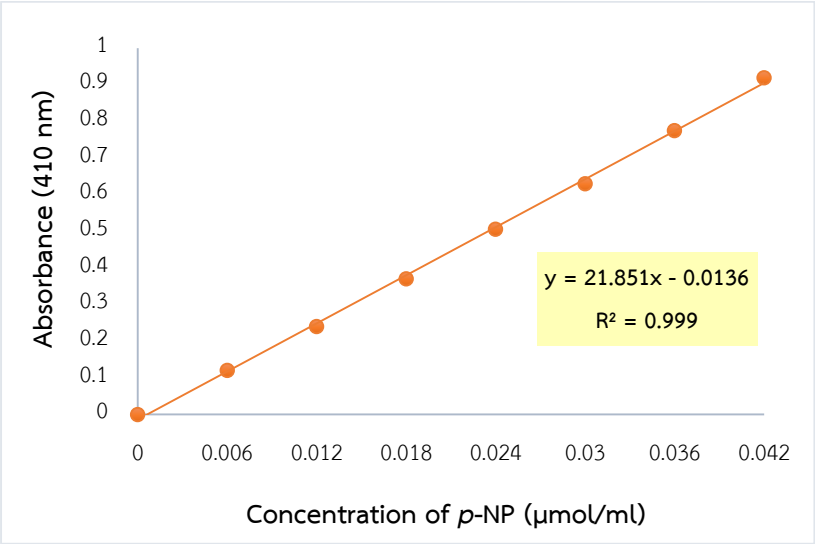

Figure A-1 Standard curve of *p*-nitrophenol (*p*-NP) concentration

1.3 Calculation of lipase activity (One unit (U) of lipase activity was defined as the amount of enzyme necessary to produce 1 µmol of *p*-nitrophenol (*p*-NP) released per min from *p*-nitrophenyl palmitate (*p*-NPP) under standard conditions).

2. Analysis of protein loading

2.1 Preparation of concentration of protein as standard curve

The concentration of protein (10 mg/ml) as stock protein solution was prepared by dissolving 80 mg of *Pseudomonas cepacia* (*P. cepacia*) in 8 ml of PBS buffer (25 mM, pH 7.0). Protein assay was performed by diluting of stock protein solution (10 mg/ml) in the range of 1-10 mg/ml. 1.0 ml of protein solution containing 1 to 10 mg/ml was pipetted into the test tubes. Then, 5 ml of protein reagent was added to the test tube and the contents mixed either by vortexing. The absorbance at 595 nm was measured after 2 min in 3 ml cuvettes against a reagent blank prepared from 1.0 ml of the appropriate PBS buffer (25 mM, pH 7.0) and 5 ml of protein reagent. The weight of protein was plotted against the corresponding absorbance resulting in a standard curve used to determine the protein in unknown samples. Results were presented in Table A-2.

Table A-2 Variation of concentration of protein

Sample number	Concentration of protein (mg/ml)	Volume of stock protein (ml)	Volume of 0.025 M, pH 7.0 PBS buffer (ml)	Volume of protein solution (ml)	Volume of protein reagent (ml)
Blank	0	0.00	1.00	0.00	5.00
1	1	0.10	0.90	1.00	5.00
2	2	0.20	0.80	1.00	5.00
3	3	0.30	0.70	1.00	5.00
4	4	0.40	0.60	1.00	5.00
5	5	0.50	0.50	1.00	5.00
6	6	0.60	0.40	1.00	5.00
7	7	0.70	0.30	1.00	5.00
8	8	0.80	0.20	1.00	5.00
9	9	0.90	0.10	1.00	5.00
10	10	1.00	0.00	1.00	5.00

2.2 The samples were measured by colorimetric method at 595 nm. The standard curve of protein concentration was shown in Figure A-2.

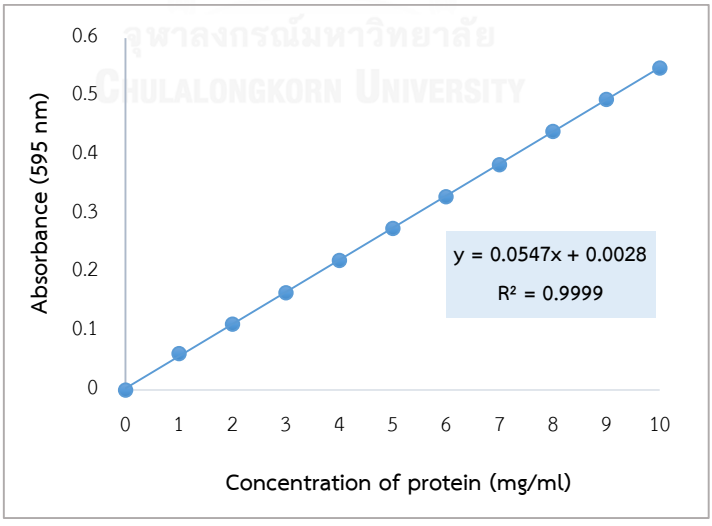

Figure A-2 Standard curve of protein concentration

2.3 Calculation of amount of protein was immobilized onto GLU-CHI-STY/PS beads. The amount of bound protein on the support was calculated from the difference between the amount of protein introduced into the reaction mixture and the amount of protein present in the solution after immobilization.

3. The ATR-FTIR spectrums of immobilized lipase

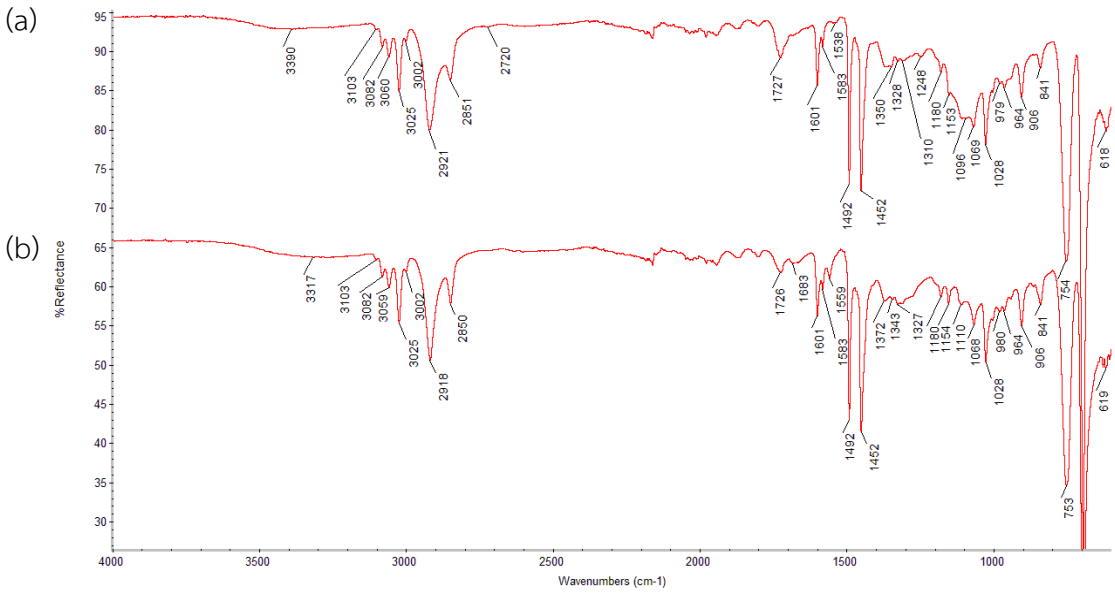

Figure A-3 Comparison of ATR-FTIR spectrums of (a) 5%GLU-1%CHI-15%STY/PS beads and (b) 18 mg of lipase immobilized onto 5%GLU-1%CHI-15%STY/PS beads at 30°C for 72 hours

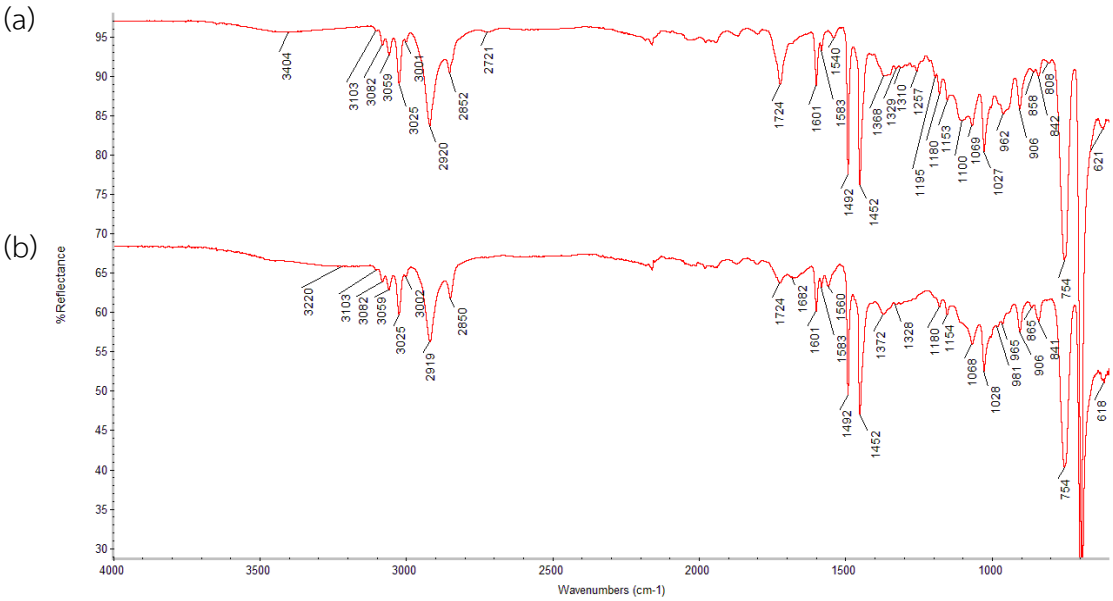

Figure A-4 Comparison of ATR-FTIR spectrums of (a) 10%GLU-1%CHI-15%STY/PS beads and (b) 18 mg of lipase immobilized onto 10%GLU-1%CHI-15%STY/PS beads at 30°C for 72 hours

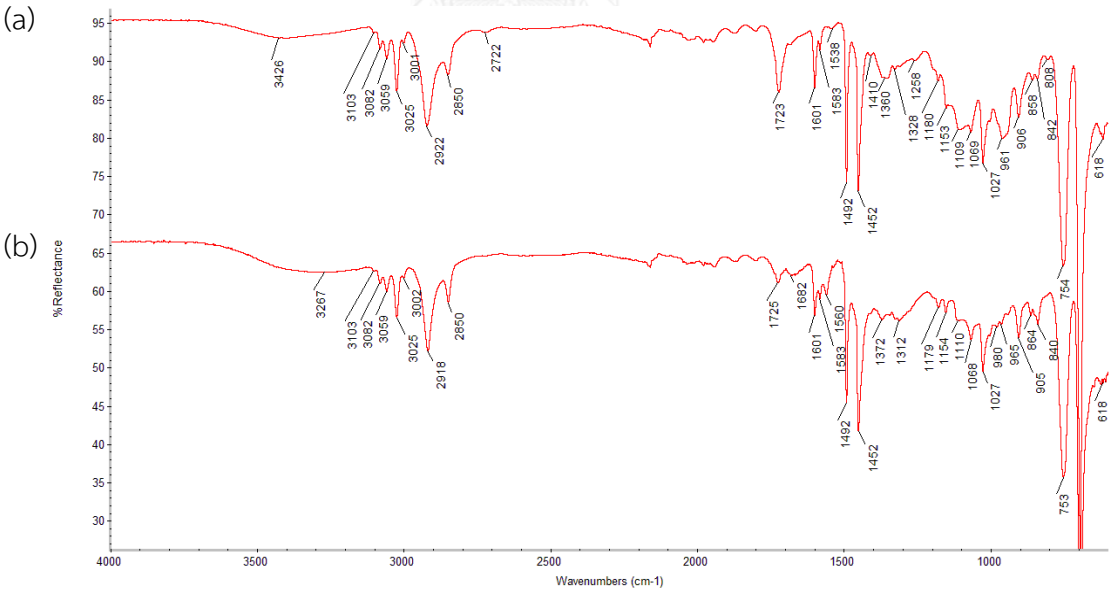

Figure A-5 Comparison of ATR-FTIR spectrums of (a) 15%GLU-1%CHI-15%STY/PS beads and (b) 18 mg of lipase immobilized onto 15%GLU-1%CHI-15%STY/PS beads at 30°C for 72 hours

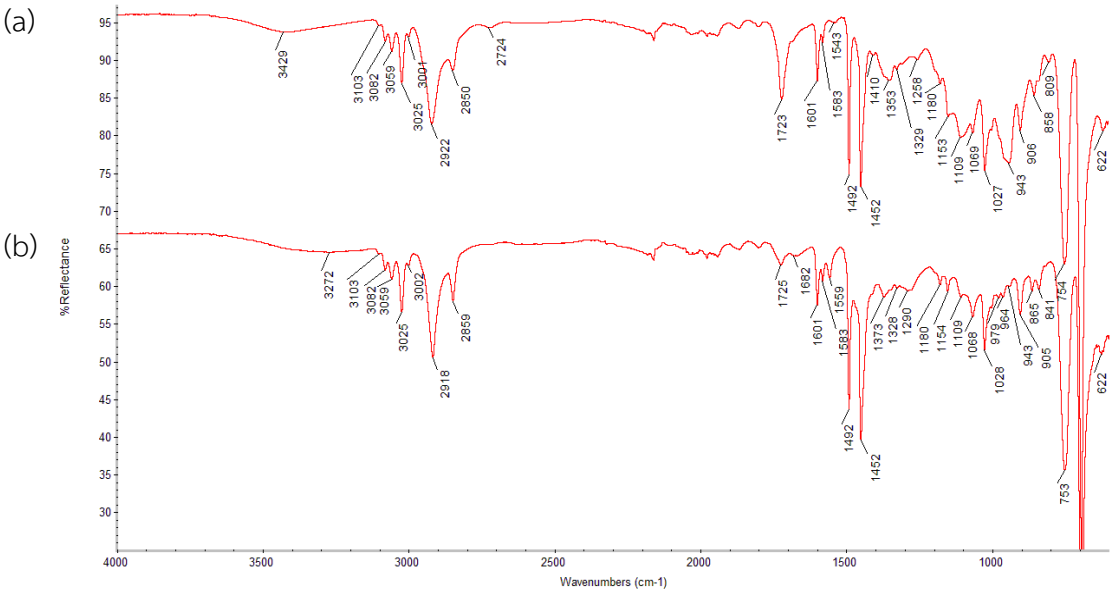

Figure A-6 Comparison of ATR-FTIR spectrums of (a) 20%GLU-1%CHI-15%STY/PS beads and (b) 18 mg of lipase immobilized onto 20%GLU-1%CHI-15%STY/PS beads at 30°C for 72 hours

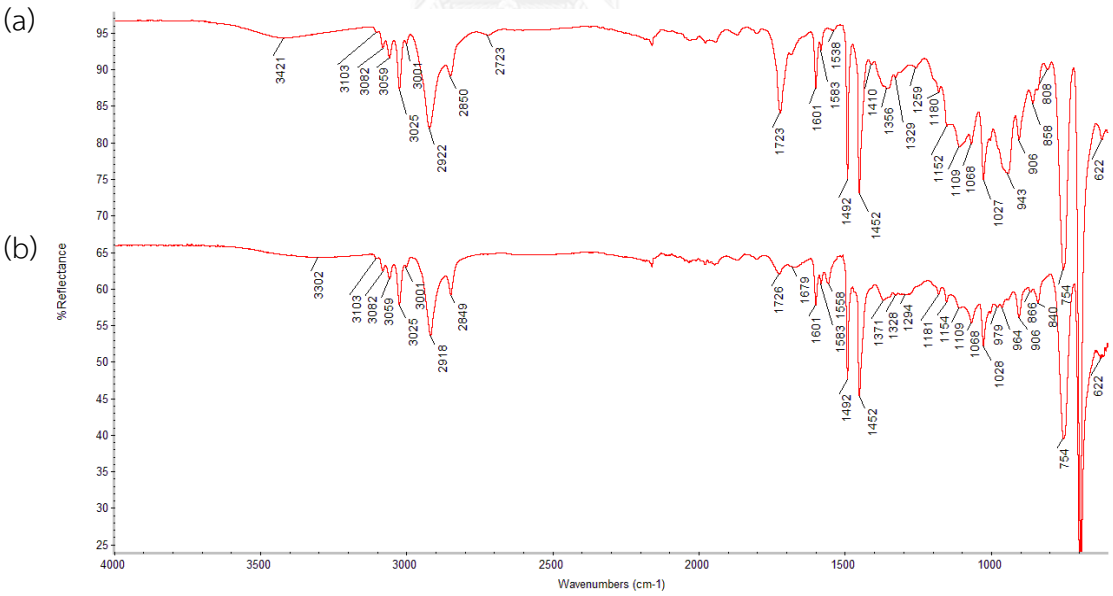

Figure A-7 Comparison of ATR-FTIR spectrums of (a) 25%GLU-1%CHI-15%STY/PS beads and (b) 18 mg of lipase immobilized onto 25%GLU-1%CHI-15%STY/PS beads at 30°C for 72 hours

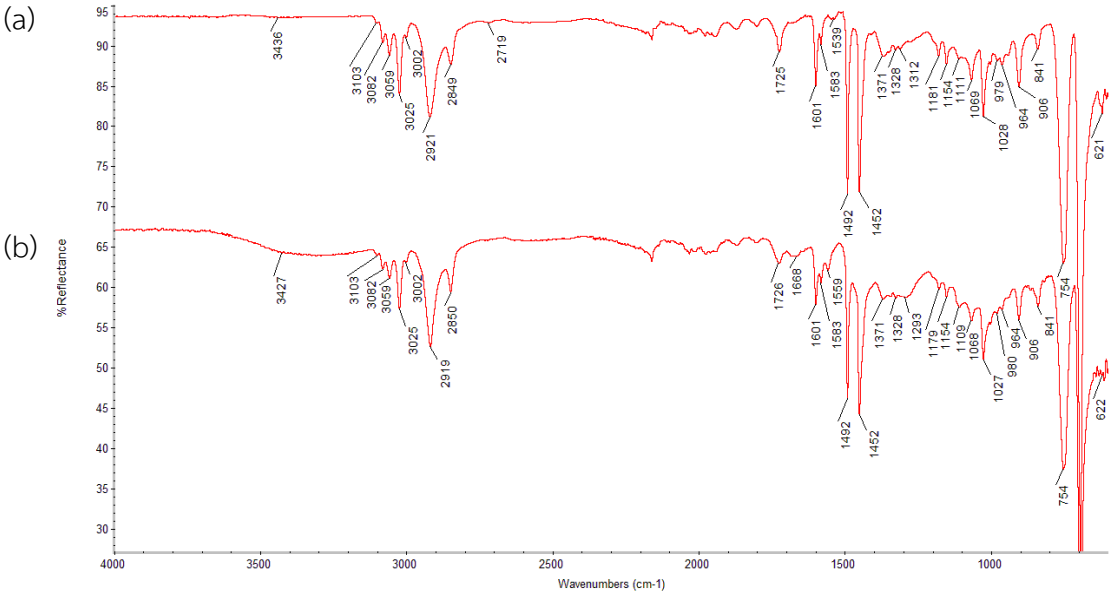

Figure A-8 Comparison of ATR-FTIR spectrums of (a) 5%GLU-2%CHI-15%STY/PS beads and (b) 18 mg of lipase immobilized onto 5%GLU-2%CHI-15%STY/PS beads at 30°C for 72 hours

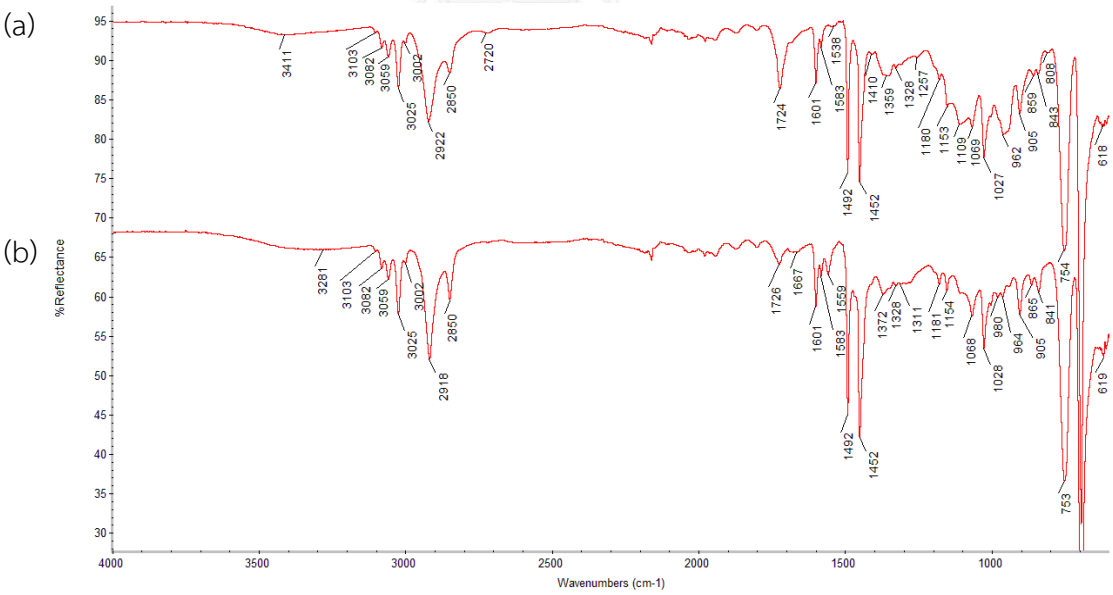

Figure A-9 Comparison of ATR-FTIR spectrums of (a) 10%GLU-2%CHI-15%STY/PS beads and (b) 18 mg of lipase immobilized onto 10%GLU-2%CHI-15%STY/PS beads at 30°C for 72 hours

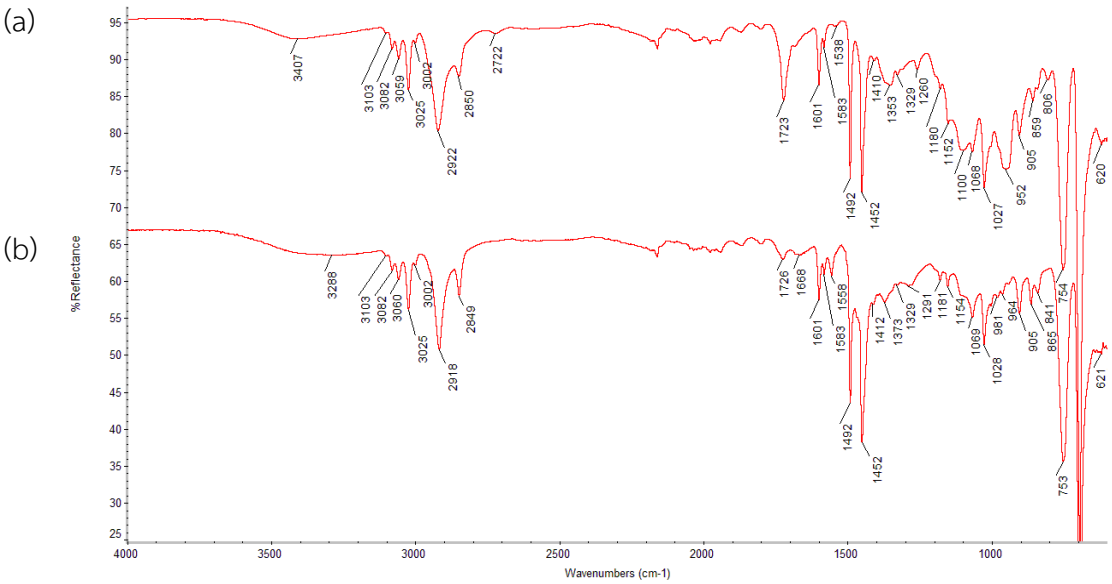

Figure A-10 Comparison of ATR-FTIR spectrums of (a) 15%GLU-2%CHI-15%STY/PS beads and (b) 18 mg of lipase immobilized onto 15%GLU-2%CHI-15%STY/PS beads at 30°C for 72 hours

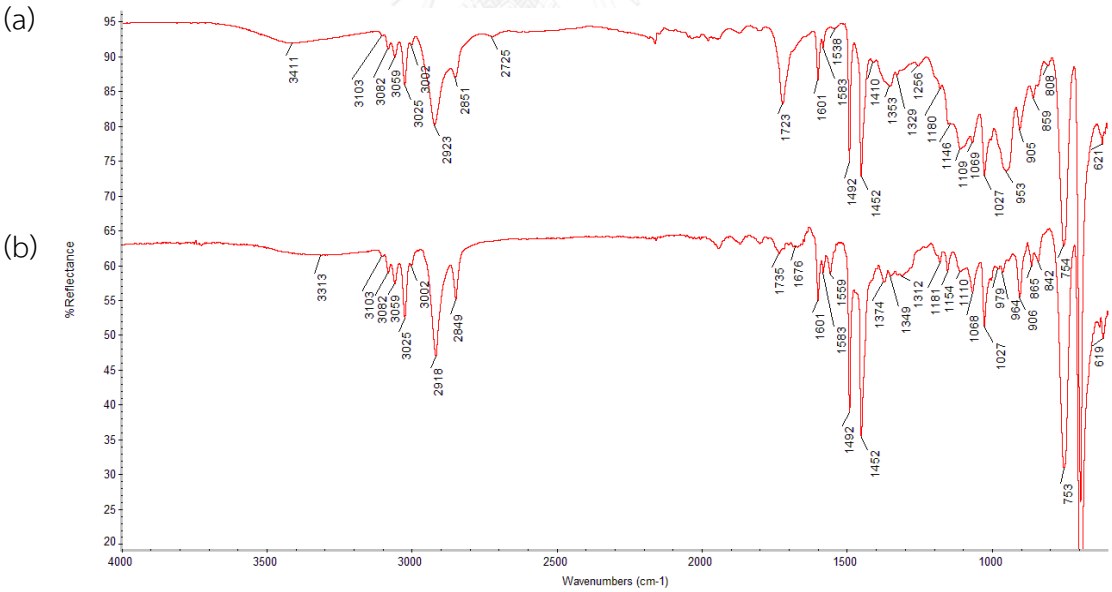

Figure A-11 Comparison of ATR-FTIR spectrums of (a) 20%GLU-2%CHI-15%STY/PS beads and (b) 18 mg of lipase immobilized onto 20%GLU-2%CHI-15%STY/PS beads at 30°C for 72 hours

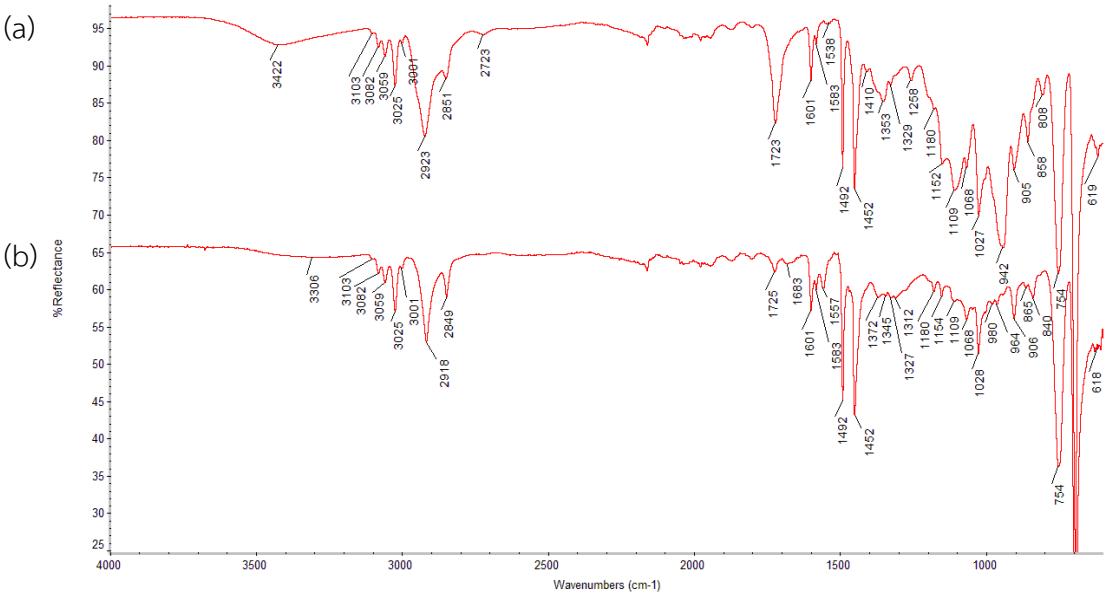

Figure A-12 Comparison of ATR-FTIR spectrums of (a) 25%GLU-2%CHI-15%STY/PS beads and (b) 18 mg of lipase immobilized onto 25%GLU-2%CHI-15%STY/PS beads at 30°C for 72 hours

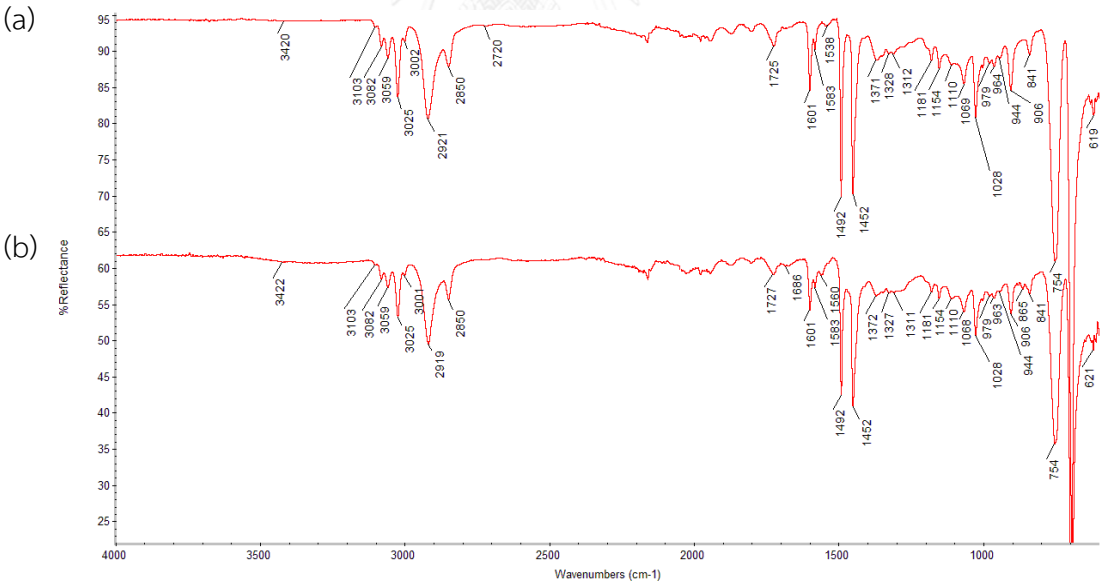

Figure A-13 Comparison of ATR-FTIR spectrums of (a) 5%GLU-3%CHI-15%STY/PS beads and (b) 18 mg of lipase immobilized onto 5%GLU-3%CHI-15%STY/PS beads at 30°C for 72 hours

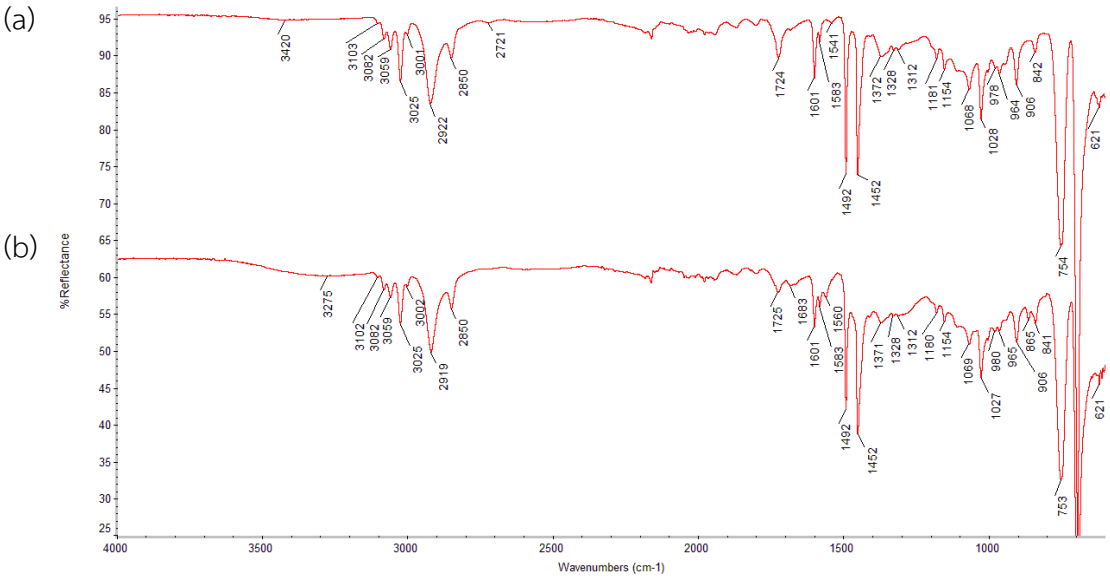

Figure A-14 Comparison of ATR-FTIR spectrums of (a) 10%GLU-3%CHI-15%STY/PS beads and (b) 18 mg of lipase immobilized onto 10%GLU-3%CHI-15%STY/PS beads at 30°C for 72 hours

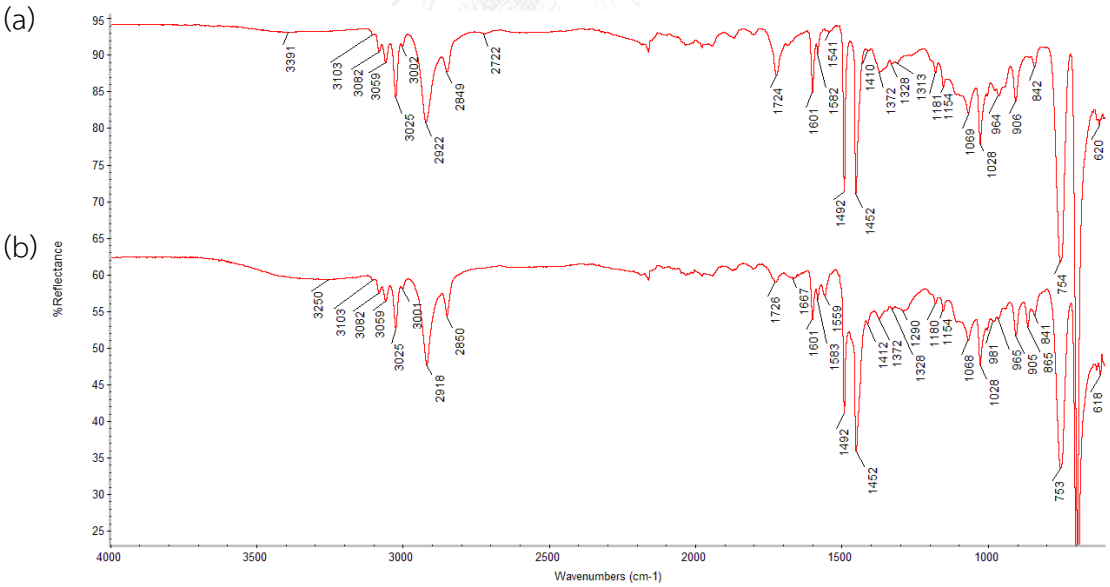

Figure A-15 Comparison of ATR-FTIR spectrums of (a) 15%GLU-3%CHI-15%STY/PS beads and (b) 18 mg of lipase immobilized onto 15%GLU-3%CHI-15%STY/PS beads at 30°C for 72 hours

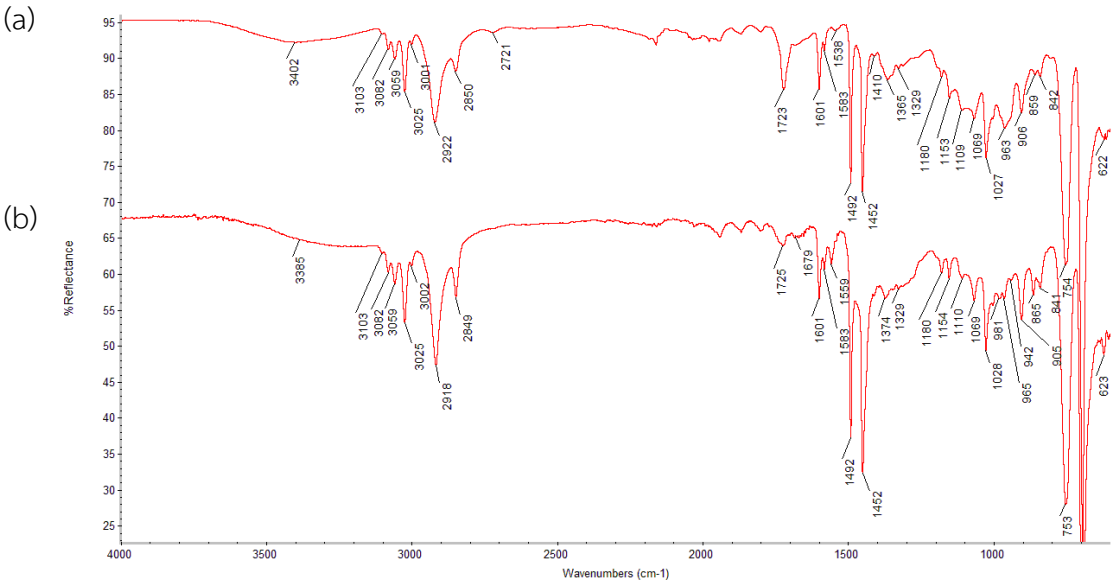

Figure A-16 Comparison of ATR-FTIR spectrums of (a) 20%GLU-3%CHI-15%STY/PS beads and (b) 18 mg of lipase immobilized onto 20%GLU-3%CHI-15%STY/PS beads at 30°C for 72 hours

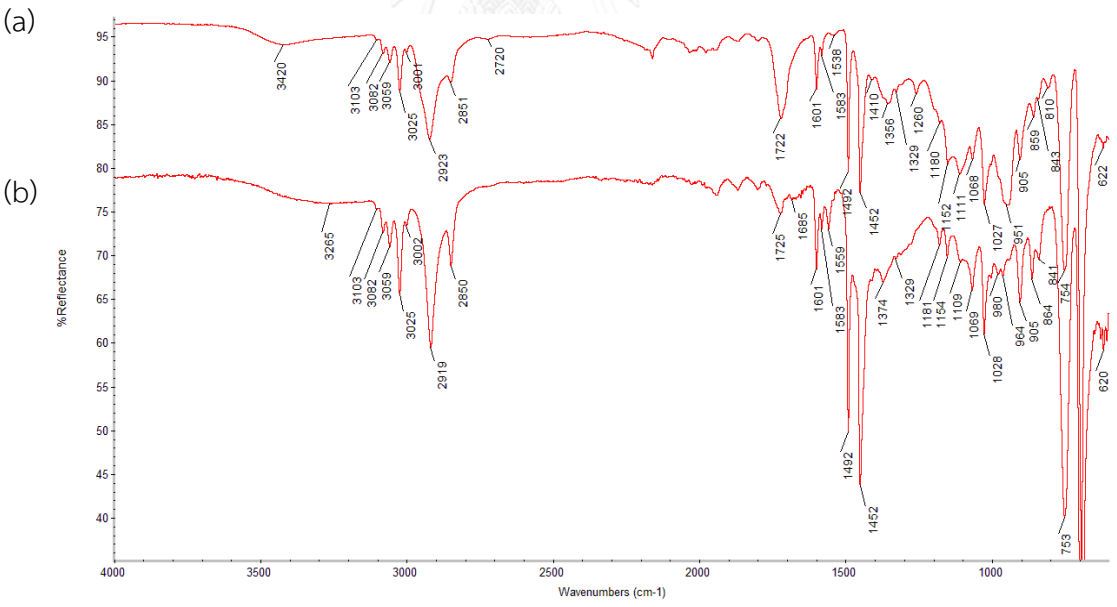

Figure A-17 Comparison of ATR-FTIR spectrums of (a) 25%GLU-3%CHI-15%STY/PS beads and (b) 18 mg of lipase immobilized onto 25%GLU-3%CHI-15%STY/PS beads at 30°C for 72 hours

APPENDIX B

CALCULATION

1. Determination of molecular weight of soybean oil

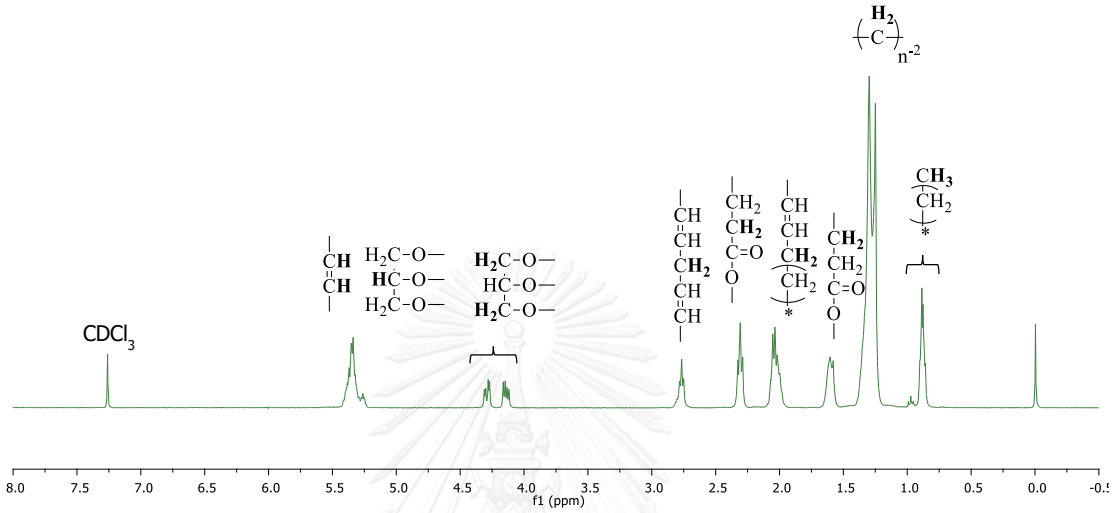

Figure B-1 ^{1}H NMR spectrum of soybean oil

1.1 The calculated molecular weight of soybean oil from saponification value

Saponification value (SN) is counted using the following formula:

$$\text{Saponification number (SN)} = \frac{MW_{KOH}\, N_{HCl}\, (V_b - V_s)}{W_s}$$

Where:

MW_{KOH} = Molecular weight of potassium hydroxide (56.109 g/mol)

N_{HCl} = Normality of hydrochloric acid (0.5 N)

V_b = Hydrochloric acid solution volume (ml) that is used for blank (without oil)

V_s = Hydrochloric acid solution volume (ml) that is used for soybean oil sample

W_s = Sample weight (g)

Table B-1 Amount of soybean oil and hydrochloric acid solution volume

Sample number	Amount of oil (g)	V_b (ml)	V_s (ml)
1	1.0021	22.90	16.10
2	1.0016	22.70	15.80
3	1.0019	22.80	15.90

$$SN_1 = \frac{(56.109\ g/mol) \times (0.5\ mol/l) \times (22.90\ ml - 16.10\ ml) \times (1\ l/1000\ ml) \times (1000\ mg/1\ g)}{1.0021\ g}$$

= 190.37 mg KOH/g oil

$$SN_2 = \frac{(56.109\ g/mol) \times (0.5\ mol/l) \times (22.70\ ml - 15.80\ ml) \times (1\ l/1000\ ml) \times (1000\ mg/1\ g)}{1.0016\ g}$$

= 193.27 mg KOH/g oil

$$SN_3 = \frac{(56.109\ g/mol) \times (0.5\ mol/l) \times (22.80\ ml - 15.90\ ml) \times (1\ l/1000\ ml) \times (1000\ mg/1\ g)}{1.0019\ g}$$

= 193.21 mg KOH/g oil

1.2 The calculated molecular weight of soybean oil from triacylglycerol molecular weight

Triacylglycerol (TAG) molecular weight is counted using the following formula:

$$\text{TAG molecule weight} = \frac{MW_{KOH}}{SN} \times \frac{1000\ mg}{1\ g} \times 3$$

Where:

MW_{KOH} = Molecular weight of potassium hydroxide (56.109 g/mol)

SN = Saponification number (mg/g)

$$\text{TAG molecule weight}_1 = \frac{MW_{KOH}}{SN_1} \times \frac{1000\ mg}{1\ g} \times 3$$

$$= \frac{56.109\ g/mol}{190.37\ mg\ KOH/g\ oil} \times \frac{1000\ mg}{1\ g} \times 3$$

$$= 884.21\ g/mol$$

$$\text{TAG molecule weight}_2 = \frac{MW_{KOH}}{SN_2} \times \frac{1000\ mg}{1\ g} \times 3$$

$$= \frac{56.109\ g/mol}{193.27\ mg\ KOH/g\ oil} \times \frac{1000\ mg}{1\ g} \times 3$$

$$= 870.96\ g/mol$$

$$\text{TAG molecule weight}_3 = \frac{MW_{KOH}}{SN_3} \times \frac{1000\ mg}{1\ g} \times 3$$

$$= \frac{56.109\ g/mol}{193.21\ mg\ KOH/g\ oil} \times \frac{1000\ mg}{1\ g} \times 3$$

$$= 871.22\ g/mol$$

The average of TAG molecule weight

$$= \frac{(884.21 + 870.96 + 871.22)\ g/mol}{3}$$

$$= 875.46\ g/mol$$

2. Calculation of % ethyl esters production

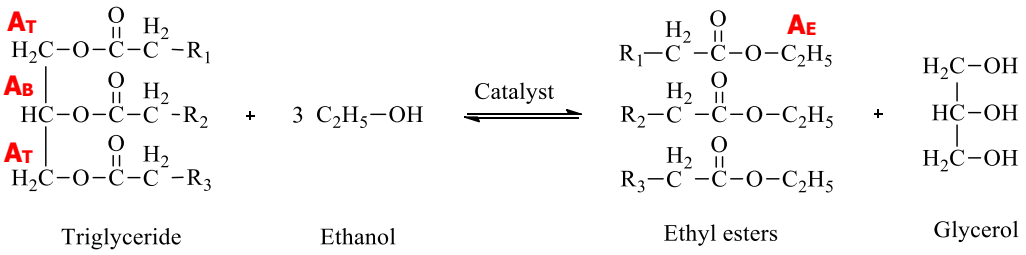

Scheme B-1 Transesterification reaction with ethanol

Where:

A_T = CH_2 protons in glycerol moiety (**δ**: 4.1-4.4 ppm)

A_B = CH proton in glycerol moiety (**δ**: 5.4 ppm)

A_E = CH_2 protons of the ethoxy group of fatty acid ethyl esters (**δ**: 4.2 ppm)

A_{CH3} = terminal methyl protons of fatty acyl moiety (**δ**: 0.9 ppm)

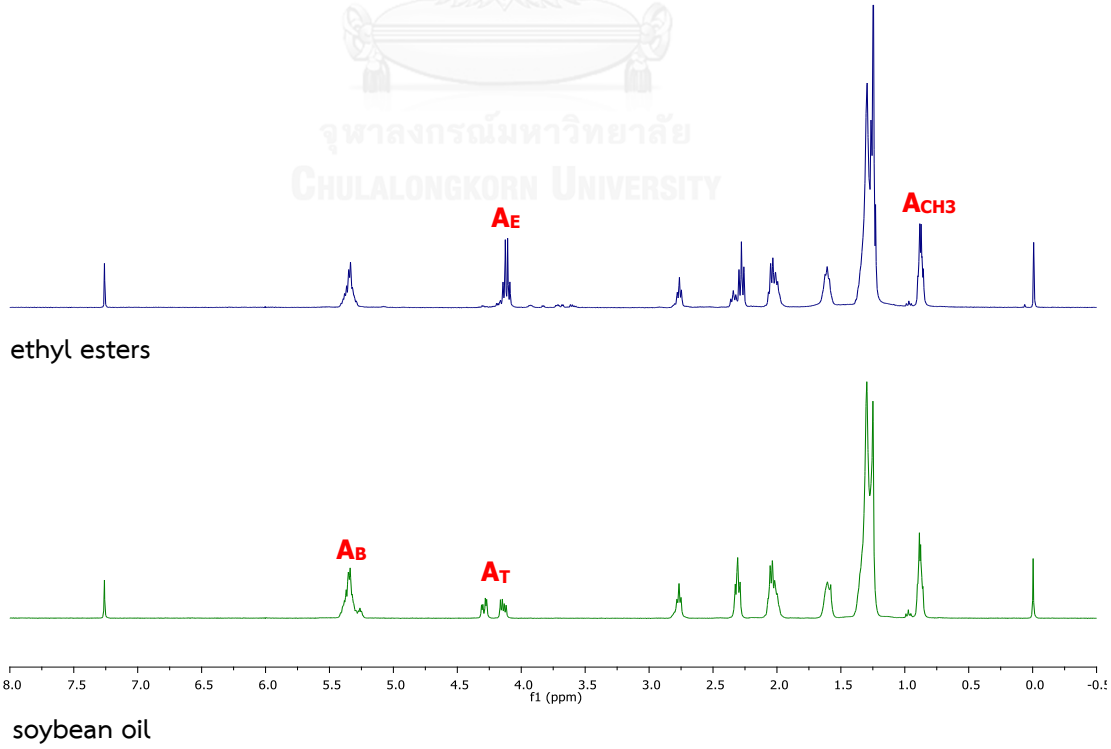

Figure B-2 ^{1}H NMR of soybean oil and ethyl esters

$$\text{Ethyl esters conversion (\%)} = \frac{\left(\frac{A_E - A_T}{2}\right)}{\left(\frac{A_{CH3}}{3}\right)} \times 100$$

Where:

A_E = Integral of CH_2 protons of the ethoxy group of fatty acid ethyl esters (**δ**: 4.2 ppm)

A_T = Integral of CH_2 protons in glycerol moiety (**δ**: 4.1-4.4 ppm)

A_{CH3} = Integral of terminal methyl protons of fatty acyl moiety (**δ**: 0.9 ppm)

3. Calculation of % methyl esters production

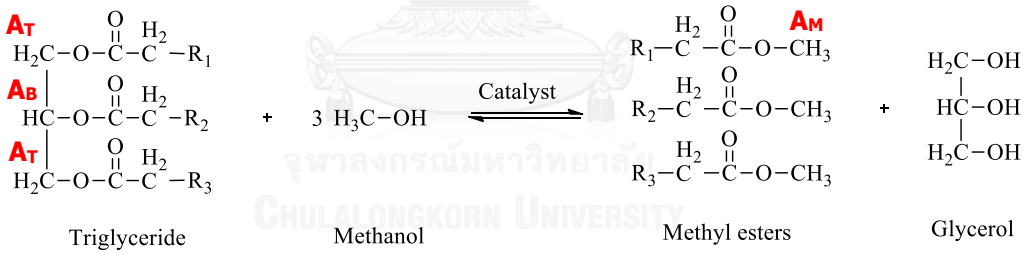

Scheme B-2 Transesterification reaction with methanol

Where:

A_T = CH_2 protons in glycerol moiety (**δ**: 4.1-4.4 ppm)

A_B = CH proton in glycerol moiety (**δ**: 5.4 ppm)

A_M = CH_2 protons of the methoxy group of fatty acid methyl esters (**δ**: 3.6 ppm)

A_{CH3} = terminal methyl protons of fatty acyl moiety (**δ**: 0.9 ppm)

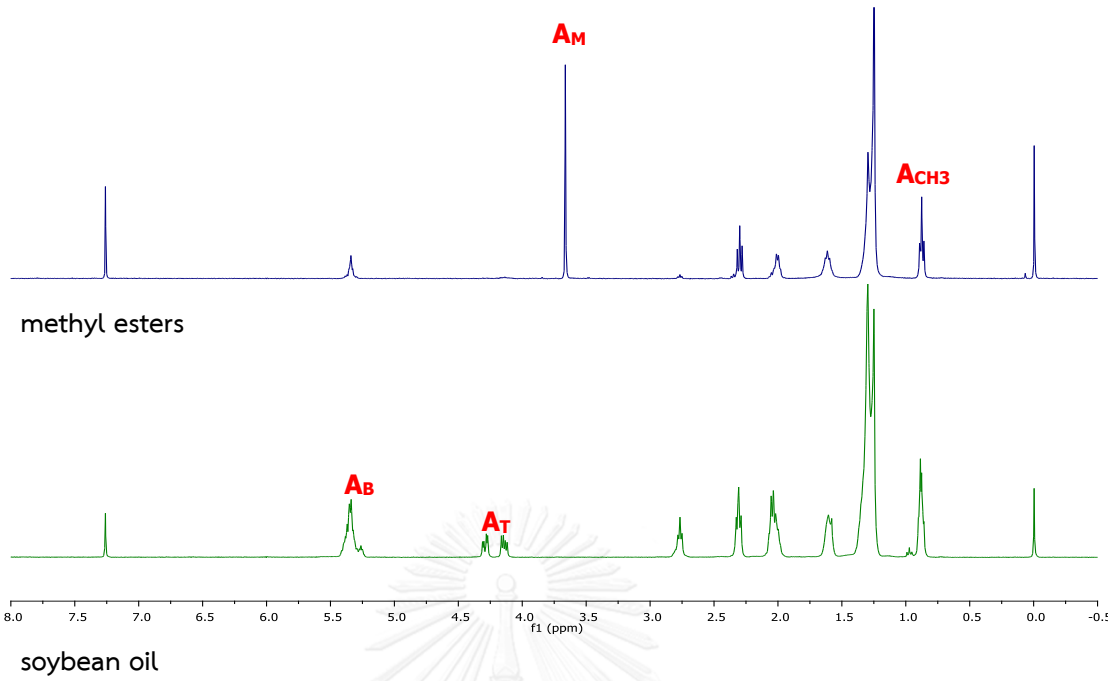

Figure B-3 ^{1}H NMR of soybean oil and methyl esters

$$\text{Methyl esters conversion (\%)} = \left(\frac{A_M}{A_{CH3}} \right) \times 100$$

Where:

A_M = Integral of CH_2 protons of the methoxy group of fatty acid methyl esters (**δ**: 3.6 ppm)

A_{CH3} = Integral of terminal methyl protons of fatty acyl moiety (**δ**: 0.9 ppm)

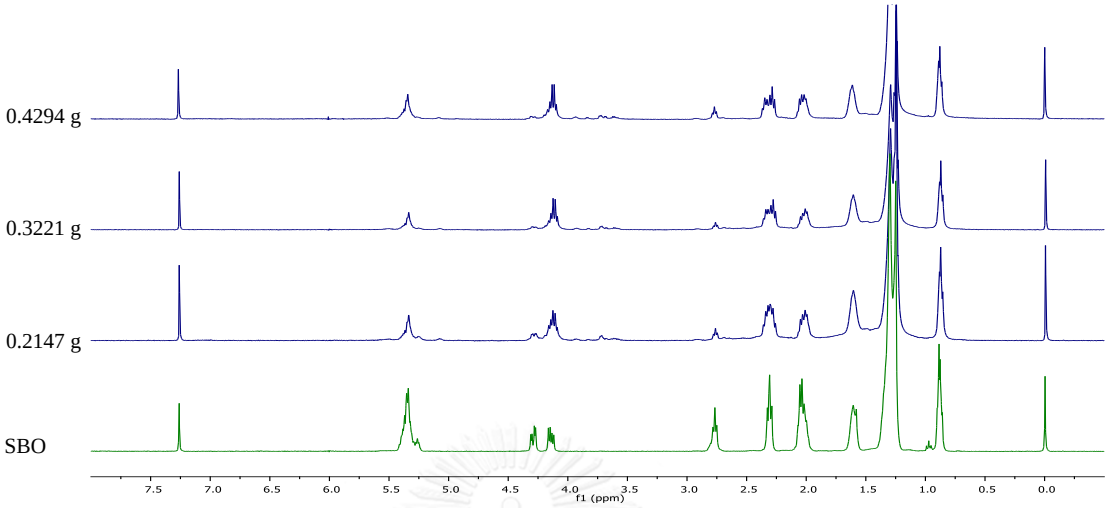

Figure B-4 ^{1}H NMR spectrums of amount of catalyst on transesterification of soybean oil. The reactions were performed with 1:3 molar ratio oil to anhydrous ethanol (one-step addition) and 10 g of soybean oil at 40°C for 192 hours

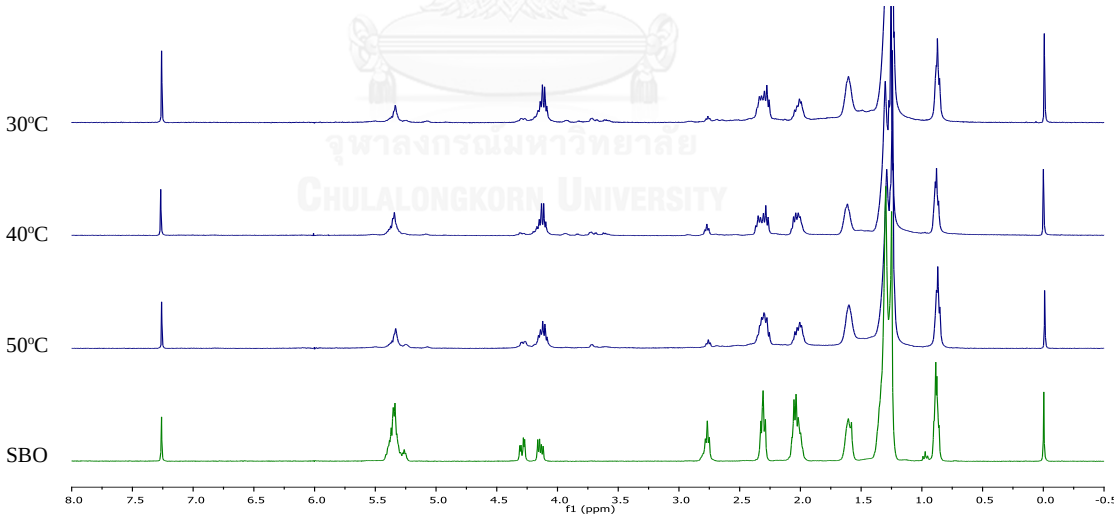

Figure B-5 ^{1}H NMR spectrums of temperature on transesterification of soybean oil. The reactions were performed with 1:3 molar ratio oil to anhydrous ethanol (one-step addition), 10 g of soybean oil and 0.4294 g of catalyst for 192 hours

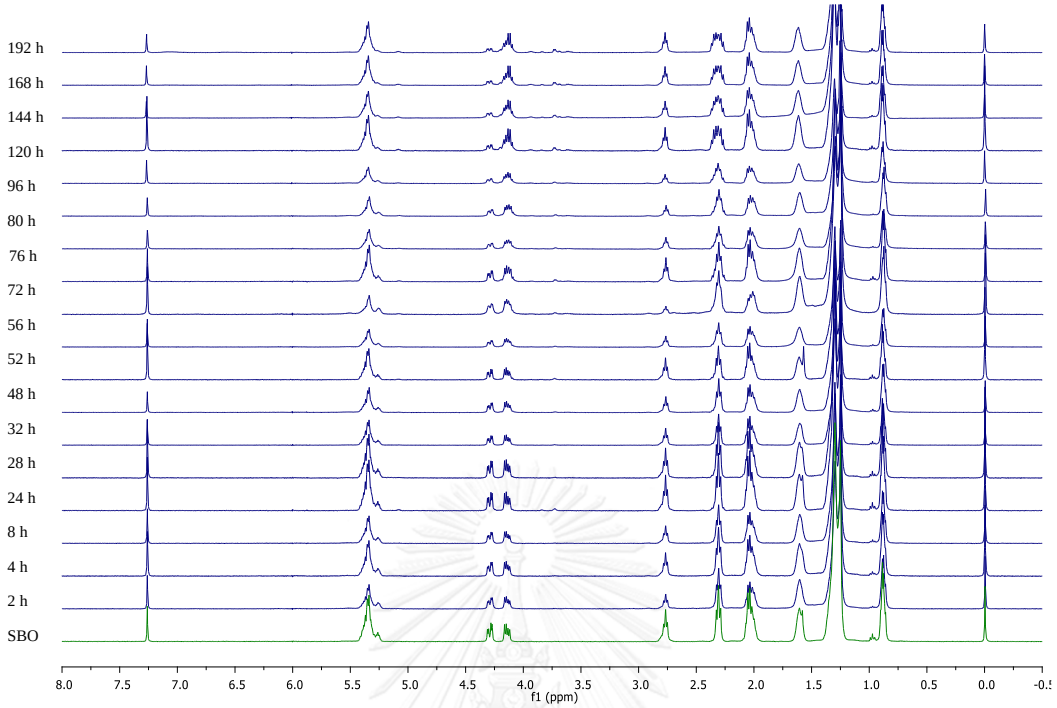

Figure B-6 ^{1}H NMR spectrums of variation of time on biodiesel conversion from soybean oil with anhydrous ethanol (1:1 molar ratio of oil to ethanol; one-step addition) at 40°C

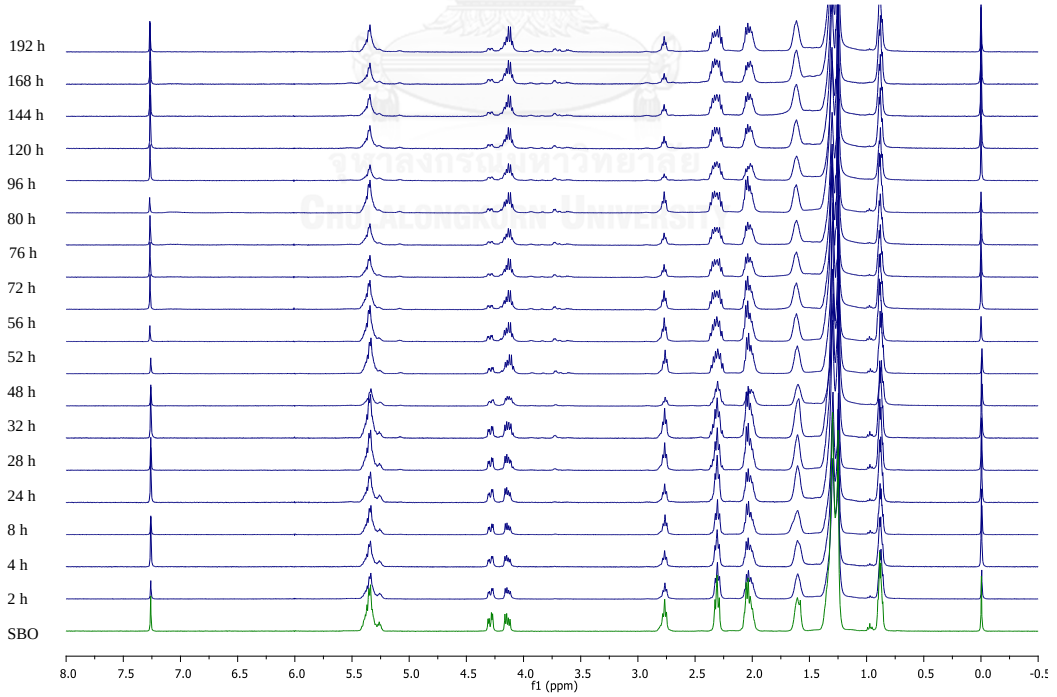

Figure B-7 ^{1}H NMR spectrums of variation of time on biodiesel conversion from soybean oil with anhydrous ethanol (1:2 molar ratio of oil to ethanol; one-step addition) at 40°C

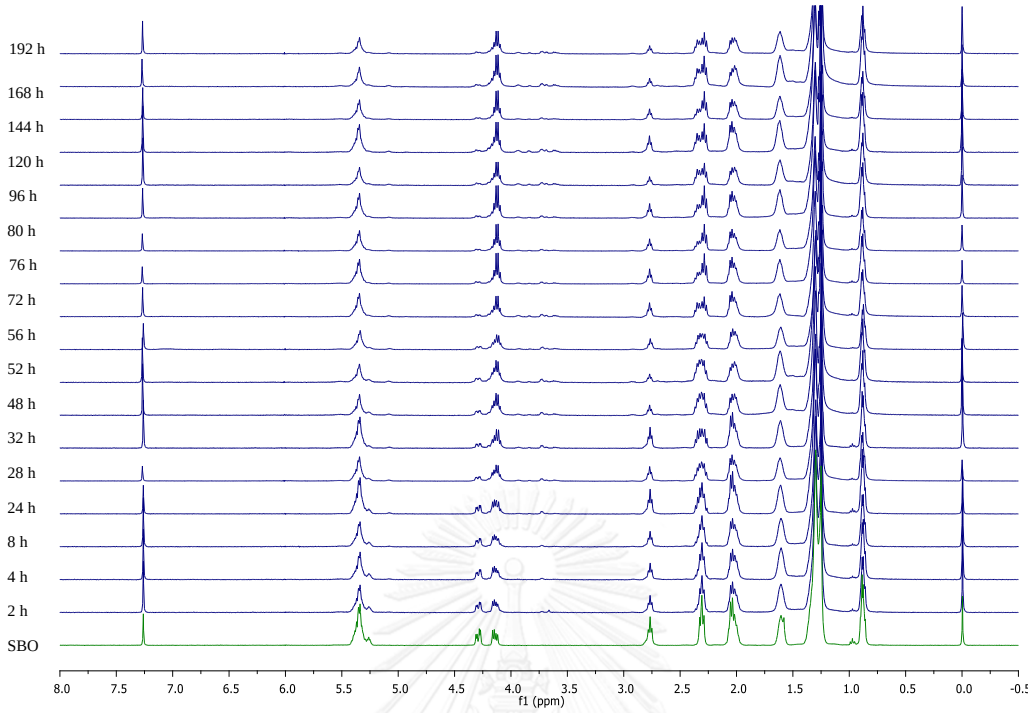

Figure B-8 ^{1}H NMR spectrums of variation of time on biodiesel conversion from soybean oil with anhydrous ethanol (1:3 molar ratio of oil to ethanol; one-step addition) at 40°C

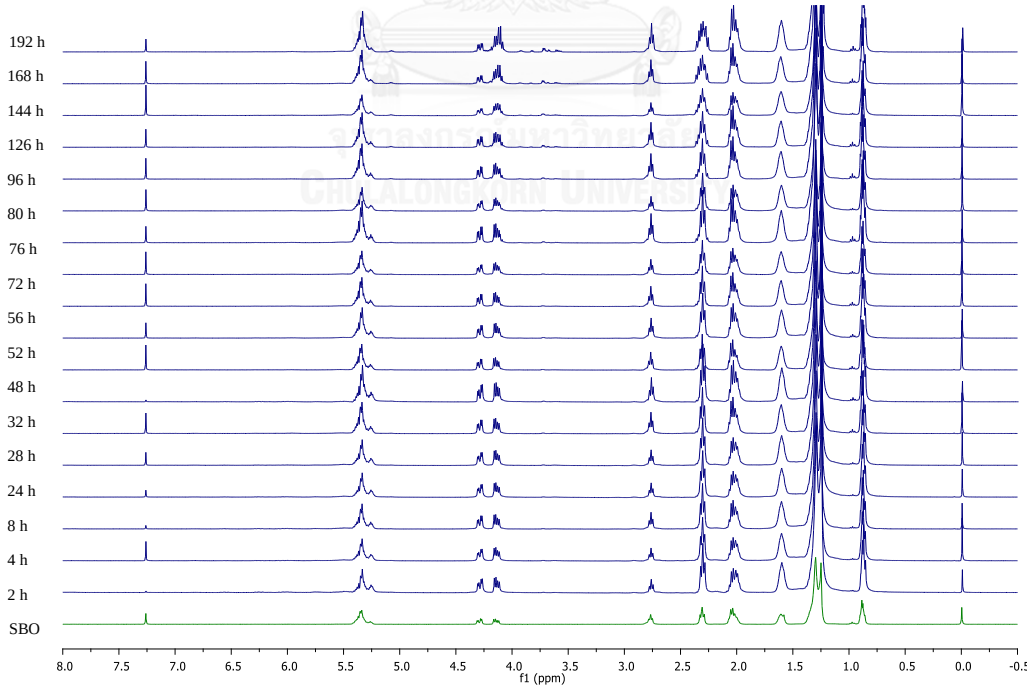

Figure B-9 ^{1}H NMR spectrums of variation of time on biodiesel conversion from soybean oil with anhydrous ethanol (1:4 molar ratio of oil to ethanol; one-step addition) at 40°C

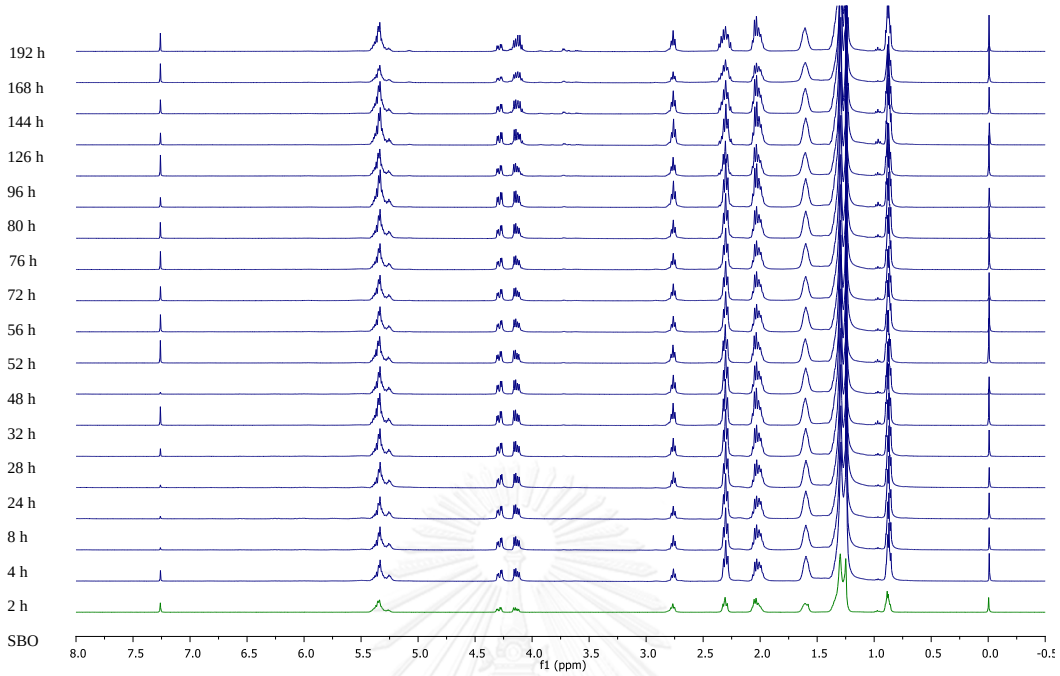

Figure B-10 ^{1}H NMR spectrums of variation of time on biodiesel conversion from soybean oil with anhydrous ethanol (1:5 molar ratio of oil to ethanol; one-step addition) at 40°C

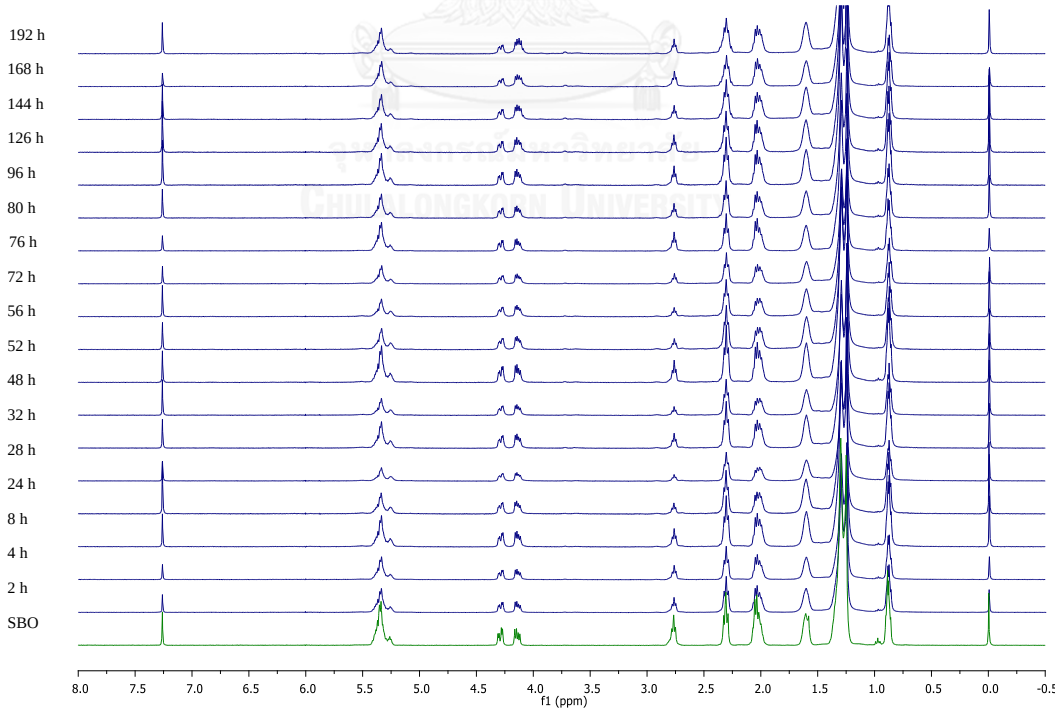

Figure B-11 ^{1}H NMR spectrums of variation of time on biodiesel conversion from soybean oil with anhydrous ethanol (1:6 molar ratio of oil to ethanol; one-step addition) at 40°C

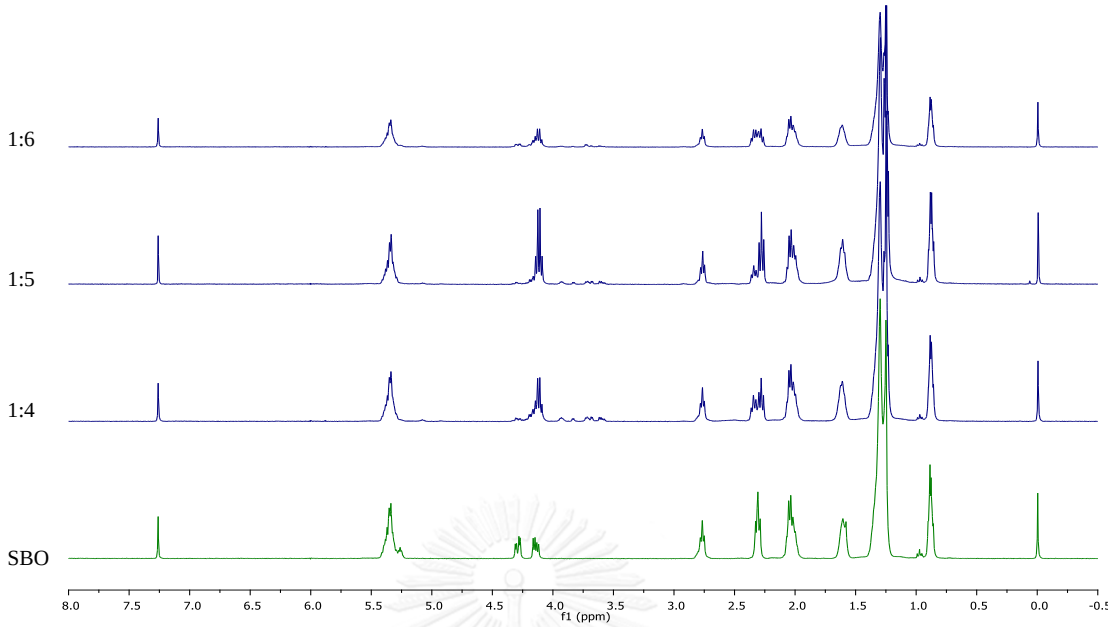

Figure B-12 ^{1}H NMR spectrums of oil/ethanol molar ratio on transesterification of soybean oil. The reactions were performed with anhydrous ethanol (three-step addition), 10 g of soybean oil and 0.4294 g of catalyst at 40°C for 32 hours

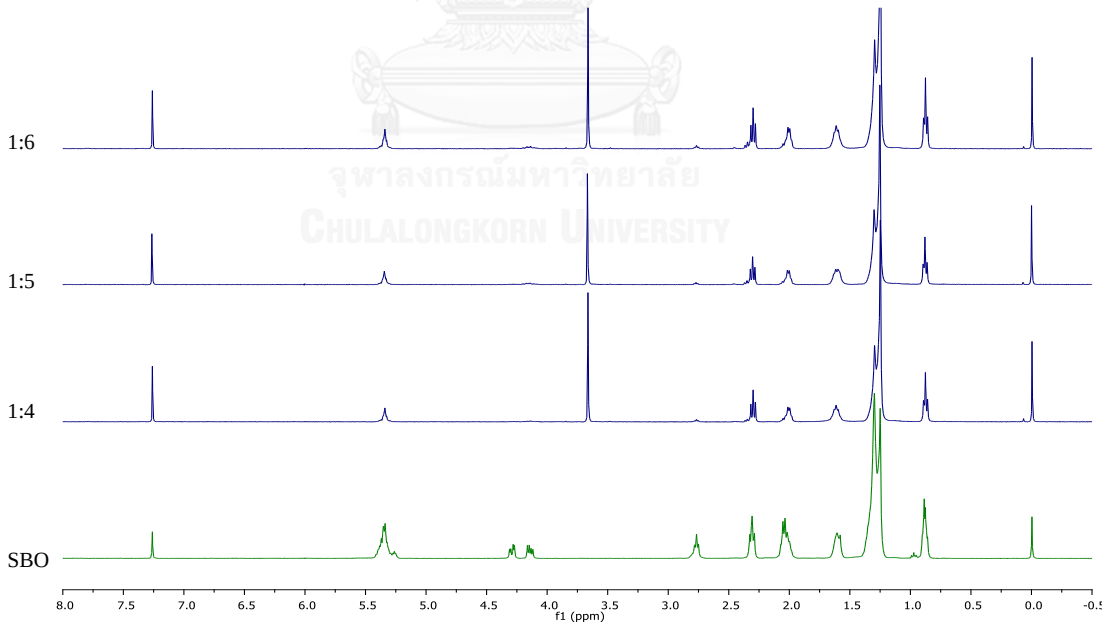

Figure B-13 ^{1}H NMR spectrums of oil/methanol molar ratio on transesterification of soybean oil. The reactions were performed with anhydrous methanol (three-step addition), 10 g of soybean oil and 0.4294 g of catalyst at 40°C for 32 hours

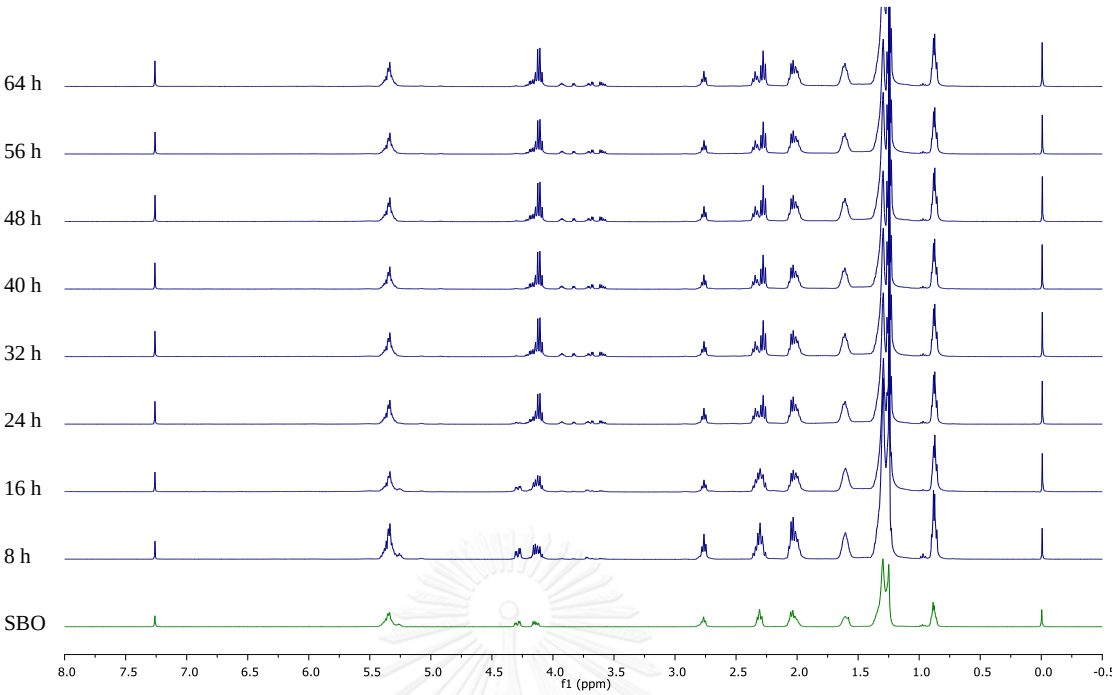

Figure B-14 ^{1}H NMR spectrums of oil/ethanol molar ratio on transesterification of soybean oil. The reactions were performed with 1:6 molar ratio oil to anhydrous ethanol (four-step addition), 10 g of soybean oil and 0.4294 g of catalyst at 40°C for 64 hours

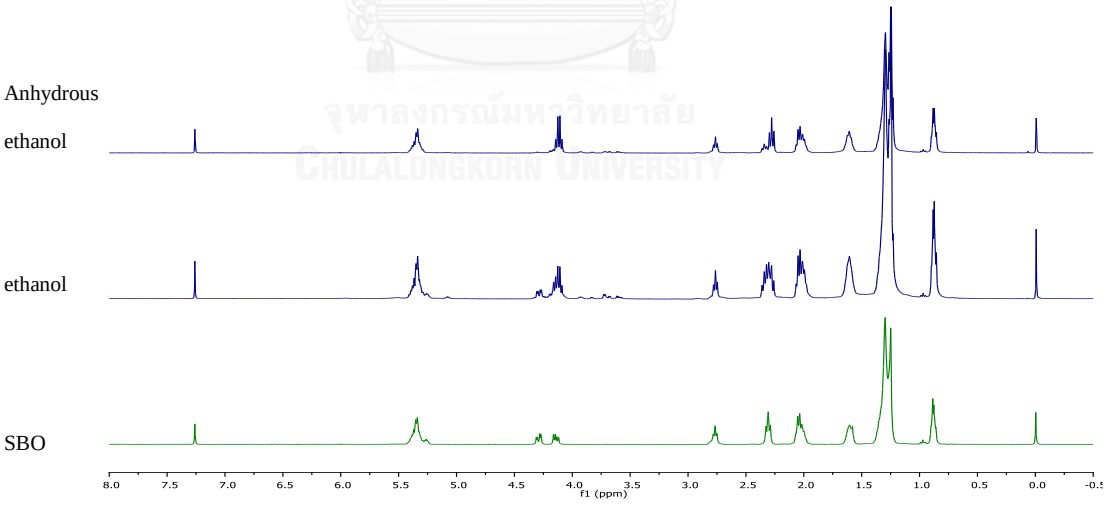

Figure B-15 ^{1}H NMR spectrums of oil/alcohol molar ratio on transesterification of soybean oil. The reactions were performed with 1:5 molar ratio oil to alcohol (three-step addition), 10 g of soybean oil and 0.4294 g of catalyst at 40°C for 32 hours

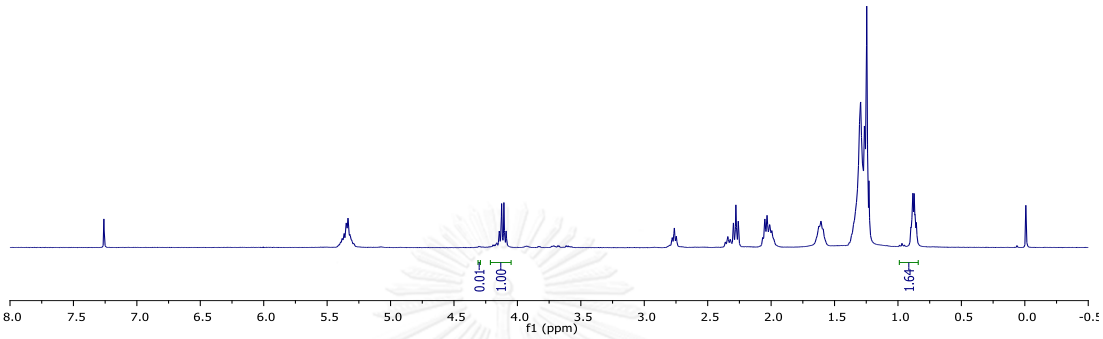

Figure B-16 ^{1}H NMR spectrums of biodiesel from soybean oil with anhydrous ethanol. The reactions were performed with 1:5 molar ratio oil to anhydrous ethanol (three-step addition), 10 g of soybean oil and 0.4294 g of catalyst at 40°C for 32 hours

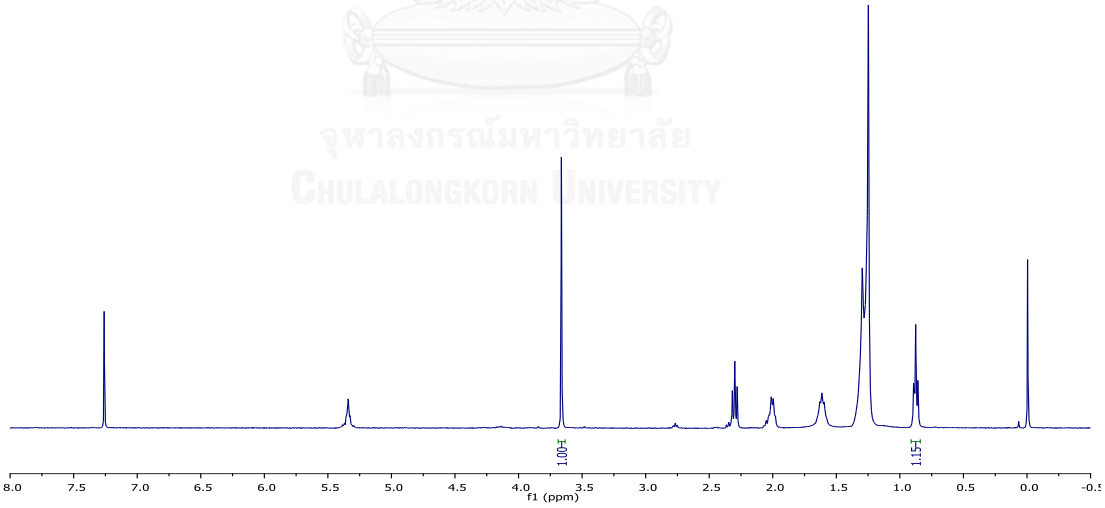

Figure B-17 ^{1}H NMR spectrums of biodiesel from soybean oil with anhydrous methanol. The reactions were performed with 1:4 molar ratio oil to anhydrous methanol (three-step addition), 10 g of soybean oil and 0.4294 g of catalyst at 40°C for 32 hours

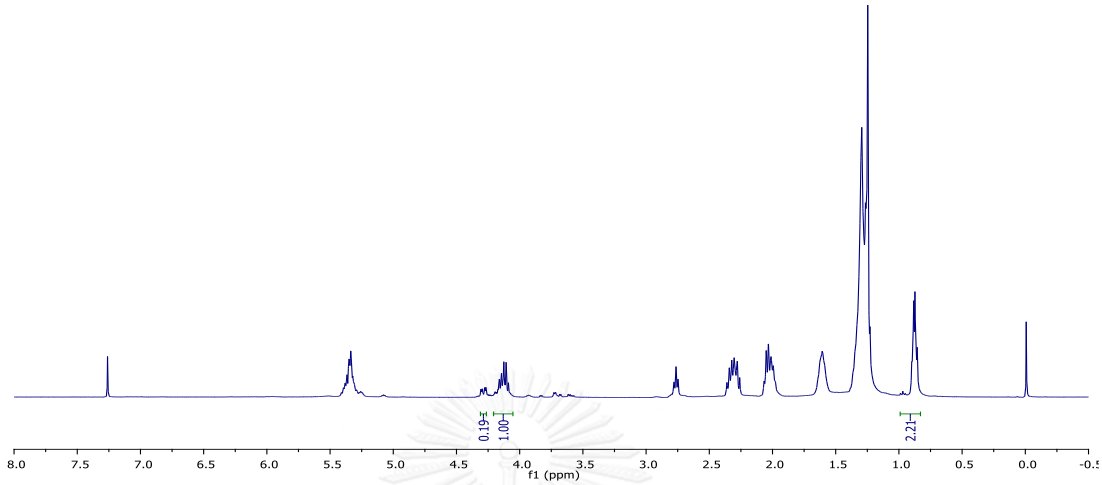

Figure B-18 ^{1}H NMR spectrums of biodiesel from soybean oil with ethanol. The reactions were performed with 1:5 molar ratio oil to ethanol (three-step addition), 10 g of soybean oil and 0.4294 g of catalyst at 40°C for 32 hours

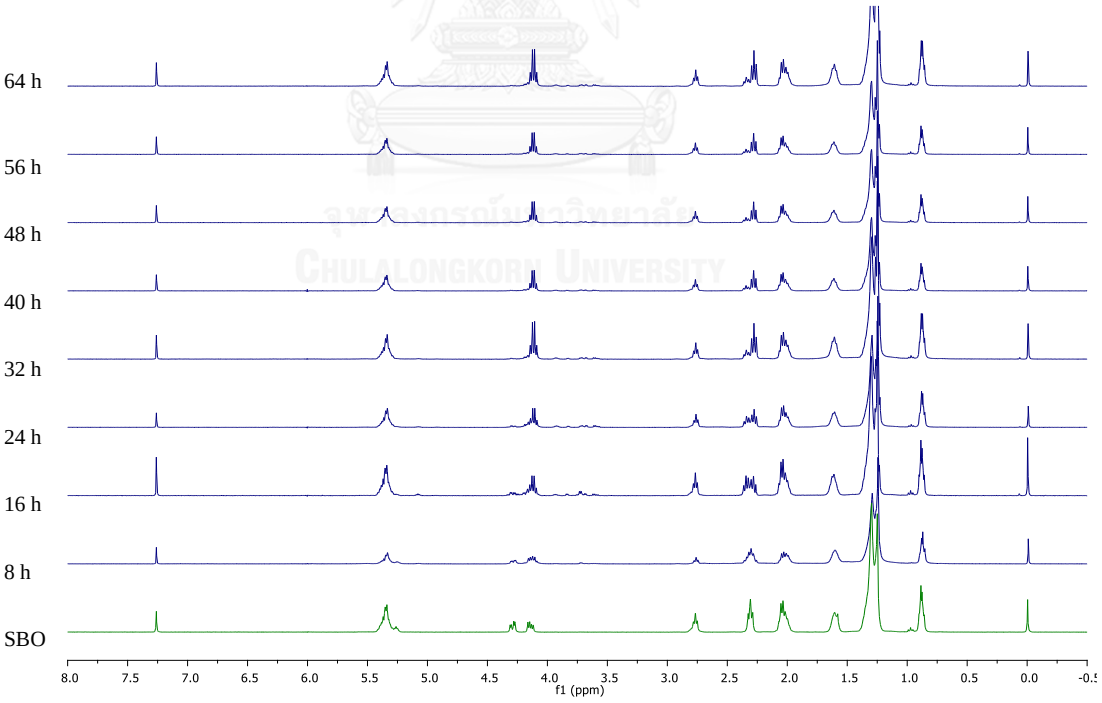

Figure B-19 ^{1}H NMR spectrums of reaction time on transesterification of soybean oil. The reactions were performed with 1:5 molar ratio oil to anhydrous ethanol (three-step addition), 10 g of soybean oil and 0.4294 g of catalyst at 40°C for 64 hours

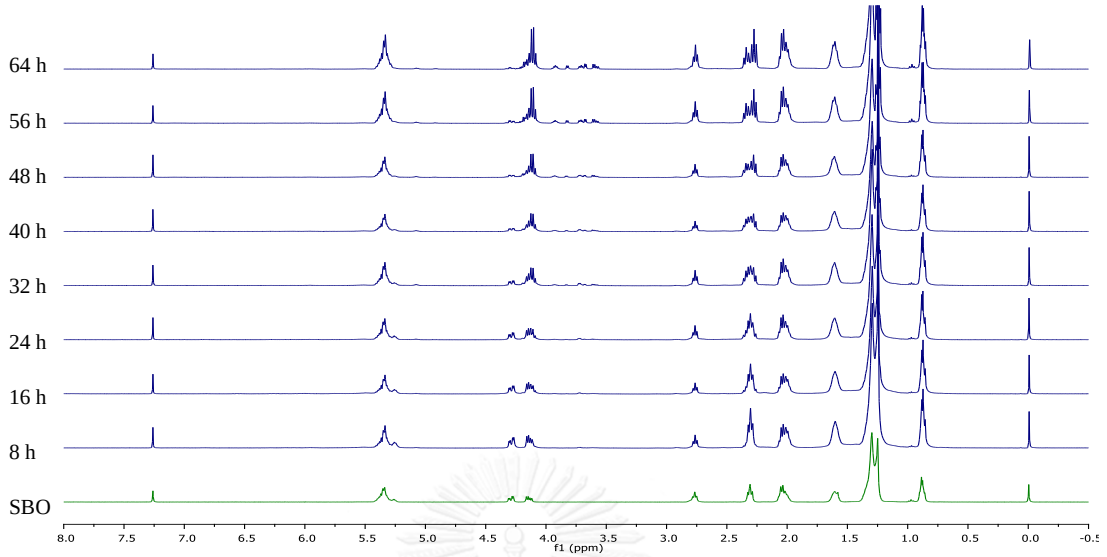

Figure B-20 ^{1}H NMR spectrums of reaction time on transesterification of soybean oil. The reactions were performed with 1:5 molar ratio oil to ethanol (three-step addition), 10 g of soybean oil and 0.4294 g of catalyst at 40°C for 64 hours

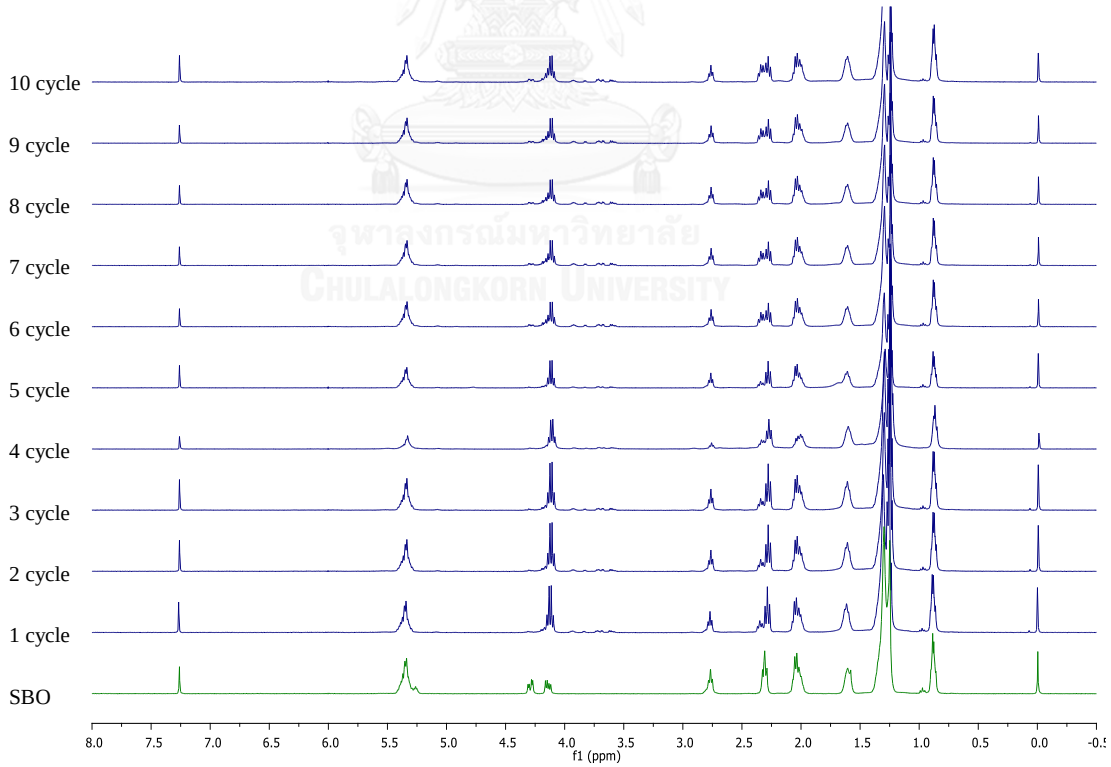

Figure B-21 ^{1}H NMR spectrums of operational stability and reusability on transesterification of soybean oil. The reactions were performed with 1:5 molar ratio oil to anhydrous ethanol (three-step addition), 10 g of soybean oil and 0.4294 g of catalyst at 40°C for 32 hours

VITA

Miss Pawinee Yuangkian was born on January 14th, 1989 in Ayutthaya, Thailand. She received a Bachelor's Degree of Science, majoring in Chemistry from Faculty of Science, Chulalongkorn University in 2011. Then, she continued her Master Degree in program of Petrochemistry and Polymer Science, Faculty of Science, Chulalongkorn University, Bangkok in 2012 and completed the program in semester 2st, 2015.

Poster presentation for the 40th Congress on Science and Technology of Thailand (STT40), which organized by Khon Kaen University in the topic of "Effect of chitosan-styrene copolymer coated onto polystyrene beads" on 2nd-4th December 2014 at Hotel Pullman Khon Kaen Raja Orchid, Khon Kaen, Thailand.